

---

# Investigating the role of FK506 binding protein 25 in cell proliferation and differentiation

---

**Tabitha Cree**

This thesis is submitted in total fulfilment of the requirements for the  
degree of Doctor of Philosophy

Supervisors: Professor John Price and Doctor Craig Goodman



**VICTORIA  
UNIVERSITY**

Institute for Health and Sport (IHeS)  
Victoria University, Melbourne, Australia

2021

## **Abstract**

Peptidyl prolyl isomerases (PPIase) are a class of enzymes that are required to catalyse the conversion of proline residues from cis to trans conformation. There are several classes of PPIase molecules, including parvulins, cyclophilins, and FK506 binding proteins (FKBPs). Among these PPIase molecules each class contains a conserved PPIase domain that facilitates protein to protein interactions. These PPIase molecules have diverse functions in cellular function and disease progression. FKBPs are a group of immunophilin molecules that are known to interact with immunosuppressant molecules FK506 and rapamycin to stop the immune response and inhibit mTOR, respectively. The structure and function of FKBPs is diverse, these proteins act to facilitate protein to protein interactions, act as co-chaperones, translocate throughout the cell in response to stress events, and bind to DNA. Importantly, FKBPs have been implicated in the pathogenesis of cancer, largely through their roles in co-chaperoning hormone receptors in hormone responsive cancers i.e. breast and prostate cancers. Of particular interest, FKBP25, a 25kDa protein that consists of two functional domains, an N terminal basic helix–loop–helix and C terminal PPIase domain. FKBP25 is known to be involved in protein folding, cytoskeletal dynamics, DNA damage repair, double stranded RNA binding, interacting with the pre-ribosome, and cellular stress responses. Despite the variety of roles that FKBP25 is known to play, there is limited research regarding FKBP25 role in disease and cell differentiation.

To address this, initial studies investigated the role of FKBP25 in breast cancer progression and epithelial to mesenchymal transition (EMT). Here it was found that FKBP25 protein expression is reduced in both mesenchymal breast cancer cell types, including BT-549, Hs578t, MDA-MB-231. To further understand the potential role of

FKBP25 in breast cancer pathogenesis, a variety of mutations that contribute to malignant transformation were examined. Here it was found that the oncogenic mutations, that are associated with growth pathways in fact increased FKBP25 expression. However, in an epidermal growth factor mediated model EMT in MDA-MB-468 breast cancer cells, it was identified that FKBP25 protein expression was reduced. This implies that the loss of FKBP25 protein expression may be required for de-differentiation and progression of cancer cells. As such, it was hypothesised that FKBP25 protein expression was correlated with the level of cellular differentiation. To examine this hypothesis, next a model of mesenchymal to epithelial transition (MET) was analysed.

The C2C12 model of myogenesis to study the role of FKBP25 in an MET-like example of cell differentiation. Previous studies have identified that FKBP25 is the most highly expressed FKBP in skeletal muscle and is expressed in the top 10% of the skeletal muscle proteome. Here it was identified that in proliferative myoblasts there is a higher level of FKBP25 protein expression compared to that of post mitotic myotubes. This was further demonstrated in a model of C2C12 quiescence where it was demonstrated that upon removal from the cell cycle, myoblasts accumulate greater levels of FKBP25 protein expression, which is then reduced upon re-entry to the cell cycle. Interestingly, this trend was not observed in human primary myoblasts, however, was identified in human rhabdomyosarcoma cells which may be due to the presence of p53 and MyoD mutations. Furthermore, *in vivo* models of muscle plasticity were examined to assess the impact of FKBP25 on skeletal muscle regeneration considering FKBP25 is the most highly expressed FKBP in mature skeletal muscle. Here it was discovered that FKBP25 protein expression is increased in models of regeneration including, chronic mechanical loading, murine muscular dystrophy (mdx), and denervation. It is

hypothesised that this was observed due to extensive cytoskeletal remodelling to repair structural damage caused by hypertrophy and atrophy of fibres.

Next, we examined the impact of FKBP25 knockdown (25KD) on cell biology and function of MDA-MB-468 and C2C12 cells. 25KD cells were developed using doxycycline inducible SMARTvector (Dharmacon, CO, USA) short hairpin RNA technology. After confirming adequate 25KD, it was observed that in both cell lines 25KD resulted in an increase in proliferation compared to respective non-targeting (NT) cells. Furthermore, in MDA-MB-468 cells, it was observed that there were no changes to invasion outgrowth or migration *in vitro*. However, it was demonstrated that 25KD resulted in decreased anchorage dependent growth, which could be explained by alterations to cytoskeletal stability. Conversely, in C2C12 myoblasts it was found that 25KD resulted in a significant increase in wound healing migration. Upon investigation of myogenic regulatory factor expression in differentiated 25KD myotubes it was revealed that there were no changes in protein expression. Furthermore, upon measurement of fibre diameter and fusion index it was found that there were no discernible changes to myotube formation.

Finally, the influence of 25KD on tubulin regulation and dynamics was assessed. Initially, the presence of microtubule (MT) post-translational modifications was assessed, including detyrosination and acetylation which are associated with MT stability. Both C2C12 and MDA-MB-468 25KD cells showed no changes to stabilising modifications. Similarly, upon examination of MT stabilising protein stathmin, both C2C12 and MDA-MB-468 25KD showed no change to stathmin expression. After this, the impact of 25KD on tubulin polymerisation under control and paclitaxel treated (induction of maximal polymerisation) conditions was explored. However, here no

differences in MT polymer content was found in either 25KD in either C2C12 or MDA-MB-468 cells.

In conclusion, this thesis has examined the potential role of FKBP25 in cell differentiation and de-differentiation in EMT and MET-like models. It was found that FKBP25 is required for some cell processes including proliferation, anchorage dependent growth, and migration. It was hypothesised that this was a result of cytoskeletal reorganisation and altered MT dynamics, however, this was unable to be demonstrated. Further studies should further examine the impact of 25KD on MT dynamics using methods less prone to error. Nonetheless, FKBP25 was demonstrated to have a role in cell proliferation and differentiation. Maintenance of FKBP25 protein in both cancers and skeletal muscle could help to preserve epithelial-like phenotype and maintain structural integrity, respectively.

## General Declaration

I, Tabitha Cree, declare that the PhD thesis entitled “Investigating the role of FK506 binding protein 25 in cell proliferation and differentiation” is no more than 80,000 words in length including quotes and exclusive of tables, figures, appendices, bibliography, references, and footnotes. This thesis contains no material that has been submitted previously, in whole or in part, for the award of any other academic degree or diploma. Except where otherwise indicated, this thesis is my own work.

I have conducted my research in alignment with the Australian Code for the Responsible Conduct of Research and Victoria University’s Higher Degree by Research Policy and Procedures.

Signature:

Date: 2/07/2021

## COVID-19 impact statement

Due to the unforeseen circumstances that arose from the 2020 COVID-19 pandemic there were substantial changes made to the studies that were undertaken in this thesis. Absence from the laboratory for extended periods of 2020 prevented the initiation of some crucial aspects of the proposed research to be undertaken. Which are outlined in the table below.

| Proposed research  | Research presented   |
|--|--|
| Generation of FKBP25 overexpression and mutant cell lines that would be used to determine the effects of each functional domain in either EMT or myogenic differentiation. | <ul style="list-style-type: none"><li>- This aspect of the study was removed due to time constraints and additional issues with lentiviral vector generation. Future studies will focus on generating these cell lines.</li><li>- Additionally, <i>in vivo</i> models of skeletal muscle plasticity were examined to describe the impacts of skeletal muscle regeneration, hypertrophy, and atrophy. These samples were kindly supplied by the EMU laboratory group at Victoria University.</li><li>- The absence of this study from the final thesis resulted in increased focus on the FKBP25 knockdown studies. This resulted in more data being recorded for this chapter compared to earlier chapters.</li><li>- The addition of microtubule studies was added to further elucidate the function of</li></ul> |

|  |  |
|--|--|
|  | <p>FKBP25 in relation to proliferation/migration studies that were hypothesised to be related to microtubule dynamics.</p>   |
| <p><i>In vivo</i> knockdown of FKBP25 in mouse hindlimb muscles using adeno-associated lentiviral vectors</p>                            | <ul style="list-style-type: none"> <li>- Due to time constraints and COVID-19 lockdown restrictions during 2020 these animal studies did not go ahead.</li> <li>- In their place, assessment of existing muscle plasticity and regeneration models were assessed (as mentioned above) to determine how FKBP25 expression is impacted by atrophy, hypertrophy, and disease states.</li> </ul>   |
| <p>RNA sequencing of either knockdown cell lines or mutant overexpression cell lines to examine the pathways that are impacted upon.</p> | <ul style="list-style-type: none"> <li>- In place of these studies, MDA-MB-468 EGF-EMT studies were completed using small molecule inhibitors to determine a mechanism that impacts upon FKBP25 expression.</li> <li>- Additional studies were planned to examine the impact of other growth factors, such as FGF-b and IGF-1, on FKBP25 expression in both MDA-MB-468 and C2C12 cell lines, however, the 2021 lockdown prevented these extended studies.</li> </ul> |

## Acknowledgments

After 4 and a half long years of endless experiments, hours of writing, and relentless editing of this document, my PhD thesis is completed. There are countless people I would like to thank for supporting me, whether it was as a mentor, friend, or smiling face in the office at 7am.

First, I would like to thank my supervisors John and Craig. You have both offered me endless support from my Honour's year in 2016, right through until I clicked submit on this thesis! Thank you for always helping me out when I was stuck, pushing me to do things out of my comfort zone, and for always having just the right advice when I needed it. You have helped me grow as both a researcher and as a person throughout my PhD journey and I cannot thank you both enough. This experience has been amazing, and I am glad I had you both to guide me through it.

All of my friends at WCHRE have made an incredible difference to my PhD. To every member of the Price lab, Charlett, Joe, Sarrabeth, Liz, CV, Asha, and Tash, you guys always made long boring days a bit more fun. You were all there to problem solve, laugh, and probably cry at some point. Your chronic optimism was absolutely invaluable to me. We are so lucky to have such a supportive and close lab group, without all of your company it would have been a lot less fun. The banh mi and gong cha lunches definitely helped too.

To my super best friends Charlett, Dean, and Lauren, you guys have listened to me whine and rave about the ups and downs of my PhD. All of the early mornings and late nights at the lab were made worth it because you guys were around to help if I needed it or even just to hang out with. Despite all of the failed westerns, tissue culture malfunctions, and stupid immuno, you guys always cheered me up. Thank you for the

millions of coffees, lunches, and everything in between. You have all made my PhD a fabulous time. Love you lots.

Also a big, big, thank you to all of my friends outside of my PhD for always appreciating how busy and unavailable I could be. Thanks for sharing memes with me, fixing my laptop, going out for dinner, random games nights, or even just texting me to check that I was alive. I will always appreciate each and every one of you.

Thank you to all of my Aunties, Uncles, cousins, and everyone in between for your words of support and curiosity about my PhD journey. I am truly lucky to have such amazing and supportive people around me – I hope that you all know how much that means to me.

Last, but certainly not least, my beautiful family (Mum, Dad, Nathan, and Jayden). You guys have put up with my stupidly long days where you would only see me for a few hours at a time, and the periods where I sat at my computer for what seemed like forever as I compiled this thesis. All of the weekends and public holidays that I missed out on things because I had to go to the lab or work on finishing a chapter. Thank you for always being patient, supportive, loving, and picking me up from the train station. Thank you for listening to me talk about things that you literally have no idea about but nodding appreciatively. Thank you for buying my favourite snacks. Thank you for always being my biggest fans. Thank you for supporting me during my long-lived university career but I promise I am finished studying now. I love you guys more than anything.

Also a special shout out to my Nan and Nuno for always asking me how my cells are going and if I am getting paid weekend rates for all the extra work I do. Bless you. You are my favourite people ever.

## Table of Contents

|   |           |
|---|-----------|
| Abstract.....   | ii        |
| General Declaration.....  | vi        |
| COVID-19 impact statement.....  | vii       |
| Acknowledgments .....   | ix        |
| List of Figures .....   | xvi       |
| List of Tables .....  | xx        |
| List of Abbreviations.....  | xxi       |
| <b>Chapter 1: Introduction</b> .....  | <b>1</b>  |
| 1.1 Peptidyl prolyl-isomerase molecules.....  | 1         |
| 1.2 Parvulins.....  | 1         |
| 1.3 Cyclophilins .....  | 4         |
| 1.4 FK506 Binding Proteins .....  | 8         |
| 1.5 FKBP12.....   | 12        |
| 1.6 FKBP52.....   | 15        |
| 1.7 FKBP51.....   | 18        |
| 1.8 FKBP38.....   | 21        |
| 1.9 FKBP25.....   | 24        |
| 1.10 The roles of FKBP25 in cancer pathogenesis .....                                 | 29        |
| 1.10.1 FKBP25 in hormone receptor expression.....                                     | 29        |
| 1.10.2 FKBP25 in cell death regulation .....  | 30        |
| 1.10.3 FKBP25 in microtubule stability.....   | 31        |
| 1.11 Nuclear FKBP25 in cancer pathogenesis .....                                      | 35        |
| 1.11.1 FKBP25 regulation of transcription factors.....                                | 35        |
| 1.11.2 FKBP25 RNA binding.....  | 36        |
| 1.11.4 FKBP25 in mesenchymal to epithelial transition (MET) cell differentiation..... | 42        |
| 1.12 Overarching aims .....   | 43        |
| <b>Chapter 2: Methods and Materials</b> .....   | <b>46</b> |
| 2.1 Plasmid purification.....   | 46        |
| 2.1.1 Bacterial Culture .....   | 46        |
| 2.1.2 Glycerol stocks.....  | 46        |
| 2.1.3 Plasmid extraction.....   | 46        |

|  |    |
|--|----|
| 2.2 Cell culture .....   | 47 |
| 2.2.1 Routine culturing of cell lines .....  | 47 |
| 2.2.2 Routine culturing of primary cell lines.....                                 | 48 |
| 2.2.3 Induction of quiescence in C2C12 cells .....                                 | 49 |
| 2.2.4 Epidermal growth factor induction of epithelial to mesenchymal transition .. | 49 |
| 2.2.5 Cryopreservation of cell lines .....   | 50 |
| 2.2.6 Generation of lentiviral particles.....                                      | 50 |
| 2.2.7 Generation of stable FKBP25 knockdown cell lines.....                        | 51 |
| 2.2.8 Doxycycline titration of FKBP25 knockdown cell lines .....                   | 53 |
| 2.3 Expression analysis.....   | 54 |
| 2.3.1 Protein extraction .....   | 54 |
| 2.3.2 Protein quantification.....  | 54 |
| 2.3.3 Western Blotting - NUPAGE .....  | 55 |
| 2.3.4 Western blotting – Bio-Rad .....   | 56 |
| 2.3.5 Microtubule polymerisation assay .....                                       | 56 |
| 2.3.6 Immunofluorescent staining .....   | 57 |
| 2.4 <i>In vitro</i> functional assays .....  | 58 |
| 2.4.1 Anchorage dependent colonisation assay.....                                  | 58 |
| 2.4.2 Matrigel invasion outgrowth assay .....                                      | 58 |
| 2.4.3 Microchemotaxis migration assay .....  | 59 |
| 2.4.4 Wound healing assay.....   | 59 |
| 2.4.5 Alamar blue viability assay .....  | 60 |
| 2.4.6 Cell density measurements.....   | 61 |
| 2.5 <i>In vivo</i> muscle hypertrophy and atrophy models.....                      | 61 |
| 2.5.1 Chronic mechanical loading .....   | 61 |
| 2.5.2 Murine muscular dystrophy (mdx).....   | 61 |
| 2.5.3 Denervation.....   | 62 |
| 2.5.4 Food deprivation .....   | 62 |
| 2.6 Statistical analysis.....  | 62 |
| 2.7 Materials.....   | 63 |
| 2.7.1 Plasmids .....   | 63 |
| 2.7.2 Reagents used for cell culture and <i>in vitro</i> assays .....              | 64 |
| 2.7.3 Reagents for expression analysis .....                                       | 66 |
| 2.7.4 General reagents .....   | 67 |
| 2.7.5 Commercial kits .....  | 68 |

|   |            |
|---|------------|
| 2.7.6 Primary antibodies .....  | 69         |
| 2.7.7 Secondary antibodies.....   | 71         |
| <b>Chapter 3: Investigating the role of FKBP25 in <i>in vitro</i> models of breast cancer de-differentiation</b> .....  | <b>72</b>  |
| 3.1 Introduction.....   | 72         |
| 3.1.1 Breast cancer .....   | 72         |
| 3.1.2 Cancer cells and the cell cycle.....  | 74         |
| 3.1.3 Epithelial to mesenchymal transition .....  | 76         |
| 3.1.4 Molecular features of EMT in breast cancer.....   | 77         |
| 3.1.5 Features of metastatic breast cancer cells.....   | 78         |
| 3.1.6 Chapter Aims: .....   | 81         |
| 3.2 Results.....  | 82         |
| 3.2.1 FKBP25 expression remains elevated in luminal and basal breast cancer cell subtypes and is reduced in mesenchymal subtypes. ....                            | 82         |
| 3.2.2 FKBP25 expression is increased upon oncogenic transformations of Ras and p53 but is reduced in metastatic clones of MDA-MB-231 cell line.....               | 85         |
| 3.2.3 FKBP25 expression is decreased upon epidermal growth factor-mediated epithelial to mesenchymal transition (EMT) in MDA-MB-468 breast cancer cell line. .... | 90         |
| 3.3 Discussion.....   | 95         |
| 3.3.1 FKBP25 expression remains elevated in luminal and basal breast cancer cell subtypes and is reduced in mesenchymal subtypes. ....                            | 95         |
| 3.3.2 FKBP25 expression is increased upon oncogenic transformation of Ras and p53 but is reduced in metastatic clones of MDA-MB-231 cell line.....                | 97         |
| 3.3.3 FKBP25 expression is decreased upon epidermal growth factor mediated epithelial to mesenchymal (EMT) in MDA-MB-468 breast cancer cell line.....             | 99         |
| 3.4 Conclusions .....   | 102        |
| <b>Chapter 4: Investigating the role of FKBP25 in models of myogenesis and muscle plasticity</b> .....  | <b>104</b> |
| 4.1 Introduction.....   | 104        |
| 4.1.1 Mesenchymal to epithelial transition (MET) and Myogenesis .....   | 104        |
| 4.1.2 Rhabdomyosarcoma (RMS).....   | 106        |
| 4.1.3 Skeletal muscle regeneration.....   | 108        |
| 4.1.4 Chapter Aims .....  | 111        |
| 4.2 Results.....  | 112        |
| 4.2.1 FKBP25 expression is increased upon C2C12 differentiation and induction of quiescence.....  | 112        |

|  |            |
|--|------------|
| 4.2.2 FKBP25 expression is increased in differentiated primary RMS cells but not differentiated primary myoblasts. ....                | 119        |
| 4.2.3 FKBP25 expression is increased in in vivo models of skeletal muscle hypertrophy and reduced in some models of atrophy. ....      | 126        |
| 4.3 Discussion.....  | 133        |
| 4.3.1 FKBP25 expression is increased upon C2C12 differentiation and induction of quiescence. ....                                      | 133        |
| 4.3.2 FKBP25 expression is increased in differentiated primary RMS cells but not differentiated primary myoblasts. ....                | 135        |
| 4.3.3 FKBP25 expression is increased in in vivo models of skeletal muscle hypertrophy and reduced in some models of atrophy .....      | 137        |
| 4.4 Conclusions .....  | 141        |
| <b>Chapter 5: The impact of FKBP25 knockdown on cell biology and function.....</b>   | <b>142</b> |
| 5.1 Introduction.....  | 142        |
| 5.1.1 The cell cycle .....   | 142        |
| 5.1.2 Cell movement .....  | 145        |
| 5.1.4 Anchorage dependence and cell growth .....   | 147        |
| 5.1.3 Implications for EMT .....   | 148        |
| 5.1.4 Chapter Aims .....   | 152        |
| 5.2 Results.....   | 153        |
| 5.2.1 Generation of doxycycline-inducible shRNA knockdown of FKBP25 in MDA-MB-468 and C2C12 cell lines.....                            | 153        |
| 5.2.2 FKBP25 knockdown increases cell viability and density over time indicating increased proliferation.....                          | 158        |
| 5.2.3 FKBP25 knockdown improves C2C12 myoblast wound healing but not chemotactic migration of MDA-MB-468 cells. ....                   | 161        |
| 5.2.4 FKBP25 knockdown reduces anchorage-dependent growth of MDA-MB-468 cells but not invasion outgrowth. ....                         | 165        |
| 5.2.5 FKBP25 knockdown does not impair markers of myogenesis or fibre size of differentiated C2C12 myotubes.....                       | 169        |
| 5.2.6 FKBP25 knockdown increases susceptibility to EGF mediated EMT by increasing markers E cadherin and vimentin. ....                | 175        |
| 5.2.7 FKBP25 knockdown does not impact upon tubulin post-translational modifications, or microtubule regulating protein stathmin ..... | 182        |
| 5.3 Discussion.....  | 190        |
| 5.3.1 FKBP25 knockdown increases cell viability and density over time indicating increased proliferation.....                          | 190        |

|  |            |
|--|------------|
| 5.3.2 FKBP25 knockdown improves C2C12 myoblast wound healing but not chemotactic migration of MDA-MB-468 cells. ....   | 191        |
| 5.3.3 FKBP25 knockdown reduces anchorage-dependent growth of MDA-MB-468 cells but not invasion outgrowth. ....   | 192        |
| 5.3.4 FKBP25 knockdown does not impair markers of myogenesis or myotube size of differentiated C2C12 myotubes.....   | 193        |
| 5.3.5 FKBP25 knockdown increases markers of epithelial to mesenchymal transition in MDA-MB-468 cells.....  | 195        |
| 5.3.6 FKBP25 knockdown alters tubulin post translational modifications associated with tubulin polymer stability in C2C12 myoblasts but not MDA-MB-468 cells.... | 196        |
| 5.4 Conclusions .....  | 199        |
| <b>Chapter 6: General discussion .....</b>   | <b>201</b> |
| 6.1 FKBP25 in breast cancer cell de-differentiation .....  | 201        |
| 6.2 The involvement of FKBP25 in myogenesis .....  | 202        |
| 6.3 FKBP25 in mature muscle plasticity.....  | 204        |
| 6.4 FKBP25 in cell biology and function.....   | 205        |
| 6.5 FKBP25 on MT polymerisation .....  | 207        |
| 6.6 Limitations of the study .....   | 209        |
| 6.7 Future directions .....  | 210        |
| References:.....   | 212        |

## List of Figures

Figure 1.1 : Conformation of proline residues in cis and trans conformations and visual description of steric hindrance

Figure 1.2: Human parvulins molecular structure

Figure 1.3: Cyclosporin A facilitation of immune suppression

Figure 1.4: Structural domains of Cyclophilin molecules

Figure 1.5: Structural domains of FK506 binding proteins

Figure 1.6: FK506 mediated immune suppression

Figure 1.7: FKBP12 and rapamycin inhibition of mTOR

Figure 1.8: FKBP12 stabilises the skeletal muscle ryanodine receptor

Figure 1.9: FKBP12 stabilises the TGF $\beta$  receptor to prevent leaky signalling

Figure 1.10: FKBP52 interaction with steroid receptors

Figure 1.11: FKBP51 regulates Akt and NF- $\kappa$ B signalling

Figure 1.12: FKBP38 implication in mTORC1 signalling

Figure 1.13: Double stranded DNA break repair

Figure 1.14: FKBP25 is a microtubule stabilising protein

Figure 1.15: Structure and components of the cytoskeleton

Figure 2.1: Elements of the SMARTvector Inducible Lentiviral shRNA vector

Figure 3.1: The functions of oncogenes and tumour suppressor genes in cell proliferation

Figure 3.2: Epithelial to mesenchymal transition (EMT)

Figure 3.3: FKBP25 expression across a panel of breast cancer cells

Figure 3.4: Localisation of FKBP25 in breast cancer cells

Figure 3.5: Expression of FKBP25 in Ras transformed mammary epithelial cell line

Figure 3.6: Expression of FKBP25 in upon p53 mutation mammary epithelial cell line

Figure 3.7: FKBP25 expression in invasive (#16) and non-invasive (#17) MDA-MB-231 clones

Figure 3.8: Epidermal Growth factor (EGF) mediated epithelial to mesenchymal transition (EMT) in MDA-MB-468 breast cancer cells

Figure 3.9: Molecular analysis of epidermal growth factor (EGF) mediated epithelial to mesenchymal transition (EMT) in MDA-MB-468 breast cancer cells

Figure 3.10: EGF mediated reduction of FKBP25 protein in MDA-MB-468 is not altered with small molecule inhibitor treatment

Figure 4.1: Mesenchymal to epithelial transition (MET)

Figure 4.2: Regulation of myogenic satellite cells in self renewal and regeneration

Figure 4.3: Comparison of differentiation and de-differentiation models

Figure 4.4: FKBP25 expression throughout C2C12 myoblast differentiation

Figure 4.5: Proposed relationship between FKBP25 and cell differentiation

Figure 4.6: Localisation of FKBP25 in C2C12 myoblasts and myotubes

Figure 4.7: Morphology of synchronous myoblasts following quiescence induction and subsequent differentiation

Figure 4.8: FKBP25 expression in synchronous, quiescent, and differentiated C2C12 myoblasts

Figure 4.9: Localisation of FKBP25 in human primary myoblast cell line MBA-135

Figure 4.10: Localisation of FKBP25 in rhabdomyosarcoma cell line Rh30

Figure 4.11: FKBP25 expression is not altered in MBA-135 human primary myoblasts and differentiated myotubes

Figure 4.12: FKBP25 expression is increased in differentiated human rhabdomyosarcoma cells

Figure 4.13 FKBP25 protein expression is not altered by EGF treatment in C2C12 myoblasts

Figure 4.14: FKBP25 protein expression is increased upon chronic mechanical overload

Figure 4.15: FKBP25 protein expression is increased in a model of murine muscular dystrophy (mdx)

Figure 4.16: FKBP25 protein expression is reduced upon hindlimb denervation

Figure 4.17: FKBP25 protein expression is unaltered in a model of food deprivation induced skeletal muscle atrophy

Figure 5.1: The cell cycle

Figure 5.2: Cell migration and principles of focal adhesion

Figure 5.3: The role of microtubule stability in cell division

Figure 5.4: Generation of a doxycycline inducible shRNA knockdown of FKBP25 in MDA-MB-468 breast cancer cells

Figure 5.5: Generation of a doxycycline inducible shRNA knockdown of FKBP25 in C2C12 myoblasts

Figure 5.6: Confirmation of FKBP25 inducible knockdown in MDA-MB-468 breast cancer cell line

Figure 5.7: Confirmation of FKBP25 knockdown in C2C12 myoblasts

Figure 5.8: FKBP25 knockdown increases cell viability and cell accumulation over time in MDA-MB-468 breast cancer cells

Figure 5.9: FKBP25 knockdown increases cell viability and cell accumulation over time in C2C12 myoblasts

Figure 5.10: FKBP25 knockdown does not impact upon chemotactic migration toward epidermal growth factor (EGF)

Figure 5.11: FKBP25 knockdown does not impact upon chemotactic migration toward fibroblast conditioned medium

Figure 5.12: FKBP25 knockdown increases wound healing migration of C2C12 myoblasts

Figure 5.13: FKBP25 knockdown results in decreased ability to form anchorage dependent colonies at both low and high seeding density

Figure 5.14: FKBP25 knockdown does not impact upon invasion out-growth

Figure 5.15: Impact upon myogenic factors following FKBP25 knockdown in C2C12 myoblasts

Figure 5.16: Impact upon myogenic factors following FKBP25 knockdown in C2C12 myotubes

Figure 5.17: FKBP25 knockdown does not impair myotube formation *in vitro*

Figure 5.18: FKBP25 knockdown does not impair myoblast fusion index

Figure 5.19: FKBP25 knockdown in addition to EGF mediated EMT does not induce further morphological change

Figure 5.20: FKBP25 knockdown exacerbates EMT markers E cadherin and vimentin upon EGF mediated EMT induction

Figure 5.21: Epidermal growth factor receptor (EGFR) signalling

Figure 5.22: FKBP25 knockdown does not alter Akt signalling in response to EGF stimulation

Figure 5.23: FKBP25 knockdown does not alter ERK signalling in response to EGF stimulation

Figure 5.24: FKBP25 knockdown in C2C12 myoblasts impairs tubulin detyrosination modification associated with microtubule polymer stability

Figure 5.25: FKBP25 knockdown in MDA-MB-468 cells does not affect tubulin modifications associated with microtubule stability

Figure 5.26: FKBP25 knockdown is not sufficient to alter the proportion of polymerised tubulin in C2C12 cells

Figure 5.27: FKBP25 knockdown is not sufficient to alter the proportion of polymerised tubulin in C2C12 cells pre-treated with paclitaxel

Figure 5.28: FKBP25 knockdown is not sufficient to alter the proportion of polymerised tubulin in MDA-MB-468 cells

Figure 5.29: FKBP25 knockdown is not sufficient to alter the proportion of polymerised tubulin in MDA-MB-468 cells pre-treated with paclitaxel

## List of Tables

Table 1.1 FKBP25 roles in EMT and cancer progression summary

Table 2.1: SMARTvector components

Table 2.2: List of SMARTvector shRNAmir sequences

Table 2.3: List of plasmids

Table 2.4: List of reagents for cell culture and *in vitro* assays

Table 2.5: List of reagents for protein expression analysis

Table 2.6: List of general reagents

Table 2.7: List of commercial kits

Table 2.8: List of primary antibodies

Table 2.9: List of secondary antibodies

Table 3.1 Breast cancer molecular subtypes

Table 3.2: Functions of phenotypic stability factors (PSFs)

Table 4.1: Myogenic regulatory factor (MRF) expression throughout myogenesis

## List of Abbreviations

$\alpha$ TAT – Alpha tubulin acetyltransferase

$\mu$ l – Microlitre

25KD – Knockdown of FKBP25

4E-BP1 – eIF4E binding protein 1

Akt – Protein kinase B

ANOVA – Analysis of variance

Apaf-1 – Apoptotic protease activating factor 1

AR – Androgen receptor

ARE – Androgen response element

ATG – Autophagy related protein

ATP – Adenosine triphosphate

BAD – Bcl-2-associated death promoter

BAK – Bcl-2 homologous antagonist killer

BAX – Bcl-2-like protein 4

BCA – Bicinchoninic acid assay

Bcl-2 – B cell lymphoma 2

Bcl-XL – B cell lymphoma extra large

BID – BH3 interacting domain death agonist

BRCA1 – Breast Cancer susceptibility protein 1

BRCA2 – Breast Cancer susceptibility protein 2

BSA – Bovine serum albumin

BTHB – Basic tilted helix loop bundle

$\text{Ca}^{2+}$  - Calcium

$\text{CaCl}_2$  – Calcium chloride

CAM – Calcium adhesion molecule

CaM – Calmodulin

CDC25 – Cell division cycle 25

CDK – Cyclin dependent kinase

CDKI – Cyclin dependent kinase inhibitor  
CFTR – Cystic fibrosis transmembrane conductance regulator  
CK2 – Casein kinase 2  
CM – Complete medium  
CML – Chronic mechanical loading  
CO<sub>2</sub> – Carbon dioxide  
CypA – Cyclophilin A  
CypB – Cyclophilin B  
CypC – Cyclophilin C  
CypD – Cyclophilin D  
CypA – Clycosporin  
DAPI – 4'6-diamidino-2-phenylindole  
DGC – Dystroglycan complex  
DMD – Duchenne muscular dystrophy  
DMEM – Dulbecco's modified eagle medium  
DMSO – Dimethyl sulfoxide  
DNA – Deoxyribose nucleic acid  
Dox – Doxycycline  
DSB – Double stranded DNA break  
dsRNA – Double stranded ribonucleic acid  
DTT – Dithiothreitol  
*E. coli - Escherichia coli*  
Eb1 – End binding protein 1  
ECL – Enhanced chemiluminescent substrate  
ECM – Extracellular matrix  
EDL – Extensor digitorum longus  
EDTA – Ethylenediaminetetraacetic acid  
EGF – Epidermal growth factor  
EGFR – Epidermal growth factor receptor

EGTA – Ethylene glycol-bis( $\beta$ -aminoethyl ether)-N,N,N',N'-tetraacetic acid

eIF4E – Eukaryotic translation initiation factor 4E

EMT – Epithelial to mesenchymal transition

ER – Endoplasmic reticulum

ER – Oestrogen receptor

Erk – Extracellular signal-regulated kinase

FAK – Focal adhesion kinase

FbCM – Fibroblast conditioned medium

FBS – Foetal bovine serum

FGF-2 – Fibroblast growth factor basic

FKBP – FK506 binding protein

FKBP12 – FK506 binding protein 12 (FKBP1A gene)

FKBP12.6 – FK506 binding protein 12.6 (FKBP1B gene)

FKBP25 – FK506 binding protein 25 (FKBP3 gene)

FKBP38 – FK506 binding protein 38 (FKBP8 gene)

FKBP51 – FK506 binding protein 51 (FKBP5 gene)

FKBP52 – FK506 binding protein 52 (FKBP4 gene)

FOXO1 – Forkhead box protein O1

GDP – Guanosine diphosphate

GFP – Green fluorescent protein

GR – Glucocorticoid receptor

GTP – Guanosine triphosphate

GTPase – GTP hydrolysis enzyme

HDAC – Histone deacetylase

HEPES - 4-(2-hydroxyethyl)-1-piperazineethanesulfonic acid

HER2 – Human epidermal growth factor receptor 2

hERG – human Ether-à-go-go-Related Gene

HIF1 $\alpha$  – Hypoxia inducible factor 1 alpha

HPA Axis – Hypothalamic pituitary adrenal axis

HR – Homologous recombination  
HSP90 – Heat shock protein 90  
IF – Intermediate filaments  
IGF – Insulin like growth factor  
IKK $\alpha$  – Nuclear factor  $\kappa$ B kinase  $\alpha$  subunit  
IL-2 – Interleukin 2  
ILK – Integrin linked kinase  
LARP6 – La-related protein 6  
LB – Luria broth  
LC3A – Microtubule-associated proteins 1A/1B light chain 3B  
LDS – Lithium dodecyl sulphate  
LN<sub>2</sub> – Liquid nitrogen  
MAP – Microtubule associated protein  
MAPK – Mitogen activated protein kinase  
MC – Methylcellulose  
MDM2 – Mouse double minute protein 2  
MDM4 – Mouse double minute protein 4  
Mdx – Murine muscular dystrophy  
MET – Mesenchymal to epithelial transition  
Mg – milligrams  
Mir2/3 – Micro RNA 2/3 (Active FKBP25 knockdown miRNA)  
miRNA/Mir – Micro RNA  
ml – Millilitre  
MLKL - Mixed lineage kinase domain like pseudokinase  
mM – Millimole  
MMP – matrix metalloproteinase  
MRF – Myogenic regulatory factor  
mRNA – Messenger ribonucleic acid  
MT – Microtubule

MTE – Myotenectionomy  
mTOR – Mammalian target of rapamycin  
MYF5 – Myogenic factor 5  
MyHC – Myosin heavy chain  
MyoD – Myoblast determination protein 1  
MyoG – Myogenin  
NaCl – Sodium chloride  
NADPH – Nicotinamide adenine dinucleotide phosphate  
NFAT - Nuclear factor of activates T cells  
NFκB – Nuclear factor kappa-light-chain-enhancer of activated B cells  
ng – Nanogram  
nm – Nanometre  
NT – Non targeting Mir  
OD – Optical Density  
P70s6-K – Ribosomal protein S6 kinase beta-1  
PA – Phosphatidic acid  
Pax – Paired box protein  
PBS – Phosphate buffered saline  
PFA – Paraformaldehyde  
PHLPP – PH domain and Leucine rich repeat Protein Phosphatases  
PI3K - Phosphatidylinositol-3-Kinase  
PINK1 – PTEN induced kinase 1  
PPIase – Peptidyl prolyl isomerase  
PR – Progesterone receptor  
PSF – Phenotypic stability factors  
PTEN – Phosphatase and tensin homolog  
PVDF – Polyvinylidene difluoride  
Rad51 – DNA repair protein RAD51  
Rad52 – DNA repair protein RAD52

Raf - Rapidly accelerated fibrosarcoma  
Rb – Retinoblastoma protein  
RBP – RNA binding protein  
RFP – Red fluorescent protein  
RFU – Relative fluorescence units  
RHEB – Ras homolog enriched in brain  
RhoA – Ras homolog family member A  
RIPA – Radioimmunoprecipitation  
RIPK1/3 - Receptor-interacting serine/threonine-protein kinases  
RMS – Rhabdomyosarcoma  
RNA – Ribose nucleic acid  
RPA – DNA replication protein A  
RPM – Rotations per minute  
RPMI – Roswell park memorial institute  
RTK – Receptor tyrosine kinase  
RyR – Ryanodine receptor  
SA – Synergist ablation  
SC – Satellite cell  
SDS – Sodium dodecyl sulphate  
SDS-PAGE – Sodium dodecyl sulphate polyacrylamide electrophoresis  
SF – Serum free medium  
SHH – Sonic hedgehog  
shRNA – Short hairpin RNA  
SMAD - Small mothers against decapentaplegic  
Sp1 – Specificity protein 1  
SR – Sarcoplasmic reticulum  
SRC – Proto-oncogene tyrosine-protein kinase Src  
SSA – Single strand annealing  
TA – Tibialis anterior

TBST – Tris buffered saline with tween-20  
TE – Tris EDTA  
TGF- $\beta$  – Transforming growth factor beta  
TM – Transmembrane domain  
TMN – Tumour node metastasis  
TNBC – Triple negative breast cancer  
TNF $\alpha$  - tumour necrosis factor alpha  
TPR – Tetracopeptide repeat  
TSC – Tuberosus sclerosis complex  
TSG – Tumour suppressor gene  
UV – Ultraviolet  
V/mV – Volts/millivolts  
v/v – Volume per volume  
VEGF – Vascular endothelial growth factor  
w/v – Weight per volume  
Wnt – Wingless/Int-1  
WT – Wild type  
WW domain – Tryptophan rich domain  
YY1 – Yin Yang 1

## Preface

This thesis aims to investigate and describe the functional roles of FKBP25 (FKBP3 gene), an FK506 binding protein that is comprised of two functional domains: a PPIase domain used to facilitate protein-protein interactions, and a basic tilted loop helix bundle domain that is required for nucleic acid binding. To date, there has been little research conducted that has examined the biological role of FKBP25 in any models. Previous unpublished research in our laboratory has focused on FK506 protein FKBP52 (FKBP4 gene), where it was identified that FKBP52 is associated with an increased metastatic phenotype both *in vitro* and *in vivo*. It was shown that loss of FKBP52 is associated with increased proliferation, anchorage dependent growth and microtubule instability (K.Waldeck PhD thesis 2008). In an effort to further characterise the expression of other FKBP proteins and their function in breast cancer, preliminary screens of assorted FKBP protein expression were conducted in a panel of breast cancer cell lines of various subtypes (Appendix 1).

Here it was first identified that FKBP25 was highly expressed in luminal and basal subtypes and expressed at comparatively low levels in mesenchymal subtypes. This led to the hypothesis that FKBP25 protein expression was associated with epithelial to mesenchymal transition, or rather the level of cellular differentiation. To comprehensively examine this hypothesis, it was decided that a second model of differentiation should be assessed. Upon investigation, it was found that FKBP25 was, in fact, expressed in the top 10% of the skeletal muscle proteome, this prompted the examination of FKBP25 in myogenesis. Myogenesis in this thesis is viewed as a process of mesenchymal to epithelial-like transition (MET), in which proliferative, mesenchymal-like myoblasts undergo a commitment or 'transition' to committed (or epithelial-like) myotubes. As such, the studies that are contained

within this thesis aim to describe the role of FKBP25 in EMT associated with breast cancer, and functions of breast cancer cells *in vitro*. Similarly, utilising the C2C12 myoblast cell line, the associated studies aim to examine the role of FKBP25 in the process of myogenesis as a model of MET. Together, these studies will be able to describe the roles of FKBP25 in cell proliferation and differentiation.

---

## Chapter 1: Introduction

---

### 1.1 Peptidyl prolyl-isomerase molecules

Peptidyl prolyl isomerases (PPIase) are a class of enzymes that facilitate the conversion of peptide bonds between proline residues and other amino acids from cis to trans conformations (**Fig 1.1**). The unusual conformation of the cyclic proline side chain leads to steric hindrance of the amino acid. However, this structure stabilizes the molecule in cis conformation. The conversion of cis to trans isomer is an energy consuming process which does not occur spontaneously and thus is a rate limiting step in protein folding. The presence of PPIase molecules is required to facilitate this conformational change in proline residues. PPIase molecules are ubiquitously expressed in both prokaryotic and eukaryotic cells, including parvulins, cyclophilins, and FK506 binding proteins.

### 1.2 Parvulins

Parvulin is a PPIase enzyme that is found in prokaryotic cells that shares no homology with mammalian PPIase molecules (1). Eukaryotic PPIase molecules include Pin1 and Par14. The structure of Pin1 consists of an N terminal WW (ligand binding domain containing two conserved tryptophan residues) domain that is required for protein-protein interaction, this region is linked to the catalytic PPIase domain by a flexible linker region (**Fig 1.2**). However, Par14 differs structurally with an N terminal basic domain linked to the catalytic PPIase domain. Pin1 is a well-researched eukaryotic parvulin molecule that is known to have roles in regulating proline-directed kinases, including extracellular receptor-regulated kinase (ERK), cyclin dependent kinases (CDKs), and glycogen synthase kinase-3 (GSK-3) (2-5). The interactions with these

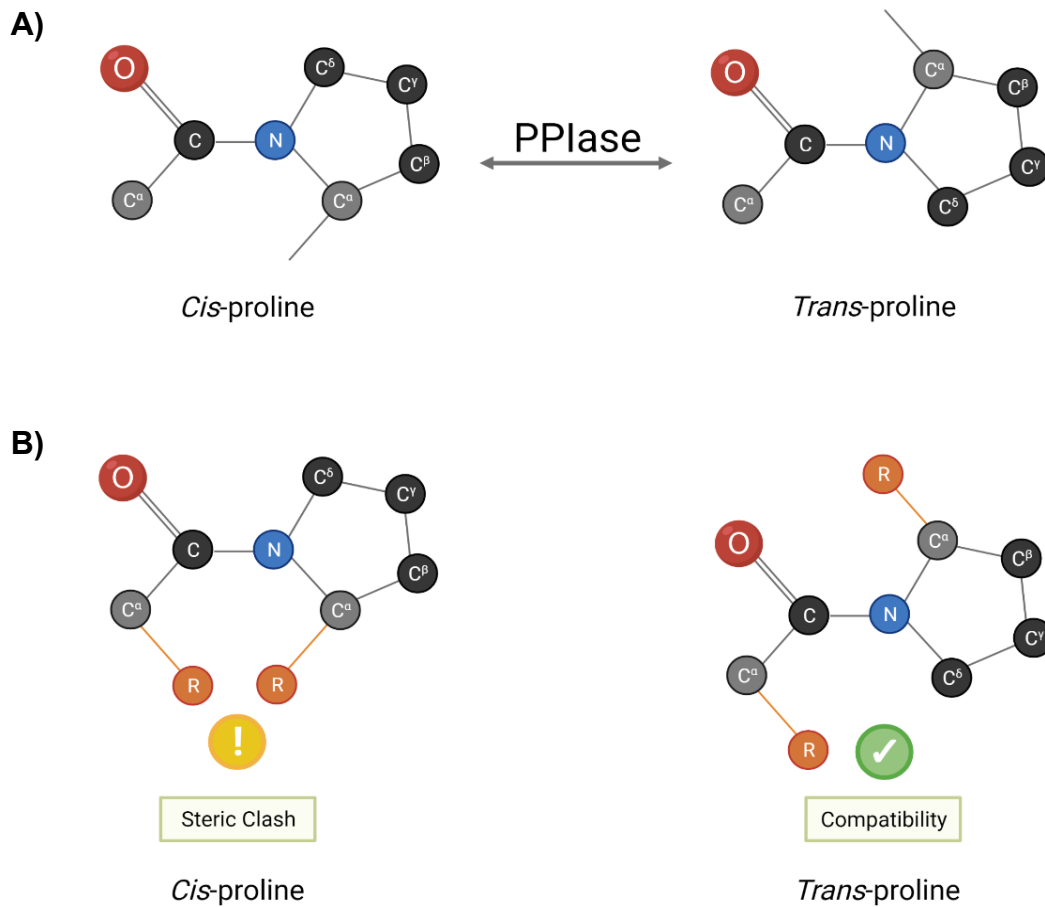


**Figure 1.1 : Conformation of proline residues in *cis* and *trans* conformations and visual description of steric hindrance**

A) Proline residues can exist in *cis* (left) conformation upon denaturation, or in some native states, however proline residues tend to exist in *trans* configurations. The *trans* (right) configuration prevents steric clashing of bound R-groups and subsequent disruption of secondary folding structures. PPlase molecules facilitate the isomerisation of proline residues from *cis* to *trans*, which would be an otherwise rate limiting step in protein folding. B) R-group binding to alpha carbons in the *cis* (left) conformation results in steric clashing of additional amino acids, which inhibits formation of peptide chains. Upon conversion to *trans* isomer (right) addition of amino acids can occur without hindrance. Made with Biorender.com.

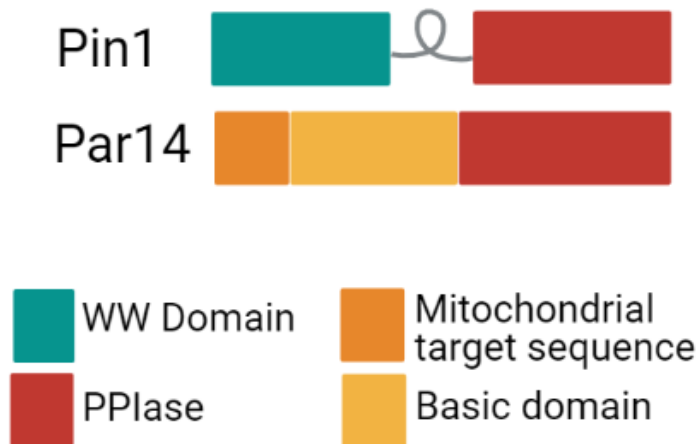


**Figure 1.2: Human parvulins molecular structure**

Human Pin1 contains a WW domain (Green) to aid protein binding linked to the PPlase site (Red) by a flexible linker region (Grey loop). Human Par14 contains a mitochondrial target sequence (Orange) followed by a basic domain that is required for DNA binding (Yellow), and an N terminal PPlase domain (Red). Made with Biorender.com.

molecules implicate Pin1 in cell proliferation and survival. Pin1 has influence over the cell cycle within each of the phases, including regulation of cyclin D expression, retinoblastoma protein (Rb) inactivation, p53 stabilization, and Cyclin E degradation (6-9). While in the G2/M transition, Pin1 is responsible for inhibition of CDC25 phosphatase activity that is required for activation of cyclin dependent kinases (10). Additionally, Pin1 is a transcriptional target of E2F. Upon overexpression of Pin1, Cyclin D1 expression is increased resulting in increased Rb phosphorylation and, thus, releasing bound E2F which can feedback and further increase Pin1 expression (11). Such that this positive feedback activates many cell growth and proliferation by increasing the stability of cyclin D and blocking activity of phosphorylated Rb (12). As such, overexpression of Pin1 has been associated with the progression of several cancers, including breast, ovarian and cervical (11, 13). The association of Pin1 with cancer progression is largely linked to its regulation of the cell cycle and stabilization

of proteins associated with cell cycle progression. Interestingly, Pin1 regulates the activity of protein phosphatase 2A, an important regulator of c-myc activity (14). c-Myc is a proto-oncogene and transcription factor that is also involved in cell cycle progression. Mutation to c-Myc results in abhorrent proliferation and, as such, is intricately linked to progression of human cancers. Other members of the parvulin family are not linked to cancer progression.

Par14 is a less characterised parvulin that exhibits a lower catalytic activity compared to Pin1 (15). It is known that Par14, and its isoform Par17, have some specific cellular compartment roles. Par14/17 act in both the cytoplasm and nucleus where they are associated with the mitotic spindle and ribosomal RNA processing (16, 17). In the nucleus, the N-terminal basic region of Par14 is responsible for DNA binding, DNA repair, and chromatin remodeling (18). Specifically, Par14 expression is increased approximately 3-fold during both S and M phases (19). The expression of Par14 is vital for cell cycle progression with blocking one or both of Pin1 or Par14 severely impairing cell proliferation (20). Despite these functions, Par14 has not been implicated in cancer development or progression.

### **1.3 Cyclophilins**

Cyclophilins are a second class of PPLase enzyme that are characterised based on their ability to bind to the immunosuppressant drug, cyclosporin A, hence their classification as immunophilin molecules. Cyclophilin binding to cyclosporin A results in inhibition of the phosphatase activity of calcineurin (CaN) in T lymphocytes, which results in inflammatory cytokine production (**Fig 1.3**) (21). There are many mammalian cyclophilin molecules, including cyclophilins A, B, C and D. These can be classified into single or multi domain cyclophilins (**Fig 1.4**) Cyclophilin A (CyPA) is the most well

characterised cyclophilin. In the absence of immune modulating drugs, CyPA is involved in protein folding of cell surface receptors, facilitating the tertiary structure of collagen, and intracellular protein trafficking (22-24). Interestingly, CyPA has been demonstrated to be secreted in response to inflammatory events such as endothelial dysfunction in early atherosclerosis.

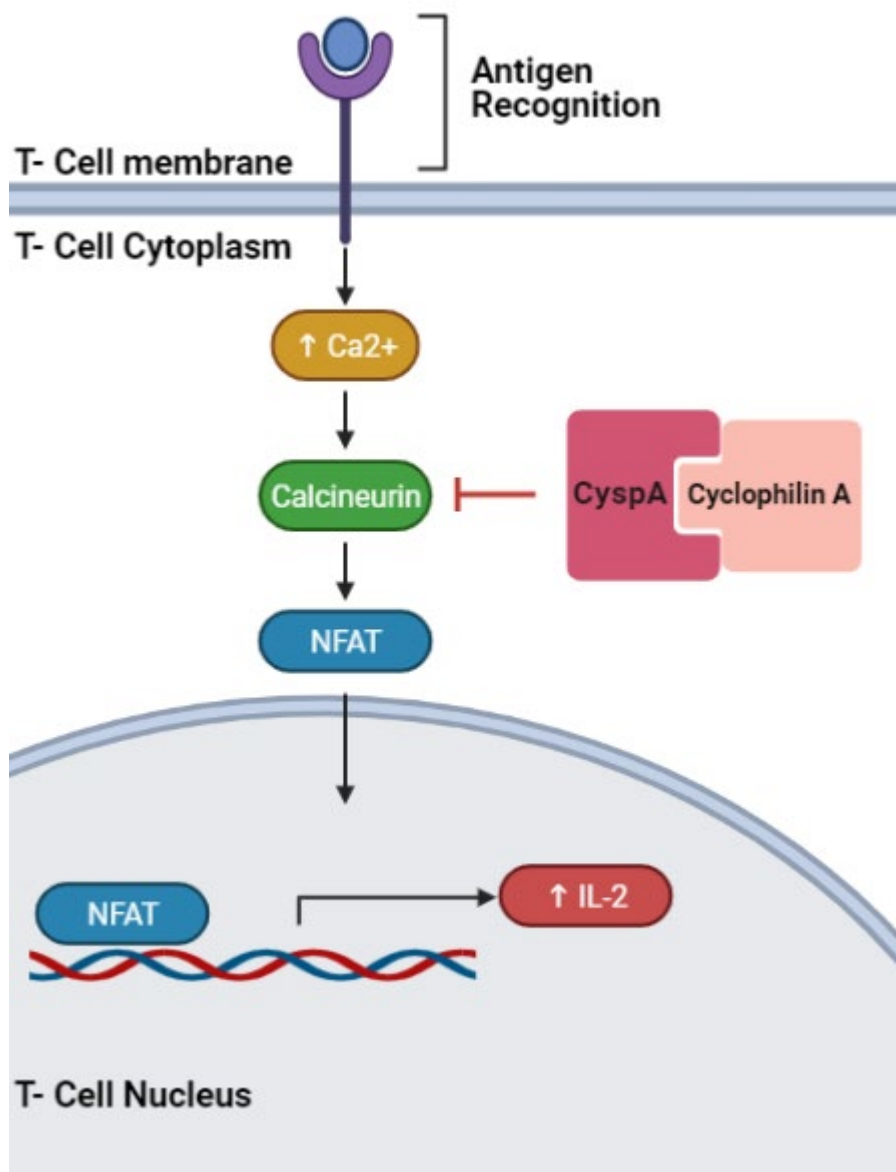


**Figure 1.3: Cyclosporin A facilitation of immune suppression**  
 Upon T cell antigen recognition an influx of  $\text{Ca}^{2+}$  activates calcineurin, a kinase enzyme that phosphorylates and activates nuclear factor of activated T cells (NFAT) resulting in interleukin-2 production and consequent amplification of the immune response. The complex formed by Cyclosporin A (CypA) and cyclophilin A act to inhibit the activity of calcineurin and thus suppress the immune response. Made with Biorender.com.

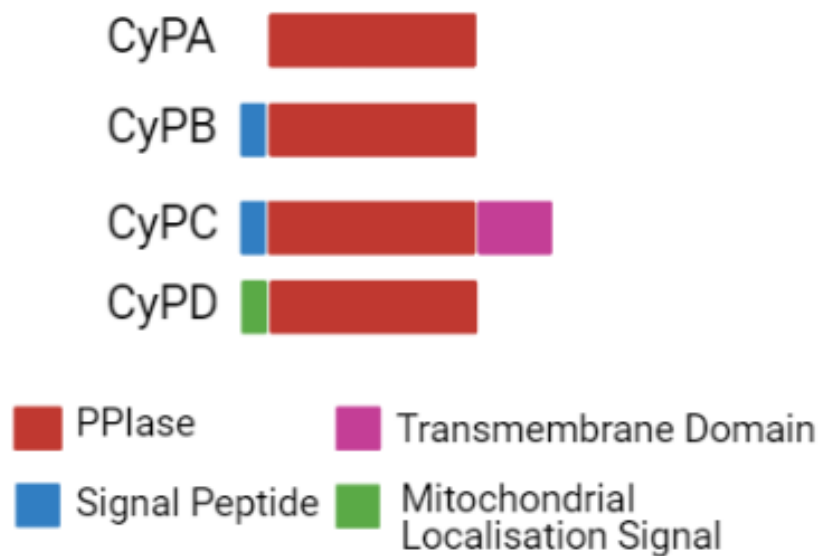


**Figure 1.4: Structural domains of Cyclophilin molecules**

Cyclophilin A consists of a single PPlase domain, known as a cyclophilin-like domain. Cyclophilins B and C contains an additional signal peptide domain that directs them to the endoplasmic reticulum (ER). Cyclophilin C contains an additional transmembrane domain for embedding in the ER. Cyclophilin D contains a mitochondrial localisation signal to allow localisation to the mitochondria. Made with Biorender.com.

CyPA is secreted from dysfunctional endothelial cells in response to the presence of reactive oxygen species to induce an inflammatory response to mitigate tissue damage (25). Furthermore, some studies have indicated that CyPA secretion stimulates cell growth and proliferation in response to damage. Specifically, exogenous CyPA was shown to activate ERK 1/2 phosphorylation and subsequent cell proliferation (26). Upregulation of CyPA has been associated with malignant transformation and cancer progression to metastasis (27, 28). In cancer cells, increased CyPA expression aids in increasing cell cycle progression and increasing overall cell proliferation (29, 30). Additionally, CyPA has been shown to block apoptotic

signals and promote migration via hypoxia inducible factor 1 $\alpha$  (HIF-1 $\alpha$ ) (31). Interestingly, CyPA transcriptional regulation has been shown to be facilitated by HIF1- $\alpha$  and tumour suppressor p53, which are two essential transcription factors required for cancer progression (32). The relationship between HIF1- $\alpha$ , p53 and CyPA is proposed to be a positive feedback loop. In this loop, the stressful environment that cancer cells survive in activates p53 and HIF1- $\alpha$  which then activate CyPA expression. Increased expression of CyPA, in turn, stabilizes p53 and leads to facilitation of proliferation and survival pathways. Further studies have demonstrated that knockdown of CyPA in lung squamous cell carcinoma results in significant reduction in tumour growth compared to controls (33). Similarly, CyPA knockdown in endometrial carcinoma cells caused a significant decrease in tumour volume over time via the induction of apoptosis (34). In addition to cancer, CyPA has been implicated in ageing, particularly in the epidermis irrespective of sun exposure (35). Furthermore, studies have found CyPA to be increased in the epidermis of aged people compared to young people, which may be linked to increased oxidative stress, and apoptosis (36). Conversely, there is evidence suggesting that CyPA expression was reduced cultured fibroblasts, which was associated with poor wound healing and metabolic impairment (37). Overall, the roles of CyPA are diverse and attribute to several essential cellular functions in addition to their classic role as an immunosuppressant binding molecule.

#### **1.4 FK506 Binding Proteins**

FK506 binding proteins (FKBP) are the final group of PPIase molecules. FKBP are a diverse family of immunophilin molecules that range in size and function (**Fig 1.5**). FKBP12 is a significant FKBP as it is involved in the mediation of immune suppression in complex with immunosuppressant drug, FK506 (Tacrolimus) (**Fig 1.6**) (38).

Additionally, FKBP12 is also able to bind to rapamycin (Sirolimus) and produce an immunosuppressant response, as well as inhibit the mammalian target of rapamycin (mTOR) mediated signaling (**Fig 1.7**) (39). All members of the FKBP family can bind to FK506 and rapamycin via their PPlase domain, FKBP12 has the highest binding affinity for these drugs (40). In addition to protein folding, FKBP's commonly function as protein chaperones. The various functions of each FKBP are dependent upon its structure and presence of functional domains (**Fig 1.5**).

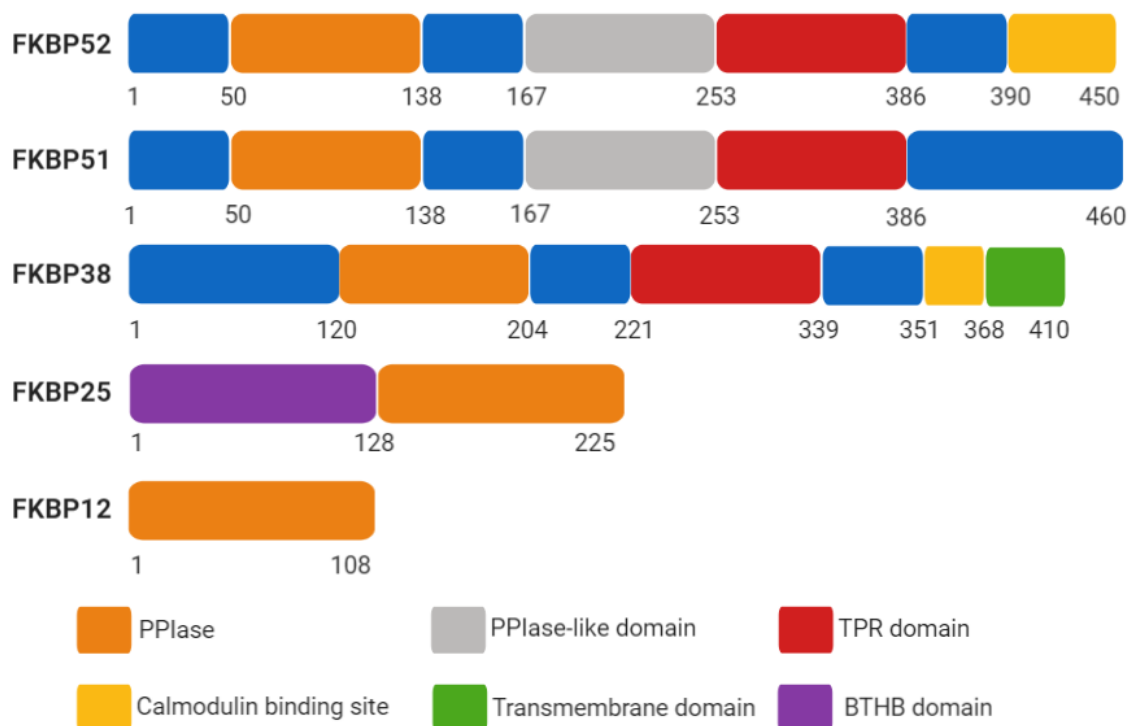


**Figure 1.5: Structural domains of FK506 binding proteins**

FK506 binding proteins tend to be larger than other PPlase molecules. High molecular weight FKBP's 52, 51 and 38 are composed of a PPlase and PPlase-like region to facilitate protein folding, in addition to a tetracopeptide repeat (TPR) domain to stabilise protein- protein interactions. FKBP52 and 38 also contain a calmodulin binding site which is proposed to modulate calmodulin activity. Low molecular weight FKBP25 is only composed of two domains, PPlase and a basic tilted helix bundle (BTHB) that is required for nucleic acid binding. The simplest of the FKBP's, FKBP12, simply contains a PPlase domain. Made with Biorender.com.

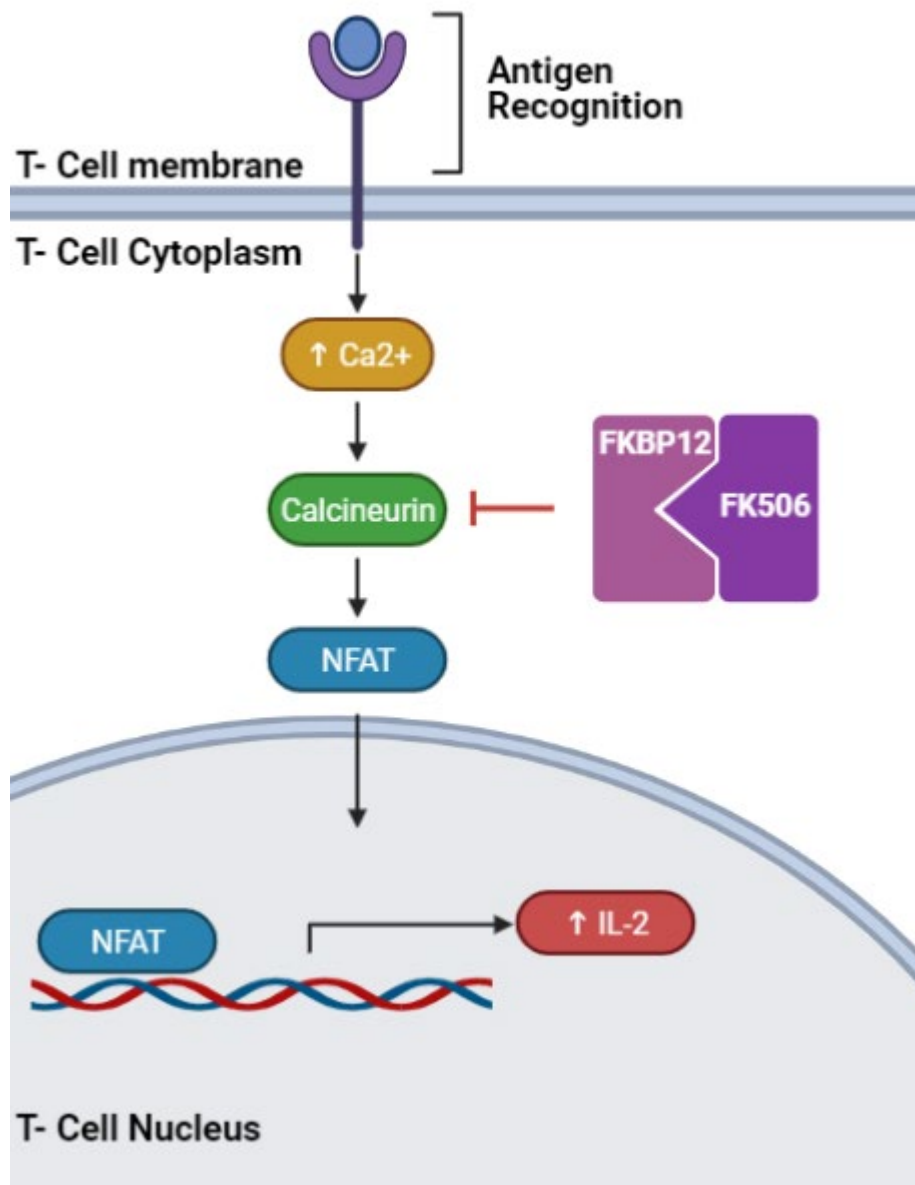


**Figure 1.6: FK506 mediated immune suppression**

Upon T cell antigen recognition an influx of Ca<sup>2+</sup> activates calcineurin, a kinase enzyme that phosphorylates and activates nuclear factor of activated T cells (NFAT) resulting in interleukin-2 production and consequent amplification of the immune response. The complex formed by FKBP12 and FK506 acts to inhibit the activity of calcineurin and thus suppress the immune response. Made with Biorender.com.

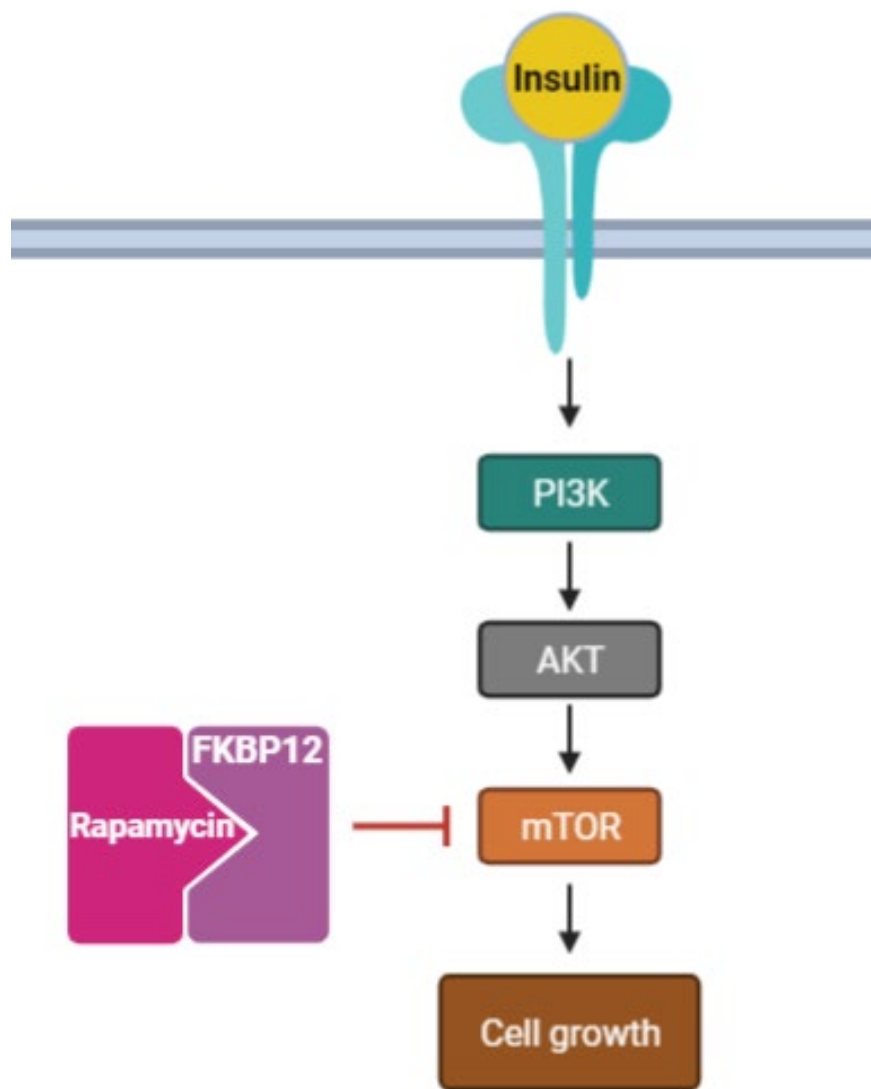


**Figure 1.7: FKBP12 and rapamycin inhibition of mTOR**  
Upon insulin binding to its receptor activation of PI3-kinase, AKT, and subsequent mTOR activation results in cell growth pathways. In the presence of rapamycin/FKBP12 complex mTORs kinase activity is inhibited causing inhibition of cell growth pathways. Made with Biorender.com.

## 1.5 FKBP12

The FKBP12 protein (*FKBP1A* gene) is comprised exclusively of the fundamental PPIase domain. Much of the previous literature has focused on the role of FKBP12 in complex with exogenous ligands (i.e. FK506 and rapamycin) and their combined effect. More recently, studies have focused on identifying the roles of FKBP12 in the absence of exogenous ligands and drugs. Interestingly, one such function of FKBP12 is association with the skeletal muscle ryanodine receptor (RyR) which is responsible for voltage-stimulated release of  $\text{Ca}^{2+}$  from the sarcoplasmic reticulum (SR) (**Fig 1.8**) (41). Upon binding to the RyR, FKBP12 has been demonstrated to enable channels to open faster and for longer periods of time. This is achieved by greater stabilization of the RyR tetramer, resulting in greater conductance required to open the voltage

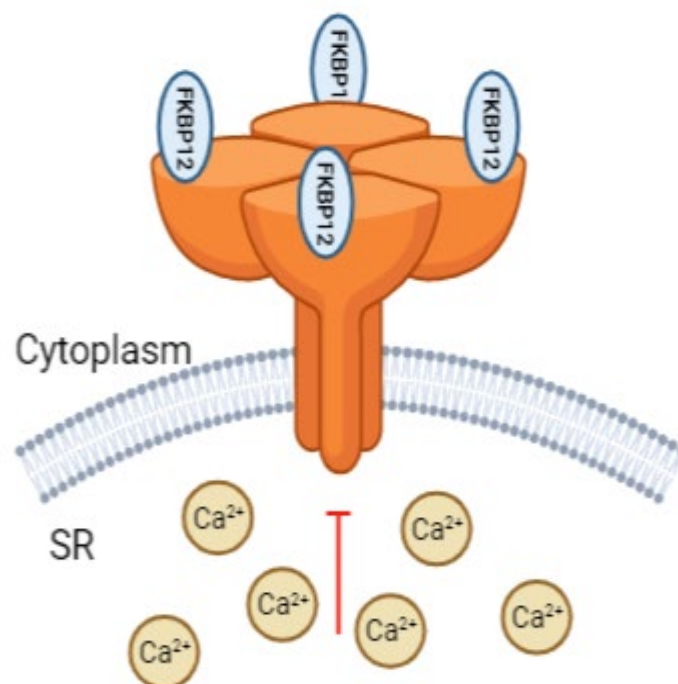


**Figure 1.8: FKBP12 stabilises the skeletal muscle ryanodine receptor**  
FKBP12 binds to the components of the ryanodine receptor (RyR) to prevent leakage of  $\text{Ca}^{2+}$  from the sarcoplasmic reticulum (SR). Made with Biorender.com.

gated channel (42), such that FKBP12 knockout animals have altered excitation contraction-coupling (43). Interestingly, an FKBP12 isoform, FKBP12.6 (*FKBP12B* gene), which differs structurally by 18 amino acids, has a binding preference for the cardiac muscle RyR2 receptor (44). It is proposed that there are 3 amino acids in FKBP12.6 that facilitate its preference for RyR2 (Gln31, Asn32, and Phe59 (45)). Regulation of the cardiac RyR2 channel is hypothesized to be dual controlled by both FKBP12 and FKBP12.6 in a feedback loop. It has been described that FKBP12 is able to activate the RyR2 and facilitate  $Ca^{2+}$  release, while FKBP12.6 antagonises FKBP12 action (46).

A second role of FKBP12 that has been described is stabilization of the transforming growth factor beta (TGF- $\beta$ ) receptor. Upon ligand binding to the type 2 TGF- $\beta$  receptor, it forms a dimer with a type 1 TGF- $\beta$ , leading to the a cascade of events that results in the phosphorylation of SMAD transcription factors which translocate to the nucleus and regulate genes involved in growth and proliferation (47). Rather than impact upon dimerization of the receptors, FKBP12 inhibits type 1 TGF- $\beta$  receptor mediated phosphorylation of the type 2 TGF- $\beta$  receptor (48). It is hypothesized that this function may be an adaptation to prevent leaky TGF- $\beta$  signaling, independent of ligand binding. Additionally, further research has demonstrated that FKBP12 is a regulator of the cell cycle, such that FKBP12 knockdown triggers enhanced intrinsic TGF- $\beta$  signaling and subsequent over expression of the cell cycle inhibitor, p21 (49). This suggests that FKBP12 must be required for inhibition of leaky TGF- $\beta$  signaling (**Fig 1.9**). Interestingly, FKBP12 has also been shown to induce chemotherapy-induced apoptosis by inhibiting p53 repressor mouse double minute protein 2 (MDM2) (50). MDM2 is an E3 ubiquitin ligase which acts to prevent p53 transcriptional activity, however, MDM4 is a regulator of MDM2's repressive activity (51). In this interaction,

FKBP12 can directly interact with MDM2 causing it to dissociate from its partner, MDM4, resulting in MDM2 auto-ubiquitination. The remaining free p53 can induce apoptosis in chemotherapy primed cells. Furthermore, FKBP12 has been revealed to play a role in instigation of necroptosis. Necroptosis is a controlled version of necrosis mediated by tumour necrosis factor alpha (TNF $\alpha$ ). This process depends on the activation of receptor-interacting serine/threonine-protein kinases 1/3 (RIPK1/3 (52)) and mixed lineage kinase domain like pseudokinase (MLKL (53)). FKBP12 was found to be indispensable for RIPK1/2 phosphorylation and formation of the necrosome (54). Overall, FKBP12 has a variety of functions in the absence of immune modulating ligands, primarily associated with receptor stabilization and regulating protein to protein interactions.

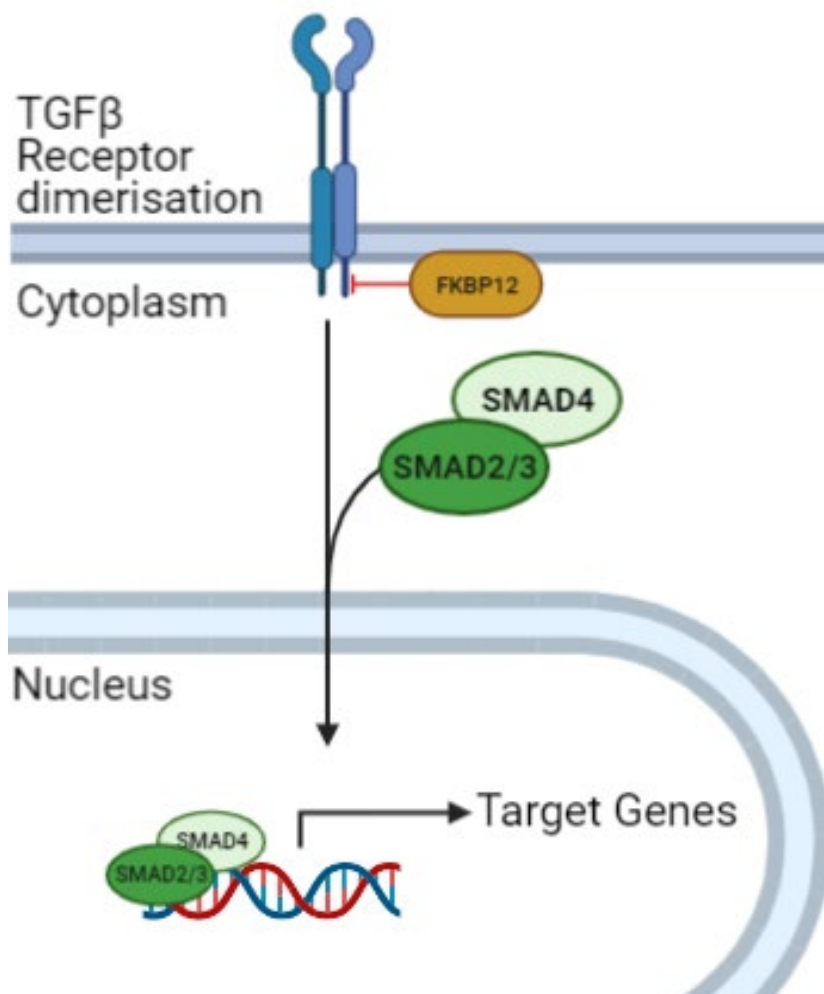


**Figure 1.9: FKBP12 stabilises the TGFβ receptor to prevent leaky signalling**  
 FKBP12 prevents spontaneous hetero dimerization of type 1 (left) and type 2 (right) TGFβ receptors. Thus, resulting in reduced leaky signalling and associated expression of target genes. Made with Biorender.com.

## 1.6 FKBP52

FKBP52 (*FKBP4* gene) is one of the largest and best characterised multidomain FKBP. The structure of FKBP52 is composed of a PPlase domain, PPlase-like domain, tetracopeptide repeat (TPR) domain, and calmodulin binding domain (See **Fig 1.5**). The PPlase domain of FKBP52 is required for its isomerase function,

however, unlike FKBP12, FKBP52 has no immunosuppressive function. This is due to one amino acid difference in the PPIase sequence of FKBP52 that makes it unable to bind and inhibit CaN (55). Similarly, the PPIase-like domain is unable to bind FK506 and has reduced PPIase activity compared to the primary PPIase domain (56). The PPIase-like domain contains an ATP/GTP-binding sequence which is required for a conformational change to enable binding to heat shock protein 90 (HSP90) (55). Importantly this region can be phosphorylated by casein kinase 2 (CK2) to prevent HSP90 binding (57). The HSP90/FKBP52 complex is a chaperone complex that is essential for intracellular trafficking of steroid receptors (**Fig 1.10**). The TPR domain of FKBP52 is required for the direct interaction with HSP90, however, HSP90 binding is also dependent on an unmodified PPIase region (58). At the C terminal of FKBP52 there is a putative calmodulin (CaM; a  $\text{Ca}^{2+}$ -sensitive second messenger) binding site. There is limited understanding of the function of this CaM binding site, however, it has been demonstrated that upon inhibition of the CaM binding site, FKBP52 has reduced client protein binding ability (59). FKBP52 is an important co-chaperone for hormone receptors, including the glucocorticoid receptor, progesterone receptor, oestrogen receptor, androgen receptor, and mineralocorticoid receptor (60-62). The most well described FKBP52/HSP90 interaction is that with the glucocorticoid receptor (GR). Activated GRs bind to the FKBP52/HSP90 complex which is shuttled to the nucleus, where genes containing a glucocorticoid response element are targeted for transcription (63). Shuttling of the FKBP52/HSP90/GR complex requires an interaction with the motor protein, dynein, which traffics the complex to the nucleus (64). This interaction is facilitated by a dual interaction with the PPIase and TPR domains of

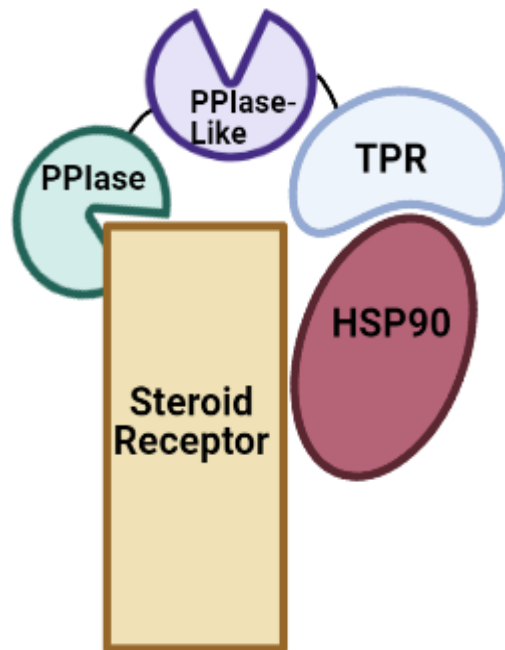


**Figure 1.10: FKBP52 interaction with steroid receptors**

FKBP52 interacts with HSP90 via its TPR domain and interacts with steroid receptors via its PPlase domain. While the PPlase-like domain does not physically interact with either client protein it is integral in maintaining the structural conformation required for these interactions. Post translational modification to the PPlase-like domain renders FKBP52 unable to bind to HSP90. Made with Biorender.com.

FKBP52. In addition to interacting with dynein, FKBP52 is a microtubule destabilising protein. FKBP52 binds to tubulin monomers via its TPR domain and subsequently prevents microtubule polymerisation. FKBP52 has been shown to colocalise with the mitotic spindle apparatus *in vitro*, and its knock down has been associated with a reduction in the growth of neural projections (65, 66). In addition to the GR, FKBP52 is known to interact with the progesterone receptor (PR) and oestrogen receptor (ER) (60, 67). The interactions with these receptors have linked FKBP52 to breast cancer pathogenesis.

Breast cancer cells are known to over express ER and consequently undergo increased proliferation which is strongly correlated to carcinogenesis (68, 69). It has been previously described that FKBP52 is expressed at different levels in normal breast tissue compared to breast carcinoma tissue (70). This is further supported by an *in vitro* study that has demonstrated that FKBP52 mRNA expression is increased in response to treatment with oestradiol (71). Interestingly, FKBP52 protein expression has been identified to be a marker of therapeutic responses to neoadjuvant therapies in breast cancer patients. Upon immunohistochemical analysis tumour samples identified as either drug sensitive, or drug resistant, it was found that FKBP52 was expressed in the cytoplasm of drug resistant tissues (72). This study suggests that FKBP52 expression may be a viable predictor of therapeutic resistance to microtubule stabilising agents such as paclitaxel as neoadjuvant therapy. A recent study has provided additional consolidation of the role of FKBP52 in breast cancer pathogenesis based upon traditional tumour-node-metastasis (TNM) cancer grading system. Specifically, increased FKBP52 mRNA expression is correlated with higher grading and worse outcomes and indicating that FKBP52 may be a viable biological marker (73). Currently there is limited research into the mechanism by which FKBP52 progresses cancer pathology. However, there is ample research suggesting that there is an intrinsic link between FKBP52 expression, cancer outcomes and cancer biology.

## **1.7 FKBP51**

FKBP51 (*FKBP5* gene) is structurally similar to FKBP52, consisting of the same domains with the exception of the calmodulin binding domain. While these proteins are structurally similar, they have several independent roles. One of the classic roles of FKBP51 is its function as a HSP90 binding protein which occurs via the TPR domain with additional stabilisation provided by amino acid interactions at the distal C-terminus

(74, 75). FKBP51 is well known to chaperone the GR within the cytoplasm of the cell. Unlike FKBP52, FKBP51 has reduced ability to translocate into the nucleus. As such, chaperoning of the GR is passed onto FKBP52 when nuclear translocation must occur (76). It has been demonstrated that GR bound to FKBP51 have reduced nuclear translocation which is likely due to FKBP51's reduced affinity for dynein compared to FKBP52 (77). A role of FKBP51 that occurs independently of FKBP52 is its association with anxiety disorders. It is hypothesised that hyperactivity of the hypothalamic–pituitary–adrenal (HPA) axis is intimately linked with the pathology of stress-related disorders. FKBP51 is responsible for chaperoning of the GR, and interestingly, FKBP51 itself is modulated by GR activation itself which inhibits FKBP51 expression, resulting in a negative feedback loop in target tissues (78, 79). FKBP51 is linked to other physiological aspects of neurological function, including synaptic transmission. It has been demonstrated that FKBP51 knockout mice had reduced long term potentiation between nerve synapses, which is indicative of neurological function and disease development, including depression (80). Another receptor that FKBP51 is intricately linked to its expression is the androgen receptor (AR) (81). Unlike its role in regulating the GR, FKBP51 is a positive regulator of AR signalling. FKBP51 is required for adequate AR signalling and transcription of AR related genes, such that FKBP51, but not FKBP52, knockdown impaired AR activity (82). Interestingly, the *FKBP5* gene itself contains an androgen responsive element (ARE) which provides a further positive feedback loop (83). This is further consolidated by studies that have examined FKBP51 overexpression in prostate cancer cells where it was found that there was increased ARE activation and increased prostate-specific antigen produced (84).

FKBP51 is also involved in the regulation of protein signalling pathways that are androgen independent. The first protein that has been demonstrated to be influenced

by FKBP51 is nuclear factor kappa-light-chain-enhancer of activated B cells (NFκB) (See **Fig 1.11**). NFκB is a protein complex transcription factor that is involved in DNA transcription, immune responses, and cell survival (85), and is rapidly activated by stress responses (i.e., UV radiation, chemotherapy, reactive oxygen species (86)). FKBP51 has previously been shown to interact with inhibitor of nuclear factor IκB kinase α subunit (IKKα), suggesting that FKBP51 may be able to influence this pathway (87). This was further supported by a study that demonstrated that in the presence of rapamycin there was an FKBP51-mediated increase in NFκB signalling that sensitises chemotherapy-treated cells to apoptosis (88, 89). Interestingly, FKBP51 has also been demonstrated to be involved in regulation of cell survival regulator, Akt, which is a known activator of NFκB activity (90). Specifically, FKBP51 has been shown to be a negative regulator of Akt activity (See **Fig 1.11**). It is proposed that FKBP51 acts as a scaffold holding Akt, and its negative regulator PH domain and Leucine rich repeat Protein Phosphatases (PHLPP), to enhance dephosphorylation of Akt serine 473 residue causing reduced enzymatic activity. Knock down of FKBP51 resulted in hyperphosphorylation of Akt and subsequent impairment of apoptosis induction (91). A recent study has proposed that these pathways are, in fact, linked via FKBP51. Specifically, Shang et al., described a PHLPP/FKBP51/IKKα complex that is competitively inhibited by long non-coding RNA (92). Displacement of FKBP51 from this complex enables PHLPP to dephosphorylate Akt, and free IKKα to inhibit NFκB in castration resistant prostate cancer. The mechanistic roles of FKBP51 have been implicated in cell biology and pathology alike and highlight the diverse nature of FKBP functions.

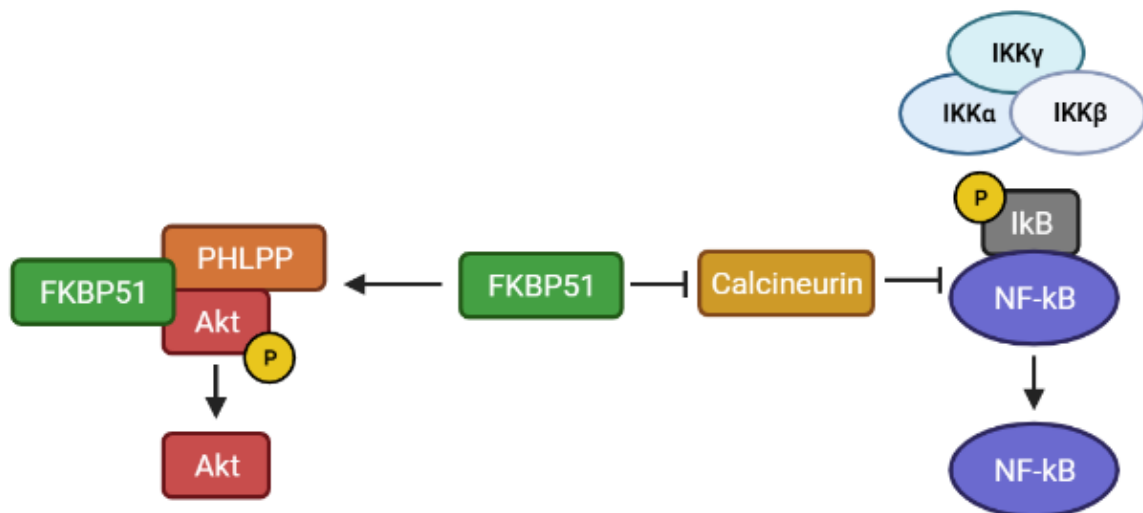


**Figure 1.11: FKBP51 regulates Akt and NF-κB signalling**  
 FKBP51 bridges the scaffold between PHLPP with Akt, resulting in enhanced Akt phosphorylation. FKBP51 also modulates NF-κB signalling by binding to IKK mediated IκB phosphorylation and subsequent NF-κB activation. FKBP51 also interacts with CaN and inhibits calcineurin dependent dephosphorylation of IκB. Adapted from Tong and Jiang, 2015, *Curr. Mol. Pharmacol.*

## 1.8 FKBP38

FKBP38 (*FKBP8* gene) is another multidomain protein that consists of both PPlase, PPlase-like, and TPR domains. Similarly, to FKBP52, FKBP38 contains a putative CaM binding domain (See **Fig 1.4**). However, FKBP38 is the only FKBP that contains a C-terminal transmembrane domain (TM). The TM domain is an essential component of FKBP38 that enables it to be anchored into the membrane of the rough endoplasmic reticulum (ER) (93). Within the lumen of the ER, FKBP38 is stabilised by HSP90 via the TPR domain. This interaction is required for the role of FKBP38 in protein folding and chaperoning of ion channels, including HERG, the alpha subunit of the voltage-dependent delayed rectifier potassium channel (94). Similarly, FKBP38 is involved in

stabilising the Cystic fibrosis transmembrane conductance regulator (CFTR) (93, 95). Interestingly, FKBP38 has recently been implicated in the induction of apoptosis from ER-related proteotoxic stress (96). FKBP38 is also known to be anchored to the mitochondrial membrane (97). Within the mitochondria, FKBP38 associated with anti-apoptotic proteins, B cell lymphoma-2 (Bcl-2) and B-cell lymphoma extra-large (Bcl-XL) (98), such that FKBP38 overexpression blocks apoptosis and blocking FKBP38 induced apoptosis. This is hypothesised to be due to FKBP38 anchoring these anti-apoptotic proteins to the inner mitochondrial membrane (97). Furthermore, FKBP38 has been associated with a mitochondrial localised form of macro-autophagy known as mitophagy. Autophagy is a self-eating process that cells undergo to remove dysfunctional components and to recycle cellular constituents. This process is mediated by autophagy-related proteins (ATGs) and lysosomal digestion (99). Other essential proteins in the execution of mitophagy are LC3A (Microtubule-associated proteins 1A/1B light chain 3B), PTEN-induced kinase 1 (PINK1) and Parkin.

FKBP38 has been demonstrated to be involved in recruiting LC3A and inducing Parkin-independent mitophagy (100). Interestingly, while FKBP38 is involved in initiating mitophagy, it is translocated to the ER upon mitophagy induction, and thus avoids degradation (101). This process enables FKBP38 to be recycled for ER protein stabilisation roles and prevent apoptosis mediated by proteotoxic stress. Another role of FKBP38 is the regulation of Ras homolog enriched in brain (RHEB), Tuberous sclerosis complex (TSC) and downstream mTOR signalling (**Fig 1.12**). The current literature does not reach a consensus on the function of FKBP38 in relation to mTOR signalling, with several studies reporting opposing data, which may be related to differing models that have been utilised. Previously, it was demonstrated that FKBP38 is required for TSC-dependent cell size regulation, which results in upregulation of

mTOR signalling (102). This is contradicted by data proposing that FKBP38 is an endogenous inhibitor of mTOR, and that FKBP38 is antagonised by Rheb to prevent the inhibition of mTOR (103). The hypothesis that FKBP38 inhibits mTOR is further supported by a study that has shown that silencing of FKBP38 activated mTOR and its associated signalling effectors: ribosomal protein S6 kinase beta-1 (p70S6K1), and eukaryotic translation initiation factor 4E (eIF4E)-binding protein 1 (4E-BP1) (104). This is further endorsed by data demonstrating that phosphatidic acid (PA), a mediator of mTOR activation, competes with FKBP38 for mTOR binding allowing allosteric stimulation of mTOR activity (105). Remarkably, Bcl-2 and Bcl-XL have also been revealed to compete with FKBP38 for mTOR activation (106). It was shown that upon respective Bcl-2 and Bcl-XL knockdown there was a corresponding reduction in phosphorylation mTOR effectors p70S6K1 and 4E-BP1. FKBP38 exerts many effects on mTOR and cell death pathways, including apoptosis and mitophagy. These effects lend important information to both cell biology and disease pathogenesis.

## 1.9 FKBP25

FKBP25 (*FKBP3* gene) is a dual domain FKBP, consisting of a C-terminal PPIase region and an N-terminal basic tilted helix bundle (BTHB) region. Similarly, to other members of the FKBP family, FKBP25 can bind both FK506 and rapamycin. Interestingly, FKBP25 has been shown to have a binding preference for rapamycin (107). However, here we are interested in understanding the roles of FKBP25 in the absence of these ligands. Upon solving the protein structure of FKBP25 it was found that the PPIase domain is required for protein binding activity and the BTLB is

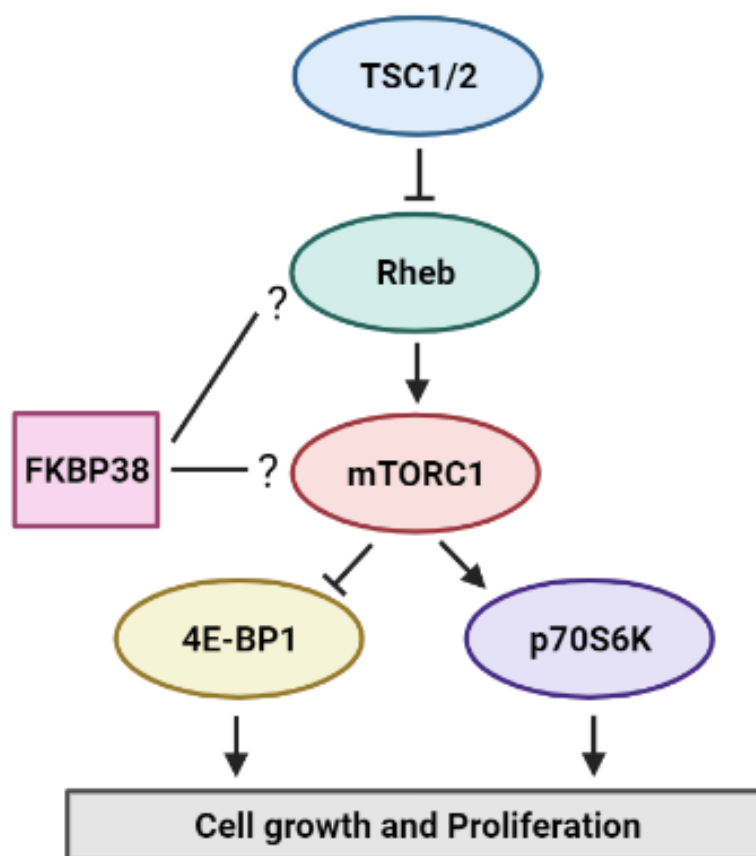


**Figure 1.12: FKBP38 implication in mTORC1 signalling**  
Activation of TSC inhibits Rheb, which in turn activates mTORC1. Activation of mTORC1 inhibits 4EBP1 and activates p70S6K, resulting in cell growth and proliferation. Made with Biorender.com.

necessary for nucleic acid binding (108). In contrast to other FKBP25s, FKBP25 is known to interact directly with DNA and RNA via its BTHB (109-111), however, it has been demonstrated to have a binding preference for double stranded RNA (dsRNA) oligonucleotides (112). Furthermore, the functions of the PPlase and BTHB regions appear to occur independently upon dsRNA binding. Additionally, FKBP25 has been shown to interact with the pre-60S ribosomal subunit (110). Here it was demonstrated that FKBP25 interacts with a variety of ribosomal proteins and processing factors, such as nucleolin. Importantly, it has been shown that FKBP25 is able to translocate to the nucleus upon stress events (113). Nucleolin is a major nucleolar protein in eukaryotic cells that is known to interact with histones and to induce decondensation of nucleolar chromatin (114). This interaction of FKBP25, nucleolin, and the pre-60S ribosomal subunit, is hypothesised to be required to chaperone the components of the large ribosomal subunits and facilitate ribosomal RNA processing.

While FKBP25 has been shown to have a binding preference for RNA, it also plays an integral role in DNA double-strand break (DSB) repair (111). DSBs can be repaired using one of two DNA repair mechanisms, homologous recombination (HR) or single-strand annealing (SSA). HR is a process that involves end processing of damaged DNA strands by HR associated protein Rad50, and strand invasion facilitated by Rad51 (115). Upon HR, damaged DNA is initially processed by DNA replication protein A (RPA) and Rad52 to resect the 3' and 5' ends at the damage site. Next, BRCA2 (Breast Cancer susceptibility protein 2) delivers Rad51 to the damage site, the DNA strands become inverted and homologous repair can begin. Here, non-damaged dsDNA is utilised as a template for repair synthesis of damaged DNA (**Fig 1.13**). Cells that are depleted of FKBP25 exhibit reduced Rad51 foci in response to double stranded breaks induced by UV (ultraviolet) light exposure. Interestingly, FKBP25 was

also demonstrated to suppress SSA by reducing expression of SSA-associated protein, Rad52 (111, 116). It appears that SSA is the preferred DNA repair mechanism in cancer cells, which may be due to the presence of BRCA mutants hindering sufficient HR (117). SSA is known to be associated with greater error incidence than other DSB repair pathways, resulting in an accumulation of somatic mutations, and as such is associated with oncogenic transformation (117, 118). FKBP25 is also known to interact with the transcription factor, p53, and p53 repressor mouse double minute protein 2 (MDM2). It was shown that FKBP25 instigates degradation of MDM2 to enable p53 activation, which may be important in the role of FKBP25 in facilitating DSB repair (119). However, this role has not been investigated in a cancer setting where p53 is mutated. Furthermore, studies have also identified FKBP25 and tubulin-associated oncoprotein, stathmin/Op18, to be reduced upon p53 induction (120). Interestingly, FKBP25 had been demonstrated to be a bona fide microtubule-associated protein that is involved in stabilising tubulin polymers (**Fig 1.14**).

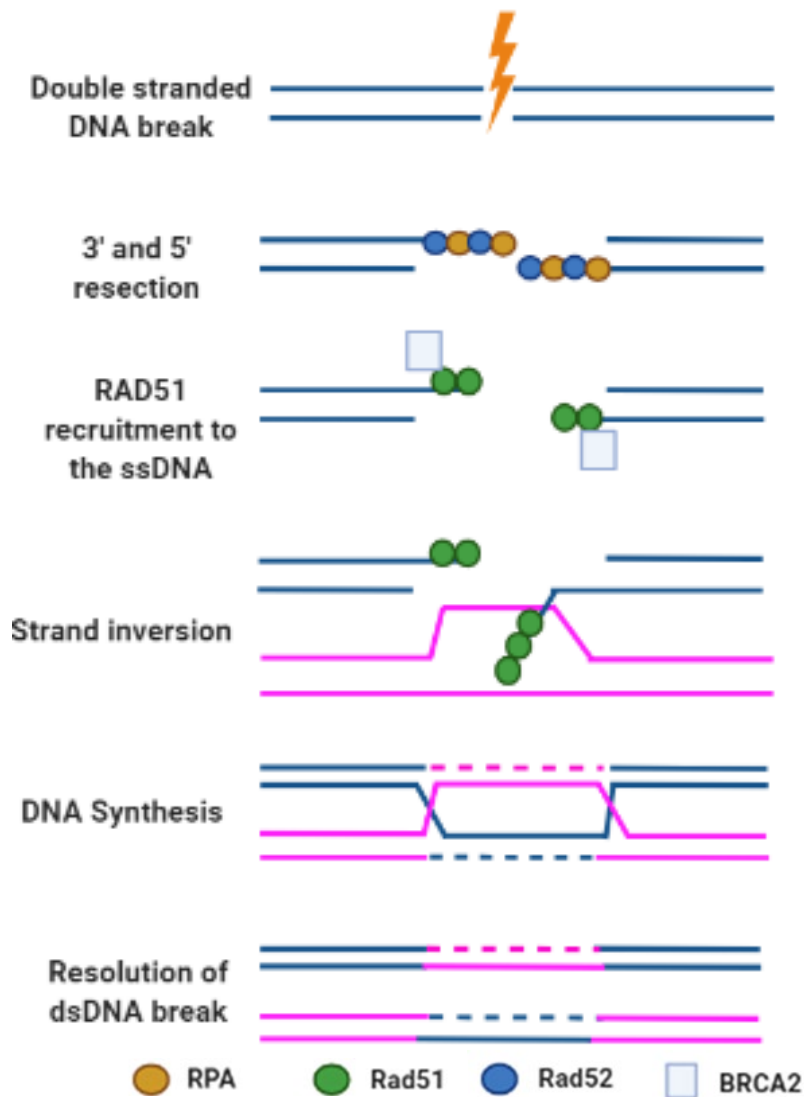


**Figure 1.13: Double stranded DNA break repair**  
 Repair of a double stranded DNA break requires resection of the 3' and 5' ends of the damage site mediated by replication protein A (RPA) and Rad 52. Rad51 is recruited to the resected ends by BRCA2 to initiate strand invasion, ligation, and DNA synthesis to repair the break. The product is a hybrid of the damaged DNA (blue) and undamaged template DNA (pink). Made with Biorender.com.

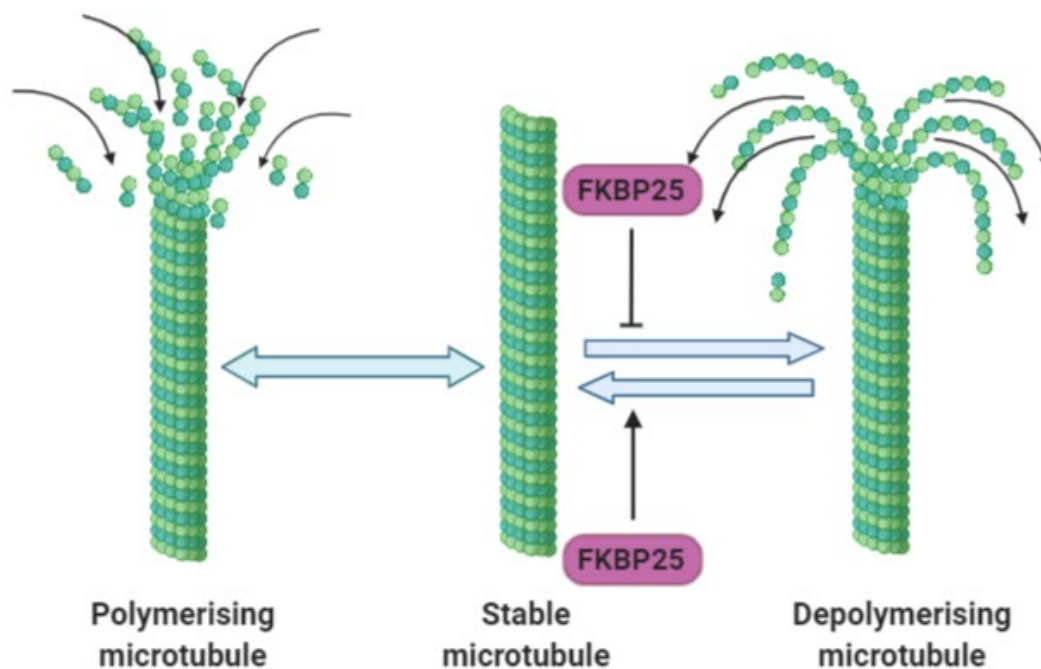


**Figure 1.14: FKBP25 is a microtubule stabilising protein**

FKBP25 is a microtubule (MT) associated protein that is required for stabilisation of MT polymers. The PPlase domain of FKBP25 is required for its interaction with tubulin polymers and has been demonstrated to be involved in stabilisation of the microtubule assemblies, including the mitotic spindle. Made with Biorender.com.

Loss of function studies have found that, in the absence of FKBP25, there are several cellular defects, including multiple nuclei and the presence of micronuclei, due to decreased stability of the mitotic spindle (109). This function was further investigated by Wang and colleagues and it was identified that depletion of FKBP25 resulted in abnormal, aneuploid oocytes, due to defective spindle-kinetochore interactions (121). These diverse roles of FKBP25 in cell biology and function have the capacity for implications in cancer pathogenesis and require further research.

## **1.10 The roles of FKBP5s in cancer pathogenesis**

### **1.10.1 FKBP5s in hormone receptor expression**

Multidomain immunophilins, FKBP51 and FKBP52, have been extensively researched regarding their role in the HSP90 chaperone complex (reviewed in (122)). The HSP90 chaperone complex is a protein complex that is responsible for a plethora of cellular functions that can lead to pathogenic changes in cancer. Of specific interest, FKBP51 and FKBP52 are intricately involved in the expression of hormone receptors (including ER, PR, and AR) in hormone receptor positive cancers, including breast and prostate cancers (67, 81). FKBP52 has been consistently demonstrated to be expressed at increased levels in ER+ breast cancer tissue and cells compared to that of normal tissue (73, 123). Increased expression of ER in breast cancer tissues results in increased proliferation of mammary tissues (124). In conjunction with other mutations that must occur to progress to an oncogenic phenotype, such as mutations to oncogenes and tumour suppressor genes, there is increased risk of cancer progression to metastatic disease (125). Similarly, FKBP52 has also been demonstrated to be shown to be involved in modulating AR activity (126). Specifically, it was found that upon inhibition of AR binding to the FKBP52-HSP90 complex there was a significant reduction in AR nuclear translocation and subsequent AR-related gene expression (127). Interestingly, FKBP52 is accepted as a positive regulator of steroid receptor expression, while FKBP51 is a negative regulator (77, 128). A notable exception of FKBP51's role as a negative regulator of steroid receptor expression is its affinity for the AR (81). In fact, FKBP51 has been shown to be expressed in an androgen-dependent manner (83), such that knockdown of FKBP51 protein expression resulted in reduced androgen dependent signalling (82). Considering the relationship between these FKBP5s and cancer progression there is some merit in

pharmacologically inhibiting these molecules. This could be accomplished either directly to inhibit FKBP-receptor interaction, or the FKBP-HSP90 interaction. A novel inhibitor of FKBP52, MJC13, which acts by preventing FKBP52 binding to the AR in prostate cancer cells by inhibiting the interaction between the AR and the FKBP52-HSP90 complex (127). Furthermore, this small molecule inhibitor was demonstrated to antagonise AR dependent gene expression and proliferation (127). Similarly, rapamycin has been demonstrated to occupy the PPIase domain of FKBP51 in prostate cancer cells and result in reduced AR-dependent signalling pathways (79). These data suggest that targeting FKBP5s in hormone dependent cancers may be a viable therapeutic option.

### 1.10.2 FKBP5s in cell death regulation

FKBP5s have also been demonstrated to be involved in regulating cell death pathways, including apoptosis and necroptosis. Cancer is a disease in which cell growth and proliferation outweighs cell death, as such, evasion of apoptosis is a key hallmark of cancer (129). Apoptosis is mediated by pro-apoptotic mediators (including BAX, BID, BAK, and BAD) and inhibited by antiapoptotic factors (Bcl-XL and Bcl-2). Proapoptotic homodimers are required to permeabilise the outer mitochondrial membrane which leads to initiation of the intrinsic apoptosis pathway (130). The intrinsic apoptotic pathway involves the release of cytochrome C from the mitochondria, activation of apoptotic protease activating factor 1 (Apaf-1) and generation of the apoptosome that mediates pro-caspases (caspase 9) cleavage, resulting in activation of pro-caspase 3 to initiate apoptosis (131). The presence of proteins that can prevent the induction of apoptosis are of interest in cancer progression. Mitophagy is an organelle specific form of autophagy, a controlled self-digestion process that involved fusion of lysosome to membrane bound targets (132). Specifically, FKBP38 has been shown to recruit

autophagy marker, LC3A, to the outer mitochondrial membrane resulting in increased mitophagy (133). Furthermore, it was demonstrated that upon induction of mitophagy, FKBP38 no longer colocalised to the mitochondria, but translocated to the ER (133, 134). While it has not been specifically shown, it is hypothesised that FKBP38 is likely to be involved in evasion of apoptosis and subsequent cancer propagation (135). Similarly, FKBP12 has been demonstrated to coordinate the formation of the necrosome, a complex of necroptotic proteins MLKL, RIPK1, and RIPK3 (54). Necroptosis has been demonstrated to have both pro- and anti- tumour effects depending on the expression of necroptosis-related proteins (136). Specifically, increased levels of RIPK1 protein and RIPK3 are associated with poor prognosis in pancreatic ductal carcinoma (137). However, reduced levels of MLKL have been correlated to poor patient outcomes in reproductive cancers (138, 139). The alterations of the expression of these proteins have been associated with chronic inflammation which is known to contribute to carcinogenesis (140, 141). Unpublished data from our laboratory has shown that FKBP12 is highly expressed in triple negative breast cancer cell lines, including MDA-MB-231, Hs578t, and BT-549 cells, while previous research shows that RIPK3 is positively correlated with triple negative and basal-like breast cancers, indicating an increased necroptotic capacity (142). This proinflammatory environment facilitates a cancer progression and advancement to metastatic disease (143). FKBP's may present an opportunistic target for therapies that aim to redirect cells to programmed cell death pathways.

### 1.10.3 FKBP's in microtubule stability

The cytoskeleton is a dynamic network consisting of three main components, microfilaments, intermediate filaments (IF), and microtubules (MT) (See **Fig 1.15**) (144). Each of these components are capable of rapid growth and disassembly to

mediate cell functions, including migration, cell division, intracellular trafficking (reviewed in (145)). Microfilaments are polymers composed of globular actin monomers that can push against a barrier, such as the cell membrane, to facilitate cell movement (146). Actin remodelling is a feature in epithelial to mesenchymal transition (EMT) that contributes to metastatic progression of cancer cells (147). It has been demonstrated that EMT induction rapidly activates RhoA, a GTPase that is involved in modulating actin organisation (148). Comparably, IFs are intricately linked to EMT in cancer cells (149). IFs are an essential component of the cytoskeleton that provide support to the plasma membrane and maintain cell shape (150). There are 6 subgroups of IFs that are specifically expressed in different types of tissues (151). Furthermore, the transition from one type of IF to another is considered a marker of EMT (152). The most notable IF transition that has been studied in the context of cancer is the expression of vimentin in epithelial cells (153). Vimentin is a typical IF that is expressed in mesenchymal cells, such as fibroblasts (154, 155). The transition to vimentin from epithelial IFs, such as keratins (156), has many implications for cell behaviours, with the transition to vimentin filaments being associated with a change in nuclear shape, loss of cell-to-cell adhesions and increase focal adhesion dynamics (157, 158). The final component of the cytoskeleton is the MT network, composed of alpha and beta tubulin dimers that form MT polymers (159). MTs are an essential component of the cytoskeleton that play roles in cell structural support, intracellular transport, motility and chromosome separation during mitosis (160). MTs are a dynamically instable polymer, meaning that they are constantly growing and disassembling at either end of the polymer (161). This feature of MTs is exploited by MT targeting drugs including taxanes (paclitaxel and docetaxel (162)) and vinca alkaloids (vincristine and vinblastine (163)). In principle, MT targeting drugs are mitotic

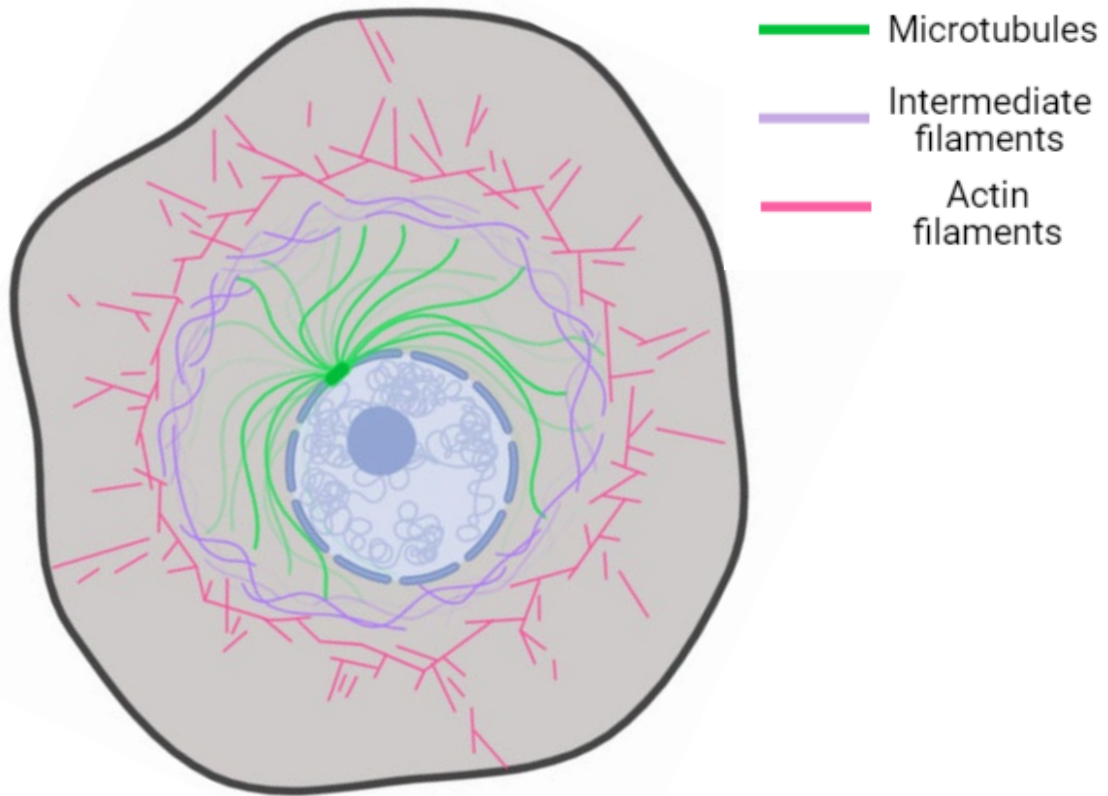


**Figure 1.15: Structure and components of the cytoskeleton**

The cytoskeleton is composed of 3 components. Microtubules (green) – mitotic spindle formation and intracellular transport; intermediate filaments (purple) – maintain cell shape and provide structural support; and actin filaments (pink) – cell motility and maintenance of cell shape. Made with Biorender.com

inhibitors that act by stabilising GDP-bound tubulin, which would normally be prone to depolymerisation (taxanes) or conversely, inhibiting tubulin dimers from polymerising into MTs (vinca alkaloids) (164, 165). The expression of selected MT-associated proteins (MAPs) has been linked to taxane resistance in cancer cells (166-168). Interestingly, FKBP52 and FKBP25 are known MT-associated proteins that destabilise and stabilise MT polymers, respectively (109, 169). Specifically, FKBP52 has been demonstrated to be a MT depolymerising molecule that results in MT catastrophe at the plus end of the polymer (169). FKBP52 is known to be upregulated in ER positive breast cancers (67, 73). Unpublished data from our Lab has demonstrated that FKBP52 knockdown, in both mouse embryonic fibroblasts and MDA-MB-231 breast cancer cells, results in increased sensitivity to paclitaxel (170). Additionally, the same unpublished study identified that FKBP52 was associated with increased metastatic propensity, increased proliferation, and alterations to cell cycle regulators. While in contrast, FKBP25 knockdown in U2OS cell line was demonstrated to result in paclitaxel resistance which is explained by the significantly reduced MT polymer content in FKBP25 knockdown cells (109). These FKBP proteins facilitate vastly different effects on cancer susceptibility to MT targeting drugs, which are first line of therapy for metastatic breast cancer (171). FKBP52 and FKBP25 should be considered as viable screening molecules when selecting appropriate treatments for cancer therapies. However, the role of FKBP25 is yet to be fully elucidated in the pathogenesis of cancer.

## **1.11 Nuclear FKBP25 in cancer pathogenesis**

### **1.11.1 FKBP25 regulation of transcription factors**

Unlike many of the other FKBP family members, FKBP25 has consistently been demonstrated to have many nuclear functions, including regulation of transcription factor expression, interaction with histones and histone modifiers, and regulation of chromatin modifications (reviewed in (172)). The nuclear activities of FKBP25 are mediated by both of its functional domains, specifically the N-terminal PPIase domain which is required for protein-protein interactions and the BTHB domain that is required to mediate interactions with nucleic acids (108). These nuclear roles of FKBP25 make it an ideal candidate for facilitating cancer pathogenesis. FKBP25 has been demonstrated to interact with YY1 (173), a transcription factor that acts as both a transcriptional activator and repressor (174). In the context of cancer progression, YY1 has multifaceted roles in promoting cancer propagation, largely surrounding transcription of regulators of proliferation. For example, YY1 inhibits p53 expression and results in subsequent increases in cell proliferation (173, 175). Further to p53 repression, YY1 has been demonstrated to inhibit p27 expression (a cyclin-dependent kinase inhibitor), resulting in increased proliferation signalling in breast cancer cells (176). In relation to FKBP25, YY1 was able to be augmented by FKBP25 expression, resulting in increased expression of histone deacetylases 1 and 2 (HDACs 1/2) (173). HDAC1 and 2 are classified as class 1 histone deacetylases, which are found ubiquitously in all tissues localised to the nucleus where they serve to cleave acetyl groups from chromatin (177). Chromatin acetylation is a process that enables histone-associated chromatin to become relaxed in order for DNA binding proteins to easily access transcription sites (178). HDACs have been described to be heavily involved in regulation of genes that are known to be beneficial to cancer progression, such as

cell cycle inhibitors (p21/p27 (179, 180)), markers of epithelial cell commitment (E cadherin (181)), and stress transcription factors (HIF1 $\alpha$ , HSP90 (182, 183)).

### 1.11.2 FKBP25 RNA binding

In yeast models, it has been demonstrated that the FKBP25 homolog, Fpr3, was found to physically associate with histone H2B and verified to be a nucleolar protein (184). In mammalian cells, FKBP25 is known to be localised to the nucleolus, in fact, FKBP25 has been demonstrated to contain several putative nuclear localisation sequences (107). These are specifically sequences that are rich in lysine residues that are located on exposed surfaces of the tertiary structure of a protein (185). While it is recognised that FKBP25 has the capacity to move between the cytoplasm and nucleus, in order to translocate to the nucleolus, FKBP25 must be bound to RNA (112). RNA binding proteins (RBPs) are critical for transcriptional control, and processing and transportation of RNA, ultimately affecting the translation of encoded proteins. RBPs have been illustrated to be involved in cancer pathogenesis of many cancers, including that of breast cancer cell EMT (186-188). RBPs have been demonstrated to protect EMT transcription factors from degradation (189). RBPs, such as Polypyrimidine tract binding protein 1 (PTPB), binding to the 3'-untranslated regions of mRNAs of EMT transcription factor, ZEB1 (a negative regulator of E cadherin) which enhances mesenchymal characteristics, including proliferation, migration and invasiveness (190). Additional mRNAs that are protected from degradation include: anti-apoptotic proteins (Bcl-2 and Bcl-XL), phosphatase and tensin homolog (PTEN; a known tumour suppressor), Cyclin E, and c-myc (191-194). Considering that FKBP25 can translocate between the nucleolus, nucleus, and cytoplasm, it is a possibility that FKBP25 is able to interact and potentially be involved in protecting EMT-associated mRNAs from degradation. A protein of interest, in relation to EMT, is La-related protein 6 (LARP6)

that has been demonstrated to facilitate upregulation of EMT characteristics in MDA-MB-231 breast cancer cells, including proliferation and invasion properties (195). Interestingly, LARP6 has been demonstrated to interact with FKBP25 and this complex was able to stabilise collagen mRNA (196). While this relationship has not been examined further, these findings suggest that FKBP25/LAP6 may be involved in stabilising other mRNAs that are associated with EMT and cancer progression. However, to date there has been no research investigating the interrelationship between FKBP25 protein expression and its function in cancer progression or EMT.

### 1.11.3 FKBP25 in epithelial to mesenchymal transition (EMT) and cancer progression

Epithelial to mesenchymal transition (EMT) is a process in which epithelial cells lose their epithelial like characteristics, gaining migratory and invasive traits and becoming mesenchymal-like cells. While EMT is a necessary process in embryonic development and wound healing (197), this process also manifests in cancer progression and metastatic initiation. Here cells from epithelial carcinomas undergo EMT, enabling them to gain invasive properties that allow them to breach the confines of the primary tumour and metastasise to a secondary site (198). A recent meta-analysis has shown that 66% of solid tumour cases result in death related to metastasis (199). Importantly, it has been shown continuously that chemotherapy treatment alone does not prevent the onset of metastatic disease (200-202). Molecular mediators of EMT and metastatic progression are of particular interest for generation of novel therapeutics to improve patient outcomes of late stage and metastatic cancers. One such example of a potential mediator of EMT and metastasis is FKBP25. FKBP25 has been demonstrated to be involved in many molecular pathways that are linked to EMT and

metastatic progression, and regulation of protein interactions that are known to propagate tumorigenic cells (See **Table 1.1**).

**Table 1.1 FKBP25 roles in EMT and cancer progression summary**

| <b>Protein</b> | <b>Interaction with FKBP25</b>  | <b>Function in EMT or cancer progression</b>   | <b>Ref</b>              |
|----------------|---|--|-------------------------|
| p53            | FKBP25 expression is repressed by WT p53.<br>FKBP25 knockdown results in reduced p53 level.   | Reduced WT p53 activity results in propagation of mutations associated with cancer progression.  | (120)<br>(119)          |
| MDM2           | FKBP25 stimulates the auto-ubiquitination of MDM2.  | Loss of MDM2 expression enables mutant p53 signalling in cancer cells.   | (119)<br>(203)          |
| YY1            | FKBP25 alters the DNA binding activity of YY1.  | YY1 increases expression of snail, which increases vimentin, N cadherin, and fibronectin expression; while decreasing E cadherin expression.   | (173)<br>(204)<br>(205) |
| HDAC2          | FKBP25 activates HDAC2 and promotes transcription factor Sp1 activity.<br>FKBP25 knockdown was demonstrated to reduce HDAC2 expression. | Increased proliferation of lung cancer cells via Sp1 activation.<br>Loss of FKBP25 demonstrated to attenuate chemoresistance <i>in vitro</i> . | (206)<br>(207)<br>(208) |

|                   |  |   |                         |
|-------------------|--|---|-------------------------|
| LARP6/<br>Acheron | FKBP25 interacts with<br>LARP6.  | LARP6 is known to enhance proliferation, invasion, increase MMP expression in breast cancer cells.                                      | (196)<br>(195)          |
| Nucleolin         | FKBP25, nucleolin, and re-60S ribosome subunits associate.                   | Nucleolin has been demonstrated to stabilize specific miRNAs involved in promoting metastatic phenotype in breast cancer cells.         | (110)<br>(209)<br>(210) |
| Rad51             | FKBP25 knockdown impairs DNA double stranded break repair mediated by Rad51. | Loss of FKBP25 forces cells to undergo error prone SSA. Cells that survive double stranded DNA breaks transition to EMT-like phenotype. | (111)<br>(211)          |

FKBP25 is known to interact with tumour suppressor protein, p53, and act as a suppressor of WT p53 activity (120). Additionally, FKBP25 knockdown has been shown to reduce p53 levels (119). The role of p53 in cancer progression has been extensively reviewed in the context of many cancers due to its high mutation frequency (Reviewed in (212, 213)). Both reduced WT p53 expression and function, and the presence of mutated p53, correlate with cancer progression and poor patient outcomes by increasing the incidence of genomic instability (214). Furthermore, FKBP25 has been shown to participate in regulation of MDM2, p53's negative regulator (119), where FKBP25 stimulates autoubiquitination of MDM2 causing it to be degraded by the proteasome (119, 203). Subsequently, this loss of p53 sequestration results in

dysregulated mutant p53 signalling resulting in proliferation of damaged cells. FKBP25 has been shown to interact with numerous proteins, which is characteristic of its role as a PPIase, and some of these interactions have been known to be related to pro-cancer roles. YY1 is a transcription factor that has been demonstrated to have increased DNA binding ability in the presence of FKBP25 in a concentration-dependent manner (173). While the transcriptome of YY1 in the presence of FKBP25 has not been fully described, YY1 is known to increase the expression of Snail, an EMT transcription factor (204). Snail and slug are known to impair the expression of E cadherin, and increase the expression of mesenchymal markers, vimentin, N cadherin, and fibronectin (215, 216). This suggests that the level of FKBP25 protein may play a role in the progression through EMT. One example of a known target of YY1 is HDAC2, which interestingly is also directly impacted upon by FKBP25 (173). HDAC2 was shown to be activated by FKBP25 and concurrently prevent degradation of transcription factor, Sp1 (206). Sp1's transcriptional target, Forkhead box protein M1 (FOXM1), is a proto-oncogene that is responsible for dysregulated proliferation in cancer cells (217). Furthermore, Sp1 has been shown to regulate acetylation of the HDAC2 promoter and FKBP25 increases HDAC2 activity, suppressing the expression of cyclin-dependent kinase inhibitor, p27 (206, 218). Another protein that FKBP25 has been identified to interact with is LARP6, an RNA binding protein that is closely related to La-protein, which is intimately involved in RNA metabolism (219). In an experimental model of liver fibrosis, it was shown that FKBP25 and LARP6 interact to stabilise collagen mRNA and increase fibrosis *in vivo* (196). In the context of cancer pathogenesis, LARP6 has been demonstrated to act as an oncogene and facilitates tumour growth, vascularisation, and production of MMPs (195). Interestingly, these functions of LARP6 are reliant on its ability to translocate to the nucleus.

As a nuclear protein, FKBP25 interacts with other nuclear and nucleolar proteins, including nucleolin (110, 209). Nucleolin is a nucleic acid binding protein that is involved in chromatin de-condensation and interaction with pre ribosomal subunits (114). Nucleolin in cancer progression has been demonstrated to be involved in stabilising micro RNAs (miRNA) that are involved in invasive breast cancer (210). There are several miRNAs that have been involved in the pathogenesis of cancer, including that of invasive breast cancer (220). Nucleolin has previously been shown to be involved in processing and maturation of miRNAs. miR-21, miR-103, miR-221, and miR-222, which are mediators of invasive and mesenchymal behaviours, including *in vivo* proliferation(221). Importantly, it was shown that upon inhibition of nucleolin reversed mesenchymal features both *in vitro* and *in vivo* (210). Finally, FKBP25 has been revealed to influence DNA repair protein, Rad51, such that depletion of FKBP25 reduces Rad51 foci at DSB sites (111). Rad51 is involved in homologous recombination, a form of DSB repair that yields a lower error rate than a second repair pathway known as single strand annealing (222). Thus, loss of FKBP25 reduces repair reliance on homologous repair (mediated by Rad51) and subsequently causes the cells to become reliant on SSA (mediated by Rad52). The ensuing reliance on SSA may increase the likelihood of accumulation of further mutations that can promote cancer progression and an EMT phenotype (211). These processes link FKBP25 to EMT and cancer progression. However, to date there has been limited research that has directly implicated FKBP25 in cancer pathogenesis.

#### 1.11.4 FKBP25 in mesenchymal to epithelial transition (MET) cell differentiation

Considering the variety of potential roles that FKBP25 plays in regulating cell function, and the associated implications for cancer progression and EMT, it is hypothesised that FKBP25 may have some roles in the opposite process, mesenchymal to epithelial transition, or MET. MET is a process in which proliferative mesenchymal cells transition to differentiated epithelial-like cells, and occurs during development, wound healing, and cellular reprogramming (223). One such model of MET is myogenesis, where proliferative, mesenchymal-like myoblasts commit and transition to epithelial-like myotubes, precursors of muscle fibres (224). Notably, FKBP25 is the mostly highly expressed of all FKBP25s in mature skeletal muscle and, in fact, it is in the top 10% of proteins expressed in the skeletal muscle proteome (225). Considering how highly expressed FKBP25 is in skeletal muscle, it is plausible that it plays a role in muscle structure or function. Again, to date, there has been no research into the role of FKBP25 in MET, myogenesis, or skeletal muscle structure and function.

## 1.12 Hypothesis

It is hypothesised that FKBP25 will play a role in proliferation and differentiation of differentiating myoblasts and de-differentiating breast cancer cells.

## 1.13 Overarching aims

The overarching aims this thesis are to examine the role of FKBP25 in cell differentiation, in terms of both physiological processes, including MET-like differentiation or myogenesis), as well as pathogenic de-differentiation (i.e. EMT/cancer progression). This will be achieved by using a variety of *in vitro* and *in vivo* models of breast cancer EMT, myogenesis and skeletal muscle plasticity. These findings will be further consolidated using *in vitro* knockdown studies to examine the impact of FKBP25 knockdown on cell biology and function. The conclusions of these studies will provide valuable insight into the roles of FKBP25 in cell differentiation and disease.

## 1.14 Specific aims

| Chapter  | Specific aims   |
|--|---|
| <b>Chapter 3:</b> To investigate the role of FKBP25 in cancer cell de-differentiation and EMT. | <ol style="list-style-type: none"><li data-bbox="708 349 1390 454">1. To investigate the expression of FKBP25 in breast cancer subtypes</li><li data-bbox="708 495 1390 674">2. To examine the impact of FKBP25 expression upon induction of oncogenic mutations.</li><li data-bbox="708 714 1390 893">3. To determine the effects of epidermal growth factor mediated EMT on FKBP25 expression.</li><li data-bbox="708 934 1390 1039">4. To determine the signalling pathways that influence FKBP25 protein expression.</li></ol>                          |
| <b>Chapter 4:</b> To describe the role of FKBP25 in myogenesis and skeletal muscle plasticity. | <ol style="list-style-type: none"><li data-bbox="708 1126 1302 1232">1. To observe FKBP25 expression in the C2C12 model of myogenesis.</li><li data-bbox="708 1272 1278 1377">2. To examine the effect of quiescence induction on FKBP25 expression.</li><li data-bbox="708 1417 1278 1597">3. To contrast the expression in human primary myoblasts and human rhabdomyosarcoma cell line Rh30</li><li data-bbox="708 1637 1366 1816">4. To examine the interaction between FKBP25 and remodelling in <i>in vivo</i> models of muscle plasticity.</li></ol> |

**Chapter 5:** To examine the impact of FKBP25 knockdown on cell biology and function of MDA-MB-468 breast cancer cells and C2C12 myoblasts.

1. Generation of doxycycline inducible shRNA knockdown of FKBP25 in MDA-MB-468 and C2C12 cell lines.
2. Examining the impact of FKBP25 knockdown on cell proliferation.
3. Examining the impact of FKBP25 knockdown on cell migration.
4. Examining the impact of FKBP25 knockdown on anchorage dependent growth and invasion outgrowth in MDA-MB-468 cells.
5. Examining the impact of FKBP25 knockdown on C2C12 differentiation.
6. Examining the impact of FKBP25 knockdown epithelial to mesenchymal transition of MDA-MB-468 cells.

---

## Chapter 2: Methods and Materials

---

### 2.1 Plasmid purification

#### 2.1.1 Bacterial Culture

Bacterial cultures containing plasmids (SMARTvector™ Inducible Lentiviral shRNA, Dharmacon, CO, USA) of interested were inoculated into 100ml of sterile Luria broth (LB; 1% tryptone, 0.5% yeast extract and 1% NaCl; Thermo Fisher, MA, USA) containing ampicillin (100µg/ml), These cultures were grown overnight at 37°C, shaking at 240 rotations per minute (RPM). Cells were pelleted at 3500 RPM for 20 minutes at 4°C and resuspended in lysis buffer for plasmid extraction as per section 2.1.5 using HI pure plasmid filter DNA purification Midi Kit (Thermo Fisher, MA, USA).

#### 2.1.2 Glycerol stocks

Bacteria cultures were inoculated into 5ml of LB broth containing appropriate antibiotics and grown overnight at 37°C with agitation (240 RPM). An 800µl aliquot of overnight culture was mixed with 200µl of 75% sterile glycerol (final concentration of 15%) in a 2ml cryotube by gentle vortexing and stored at -80°C.

#### 2.1.3 Plasmid extraction

Lysed bacterial cells were prepared using the pure link HI pure plasmid filter DNA purification Midi Kit (Thermo Fisher, MA, USA) as per the manufacturer's instructions. In brief, pelleted bacterial cells were resuspended, lysed, and plasmid DNA was precipitated from the solution and extracted via column separation. The plasmid DNA was washed, eluted from the column, and precipitated with isopropanol (Sigma Aldrich, MO, USA). The plasmid suspension was centrifuged at 13.3 RPM for 30 minutes at 4°C. Supernatant was discarded and the pellet resuspended in 70% (v/v)

ethanol and the spin was repeated. The pelleted plasmid was left to dry at room temperature. The dried pellets were resuspended in Tris-EDTA (TE) buffer for storage (-20°C) and use. The plasmid concentrations were analysed using Nanodrop spectrophotometer (Thermo Fisher, MA, USA); including plasmid concentration, and measures of purity (260:280, 260:230 ratio).

Due to the proprietary nature of the SMARTvector backbone, no restriction digests were able to be performed to confirm plasmid DNA (See Figure 2.1).

## **2.2 Cell culture**

### **2.2.1 Routine culturing of cell lines**

Breast cancer cell lines, including MDA-MB-231, MBA-MB-468; myoblast cell line C2C12, and human embryonic kidney cell line HEK293t, were cultured in Dulbecco's modified eagle medium (DMEM, Thermo Fisher, MA, USA) supplemented with 10% foetal bovine serum (FBS), antibiotic/antimycotic (1%, Invitrogen, CA, USA), Glutamax (1%, stable L-glutamine substitute, Thermo Fisher, MA, USA), sodium pyruvate (1mM/110mg/L, Thermo Fisher, MA, USA), and HEPES (25mM/5.9g/L, Thermo Fisher, MA, USA). Other breast cancer cells including T47D, were maintained in Roswell Park Memorial Institute (RPMI, Gibco, MA, USA) containing the same supplements. Immortalised mammary epithelial cell line, MCF10A, was maintained in a DMEM/F12 formulation containing epidermal growth factor (EGF, Thermo Fisher, MA, USA), cholera toxin (Sigma Aldrich, MO, USA), insulin (Thermo Fisher, MA, USA), and horse serum (5%, Thermo Fisher, MA, USA).

Cells were grown to 80% confluency before passaging, where media was removed, and cells were rinsed with phosphate buffered saline (PBS). Cells were then incubated with TrypLE Express (Stable trypsin alternative, Thermo Fisher, MS, USA) for

approximately 5 minutes at 37°C with 5% CO<sub>2</sub> to dissociate cells from the culture vessel.

MCF10A cells were dissociated using TrypLE Express and collected in resuspension medium (growth medium with 20% horse serum, as serum is required to inactivate trypsin), the resuspension was then centrifuged at 1500 RPM for 5 minutes to pellet the cells. The resuspension media was discarded, and the pellet resuspended in growth media for passaging. All cells were diluted at an appropriate dilution for the cell line and incubated at 37°C with 5% CO<sub>2</sub>.

C2C12 myoblasts were differentiated by changing media to differentiation medium, DMEM containing 2% horse serum (Thermo Fisher, MA, USA) containing the same supplements as previously described. C2C12 myoblasts were plated at high confluency (80-90%) for 24 hours prior to changing to differentiation medium for 4-5 days to form myotubes.

### 2.2.2 Routine culturing of primary cell lines

Human primary myoblast (MDA-135) and rhabdomyosarcoma (Rh30) cell lines were provided by Kevin Watt. Both MDA-135 and Rh30 primary cell lines were cultured and maintained in Hams/F10 medium (HyClone medium, Amersham, Piscataway, NJ, USA), supplemented with fibroblast growth factor basic (FGF-2, 25µg/ml, Peprotech, NJ, USA), 10% FBS (Thermo Fisher, Australia) and 1% antibiotic/antimycotic (Thermo Fisher, MA, USA). Cells were maintained at approximately 60% confluence to prevent premature differentiation as a result of increased confluency. For differentiation cells were plated at high confluency (80-90%) for 24 hours before being transitioned to differentiation medium, alpha minimum essential medium (alpha MEM, Gibco, MA, USA) supplemented with insulin/selenium solution (0.5% of 100x stock solution,

Thermo Fisher, MA, USA), B27 supplement (2% of 50X stock solution, Thermo Fisher, MA, USA) and horse serum (2%, Thermo Fisher, MA, USA). Cells cultured in differentiation medium fused into myotubes in 3-4 days stored at 37°C with 5% CO<sub>2</sub>.

### 2.2.3 Induction of quiescence in C2C12 cells

C2C12 cells were grown to 70% confluency in T75 flasks and lifted as described in 2.2.1. A viscous suspension medium containing 4% methylcellulose (MC)/DMEM (MC/DMEM (w/v)) was prepared according to Subramanian et al. to suspend C2C12 cells and prevent adherence, thus arresting cells in G0 phase (i.e. quiescence). Additionally, a suspension mix was prepared containing 20% FBS, 4mM Glutamax, 1x antibiotic/antimycotic, and 10nM HEPES which was added to 6.6mL of MC/DMEM to a total of 10mL in a 50mL falcon tube (Corning). Cells were counted and adjusted to 1x10<sup>6</sup> cells per mL and 1mL was added to the MC/DMEM solution. The solution containing the cells was gently rolled to ensure the cells were distributed in the solution. The tubes were stored upright at 37°C with 5% CO<sub>2</sub> and agitated daily to ensure the cells did not settle. Cells were collected over various time points by centrifugation, whereby the suspension was diluted with PBS and the tubes were centrifuged at 1250G for 25 minutes. Centrifugation was repeated several times to remove all MC in the cell suspension. Cells were then either lysed for protein collection (as per 2.3.1), or resuspended and replated under normal culture conditions for further analysis.

### 2.2.4 Epidermal growth factor induction of epithelial to mesenchymal transition

MDA-MB-468 cells were grown and lifted as per section 2.2.1, replated at low (approximately 50%) confluency and allowed to adhere overnight. Following this, the

complete medium was replaced with serum free medium (DMEM, Gibco, MA, USA) for 16 hours. Finally, the cells were treated with 50ng/ml epidermal growth factor (EGF, Corning, NY, USA) in complete growth media for 72 hours. Cells were imaged using the Olympus IX81 microscope to observe morphological changes. In knockdown experiments, cells were treated with doxycycline (dox, at 0.5µg/ml) starting 24h prior to serum deprivation. Then continued as described above in the presence of dox.

### 2.2.5 Cryopreservation of cell lines

Cell lines were grown to confluency in T75 flasks and passaged as per 2.2.1. Cells were lifted and centrifuged in growth media for 5 minutes at 1500 RPM, after which the pellet was held on ice. The cells were then resuspended in 4mL of freezing medium (90% FBS and 10% dimethyl sulfoxide (DMSO)), 1mL of cell suspension was added per cryotubes (Nunc, Thermo Fisher, MA, USA). Filled cryotubes were placed on ice for approximately 5 minutes before being transferred to a cold (4°C) Mr. Frosty cryo-container (Thermo Fisher, MA, USA). This was stored at -80°C for 24 hours, after which the cells were transferred to liquid nitrogen (LN<sub>2</sub>) for long term storage.

### 2.2.6 Generation of lentiviral particles

HEK293t cells were grown to 80% confluency in T75 flasks (Corning), lifted and reseeded at medium confluency in either 6 well plate (1x10<sup>5</sup> cell per well) or 10cm dish (1x10<sup>6</sup> cells) (Corning) and left to adhere overnight at 37°C with 5% CO<sub>2</sub>. Prior to transfection, cells were changed to DMEM containing no antibiotic/antimycotic. For lentiviral transfection 5µg of psPAX.2 and 2.5µg of pMD2.g were combined with 7µg of plasmid DNA in 2mL DMEM and mixed thoroughly. Next, 14µl of PLUS reagent (Invitrogen, MO, USA) was added and incubated at room temperature for 5 minutes. 12µl of Lipofectamine LTX (Invitrogen, MO, USA) was added to the mixture and

incubated for 30 minutes at room temperature (Lipofectamine is used to create lipid bound vesicles which deliver the viral components into the packaging cells). The DNA-lipid complex solution was added to the cells in a dropwise manner, gently rocked to mix, and then incubated for 16 hours at 37°C with 5% CO<sub>2</sub>. After 16 hours the supernatant is removed and replaced with harvesting media (i.e. the growth medium of cells of recipient cells, DMEM with 10% FBS), which was collected after 48 hours. The virus containing supernatant was centrifuged briefly to pellet any cells and filtered using a 0.4µm polyvinylidene difluoride (PVDF) filter, aliquoted and stored at -80°C for future use.

### 2.2.7 Generation of stable FKBP25 knockdown cell lines

Cells of interest, namely MDA-MB-468 and C2C12, respectively, were plated at 1x10<sup>6</sup> cells in a T25 flask (Corning) and allowed to adhere overnight at 37°C with 5% CO<sub>2</sub>. The growth medium was removed and replaced with 2mL of DMEM containing lentiviral particles (1 in 3 dilution), and 10µg/mL of polybrene which was incubated for 24 hours. After 24 hours the virus containing media was discarded and replaced with growth medium for a recovery period of 24 hours. Following this cells that were successfully transfected were selected using the selection marker contained on the plasmid, i.e. puromycin resistance. Cells were cultured in medium containing 2-5µg/mL of puromycin (Sigma Aldrich, MO, USA) (MDA-MB-468 2µg/mL, C2C12 5µg/mL) which was replaced or passaged every 2-3 days, for 10 days.

To induce FKBP25 knockdown in C2C12 myotubes, myoblasts were treated with 0.5µg/ml doxycycline in growth medium for 72 hours prior to transition to differentiation medium (as per 2.2.1)

**Table 2.1: SMARTvector components**

| <b>Vector component</b>        | <b>Description</b>  |
|--------------------------------|---|
| 5' LTR                         | 5 prime long terminal repeat is required for vector integration into the host cell genome.  |
| Ψ (Psi)                        | Psi packaging sequence allows the lentiviral genome to be packed by exogenous systems.  |
| RRE                            | Rev response element enhances packaging efficiency.   |
| TRE3G                          | Inducible tetracycline response element which is activated by Tet-on 3G in the presence of a Tet/Tet derivative (i.e. Doxycycline). |
| T GFP/ T RFP                   | Turbo green fluorescent protein, or turbo red fluorescent protein reporter; visual reporter of Tet-inducible activation.            |
| SMARTvector universal scaffold | A proprietary scaffold developed by Dharmacon based on microRNA-gene targeting sequences.   |
| hEF1α                          | Human elongation factor-1 alpha constitutive promoter required to drive non-Tet regulated vector elements.                          |
| Puro <sup>R</sup>              | Puromycin resistance gene which allows for selection of transfected cells.  |
| 2A                             | A self-cleaving peptide chain that enables expression of Puro <sup>R</sup> and Tet-On-3G from RNA pol-2 promoter.                   |
| Tet-On 3G                      | Tet-regulated transactivator protein which binds to TRE3G in the presence of doxycycline.   |
| WPRE                           | Woodchuck Hepatitis post-transcriptional Regulatory Element enhances shRNA expression in target cells.                              |
| 3' SIN LTR                     | 3 prime Self Inactivating Long Terminal Repeat for generation of replication incompetent viral particles.                           |

## 2.2.8 Doxycycline titration of FKBP25 knockdown cell lines

SMARTvector™ Inducible Lentiviral shRNA (Dharmacon, CO, USA) is a tetracycline inducible shRNA system that is more sensitive than previous systems. As such, the concentration of doxycycline (Sigma Aldrich, MO, USA) was titrated to ensure the minimal dose was used to induce knockdown. After selection, cells were plated at approximately 60% confluency in 6 well plates and treated with a range of doxycycline concentrations (from 0.1-2µg/mL) for 72 hours to induce maximal shRNA induction. In addition to puromycin resistance, SMARTvector contain a red fluorescent protein (RFP) reporter that is activated when doxycycline is present (See **Fig 2.1** and **Tables 2.1** and **2.2**). Fluorescence images were taken to confirm RFP expression using the Olympus IX81 fluorescence microscope.

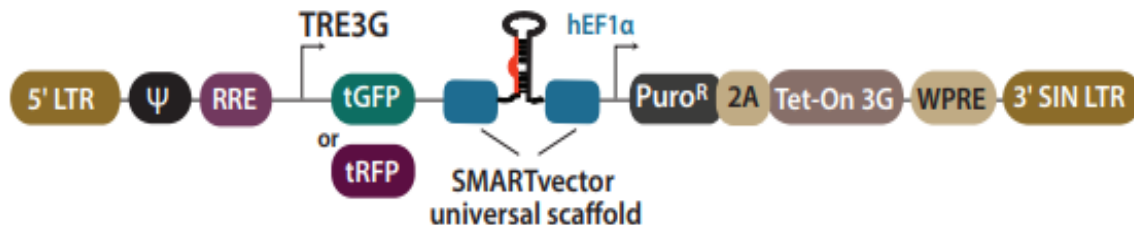


**Figure 2.1: Elements of the SMARTvector Inducible Lentiviral shRNA vector**

The SMARTvector shRNA vector contains a series of features that enable safe and effective shRNA mediated knockdown utilising TET-on technology. The SMARTvector design contains a proprietary 'universal scaffold' based on microRNA gene targeting sequences. See Table 2.1 for descriptors.

**Table 2.1: List of SMARTvector shRNAmir sequences**

| Construct  | Sequence                            |
|--|-------------------------------------|
| V3SH11252-225035425<br>(shRNAmir1/Non targeting) | TTATTAGTGGCTCATTGGT (targets 3'UTR) |
| V3SH11252-225145909<br>(shRNAmir2)               | TTTCAGTACCCTTAAAACG (targets ORF)   |
| V3SH11252-226953220<br>(shRNAmir3)               | AAACGAATCTGAACCGTGT (targets ORF)   |

## 2.3 Expression analysis

### 2.3.1 Protein extraction

Cells were plated in 6 well plates for protein extraction. Plates were placed on ice and rinsed with ice cold PBS before lysis with a modified radio-immunoprecipitation assay buffer (RIPA buffer -1mM EDTA, 0.5mM EGTA, 10mM Tris-HCl, 140mM sodium chloride, 10% sodium deoxycholate, and 1% triton-X 100, containing protease and phosphatase inhibitor cocktails (Sigma Aldrich, MO, USA). Plates scraped using a cell scraper, lysates were collected and triturated to shear any remaining cellular debris. Next, the lysates were centrifuged at maximum speed (13,000 RPM) at 4°C for 30 minutes. The supernatants were collected and stored at -80°C and the pellets discarded.

### 2.3.2 Protein quantification

Cell lysates were quantified using the bicinchoninic acid assay (BCA, Pierce Biotechnology, IL, USA) as per manufacturer's instructions. In brief, a standard curve of known protein concentrations was generated by a serial dilution of 2-0.03125mg/ml of bovine serum albumin (BSA). Unknown samples were plated in triplicate (in addition

to the standard curve samples) in a 96 well plate to which the BCA reagent was added. The plates were incubated at 37°C for 30 minutes for colour development. The plates were read in the Varioskan Flash plate reader using SkanIt RE software (Thermo Fisher, MA, USA) at 562nm. Protein concentrations were established by referencing the standard curve.

### 2.3.3 Western Blotting - NUPAGE

Aliquots of protein lysates (10-20µg) were combined with 4x lithium dodecyl sulphate (LDS) loading dye (Invitrogen, MO, USA), containing 10% NUPAGE reducing agent (Dithiothreitol/DTT, Invitrogen, MO, USA), and denatured at 95°C for 5 minutes. Protein samples were loaded into NUPAGE Novex 4-12% Bis-Tris precast gradient gels (Invitrogen, MO, USA). Proteins were electrophoresed at 150 volts for 80 minutes in NUPAGE 1X MES (2-ethanesulfonic acid) running buffer (Invitrogen, MO, USA). Following electrophoretic separation of proteins, the gels were equilibrated in 20% ethanol, and transferred onto a polyvinylidene difluoride (PVDF) membrane using the iBlot2 dry blotting system (Invitrogen, MO, USA). Dry blotting involved applying 20-25 volts to the transfer stack for 5-8 minutes. Membranes were blocked in 3% skim milk powder (w/v) in tris-buffered saline with 0.1% tween-20 (TBST, pH 7.4) for 60 minutes at room temperature with gentle agitation. Primary antibodies were used at appropriate dilutions in 3% skim milk/TBST and incubated at 4°C overnight.

The next day, membranes were washed in TBST for 10 minutes at 240 RPM three times to ensure adequate removal of non-specific antibody binding. Next, the secondary antibodies were applied in 3% skim milk/TBST (horse radish peroxidase conjugated secondary antibodies, Invitrogen), followed by the same washing procedure. The membranes were then incubated in SuperSignal™ West Pico PLUS enhanced chemiluminescence reagent (ECL, Pierce Biotechnology, IL, USA) for 5

minutes to develop luminescence. The membranes were imaged in the Vilber Lourmat imaging system (Vilber Lourmat, Germany). Densitometric measurements of the protein of interest were quantified using Fusion CAPT Advance software (Vilber Lourmat, Germany). Upon analysis of protein expression results were normalised to a loading control (beta actin) and expressed as either a proportion of beta actin expression or normalised to non-dox treated controls.

#### 2.3.4 Western blotting – Bio-Rad

Whole tissue homologues were analysed using 10% SDS PAGE gels poured freshly on the day of analysis. Up to 50g of protein was combined with 2x SDS sample buffer (20% glycerol; 100mM Tris, pH 6.8; 4% SDS; 0.017% bromophenol blue; 0.25M dithiothreitol (DTT)) and boiled at 95°C for 5 minutes to denature proteins and run at 100V in running buffer (containing: Tris, SDS, glycine). Following electrophoresis, proteins were transferred to a PVDF membrane in transfer buffer (containing Tris, glycine, and 20% methanol) for 1 hour at 300mV. Blocking, incubation, and washing steps are as per section 2.3.3 above. Expression quantification differed to 2.3.3 by normalising protein expression to total protein (using Coomassie Brilliant Blue) which was also imaged and quantified using Fusion CAPT Advance software (Vilber Lourmat, Germany).

#### 2.3.5 Microtubule polymerisation assay

The ratio of microtubule to free tubulin was determined using a Microtubule/Tubulin In Vivo Assay Biochem Kit (Cytoskeleton, CO, USA). In brief, cells were pre-treated with doxycycline to induce FKBP25 knockdown, and plated at 80% confluency 24 hours prior to the assay. Each sample was treated with 1uM Taxol to induce polymerisation of the microtubules (MT) (1 hour at 37°C) as well as untreated control cells. All

reagents were warmed to 37°C unless otherwise specified. Cells were washed in PBS lysed and collected in 80µl of buffer the lysates were pipetted up and down to ensure adequate shearing of cell membranes. Lysates were centrifuged at 1500 RPM for 5 minutes to pellet large complexes in the lysate. Next, the supernatant from the low-speed spin was aliquoted into 1ml ultracentrifuge tubes and centrifuged at 100,000 RPM for 1 hour at 37°C. The supernatant from the ultracentrifugation contained the free tubulin fraction, and the pellet contained the polymerised MT fraction. The pelleted MTs were resuspended in 80µl of MT stabilisation buffer, and 20µl of 5x SDS buffer. 15µl of 5x SDS buffer was added to the supernatant. The samples were left to stabilise at room temperature for 15 minutes before being subjected to SDS PAGE as per section 2.3.3. Membranes were incubated with anti-sheep pan tubulin antibody provided by Cytoskeleton.

### 2.3.6 Immunofluorescent staining

Cells were grown on Millicell EZ Slides (Merk Millipore, Germany) or 150µm thick poly-D-lysine coated glass coverslips (Nue Vitro Corporation, WA, USA), following treatment/induction of knockdown. Cells were fixed with 4% paraformaldehyde (PFA) at 37°C for 5 minutes, followed by room temperature for 25 minutes. Fixed cells were washed 5 times with PBS or PBS with 0.1% tween-20 (PBST). Cells were then incubated in blocking and permeabilising buffer (0.2% skim milk powder, 0.1M glycine, 1% BSA, 0.01% triton-X in PBS) at room temperature for 30 minutes, followed by three PBS washes. The primary antibodies were made up in 0.1% BSA/PBST and incubated at room temperature for 60 minutes. The fluorophore conjugated secondary antibodies were diluted in 0.1% BSA/PBS and incubated for 30 minutes at room temperature protected from light. Slides were washed five times in PBS and the nuclei counterstained with 1µg/ml 4'6-diamidino-2-phenylindole (DAPI; Sigma Aldrich, MO,

USA) for 10 minutes and wash steps were repeated. Finally, slides were mounted with a coverslip using Fluoroshield anti-fade mounting media (Sigma Aldrich, MO, USA) and dried overnight before imaging with the BX53 Olympus microscope.

## **2.4 *In vitro* functional assays**

### **2.4.1 Anchorage dependent colonisation assay**

Cells were lifted and resuspended as per section 2.1.1. Cells were resuspended at  $1 \times 10^3$  cells/mL, and 100 $\mu$ L (100 cells) or 500 $\mu$ L (500 cells) and were aliquoted into 1mL of media per well in a 6 well plate. Cells were left to colonise for 14 days, including media change every 2-3 days. Upon collection, plated were rinsed with ice cold PBS and fixed with 100% methanol, followed by Diff-Quick staining (Histolabs, Australia), and rinsed in distilled water. Plates were dried over night before being scanned and analysed using manual counting of visible colonies on ImageJ (NIH; <http://rsb.info.nih.gov/nih-image/>). All values were normalised and expressed as proportions of non-dox treated controls

### **2.4.2 Matrigel invasion outgrowth assay**

Ice cold Geltrex (Thermo Fisher, MA, USA) was plated into the wells of a 96 well plate and allowed to set for 10 minutes at 37°C. Cells were lifted and resuspended at  $2 \times 10^5$  cells/mL as per section 2.1.1. Using the 'top' method 5 $\mu$ L of cells was diluted in 200 $\mu$ L of growth medium and seeded on top of the base layer. The cells were left to colonise for up to 10 days and were imaged regularly at low magnification using IX81 Olympus microscope. Upon completion, the colonies were measured (diameter,  $\mu\text{m}^2$ ) using Olympus CellSens software (Olympus, Tokyo, Japan).

### 2.4.3 Microchemotaxis migration assay

The Microchemotaxis assay is used to determine the ability of cells to migrate toward a chemotactic gradient through a porous membrane (8µm-pore polyvinyl pyrrolidone-free polycarbonate membranes, Neuro Probe Inc., MD, USA) using the Boyden chamber apparatus. Cells were non-enzymatically lifted using PBS/EDTA solution and resuspended at  $1 \times 10^6$  cells/mL in DMEM containing 0.1% FBS. The lower compartments of the chambers were filled with chemo attractants including EGF, fibroblast conditioned media, and 10% FBS, as well as a 0.1% BSA background control carefully loaded to ensure that no bubbles are introduced. Cells were loaded into the top compartment of the Boyden chamber (56µl), the apparatus was then incubated at 37°C with 5% CO<sub>2</sub> for 6 hours. After incubation, the membrane was removed, fixed in 100% methanol, and stained with Diff-Quick (Histolabs, Australia) before being mounted on a microscope slide. Cells that remained on the top side of the membrane were wiped away before imaging. Cell migration was quantified by imaging the slides high powered magnification using the Olympus IX81 microscope and migrated cells were manually counted using ImageJ (NIH; <http://rsb.info.nih.gov/nih-image/>).

### 2.4.4 Wound healing assay

C2C12 cells were cultured and lifted as per section 2.1.1 and reseeded on a 6-well plate (Corning) at approximately 90% confluence. FKBP25 knockdown cells were induced with doxycycline for 72 hours prior to replating and maintained in appropriate doxycycline concentration. Cells were left to adhere overnight before being scratched with a 200µl pipette tip. The media was replaced with complete medium containing 5ng/ml Mitomycin C (Sigma Aldrich, MO, USA) to prevent proliferation during wound healing. Coordinates were set within the scratch wound using NIS Elements software

on the Nikon Eclipse Ti-E inverted widefield microscope (Nikon, Tokyo, Japan) to image each wound every 15 minutes for up to 24 hours at 4x magnification. The images were compiled into a film clip and analysed using NIS Elements software (Nikon, Tokyo, Japan) to determine the wound closure time. Wound healing was analysed by determining the percentage of wound closure (area in the wound  $\mu\text{m}^2$ ) in 20 hours.

#### 2.4.5 Alamar blue viability assay

AlamarBlue (resazurin salt) viability assay (Sigma Aldrich, MO, USA) was used to measure viable, proliferating cells in a population. Specifically, the AlamarBlue reagent is a commercially available product that contains resazurin, a weakly fluorescent blue dye. Upon reduction (by NADPH dehydrogenase, a mitochondrial enzyme) resazurin changes into a pink coloured and highly fluorescent dye resorufin. As such, increased fluorescence indicates increased viability in the sample.

Cells were grown and lifted as per section 2.1.1 and resuspended at  $1 \times 10^4$  cells/mL. Cells were seeded at different densities depending on the cell type, i.e. MDA-MB-468 cells were plated at 2000 cells/well (100 $\mu\text{l}$ ), and C2C12 cells were plated at 1000 cells/well (50 $\mu\text{l}$ ). Each well was filled to contain 200 $\mu\text{l}$  of media. Cells were left to incubate overnight before Alamar blue dye was added (Alamar blue working solution was prepared as a 1:10 dilution in complete medium/DMEM). Once the dye was added the plate was shielded from light and stored in the at 37°C with 5% CO<sub>2</sub> for two hours. After the incubation period the supernatant was transferred to a white opaque 96 well plate for fluorometric reading in the Varioskan Flash plate reader using SkanIt RE software (Thermo Fisher, MA, USA) at 580-610nm (peak emission is 585nm). The cells were replaced with fresh media and placed back into the incubator; this assay

was repeated for 5 days. Measured relative fluorescence units (RFU) values were plotted for each time point.

#### 2.4.6 Cell density measurements

Following alamar blue viability assays, the cells were fixed and stained with Diff-Quick stain (Histolabs, Australia) as per 2.4.1. The plates were then left to dry overnight and before being scanned for analysis. Mean relative density measurements were read using ImageJ (NIH; <http://rsb.info.nih.gov/nih-image/>) and normalised to non-dox treated controls.

### 2.5 *In vivo* muscle hypertrophy and atrophy models

These *in vivo* studies were not performed as part of this thesis but were kindly provided by the Exercise Metabolism Unit (EMU; Victoria University, Melbourne, Victoria).

#### 2.5.1 Chronic mechanical loading

Eight- to ten-week-old female FVB/N mice were subjected to either synergist ablation (SA), myotectomy (MTE), or sham surgery. In short, animals subject to SA surgery involved bilateral removal of the soleus and distal half of the gastrocnemius. MTE surgery involved removing only the achilles tendon rather than the entire gastrocnemius muscle, and the soleus remains intact. Sham surgery involved surgical incision in the lower leg which was closed immediately after. Tissues were harvested 7 and 14 days after surgeries were performed (226, 227).

#### 2.5.2 Murine muscular dystrophy (mdx)

Eight-week-old male C57Bl/10ScSn (normal wild-type strain; CON) and C57Bl/10mdx (mdx) mice were purchased from Animal Resources Centre (Western Australia,

Australia). The mice were not subjected to any treatment or procedures. Upon non-recovery surgery all muscles and organs were harvested for analysis (228).

### 2.5.3 Denervation

Eight-week-old male C57BL/6 male mice were subjected to denervation surgery, this involved creating a small incision in the distal knee compartment to expose the peroneal nerve which was excised. The wounds were closed, and mice were given appropriate recovery periods. Tissues were harvested at 7 and 14 days after surgeries were performed (229).

### 2.5.4 Food deprivation

Eight- to ten-week-old female FVB/N mice were deprived of food for a 48-hour period, while maintaining *ad libitum* access to drinking water. Control mice continued *ad libitum* access to both food and water. Following the 48-hour deprivation period the mice underwent non-recovery surgery where all tissues were harvested for analysis (227).

## 2.6 Statistical analysis

All experiments were performed at least three times using biological replicates. Graph Pad Prism was used to analyse all data sets. All experiments pertaining to doxycycline inducible cell lines were analysed using a 2-way analysis of variance (ANOVA). While treatments and conditions undertaken on parental cell lines were analysed with independent T-tests or one-way ANOVA depending on the variables. Throughout the studies significance was reported at  $p \leq 0.05$ , and data was presented as mean  $\pm$  standard deviation.

## 2.7 Materials

### 2.7.1 Plasmids

**Table 2.3: List of plasmids**

| Plasmids                                      | Source                      |
|---|-----------------------------|
| pDGM2.4                                       | Open Biosystems, USA        |
| pMD2.G  | Addgene, Massachusetts, USA |
| pMDLg/pRRE                                    | Addgene, Massachusetts, USA |
| pRSV Rev                                      | Addgene, Massachusetts, USA |
| psPAX   | Open Biosystems, USA        |
| V3SH11252-225035425 (shRNAmir1/Non targeting) | Dharmacon, Colorado, USA    |
| V3SH11252-225145909 (shRNAmir2)               | Dharmacon, Colorado, USA    |
| V3SH11252-226953220 (shRNAmir3)               | Dharmacon, Colorado, USA    |

## 2.7.2 Reagents used for cell culture and in vitro assays

**Table 2.4: List of reagents for cell culture and in vitro assays**

| <b>Item</b>   | <b>Source</b>                                    |
|---|--|
| 100X Antibiotic/Antimycotic   | Gibco Invitrogen, California, USA                |
| Alamar Blue (Resazurin sodium salt)   | Sigma-Aldrich, Missouri, USA                     |
| Basic fibroblast growth factor (FGF-2)  | Peptotech. New Jersey, USA                       |
| Bovine serum albumin (BSA)  | Sigma-Aldrich, Missouri, USA                     |
| B27 Supplement  | Invitrogen, California, USA                      |
| Cholera toxin   | Sigma-Aldrich, Missouri, USA                     |
| Collagen I  | Sigma-Aldrich, Missouri, USA                     |
| Diff Quick Dyes   | Fronine Lab Supplies, New South Wales, Australia |
| Doxycycline   | Sigma-Aldrich, Missouri, USA                     |
| Dulbecco's modified Eagle Medium (DMEM)   | Gibco Invitrogen, California, USA                |
| Dulbecco's modified Eagle Medium (DMEM)/<br>Ham's nutrient mixture F12 (DMEM/F12) | Gibco Invitrogen, California, USA                |
| Epidermal growth factor (EGF)   | BD Biosciences, California, USA                  |
| Foetal bovine serum (FBS)   | Thermo Scientific, California, USA               |
| Geltrex™ Basement Membrane Matrix   | Thermo Scientific, California, USA               |
| Glutamax  | Gibco Invitrogen, California, USA                |
| HEPES   | Gibco Invitrogen, California, USA                |
| Horse serum (HS)  | Gibco Invitrogen, California, USA                |

|  |  |
|--|--|
| HyClone AdvanceSTEM cell culture media       | GE Healthcare Biosciences, Pennsylvania, USA |
| Hygromycin B                                 | Sigma-Aldrich, Missouri, USA                 |
| Hydrocortisone                               | Sigma-Aldrich, Missouri, USA                 |
| Insulin from Bovine pancreas                 | Sigma-Aldrich, Missouri, USA                 |
| Insulin, transferrin, selenium (ITS, 100X)   | Gibco Invitrogen, California, USA            |
| Lipofectamine LTX PLUS                       | Invitrogen, California, USA                  |
| LY294002                                     | Sigma-Aldrich, Missouri, USA                 |
| Methanol                                     | Sigma-Aldrich, Missouri, USA                 |
| Methylcellulose                              | Sigma-Aldrich, Missouri, USA                 |
| Mitomycin C                                  | Sigma-Aldrich, Missouri, USA                 |
| PD- 325901                                   | Sigma-Aldrich, Missouri, USA                 |
| Polybrene (hexadimethrine bromide)           | Sigma-Aldrich, Missouri, USA                 |
| Puromycin                                    | Sigma-Aldrich, Missouri, USA                 |
| Rapamycin                                    | Sigma-Aldrich, Missouri, USA                 |
| Roswell Park Memorial Insitute (RPMI) medium | Gibco Invitrogen, California, USA            |
| Terg-a-Zyme                                  | Alconox Inc., New York, USA                  |
| TrypLE Express (stable trypsin replacement)  | Gibco Invitrogen, California, USA            |

### 2.7.3 Reagents for expression analysis

**Table 2.5: List of reagents for protein expression analysis**

| Item   | Supplier                     |
|--|------------------------------|
| 10x Reducing agent (500 mM dithiothreitol (DTT)) | Invitrogen, California, USA  |
| 4',6-diamidino-2-phenylindole (DAPI)             | Invitrogen, California, USA  |
| 4x Loading buffer                                | Invitrogen, California, USA  |
| Antioxidant reagent                              | Invitrogen, California, USA  |
| Coomassie Brilliant blue R-250                   | Bio-Rad, California, USA     |
| iBlot PVDF Transfer stacks (Midi and Mini size)  | Invitrogen, California, USA  |
| MES running buffer                               | Invitrogen, California, USA  |
| Novex Sharp pre stained protein standard         | Invitrogen, California, USA  |
| NUPAGE 10, 12, 15, 20 well gels (Bis-Tris 4-20%) | Invitrogen, California, USA  |
| Phosphatase inhibitor                            | Sigma-Aldrich, Missouri, USA |
| Protease inhibitor                               | Sigma-Aldrich, Missouri, USA |
| Restore plus stripping buffer                    | Invitrogen, California, USA  |
| Skim milk powder                                 | Diploma, Victoria, Australia |
| Triton-X 100                                     | Sigma-Aldrich, Missouri, USA |
| Tween-20   | Sigma-Aldrich, Missouri, USA |

## 2.7.4 General reagents

**Table 2.6: List of general reagents**

| <b>Item</b>  | <b>Supplier</b>              |
|--|------------------------------|
| Acetic acid  | Sigma-Aldrich, Missouri, USA |
| Ampicillin   | Sigma-Aldrich, Missouri, USA |
| Dimethyl sulfoxide (DMSO)  | Sigma-Aldrich, Missouri, USA |
| Disodium phosphate ( $\text{Na}_2\text{HPO}_4$ )                         | Sigma-Aldrich, Missouri, USA |
| Ethanol  | Merck, New Jersey, USA       |
| Ethylenediaminetetraacetic acid (EDTA)                                   | Sigma-Aldrich, Missouri, USA |
| Ethylene glycol-bis ( $\beta$ -aminoethyl ether) tetraacetic acid (EGTA) | Sigma-Aldrich, Missouri, USA |
| Glycerol   | Sigma-Aldrich, Missouri, USA |
| Glycine  | Sigma-Aldrich, Missouri, USA |
| Hydrochloric acid (HCl)  | Sigma-Aldrich, Missouri, USA |
| Isopropanol  | Sigma-Aldrich, Missouri, USA |
| Luria Broth  | Sigma-Aldrich, Missouri, USA |
| Potassium chloride (KCl)   | Sigma-Aldrich, Missouri, USA |
| Potassium dihydrogen phosphate ( $\text{KH}_2\text{PO}_4$ )              | Sigma-Aldrich, Missouri, USA |
| Sodium chloride (NaCl)   | Sigma-Aldrich, Missouri, USA |
| Sodium deoxycholate  | Sigma-Aldrich, Missouri, USA |
| Sodium dodecyl sulphate (SDS)  | Sigma-Aldrich, Missouri, USA |
| Tris hydrochloride   | Sigma-Aldrich, Missouri, USA |

## 2.7.5 Commercial kits

**Table 2.7: List of commercial kits**

| Item   | Supplier                            |
|--|-------------------------------------|
| BCA protein assay kit                                  | Pierce Biotechnology, Illinois, USA |
| Microtubule/Tubulin In Vivo Assay Biochem Kit          | Cytoskeleton, Colorado, USA         |
| PureLink™ HiPure Plasmid Midiprep Kit                  | Invitrogen, California, USA         |
| SuperSignal™ West Pico PLUS Chemiluminescent Substrate | Pierce Biotechnology, Illinois, USA |

## 2.7.6 Primary antibodies

**Table 2.8: List of primary antibodies**

| Item                        | Catalogue Number | Supplier                               |
|-----------------------------|------------------|--|
| Alpha Tubulin               | SC-8035          | Santa Cruz Biotech.,<br>Texas, USA     |
| Acetylated tubulin          | 32-2700          | Invitrogen, California, USA            |
| Akt (Total)                 | 4691             | Cell Signalling,<br>Massachusetts, USA |
| Akt (Ph Ser473)             | 4060             | Cell Signalling,<br>Massachusetts, USA |
| Akt (Ph Thr308)             | 13038            | Cell Signalling,<br>Massachusetts, USA |
| Beta actin                  | 4970             | Cell Signalling,<br>Massachusetts, USA |
| Cyclin D1                   | 2926             | Cell Signalling,<br>Massachusetts, USA |
| Detyrosinated alpha tubulin | ab48389          | Abcam, Cambridge, UK                   |
| E Cadherin                  | 3195             | Cell Signalling,<br>Massachusetts, USA |
| Fast myosin heavy chain     | ab51263          | Abcam, Cambridge, UK                   |
| FKBP25 (WB)                 | MAB3955          | R&D systems, Minnesota,<br>USA         |
| FKBP25 (IF)                 | ab16654          | Abcam, Cambridge, UK                   |
| Erk 1/2 (Total)             | 9102             | Cell Signalling,<br>Massachusetts, USA |
| Erk 1/2 (Ph Thr202/Tyr204)  | 9101             | Cell Signalling,<br>Massachusetts, USA |
| MyoD 1                      | ab16148          | Cell Signalling,<br>Massachusetts, USA |

|                           |          |                                     |
|---------------------------|----------|-------------------------------------|
| Myogenin                  | ab124800 | Abcam, Cambridge, UK                |
| MDM2                      | ab16895  | Abcam, Cambridge, UK                |
| p21 <sup>CIP1/WAF1</sup>  | 2947     | Cell Signalling, Massachusetts, USA |
| Pan Tubulin               | ATN02    | Cytoskeleton, Colorado, USA         |
| p70-S6 Kinase (Total)     | 2708     | Cell Signalling, Massachusetts, USA |
| p70-S6 Kinase (Ph Thr389) | 9234     | Cell Signalling, Massachusetts, USA |
| p53                       | 2324     | Cell Signalling, Massachusetts, USA |
| Stathmin                  | 3352     | Cell Signalling, Massachusetts, USA |
| Vimentin                  | 5741     | Cell Signalling, Massachusetts, USA |

## 2.7.7 Secondary antibodies

**Table 2.9: List of secondary antibodies**

| Item  | Catalogue Number | Supplier                             |
|---|------------------|--------------------------------------|
| Anti-sheep HRP conjugated secondary antibody                        | GL21             | Cytoskeleton, Colorado, USA          |
| Goat anti-Mouse IgG (H+L) Secondary Antibody, HRP conjugated        | 31430            | Invitrogen, California, USA          |
| Goat anti-Rabbit IgG (H+L) Secondary Antibody, HRP conjugated       | 31460            | Invitrogen, California, USA          |
| Goat anti-Rat IgG (H+L) Secondary Antibody, HRP conjugated          | PI-9400          | Vector Laboratories, California, USA |
| Goat anti-Mouse IgG (H+L) Cross-Adsorbed Alexa Fluor 488 conjugate  | A-11017          | Invitrogen, California, USA          |
| Goat anti-Mouse IgG (H+L) Cross-Adsorbed Alexa Fluor 594 conjugate  | A-11005          | Invitrogen, California, USA          |
| Goat anti-Rabbit IgG (H+L) Cross-Adsorbed Alexa Fluor 488 conjugate | A-11070          | Invitrogen, California, USA          |
| Goat anti-Rabbit IgG (H+L) Cross-Adsorbed Alexa Fluor 594 conjugate | A-11012          | Invitrogen, California, USA          |

---

## Chapter 3: Investigating the role of FKBP25 in *in vitro* models of breast cancer de-differentiation

---

### 3.1 Introduction

#### 3.1.1 Breast cancer

Cancer is one of the leading causes of death in the developed world. In Australia, it is estimated that 1 in 2 people will develop cancer in their lifetime (230). In 2021, it is projected that breast cancer will be the most commonly diagnosed cancer according to statistics from the World Health Organisation (231). Worldwide in 2020 alone, breast cancer was the most frequently diagnosed cancer. Breast cancers arise from different types of cells that can be categorised into three broad subtypes, including luminal, human epidermal growth factor receptor 2 (HER2) positive, and triple negative (See **Table 3.1**).

Luminal breast cancer cells express the oestrogen and/or progesterone receptor, while HER2+ express the HER2 receptor in addition to, or in the absence of, ER and PR. In contrast to these cancer types, the triple negative cells do not express any of these receptors. Luminal breast cancers tend to remain as a differentiated tissue, proliferate at a slower pace, and maintain an epithelial phenotype (232). HER2+ breast cancers are increasingly proliferative and begin to lose differentiation of their original cell type (233). Luminal and HER2+ subtypes require hormone stimulation to initiate proliferation, however, triple negative breast cancer cells do not require this stimulation (234). The presence of growth factor receptors and hormone receptors on the surface of cancer cells enables magnified growth and proliferation signalling. This forces cells to proliferate, even in circumstances when they would not usually,

including environmental stresses, such as nutrient or oxygen deprivation. These adaptations allow cells that would usually not survive to thrive.

**Table 3.1 Breast cancer molecular subtypes**

| <b>Subtype</b>               | <b>Luminal</b>  | <b>HER2 +</b>  | <b>Triple negative</b>  |
|------------------------------|---|--|---|
| <b>Molecular Features</b>    | <ul style="list-style-type: none"> <li>• ER or PR positive</li> <li>• HER2 negative</li> </ul>                                      | <ul style="list-style-type: none"> <li>• ER and/or PR positive</li> <li>• HER2 positive</li> </ul>   | <ul style="list-style-type: none"> <li>• ER and PR negative</li> <li>• HER2 negative</li> </ul>                             |
| <b>Morphology</b>            | <ul style="list-style-type: none"> <li>• Round</li> <li>• Epithelial</li> </ul>   | <ul style="list-style-type: none"> <li>• Dependent on molecular signature</li> <li>• Can be more or less mesenchymal</li> </ul>              | <ul style="list-style-type: none"> <li>• Polar</li> <li>• Spindle shaped</li> </ul>   |
| <b>Response to treatment</b> | <ul style="list-style-type: none"> <li>• Responsive to chemotherapy</li> <li>• Responsive to monoclonal antibody therapy</li> </ul> | <ul style="list-style-type: none"> <li>• Somewhat responsive to chemotherapy</li> <li>• Responsive to monoclonal antibody therapy</li> </ul> | <ul style="list-style-type: none"> <li>• Least responsive to chemotherapy</li> <li>• Limited therapies available</li> </ul> |

### 3.1.2 Cancer cells and the cell cycle

As the cancer cells rapidly proliferate which leads to an accumulation of mutations in the regulators of cell cycle progression, and cell cycle checkpoints can become dysregulated and ultimately skipped. This leads to a feed forward loop contributing to excessive proliferation. Proto-oncogenes and tumour suppressor genes are commonly mutated in (See **Figure 3.1**). Proto-oncogenes are genes that are involved in promotion of proliferation signals (236). Mutation to these proto-oncogenes (now called an oncogene) results in the production of mutant proteins that allow cells to rapidly proliferate. Common examples of oncogenes are receptor tyrosine kinases (RTK, e.g., epidermal growth factor receptor/EGFR), regulatory GTPases (Ras), and transcription factors (Myc) (237, 238). Conversely, tumour suppressor genes (TSGs)

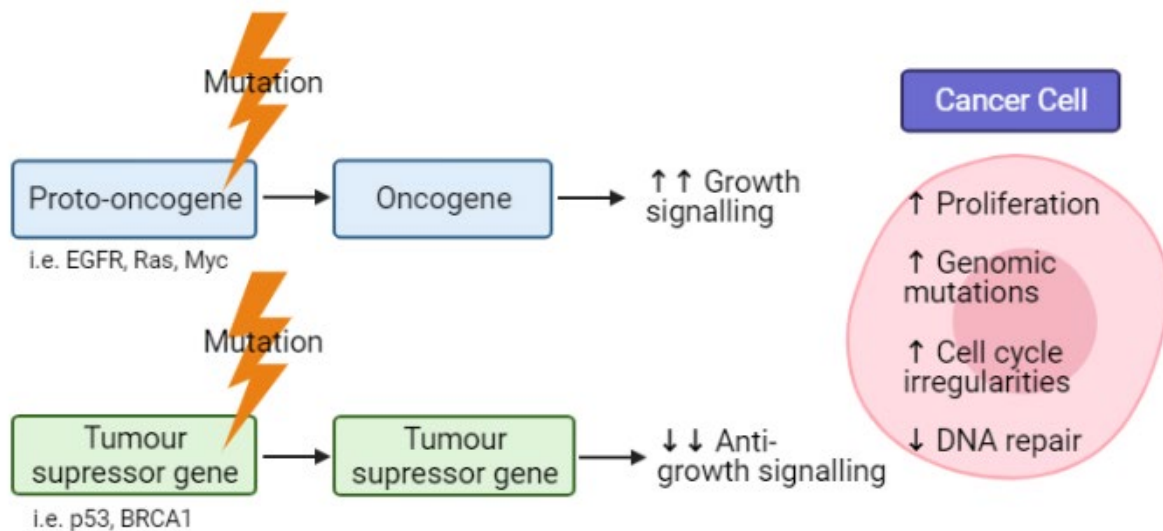


**Figure 3.1: The functions of oncogenes and tumour suppressor genes in cell proliferation**

Oncogenes and tumour suppressor genes are involved in the progression of cancer by increasing growth signalling and decreasing anti-growth signalling, respectively. In combination these functions result in increased proliferation, genomic mutations, and cell cycle irregularities (specifically lack of removal of abnormal cells) and decreased/defective DNA repair. Made with Biorender.com.

are involved in producing anti-growth signals. Proteins that are encoded by TSGs are responsible for regulation of the cell cycle, detecting genomic mutations, and induction of apoptosis of mutant cells (239). Thus, mutations to TSG cause loss of function and subsequent continuation of growth signalling to cells that would, under normal circumstances, be removed from the cell cycle (239). The most commonly mutated TSG is p53, which is mutated in ~50% of human cancers (214). p53 is transcription factor that is responsible for activation of DNA repair and removal of cells containing mutant DNA from the cell cycle through the induction of cyclin dependant kinase inhibitor, p21 (240). Similarly, in the case of breast cancer, a TSG known as Breast cancer type 1 (BRCA1) encodes a DNA repair enzyme that is frequently mutated and is utilised as a predictive marker of familial breast cancer susceptibility (241-243). Triple negative breast cancer has a strong association with both BRCA1 and p53 mutations that, in turn, results in aggressive, heterogenous disease (244). As such, triple negative breast cancer cells can proliferate freely, readily de-differentiate and become increasingly mesenchymal.

### 3.1.3 Epithelial to mesenchymal transition

The transition of breast cancer cells from epithelial to mesenchymal (epithelial to mesenchymal transition, EMT; See **Fig 3.2**) is an essential process that is required for progression to metastatic disease (235, 236). Importantly, to effectively treat these aggressive cancers, first the molecular mechanisms that enable cells to survive must be understood. In our preliminary studies (to be discussed in this chapter), it was identified that FK506 binding protein 25 (FKBP25) is lost in dedifferentiated mesenchymal type cells. Previous studies have described the role of FKBP25 in proliferation, tubulin dynamics, DNA double stranded break repair, and p53 regulation, all of which are essential processes involved in cancer progression (109, 119, 237). The role of FKBP25 in cancer progression and epithelial to mesenchymal transition, however, is yet to be examined prior to this thesis.

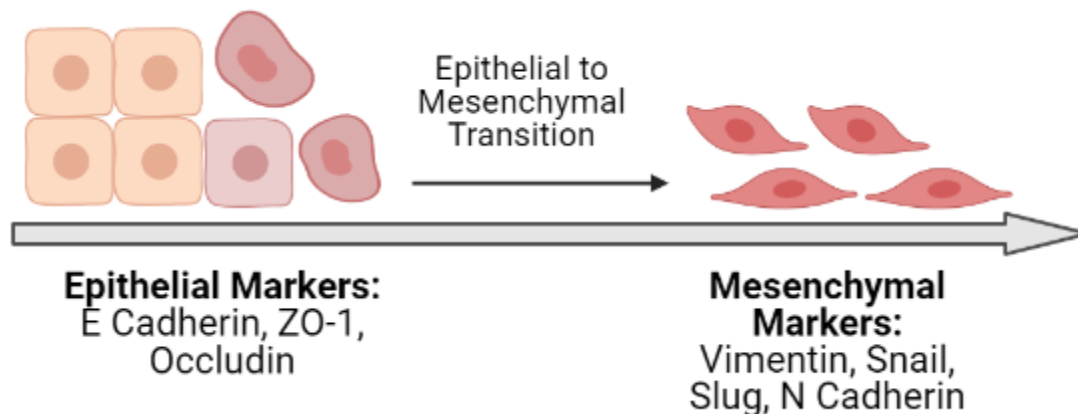


**Figure 3.2: Epithelial to mesenchymal transition (EMT)**

EMT refers to the process of epithelial cells lose their polarity and gain migratory and invasive characteristics. EMT is seen in cancer metastasis, tissue fibrosis, and wound healing. Epithelial phenotype markers include E cadherin, ZO-1, and occludin. These molecules are tight junction molecules that anchor epithelial cells together. Mesenchymal phenotype markers include vimentin, Snail, Slug, and N-cadherin. Vimentin and N cadherin are structural molecules that are advantageous to the mesenchymal phenotype. Snail and Slug are mesenchymal transcription factors that impair epithelial-associated gene expression (i.e. E cadherin). Made with Biorender.com.

### 3.1.4 Molecular features of EMT in breast cancer

Within a solid tumour, the cells are able to maintain epithelial characteristics including, polarity, cell to cell adhesions, and adhesion to a basement membrane (238). Conversely, mesenchymal cells lose these features and gain invasive and migratory abilities (238). EMT requires a plethora of mutations and molecular alterations to maintain and induce a mesenchymal phenotype. Upon induction of the EMT program, mesenchymal zinc finger transcription factors, including SNAI1 (Snail), SNAI2 (Slug), ZEB1, and ZEB2 are transcribed to facilitate a more mesenchymal phenotype. These EMT transcription factors have been demonstrated to repress E cadherin expression, an essential epithelial cell adhesion molecule (239, 240). Cadherins are a family of calcium-dependent adhesion molecules (CAMs) that form adherens junctions between cells, which are required to maintain epithelial cell structure, function, and importantly, cell polarity. E-cadherin is a transmembrane protein that is bound to catenin molecules on its cytoplasmic domain. Catenin molecules act as an anchor between cadherins and the actin cytoskeleton and are involved in stimulation of the Wnt signalling pathway (241). Wnt signalling is associated with tissue regeneration, cell polarity and intracellular calcium handling (242-244). The loss of E cadherin is a vital event in the EMT program. For example, suppressed E cadherin expression can result in disrupted cell-cell adhesion and distorted Wnt signalling. Common cancer associated effects of Wnt signalling include, rapid cell division and the onset of cell migration, which intimately links Wnt signalling with the onset of metastasis. Additionally, the EMT transcription factor, Snail, has also been shown to facilitate expression of mesenchymal proteins including, vimentin, an intermediate filament that is expressed in mesenchymal cells (245). Vimentin is an important marker of the transition of cells from epithelial to mesenchymal phenotype. While vimentin

expression is commonly used to identify mesenchymal tissue in cancers, the function of vimentin in the progression of cancer is poorly understood. However, there is some literature that suggests that vimentin is associated with increased migration capacity and facilitation of mutant H-Ras signalling events (246, 247). Upon activation of these pathways the transitioned cells begin to exhibit mesenchymal characteristics which are, in fact, similar to the features of developmental and precursor tissue/cells.

### 3.1.5 Features of metastatic breast cancer cells

An important feature of mesenchymal cells is their ability to metastasise from a primary site to a secondary site and colonise a secondary tumour (248). Breast cancer cells undergo rigorous selection that enables their survival through the process of metastasis. Adequate transition from epithelial to mesenchymal phenotype is the most prominent factor influencing metastatic success (249). An important feature of metastatic mesenchymal cancer cells is their ability to migrate and invade. Konen et al., described a profile for successful metastatic cells which they have termed “leader cells” (250). This profile depicts leader cells as cells that have an increased capacity for focal adhesion-kinase signalling which forges a pathway for the rest of the metastatic population termed “follower cells” (250). Follower cells are depicted as cells that trail behind the leader cells that drive invasion, and importantly, are the cells that propagate at a secondary site (250). It is essential that basal/differentiated cancer cells are able to switch on EMT-related gene expression to promote their survival as an invasive and de-differentiated phenotype (251). It has been described that *in vitro*, invasive leader cells can be further characterised by their ability to express basal markers, including cytokeratin-14, p63, P-cadherin, and cytokeratin-5 (251). Interestingly, leader cells were also demonstrated not to express Twist, Slug, or vimentin, which are classically associated with EMT (251). The ability of these cells to

maintain expression of basal markers enables them to switch from a mesenchymal phenotype back to an epithelial-like phenotype to colonise at a secondary site, suggesting a only a partial EMT (252). These partially committed mesenchymal cells follow leader cells in regard to migration and invasion, however, can become fully de-differentiated into a mesenchymal cell by environmental factors such as stress or hypoxia (253). Alternatively, phenotypic stability factors (PSFs) are involved in maintaining an intermediate phenotype between epithelial-like and mesenchymal. Notable PSFs include OVOL, NRF2, GRHL2, NUMB, and NFAT ((254-258) See **Table 3.2**). These PSFs, respectively, have been shown to impair complete EMT, such that knockdown of these proteins *in vitro* has been demonstrated to impair EMT behaviours, such as collective migration (255, 257). These features of EMT can be exploited to develop novel therapeutics that can prevent complete mesenchymal transition. As such, it is vital that facilitators and inhibitors of EMT are identified to develop appropriate interventions.

Considering the proposed roles of other FKBP molecules (including FKBP51 and FKBP52) in the pathogenesis of cancers and promotion of EMT, it is plausible that FKBP25 may also be involved in these processes. Although, to date, there has been limited studies that examine a biological role of FKBP25, especially in a cancer setting. However, these studies have given valuable insight to the molecular interactions and potential pathways that could contribute to cancer related de-differentiation.

**Table 3.1: Functions of phenotypic stability factors (PSFs)**

| <b>PSF</b> | <b>Function</b>  |
|------------|--|
| OVOL1/2    | OVOL inhibits transcription of Zeb1 protein.   |
| NRF2       | NRF2 inhibits Snail activation, which consequently prevents E cadherin and Zeb1 degradation.       |
| GRHL2      | GRLH2 induces E cadherin expression and inhibits Zeb1.   |
| NUMB2      | NUMB2 inhibits Notch signalling (i.e. Notch receptor, Delta, Jagged, Notch intra-cellular domain). |
| NFAT       | NFAT activation promotes E cadherin expression.  |

### 3.1.6 Chapter Aims:

In the first chapter of this thesis, the aims are to investigate the role of FKBP25 in a variety of breast cancer EMT and de-differentiation models.

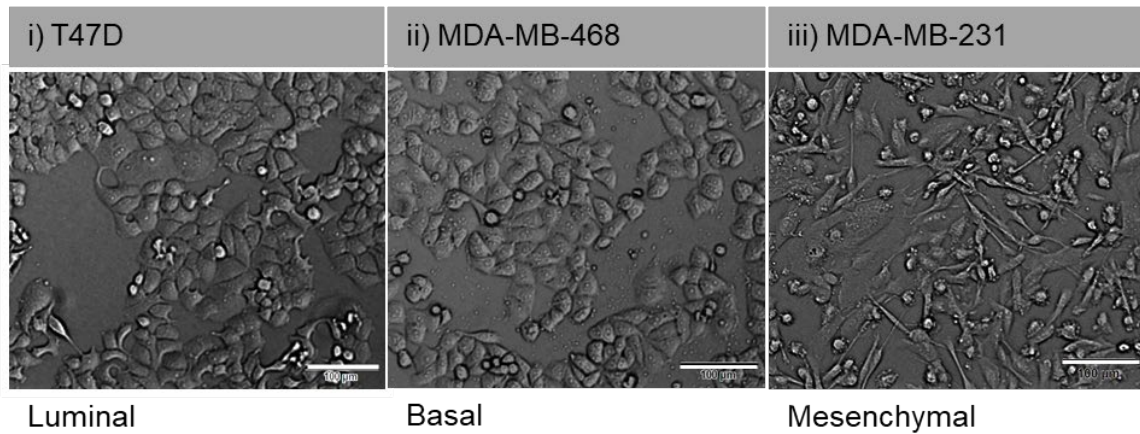
1. To investigate the expression of FKBP25 in breast cancer subtypes
2. To examine the impact of FKBP25 expression upon induction of oncogenic mutations.
3. To determine the effects of epidermal growth factor mediated EMT on FKBP25 expression.
4. To determine the signalling pathways that influence FKBP25 protein expression.

## 3.2 Results

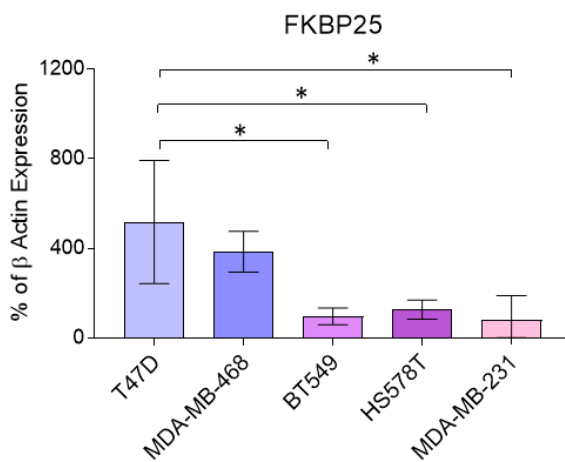
### 3.2.1 FKBP25 expression remains elevated in luminal and basal breast cancer cell subtypes and is reduced in mesenchymal subtypes.

To examine the expression of FKBP25 throughout breast cancer progression, a panel of different breast cancer cells and subtypes were assessed. These subtypes ranged from epithelial-like luminal cells (T47D, **Fig 3.3 A i**), triple negative basal cells (MDA-MB-468, **Fig 3.3 A ii**), and triple negative mesenchymal cells (BT 549, HS578T and MDA-MB-231 pictured in **Fig. 3.3 A iii**). It was found that these cell lines displayed differential expression patterns, in which the mesenchymal subtype had significantly reduced FKBP25 expression compared to the luminal subtype (**Fig 3.3 B and C**). To further examine the differential expression of FKBP25, localisation immunofluorescent staining was performed. Here it was identified that in normal mammary epithelium (MCF10A cells, **Fig 3.4 A**) FKBP25 is evenly dispersed throughout the cytoplasmic and nuclear compartments, a pattern also seen in T47D and MDA-MB-468 cells (**Fig 3.4 B and C**, respectively), while MDA-MB-231 cells showed less staining in the nuclear compartment (**Fig 3.4 D**). This reduction in protein dispersion in the cell may be accounted for by the reduction in overall expression in mesenchymal cell types. The reduction in FKBP25 protein expression described in Figure 3.3 was not observed in immunofluorescent staining as these experiments were undertaken to localise FKBP25 rather than quantify protein expression.

A)



B)



C)

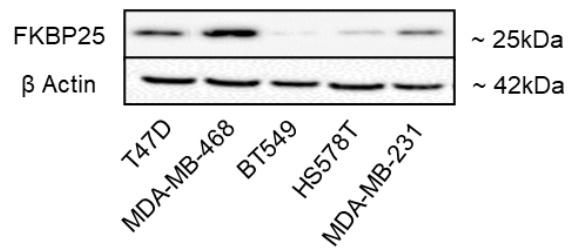


**Figure 3.3: FKBP25 expression across a panel of breast cancer cells**

**A)** Morphology of breast cancer cell lines, including luminal (T47D) and triple negative subtypes basal (MDA-MB-468) and mesenchymal (MDA-MB-231). **B)** FKBP25 is highly expressed in epithelial-like cell lines T47D and MDA-MB-468, compared to that of mesenchymal cell lines. **C)** Representative blot of FKBP25. Scale bar = 100µm. Data presented as mean  $\pm$  SD of n=3, \* = p<0.05

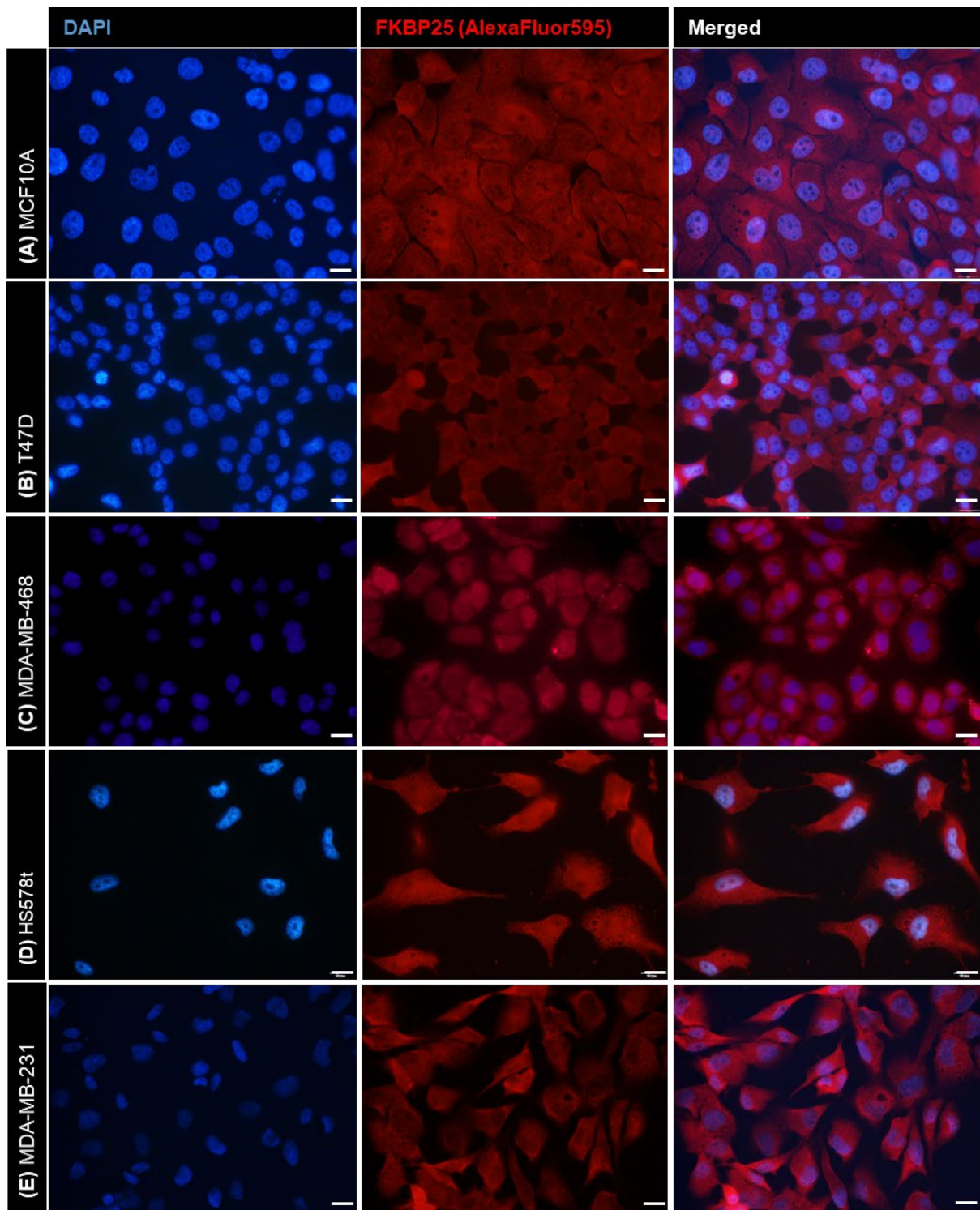


**Figure 3.4: Localisation of FKBP25 in breast cancer cell subtypes**  
 FKBP25 is located in the cytoplasm of immortalised mammary epithelial cells (A) MCF10A, Luminal cell line (B) T47D, basal cell line (C) MDA-MB-468, and mesenchymal cell lines (D) MDA-MB-231 and (E) HS578t. Images taken at X60 magnification, scale bar = 10µm. N=3

### 3.2.2 FKBP25 expression is increased upon oncogenic transformations of Ras and p53 but is reduced in metastatic clones of MDA-MB-231 cell line.

Next, it was assessed how oncogenic transformations alter FKBP25 expression in mammary epithelial cell line, MCF10A. The first mutations to be assessed were two common p53 mutations, WT knockdown (shown as Mir 4, with mCherry expression vector control) and a gain of function mutation (shown as p53<sup>R273H</sup>, with GFP expression vector control). This R273H p53 mutation is described as dominant negative i.e. this mutation will override WT p53 function to facilitate an invasive and migratory phenotype (259). While these mutations result in changes to in vitro cell behaviours (260), there are no notable morphological changes to the MCF10A cells when grown in a 2D culture (**Fig 3.5 A**). In response to these p53 mutations, it was found that there is an additive increase in FKBP25 expression upon WT p53 knock down and p53<sup>R273H</sup> expression (**Fig 3.5 B**). Additionally, in response to these p53 mutations, there are reductions in both MDM2 and p21, the repressor and product of WT p53 activation compared to WT control (mCherry/GFP, **Fig 3.5 C**). The second mutation that was assessed was Ras<sup>V12</sup>, a constitutively active mutation resulting in hyper activation of the Ras signalling cascade (261). In MCF10A cells, the Ras<sup>V12</sup> mutation resulted in an altered morphology in which the cell's characteristic cobble stone appearance is lost and adopts a spindle-like morphology (**Fig 3.6 A**). Similar to the p53 model, there was an increase in FKBP25 expression upon Ras<sup>V12</sup> mutation (**Fig 3.6 B and C**).

While these single mutations are not representative of a complete oncogenic transformation and dedifferentiation, they are able to give some insight to the biological

role of FKBP25 in the associated signalling pathways (i.e. Ras and p53 signalling). To further elucidate the impact of dedifferentiation on FKBP25, the next model to be examined were clones of the parental MDA-MB-231 cell line, referred to as clones #16 and #17. Upon preparation of these clones, cells were transfected with ectopic matrix metalloproteinase 2 (MMP-2), an enzyme that is required to degrade the extracellular matrix, which is required to allow malignant cells to evade their site of origin (262). Single clones were selected and propagated, which resulted in populations of cells which exhibited vastly different behaviours. While both clones over expressed MMP-2, it was found that they had substantial morphological and behavioural differences. It was found that clone #16 was more migratory and invasive with increased propensity to metastasise to bone *in vivo*, while #17 is highly proliferative but not invasive (Unpublished Price lab data). The morphology of these cells was observed to be slightly different, whereby #16 cells are long, and spindle shaped, and #17 cells tended to be more rounded and shorter (**Fig 3.7 A**). While clone #17 was highly proliferative it lacked the migratory and invasive capacity of clone #16. Interestingly, FKBP25 was found to be increased in the proliferative non-invasive #17 clone compared to invasive #16 (**Fig 3.7 B and C**). These findings support the initial hypothesis that loss of FKBP25 expression is associated with a mesenchymal phenotype (#16), while greater FKBP25 expression is associated with a differentiated, more epithelial-like phenotype (#17).

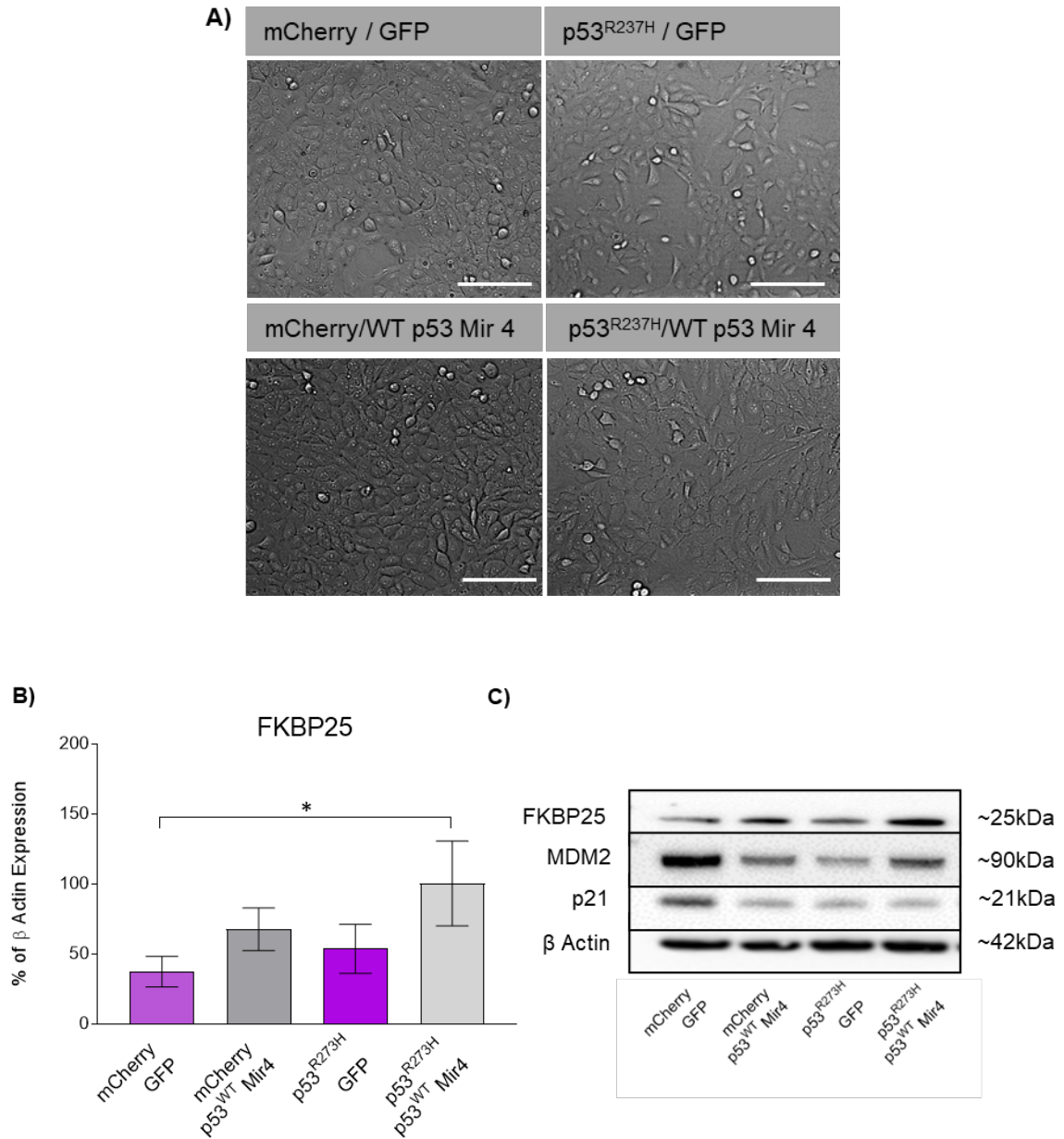


**Figure 3.5: Expression of FKBP25 in p53 mutant mammary epithelial cell line**

**A)** Morphology of MCF10A cells containing one or both of p53<sup>R237H</sup> mutation (with control mCherry), and wild type (WT) p53 knockdown (Mir 4, with GFP control). **B)** FKBP25 expression is increased with both p53 mutant and WT knockdown compared to mCherry/GFP control. **C)** Representative blot. Scale bar = 100 $\mu$ m. Data presented as mean  $\pm$  SD of n=3, \* =  $p \leq 0.05$

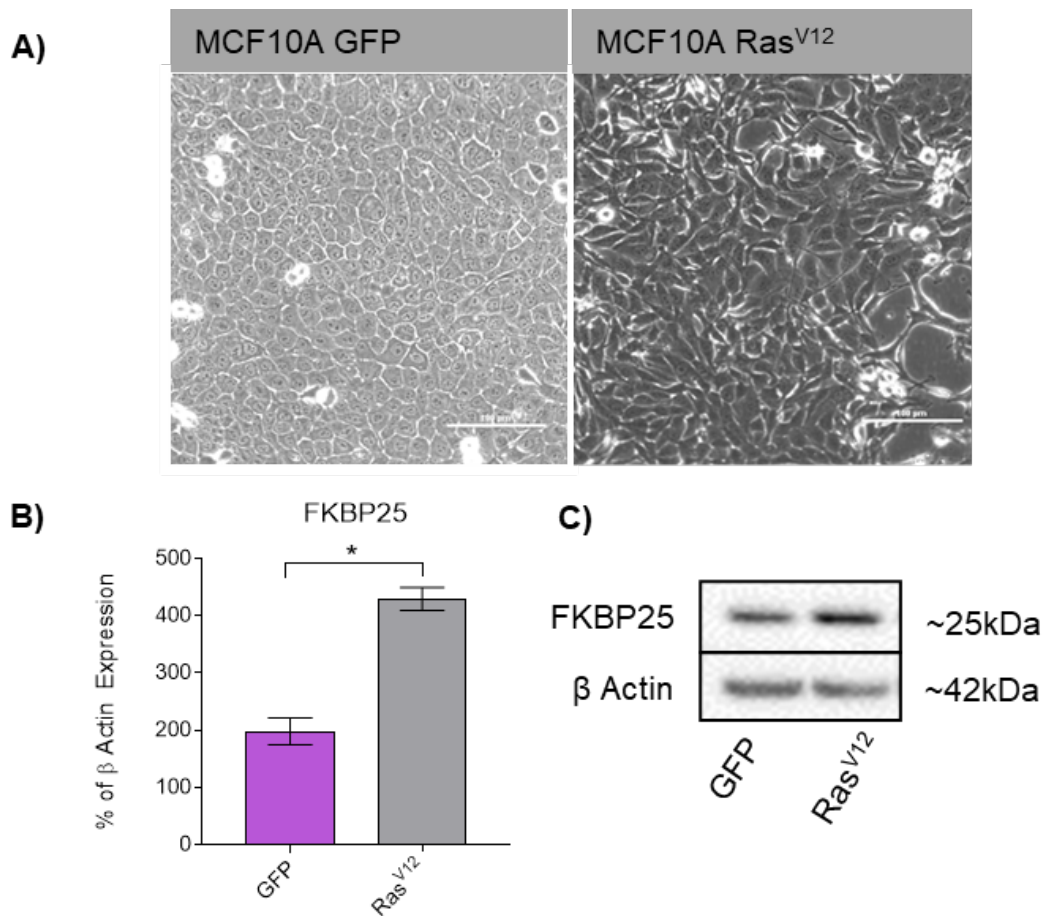


**Figure 3.6: Expression of FKBP25 in Ras transformed mammary epithelial cell line**

**A)** Morphology of MCF10A GFP (immortalised breast epithelium) and MCF10A Ras<sup>V12</sup> (breast epithelium transformed with constitutively active Ras mutation). **B)** MCF10A GFP, a cell line with epithelial morphology expresses lower levels of FKBP25, compared to MCF10A Ras<sup>V12</sup> which is mesenchymal. **C)** Representative blot of FKBP25 expression. Scale bar = 100 $\mu$ m. Data presented as mean  $\pm$  SD of n=3, \* =  $p \leq 0.05$

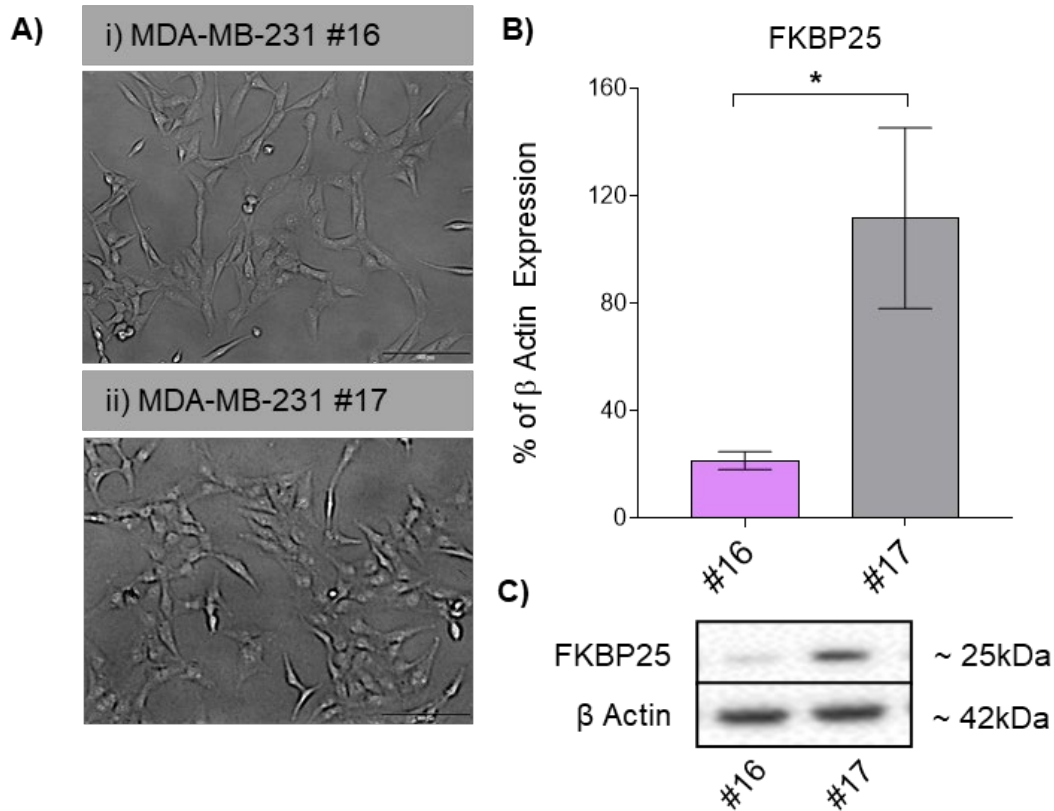


**Figure 3.7: FKBP25 expression in invasive (#16) and non-invasive (#17) MDA-MB-231 clones**

**A)** Morphology of MDA-MB-231 clones i) #16, a highly invasive clone, and ii) #17, a proliferative, non-invasive clone. **B)** FKBP25 expression is reduced in the invasive clone #16 compared to non-invasive #17. **C)** Representative blot of FKBP25 expression. Scale bar = 100 $\mu$ m. Data presented as mean  $\pm$  SD of n=3, \* =  $p \leq 0.05$

### 3.2.3 FKBP25 expression is decreased upon epidermal growth factor-mediated epithelial to mesenchymal transition (EMT) in MDA-MB-468 breast cancer cell line.

To examine the impact of EMT on FKBP25 expression, next an EGF-mediated EMT model in MDA-MB-468 cells was assessed. The MDA-MB-468 breast cancer cell line is known to over express the EGF receptor, which is characteristic of triple negative breast cancer cell lines (263, 264). It is a well-established method to induce EMT in MDA-MB-468 cells by stimulating them with EGF over a period of time (265-269). Upon induction of EMT, cells begin to express mesenchymal markers including, intermediate filament, vimentin, and transcription factors including, snail and slug (270).

Additionally, cells that have undergone EMT will display a reduction in epithelial markers, including that of E cadherin (271). Upon 72-hour stimulation with 50ng/ml of recombinant EGF, a clear morphological change was observed in the epithelial-like basal MDA-MB-468 cells (**Fig 3.8 A i**) to a spindle shaped mesenchymal morphology (**Fig 3.8 A ii**). In addition, it was observed that upon E cadherin staining there was a reduction and shift in localisation away from the cell periphery (**Fig 3.8 B i and ii**), where E cadherin normally functions as a cell adhesion molecule. Furthermore, it was demonstrated by immunoblot that there was a significant reduction in E cadherin and an increase in vimentin expression (**Fig 3.9 A, B and D**). Importantly, EGF-induced EMT was also associated with a reduction in FKBP25 (**Fig 3.9 C and D**). These data suggest that, as breast cancer cells undergo EMT, and become more dedifferentiated, there is a parallel loss of FKBP25 expression. To establish the mechanism by which this reduction of FKBP25 occurs, next examined EGF stimulated MDA-MB-468 cells

treated with a series of small molecule inhibitors, including LY294002 (25 $\mu$ M; PI3K inhibitor), PD325901 (100nM; Mek inhibitor), and rapamycin (50nM; mTOR inhibitor). Cells were plated and pre-treated with 50ng/ml of EGF as per previous EMT experiments (See **Fig 3.8 and 3.9**), followed by a 24-hour treatment with respective inhibitors. It was observed that while FKBP25 reduction was achieved upon EGF treatment, there were no changes to FKBP25 protein expression in response to inhibitor treatment (**Fig 3.10 A**). Upon examination of inhibitor pathways, it was determined that LY294002 did not alter the ratio of total Akt to phosphorylated Akt (**Fig 3.10 B**). However, it was able to reduce total Akt protein (See blot **Fig 3.10 E**). PD325901 treatment was not found to impair Erk phosphorylation in an unstimulated state, however, upon EGF stimulation Erk phosphorylation is blunted (**Fig 3.10 C**). Finally, p70s6K phosphorylation was demonstrated to be reduced by both LY294002 and rapamycin (**Fig 3.10 D**). Considering LY294002 should inhibit Akt, and thus indirectly inhibit mTOR mediated phosphorylation of p70s6K, this reduction was anticipated. Together, this data suggests that none of these pathways are involved in the EGF-mediated reduction in FKBP25 protein expression.

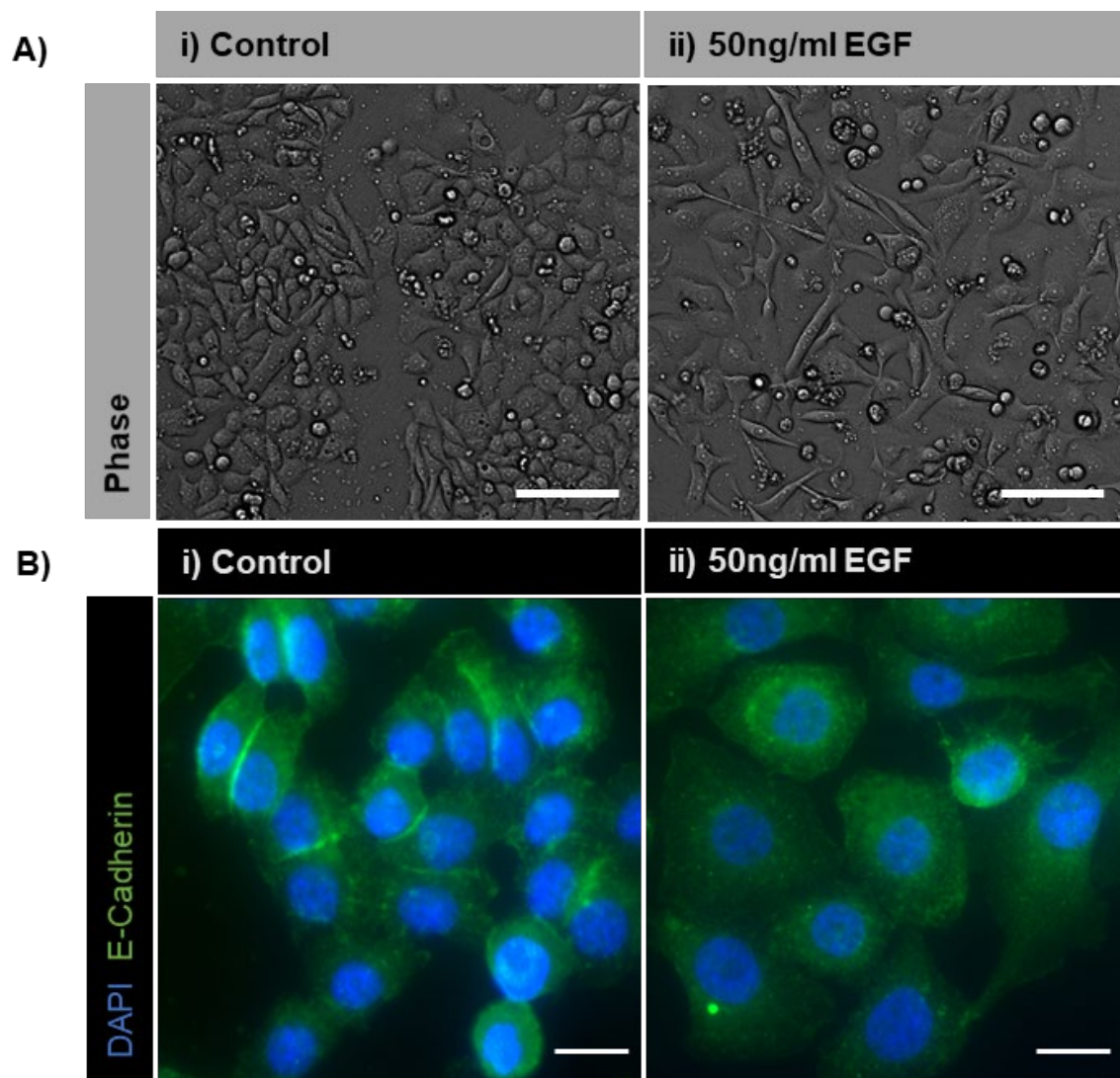


**Figure 3.8: Epidermal Growth factor (EGF) mediated epithelial to mesenchymal transition (EMT) in MDA-MB-468 breast cancer cells**  
**A)** Morphological changes of MDA-MB-468 cells (i) control or treated with (ii) 50ng/ml EGF displaying loss of round epithelial shape and shifting to an elongated spindle shape. **B)** Immunofluorescence of MDA-MB-468 cells (i) control or treated with (ii) 50ng/ml EGF stained with E cadherin and DAPI. Treated cells show loss of membrane bound E cadherin and redistribution to the cytoplasm. Top scale bars = 100 $\mu$ m, Bottom scale bars = 20 $\mu$ m. Data presented as mean  $\pm$  SD of n=3, \* = p $\leq$ 0.05

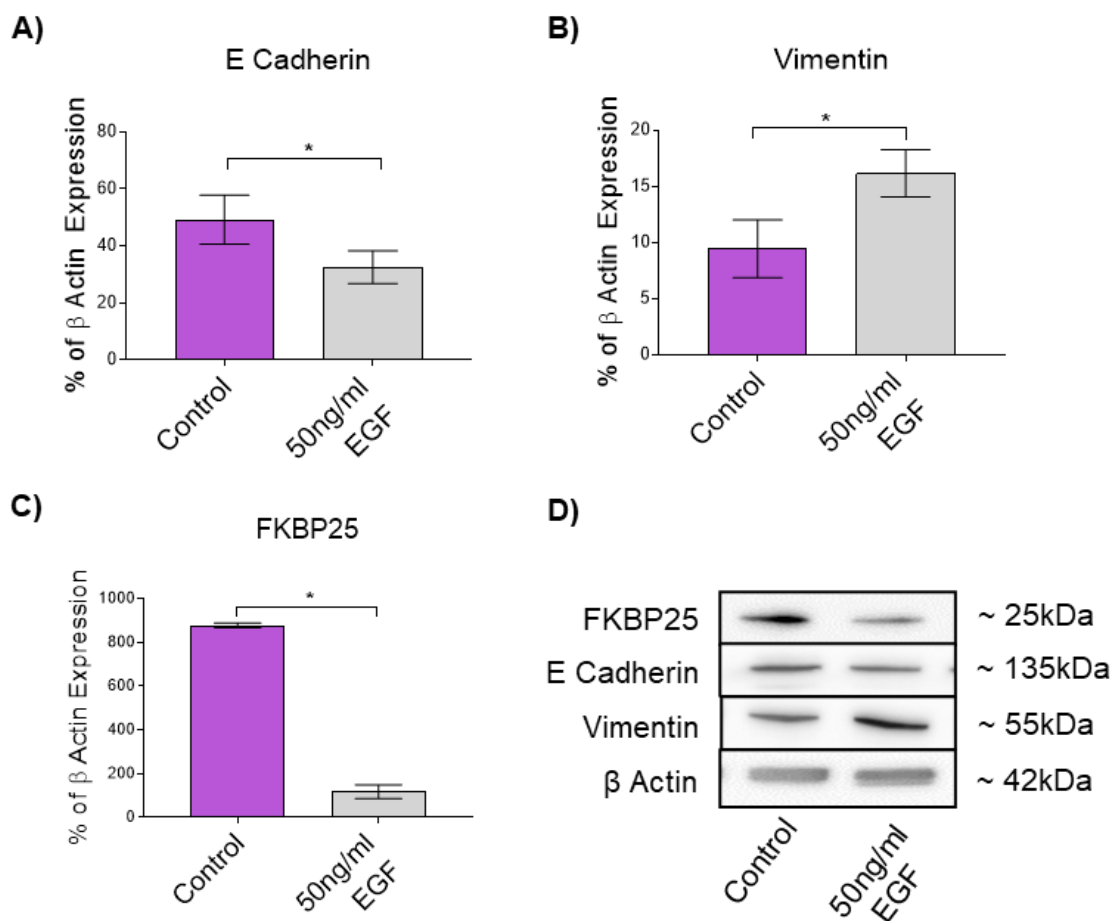


**Figure 3.9: Epidermal growth factor (EGF) mediated epithelial to mesenchymal transition in MDA-MB-468 breast cancer cells**  
 Upon treatment with 50ng/ml EGF MDA-MB-468 cells express reduced levels of **A)** E cadherin, and **B)** vimentin, and results in reduced levels of **C)** FKBP25. **D)** Representative blots. Data presented as mean  $\pm$  SD of n=3, \* =  $p \leq 0.05$

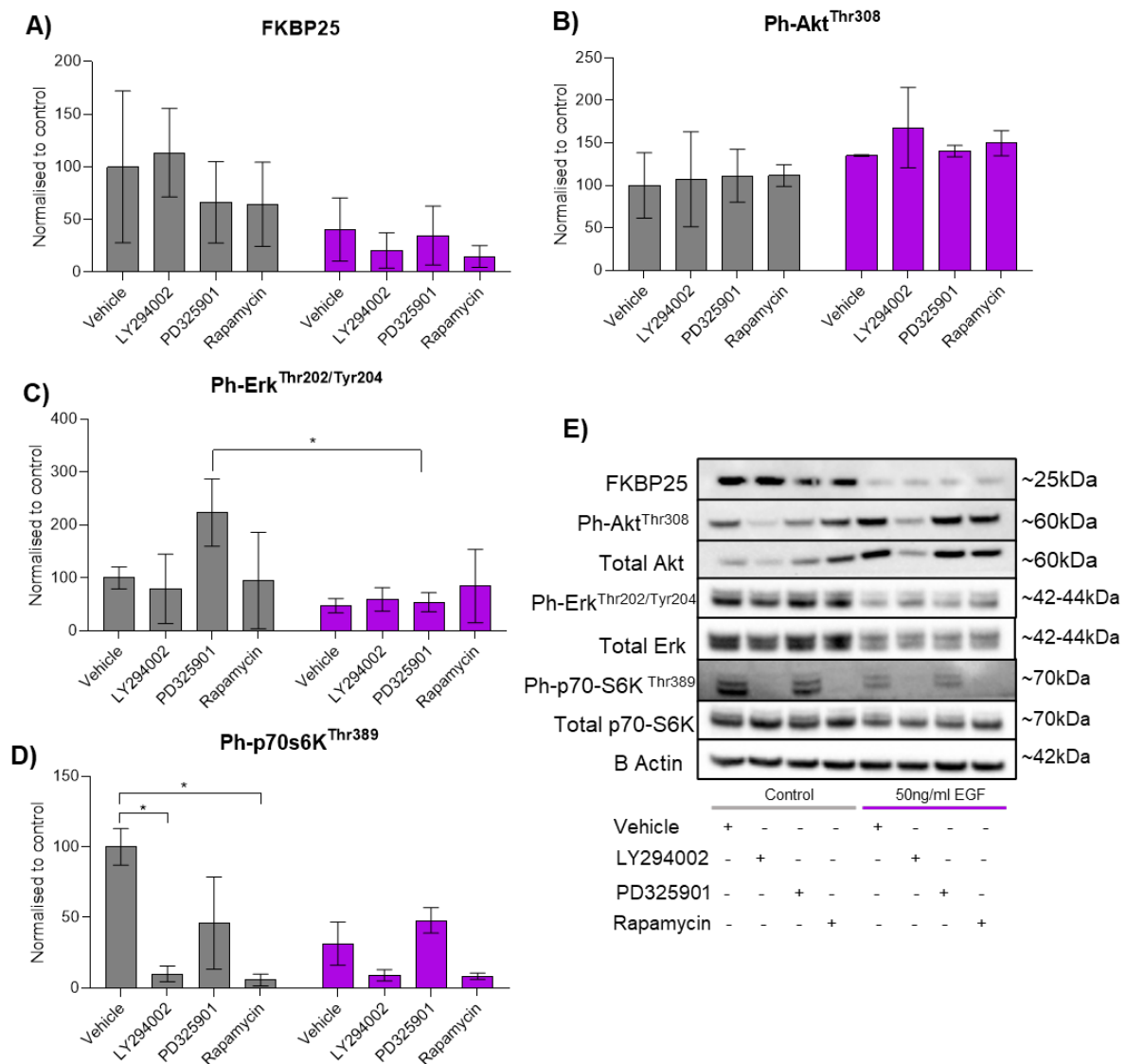


**Figure 3.10: The EGF-mediated reduction of FKBP25 protein in MDA-MB-468 is not altered with small molecule inhibitor treatment** MDA-MB-468 cells were treated for 24 hours with one of, DMSO vehicle (0.001% (v/v)), LY294002 (PI3K inhibitor, at 25µM), PD325901 (Mek inhibitor, at 100nM), or rapamycin (mTOR inhibitor, at 50nM) in the presence or absence of EGF. All data is presented as a phosphorylated to total protein ratio, normalised to vehicle expression. **A)** FKBP25 protein expression was reduced upon EGF treatment. **B)** Phosphorylation of Akt<sup>Thr308</sup> was unaltered upon drug treatments. **C)** Phosphorylation of Erk<sup>Thr202/Tyr204</sup> was unaltered with drug treatment. **D)** Phosphorylation of p70s6K<sup>Thr389</sup> was reduced with both LY294002 and Rapamycin. **E)** Representative blots. All data is presented as mean±SD, n=3, \*p≤0.05.

### 3.3 Discussion

#### 3.3.1 FKBP25 expression remains elevated in luminal and basal breast cancer cell subtypes and is reduced in mesenchymal subtypes.

In this study, we have examined breast cancer cells from both the luminal (T47D) and triple negative subtypes (MDA-MB-468, HS578t, BT549, and MDA-MB-231). Triple negative breast cancer cells can be further subdivided into two subtypes, basal and claudin-low. Basal-like breast cancer cells maintain more epithelial features, such as cytokeratin filaments, which enable them to remain anchored within the tissue and maintain epithelial morphology (248). Claudin-low cells are highly mesenchymal and do not express tight junction adhesion molecules (such as claudin) which enables them to migrate and metastasise easily (272). Our studies have revealed an expression pattern in which FKBP25 is expressed highly in breast cancer cells with a more epithelial phenotype, i.e., luminal, and basal cell types, compared to those with a mesenchymal phenotype i.e., claudin low (**Fig 3.2**), suggesting that the loss of FKBP25 expression may be beneficial for the mesenchymal phenotype of breast cancer cells.

Current literature suggests that FKBP25 is required for the formation and stability of both the meiotic and mitotic spindles (109, 121). It has also been demonstrated that FKBP25 is a microtubule stabiliser, playing an essential role in forming the mitotic spindle and that the loss of FKBP25 resulted in dysregulated cell division (273). However, this mechanism has not been examined in the context of cancer cells, specifically that of mesenchymal breast cancer cells. It is well documented that the acquisition of genomic instability and mutations is a classic hallmark of cancer (129), and some findings suggest that decreased microtubule stability is a hallmark of EMT,

being beneficial for cell migration and polarity (274). This appears to be contradicted in #17 clones, which express significantly higher levels of FKBP25 compared to #16 clones. However, typical MDA-MB-231 cells were demonstrated to express low levels of FKBP25 (**Fig 3.3**), similar to #16 clones. Considering #17 clones display less invasive behaviours, which may be comparable to MDA-MB-468 cells, which were shown to express high levels of FKBP25. Thus, this data supports the hypothesis that FKBP25 is highly expressed in breast cancer cell lines with an epithelial-like phenotype.

To further examine the involvement of FKBP25 in breast cancer cells, the localisation of FKBP25 was examined in a variety of cell lines.. Under normal conditions it was found that, in MCF10A, T47D, MDA-MB-468, and MDA-MB-231 cells, FKBP25 is located in both the cytoplasm and nucleus of the cells (**Fig 3.3**). Current literature has shown that FKBP25 is able to be shuttled between the nucleus and cytoplasm which is mediated by the N-terminal PPlase domain upon exposure to stress (113). This suggests that the ubiquitous localisation of FKBP25 throughout the cells describes a basal amount of stress in these breast cancer cells. It is also known that FKBP25 has several functions in the cytoplasm, including interaction with the pre-60S ribosome (110), microtubule stabilisation (109), and interactions with double stranded RNA (dsDNA; structure is transfer RNA, ribosomal RNA, and microRNA (275)) (112). Further studies on these multifaceted roles of FKBP25 are required to fully elucidate the role of FKBP25 in the mesenchymal phenotype.

### 3.3.2 FKBP25 expression is increased upon oncogenic transformation of Ras and p53 but is reduced in metastatic clones of MDA-MB-231 cell line.

To begin the characterisation of FKBP25 in oncogenic transformation the MCF10A immortalised mammary epithelial cell line with constitutively expressed mutant p53, or wild type (WT) knockdown was examined (**Fig 3.6**). The p53<sup>R237H</sup> mutant, is a gain of function mutation which causes increased proliferation, migration, and invasion abilities in numerous cell lines (276). Upon knockdown of WT p53, there is an increase in FKBP25 protein expression. While the expression of the mutant p53<sup>R237H</sup> had little effect of FKBP25, the dual expression of mutant p53 and WT knockdown resulted in a significant increase in FKBP25, suggesting that mutant p53 is a driver of FKBP25 expression. Upon manipulation of p53 there were also clear reductions in p53 repressor, mouse double minute 2 (MDM2), and p53 target protein, p21 (**Fig 3.4 C**).

Interestingly, FKBP25 induces autoubiquitination of MDM2, a repressor of WT p53, resulting in its degradation (119). In mCherry/GFP (containing WT p53) cells, it was observed that there was low FKBP25 expression, which increased the expression of MDM2 and p21 (**Fig 3.4 C**). However, when p53 was manipulated, with either WT KD (Mir4) or expression of p53<sup>R237H</sup>, there were aberrations to both MDM2 and p21 protein expression (**Fig 3.4 C**). This model has enabled us to confirm a relationship between p53 mutation and FKBP25 expression which may be involved in de-differentiation and transition to a mesenchymal phenotype.

The next model to be examined was the MCF10A cell line with a constitutively active H-Ras<sup>V12</sup> mutation. H-Ras is a small GTPase second messenger protein that is involved in several signalling cascades, including MAPK/ERK signalling and PI3K

pathways (277) Under normal conditions, Ras GTPases exist as an inactivate GDP bound form which, upon receptor binding, is phosphorylated into its active GTP-bound form. Ras family members, including H-Ras, K-Ras, and N-Ras, are well characterised proto-oncogenes that frequently acquire hotspot mutations in many human cancers (278, 279). Upon mutation to Ras GTPases, namely a glycine to valine substitution at position 12 (H-Ras<sup>V12</sup>), renders the molecule permanently 'switched on' and unable to hydrolyse bound GTP to GDP, ultimately resulting in uncontrolled proliferation signals (280). To examine the role of FKBP25 in cell growth and proliferation, we examined FKBP25 expression in this MCF10A H-Ras<sup>V12</sup> model. It was observed that constitutive activation of Ras was associated with an increase in FKBP25 expression (**Fig 3.5**) Again, contrary to our hypothesis, this proliferative, mesenchymal model displays increased expression of FKBP25. Considering the findings that FKBP25 protein expression is decreased in mesenchymal breast cancer cells (**Fig 3.3**) and in EGF mediated EMT (**Fig 3.4**) it was anticipated that this H-Ras mutant phenotype would also result in reduced FKBP25 expression. It is important to appreciate, however, that while this model contains a H-Ras mutation, the MCF10A cells are otherwise normal immortalised mammary epithelium (281). This may indicate that alterations to FKBP25 expression in mesenchymal cells is multifaceted and reliant on acquisition of other mutations associated with cancer progression. Similarly, in the p53 model previously described, this model contains one oncogenic transformation that is insufficient to induce a complete neoplastic transformation. These findings highlight those multiple mutations are required for de-differentiation associated with the mesenchymal phenotype.

To further elucidate the potential role of FKBP25 in proliferation and dedifferentiation of breast cancer cells, a pair of MDA-MB-231 breast cancer cell line clones with

different proliferative and metastatic phenotypes was examined. These studies identified that FKBP25 expression is significantly reduced in clone #16 cells compared to #17 cells (**Fig 3.6**). This model demonstrates that FKBP25 expression is increased in the proliferative, less invasive clone (#17), compared to the less proliferative, invasive clone (#16). These data consolidate our previous findings in section 3.2.1, where it was identified that FKBP25 protein expression is low in de-differentiated, mesenchymal breast cancer subtypes (**Fig 3.2**). While it was demonstrated a difference in FKBP25 expression in these MDA-MB-231 clones, further investigation is required to understand the role of FKBP25 in the mesenchymal phenotype.

### 3.3.3 FKBP25 expression is decreased upon epidermal growth factor mediated epithelial to mesenchymal (EMT) in MDA-MB-468 breast cancer cell line.

Hormone receptor signalling and breast cancer are intricately linked in the pathogenesis of the disease. Breast cancers are typically associated with amplified expression of ER, PR, or HER2 which result in dysregulated and excessive proliferation (282). Similar to HER2, the epidermal growth factor receptor (EGFR/HER1) is a tyrosine kinase receptor that facilitates cell proliferation and growth (283). Importantly in breast tissue, EGFR signalling is integral for mammary development whereby loss of receptor signalling results in impaired ductal and epithelial growth (284). In many human cancers, EGFR is amplified or mutated resulting in aberrant signalling and, as such, has become an attractive target for antiproliferative drugs in many cancer types, including lung (285) and breast (286). Overstimulation of these receptor pathways can result in epithelial to mesenchymal transition in effected cells (EMT) (287).

The process of EMT occurs when epithelial cells lose epithelial features, such as cell adhesion and cell polarity, and acquire invasive mesenchymal characteristics. When cells undergo EMT there are several steps which must occur including loss of cell to cell adhesion, and the ability to degrade and invade the basement membrane and enter the vasculature (288). The initiation of EMT is a complex process that involves activation of transcription factors, switching of structural proteins to facilitate movement, and activation of stem-like properties (235, 289, 290). Interestingly, FKBP12 has been demonstrated to have suppressive effects on EGFR autophosphorylation in vitro where addition of exogenous FKBP12 was found to reduce phosphorylation of the EGFR at all activation sites (291). Similarly, FKBP12 has also been shown to suppress activation of the transforming growth factor beta (TGF $\beta$ ) receptor and ryanodine receptor (RyR) resulting in inhibition of their associated signalling pathways (292, 293). Considering the similar homology between FKBP12 and FKBP25 (294), there may be some cross over of these roles for FKBP25.

To investigate the involvement of FKBP25 in EMT, the MDA-MB-468 cell line was utilised, which was previously identified as having high levels of FKBP25 expression (**Fig 3.2**). Additionally, MDA-MB-468 cells express high levels of EGFR which can be exploited to create an in vitro model of EMT (295). Upon stimulation with EGF, MDA-MB-468 cells undergo a morphological shift whereby the cells become elongated and multipolar in conjunction with a redistribution of E cadherin from the cell periphery (**Fig 3.7**). Once EMT was visually confirmed, the analysis moved onto a molecular confirmation where a reduction in E cadherin and increase in vimentin were observed. Importantly, this coincided with a decrease in FKBP25 (**Fig 3.8**). This evidence supports the hypothesis that a mesenchymal phenotype is associated with reduced FKBP25 expression.

This observed reduction in FKBP25 in EGF-mediated EMT may be caused by a variety of factors. In this study it was discovered that the FKBP25 reduction observed by EGF-mediated EMT is unlikely to be caused through signalling via PI3K, Mek, or mTOR (**Fig 3.10**). However, these studies could be improved by trialling drug doses and time courses to optimise molecular inhibition. Considering the multifaceted roles of FKBP25 in cell biology there are many other avenues that could be examined to explain FKBP25 protein reduction in response to EGF-mediated EMT. One such mechanism may be that FKBP25 in EGF-mediated EMT is altered calcium handling. The role of calcium signalling and handling in EGF-mediated EMT in MDA-MB-468 cells has been extensively studied. It was demonstrated that MDA-MB-468 cells treated with EGF provokes an intracellular influx of calcium (266). Furthermore, it was shown that chelation of calcium in EGF treated cells impairs mRNA expression of EMT markers, vimentin, N cadherin and twist; suggesting that the process of EGF-mediated EMT is, in part, calcium-dependent (265). However, some markers, including snail, were upregulated in response to calcium chelation, indicating not all mediators of EMT are impacted by calcium. Interestingly, FKBP25 has been shown to interact with transient receptor potential channel 6 (TRPC6), a component of the heterodimer channel that facilitates non-capacitative calcium entry into cells (296). Upon knockdown of FKBP25, it was shown that calcium entry into cells was reduced in HEK293T cells, however, this mechanism has not been examined in breast cancer cells.

Another mechanism that may implicate FKBP25 in EMT in breast cancer cells is FKBP25's role as a microtubule stabiliser (109). In this model of EGF-mediated EMT in MDA-MB-468 cells, it was identified that FKBP25 levels decrease upon EMT induction, suggesting that there may be a decrease in microtubule stability in the

absence of FKBP25 (273). In this instance, it may occur that the microtubule assemblies are, in fact, more dynamic without a microtubule-associated protein, such as FKBP25, enabling faster formation of the mitotic spindle and, as such, faster cell proliferation. In addition to this, the decreased stability of the mitotic spindle may increase the likelihood of genomic damage occurring during metaphase. Specifically, this scenario could occur during metaphase chromosome separation if the spindles are not stable enough to adequately separate the chromatids (297). In the context of mesenchymal progression, it would be essential to gain genomic mutations to facilitate further growth and survival of the mutant cells (298). To this end it is important to further elucidate the role of FKBP25 in breast cancer cell epithelial to mesenchymal transition.

### **3.4 Conclusions**

This chapter has described the role FKBP25 in models of breast cancer cell de-differentiation and EMT *in vitro*. It was found that FKBP25 protein expression is reduced in mesenchymal breast cancer cell types compared to that of more epithelial-like basal subtypes. Specific mutations that are associated with the mesenchymal phenotype, Ras<sup>v12</sup> and p53<sup>R273H</sup>, were examined in immortalised mammary epithelial cell line MCF10A. Contrary to our hypothesis and previous findings, these models demonstrated an increase in FKBP25. These studies highlight that the regulation of FKBP25 in breast cancer cell de-differentiation is not dependent on a single mutation and must encompass a variety of factors. Our studies have also demonstrated consistently that EGF-mediated EMT results in a reduction of FKBP25 protein. Additionally, it was demonstrated that the reduction in FKBP25 is impaired by inhibiting small molecules that are involved in the EGF signalling cascade (including PI3K, Akt, and mTOR). Considering these findings it

may be that EGF is having other effects on cell biology and behaviour that influence FKBP25, such as MT stability and dynamics. It would be important to examine additional models of EMT, that are under both genetic and exogenous ligand control to comprehensively assess the impact of EMT on FKBP25 protein expression.

---

## Chapter 4: Investigating the role of FKBP25 in models of myogenesis and muscle plasticity

---

### 4.1 Introduction

#### 4.1.1 Mesenchymal to epithelial transition (MET) and Myogenesis

The process of MET is required for the transition of motile mesenchymal cells into polarised epithelial cells, which is seen in tissue development. The reverse process of EMT is referred to as mesenchymal to epithelial transition (MET; **Figure 4.1**). One example of MET of interest is myogenesis (299). Myogenesis is the process of skeletal muscle cell differentiation from a proliferative progenitor cell, known as myoblasts, to mature differentiated muscle fibres, or myotubes (300). Comparably to EMT, this form of MET requires expression of myogenic factors to occur. Upon induction of myoblast

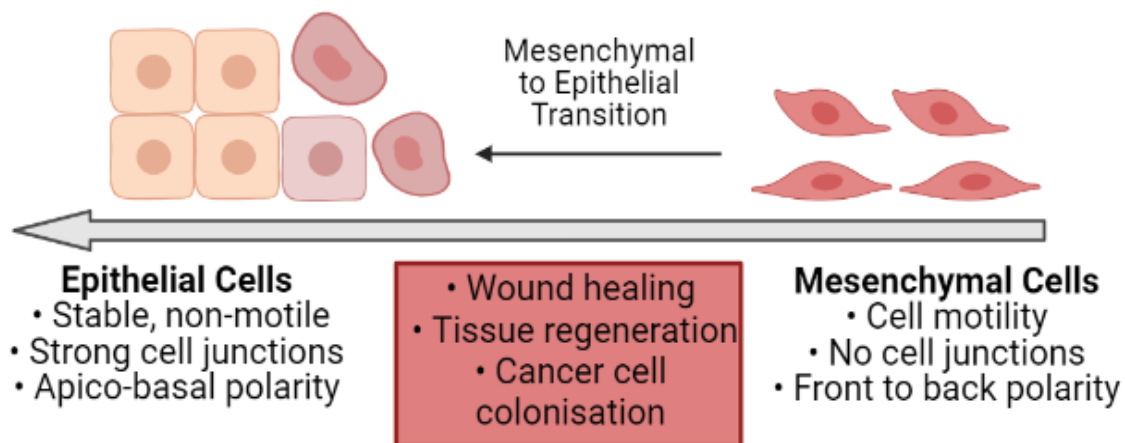


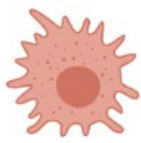
**Figure 4.1: Mesenchymal to epithelial transition (MET)**

MET refers to mesenchymal cell committing to epithelial lineage where cells lose their motility, cell-cell junctions and front/back polarity which are mesenchymal characteristics. Upon loss of these features, cells transition to a stable non-motile phenotype with strong cell junctions and apico-basal polarity – which are characteristic of epithelial cells. Made with Biorender.com.

differentiation, a cascade of myogenic regulatory factors (MRFs) begin to be

transcribed to facilitate the transition to mature myotubes (**Table 4.1**). These factors include myoblast determination protein 1 (MyoD), myogenic factor 5 (MYF5), myogenic factor 4 (myogenin/MyoG) (301). These factors are repressed in proliferative myoblasts and are activated upon induction of differentiation. Specifically, these MRFs are activated by cessation of cyclin dependent kinase activity corresponding with removal of myoblasts from the cell cycle to undergo terminal differentiation (302). In contrast to post mitotic myotubes, myogenic precursors cells can also exist as quiescent satellite cells. Satellite cells are the stem population within the skeletal muscle that enable regeneration and healing in response to muscle damage (303). An important identification factor in the satellite cell population are the paired box proteins (Pax proteins, PAX3 and PAX7), however, little is known about the function of these proteins in satellite cells (304). Upon activation of satellite cells by injury, the cells divide to replenish their stem-population.

**Table 4.1: Myogenic regulatory factor (MRF) expression throughout myogenesis**

| <br>Satellite cell | <br>Activated satellite cell | <br>Myoblast | <br>Myocyte | <br>Myotube |
|---|---|---|---|--|
| PAX7  |   |   |   |  |
| PAX3  |   |   |   |  |
| Myf5  |   |   |   |  |
|   | MyoD  |   |   |  |
|   |   | Myogenin  |   |  |
|   |   |   | Contractile proteins (MyHC)   |  |

After which a daughter cell is able to migrate to the damaged site, fuse into the myofibres and initiate regeneration (305). This process is essential for the maintenance and function of healthy mature skeletal muscle. It has previously been identified that FKBP25 is expressed in the top 10% of the skeletal muscle proteome (225), suggesting that FKP25 may play some role in muscle fibre maintenance or function.

#### 4.1.2 Rhabdomyosarcoma (RMS)

Interestingly, there is a group of aggressive skeletal muscle cancers in which the myoblasts fail to fully differentiate, which results in proliferation of immature myocytes known as rhabdomyoblasts (306). The accumulation of these immature tumour cells is known as rhabdomyosarcoma (RMS). RMS can be subdivided into three major

subgroups based on histological features: embryonal, alveolar, and anaplastic RMS. These cancers primarily affect children under the age of 18 and has an approximate 5 year survival rate dependent on the RMS subtype (307). RMS tends to be highly heterogenous and lacks defined genetic features and, as such, is difficult to diagnose. However, one key cytogenetic feature of RMS is the presence of fusion genes, notably the fusion of PAX3/7-FOXO1 in alveolar RMS (308, 309). The presence of this gene fusion is correlated with poor patient outcomes. The prognosis of RMS can be worsened by the activation of super enhancers (BET bromodomain protein; BRD4) to autoactivate master regulators in RMS: MYOD, MYOG, and MYCN (310). Activation of these master regulators results in accelerated tumour progression and propagation of mutant cells. A second notable genetic trait of RMS cells is the presence of p53 mutations (311). It has also been identified that, while less common, Ras (N-Ras and K-Ras) mutations are relevant to RMS pathogenesis (312, 313). The link between oncogenic Ras and myogenic differentiation blockade is poorly understood. Current evidence suggests that oncogenic Ras signalling represses expression of the pro-myogenic factor, MYOG, which results in propagation of rhabdomyoblasts (314). This model of poorly differentiated myogenic cells may serve as an apt model to study the role of FKBP25 in differentiation and models of progressive de-differentiation. Throughout this chapter the aim is to investigate the role of FKBP25 in cell models of differentiation to assess its function in the maintenance of cell phenotypes. The use of pathological breast cancer, EMT, and physiological myogenesis models will comprehensively shed light on the poorly defined function of FKBP25 in cell differentiation.

### 4.1.3 Skeletal muscle regeneration

Upon completion of myogenic differentiation, skeletal muscle cells are considered terminally differentiated. Mature skeletal muscle becomes post mitotic and permanently withdraws from the cell cycle to cease active proliferation. Despite being a post mitotic tissue, skeletal muscle has a significant capacity to regenerate and overcome injury. Skeletal muscle myofibres contain a subpopulation of quiescent myogenic precursor cells known as satellite cells (SCs) that are able to initiate MET (315). The SC population reside between the basement membrane and sarcolemma of the myofibres (316). In healthy, undamaged muscle SCs lie dormant, however, upon damage become activated (317). Activation of SCs stimulates re-entry to the cell cycle where the cell divides into 2 daughter cells which can undergo one of two fates. These daughter cells express myogenic markers PAX7/3 and MyoD (318). SCs can then either commit to myogenic lineage as marked by expression of Myf5 (319), or alternatively lose MyoD expression and re-enter the SC pool for further regenerative capacity (319) (**Fig 4.2**). Upon activation satellite cells must migrate from the basal lamina to the site of damage, which is mediated by chemoattraction toward insulin-like growth factor (IGF-1) that is secreted from damaged muscle fibres (320). Specifically, cellular migration is mediated by CD34 and CD44 cell surface receptors that are able to interact with ECM proteins including collagen, fibronectins, and laminin (321, 322). Additionally it is essential for myogenic precursor cells to produce matrix metalloproteinases (MMPs), which are required for ECM degradation to enable invasion of cells through the basal lamina (323, 324). Upon entry to the damage site both proinflammatory cytokines (including interleukin-6 (325)) and growth factors (IGF-1 and fibroblast growth factor (FGF-b) (326)) stimulate cell proliferation.

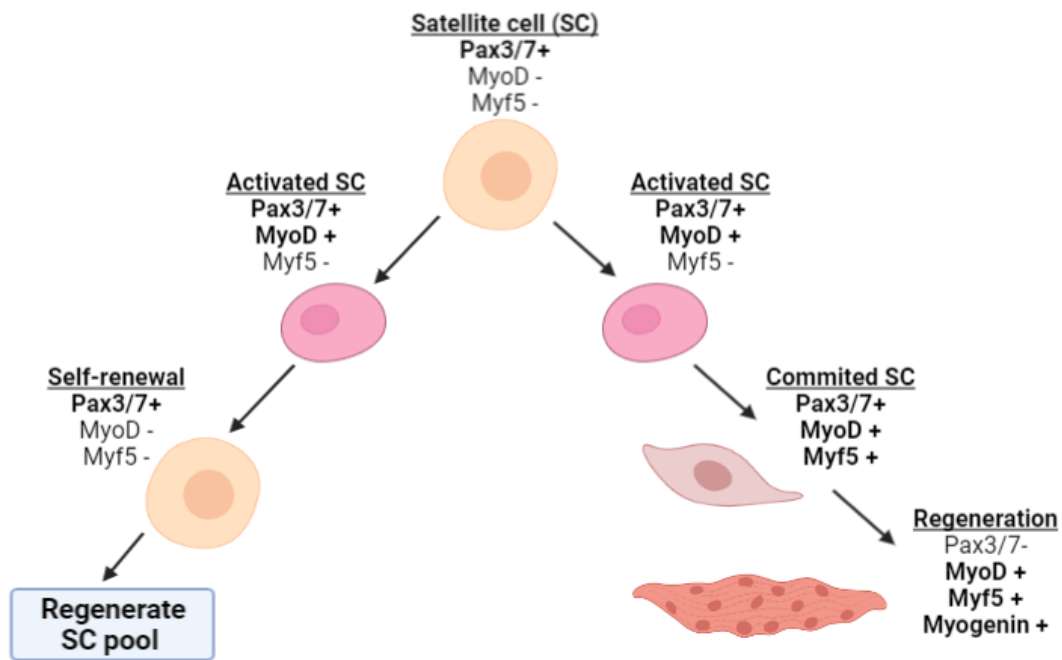


**Figure 4.2: Regulation of myogenic satellite cells in self renewal and regeneration**

Satellite cells (SC) exist in skeletal muscle to proliferate and regenerate damaged fibres. SC markers Pax3/7 are expressed in quiescent SCs. Upon activation by a damage event, SC become activated and express MyoD. Next, SCs will either return back to quiescence and contribute to self-renewal of the SC pool (and lose MyoD expression, left), or commit to proliferation and differentiation (as such express Myf5 and myogenin, right). Adapted from Amalda and Wagers 2016. Made with Biorender.com.

Fusion of regenerated myoblasts into the damaged muscle is the final event that must take place to rebuild the tissue, and this complete the MET process. Myoblasts express an intracellular adhesion molecule, M-cadherin, that is required for anchorage of myoblasts into the muscle (327). Upon adhesion and fusion to the muscle fibre, the nuclei of the fusing myoblasts evenly distribute in the centre of the fibre, known as centration (328). The centrally localised nuclei must be redistributed to the periphery of the muscle fibres which is essential for appropriate functioning of regenerated muscles (329). Nuclei are repositioned by microtubules and microtubule associated motor proteins, such as dynein (330). MTs are anchored to the microtubule organising

centres that are located on the nuclear envelope, and the cell cortex which enable the nuclei to be pulled toward the fibre periphery (331). It has been consistently described that there is significant MT remodelling upon skeletal muscle damage and regeneration, however the mechanisms are poorly understood (332-334). It has been hypothesised that the reason for extensive remodelling is due to constant repositioning of the nuclei within a regenerating tissue. Specifically, that motor proteins (kinesin-1 and dynein) compete for MT interaction to facilitate nuclear movement to mature the regenerated fibres (335). In order to facilitate movement the MTs should be stable, as such regenerating muscle fibres contain increased stable tubulin polymers and reduced MT dynamics (335). FKBP25 is a known MT stabilising protein, and interestingly is the most highly expressed FKBP in mature skeletal muscle (225). These factors may implicate FKBP25 in facilitating MT stability in muscle regeneration in addition to a potential role on myogenic differentiation.

#### 4.1.4 Chapter Aims

This chapter aims to identify and describe the relationship between FKBP25, cell differentiation, and regeneration using a variety of *in vitro* and *in vivo* models.

1. To observe FKBP25 expression in the C2C12 model of myogenesis.
2. To examine the effect of quiescence induction on FKBP25 expression.
3. To contrast the expression in human primary myoblasts and human rhabdomyosarcoma cell line Rh30
4. To examine the interaction between FKBP25 and remodelling in *in vivo* models of muscle regeneration and plasticity.

## 4.2 Results

### 4.2.1 FKBP25 expression is increased upon C2C12 differentiation and induction of quiescence.

To further examine the role of FKBP25 in the processes of differentiation and dedifferentiation, next the role of FKBP25 in a normal physiological model of differentiation was assessed. This model of differentiation, the C2C12 myoblast model, is, in effect, the opposite of the EMT and could be considered MET (mesenchymal to epithelial transition, **4.3**). Upon differentiation, the proliferative progenitor myoblasts

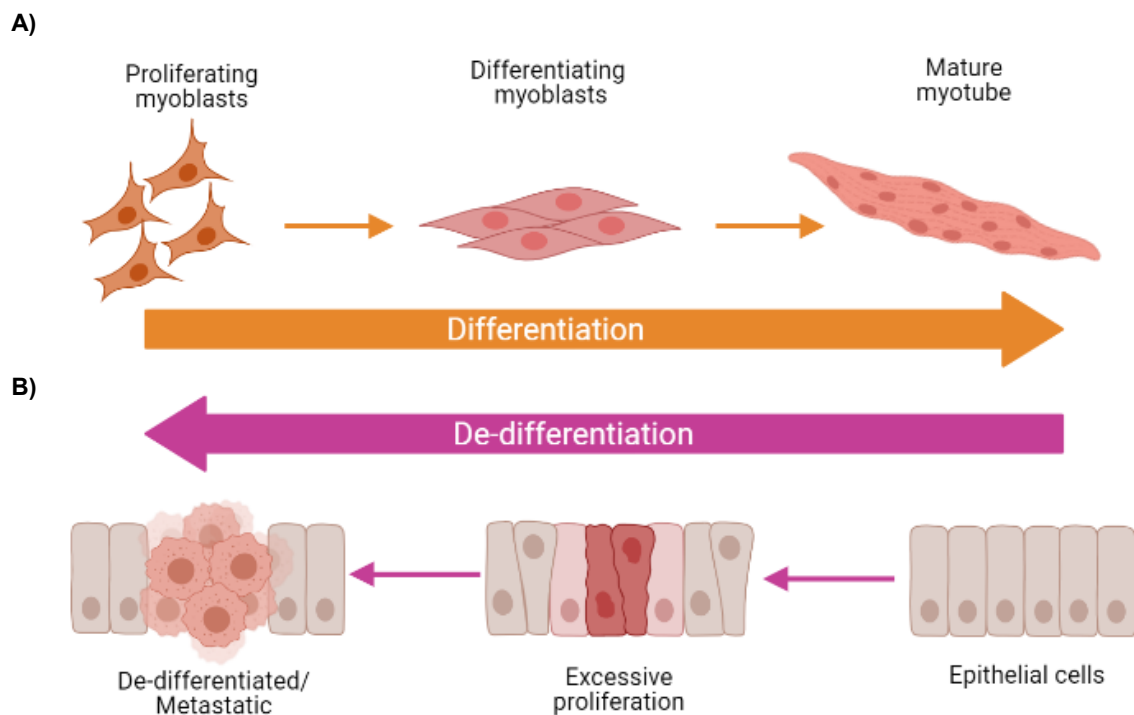


**Figure 4.3: Comparison of differentiation and de-differentiation models**

**A)** The C2C12 differentiation model involves the progression from proliferative myoblast to differentiation myoblasts, and finally to mature myoblasts via removal from the cell cycle and post mitotic myogenic commitment. **B)** Conversely, de-differentiation involves chronic stimulation of the cell cycle resulting in excessive proliferation. Accumulation of mutations and progressive de-differentiation results in cells that are mesenchymal and have increased metastatic potential. Made with Biorender.com.

commit to differentiation, which is marked by expression of myogenic factors, and exit of the cell cycle to become post mitotic (336, 337). Induction of differentiation of C2C12 myoblasts is initiated by serum deprivation, which forces the cells to cease proliferating and begin to fuse. Throughout the 96 hours of differentiation, the C2C12 cells fuse together to form myotubes (**Fig 4.4 A**). Importantly, throughout this differentiation process, it was observed that there was an increase in fast myosin heavy chain, myogenin, and MyoD, which indicate commitment to myogenesis, and a decrease in cyclin D representing cessation of proliferation (**Fig 4.4 B**). Importantly, throughout this differentiation process, it was observed that FKBP25 expression increases significantly (**Fig 4.3 C**). This data is reflective of the findings from section 3.2.4, where it was observed that FKBP25 protein expression is reduced in MDA-MB-468 cells that have undergone EMT and consequent de-differentiation from their epithelial phenotype (**Fig 3.9**). Similarly in this C2C12 model, we have identified that FKBP25 protein expression is increased as C2C12 myoblasts differentiate into myotubes, representing a type of MET – the reverse process of EMT (Displayed in **Fig 4.4**). Which led us to generate the hypothesis that FKBP25 protein is expressed at a low level in differentiated or mesenchymal-type cells, such as C2C12 myoblasts or mesenchymal breast cancer cells. Whereas differentiated or epithelial-like cells including C2C12 myotubes, or luminal and basal breast cancer subtypes express much higher levels of FKBP25 protein.

To further describe the function of FKBP25 in the process of differentiation we next assessed FKBP25 localisation. Within the C2C12 cells, FKBP25 is localised throughout the cells, i.e., the nuclear and cytoplasmic compartments of both myoblasts and myotubes (**Fig 4.6**). As the myotube network becomes more complex there is a more intense staining of FKBP25 corresponding with the increase in cytoplasmic

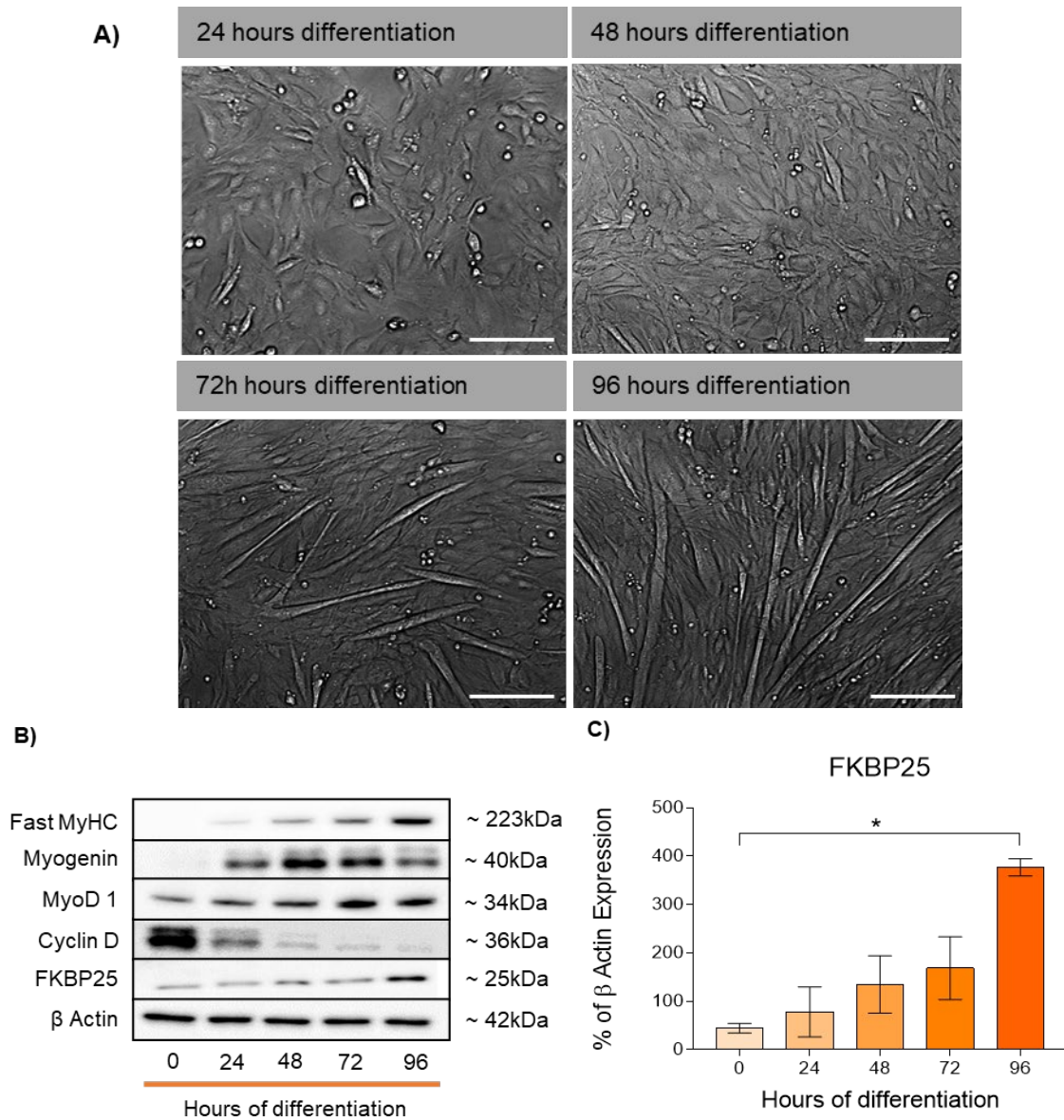


**Figure 4.4: FKBP25 expression throughout C2C12 myoblast differentiation**

**A)** C212 morphology throughout differentiation from an immature myoblast cell to mature myotube (i-iv). **B)** Representative blots of FKBP25 expression, myogenic and proliferation markers **C)** FKBP25 expression increases throughout C2C12 myogenesis. Scale bar = 100 $\mu$ m. Data presented as mean  $\pm$  SD of n=3, \* =  $p \leq 0.05$

space. It is known that as myoblasts differentiate to myotubes the cells withdraw from the cell cycle and become terminally differentiated, or post mitotic. This feature of myotubes begged the question of whether the change in FKBP25 protein expression is linked to the differentiation status of the cells, or rather the ability to proliferate. To address this, a model of quiescence in which the C2C12 myoblasts was developed, to remove cells from the cell cycle and, as such, stop proliferation. To induce quiescence, cells were suspended in a semi solid medium to prevent adhesion dependant growth. Once released from quiescence, i.e., replating onto a solid substratum, the C2C12 cells were able to proliferate and differentiate as normal (**Fig 4.7**). Upon quiescence induction, there is an increase in FKBP25 expression compared to replated proliferating myoblasts, which continues to increase into differentiation (**Fig 4.8 A**). This increase in FKBP25 with differentiation coincides with a decrease in proliferation that is seen in both quiescent and differentiated myotubes (See Cyclin D **Fig 4.8 B**). These data suggest that increased FKBP25 expression in C2C12 myotubes may be related to reduced proliferation rather than differentiation per se.

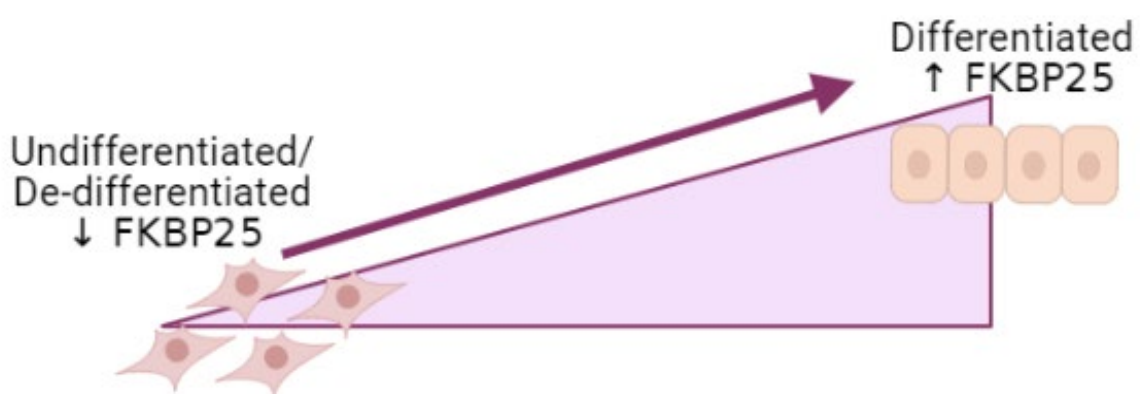


**Figure 4.5: Proposed relationship between FKBP25 and cell differentiation.** High levels of FKBP25 protein are associated with differentiated cell types, including epithelial cells, and differentiated skeletal muscle myotubes. While low levels of FKBP25 protein is associated with poorly differentiated mesenchymal breast cancer cells and immature myoblasts. Made with Biorender.com.

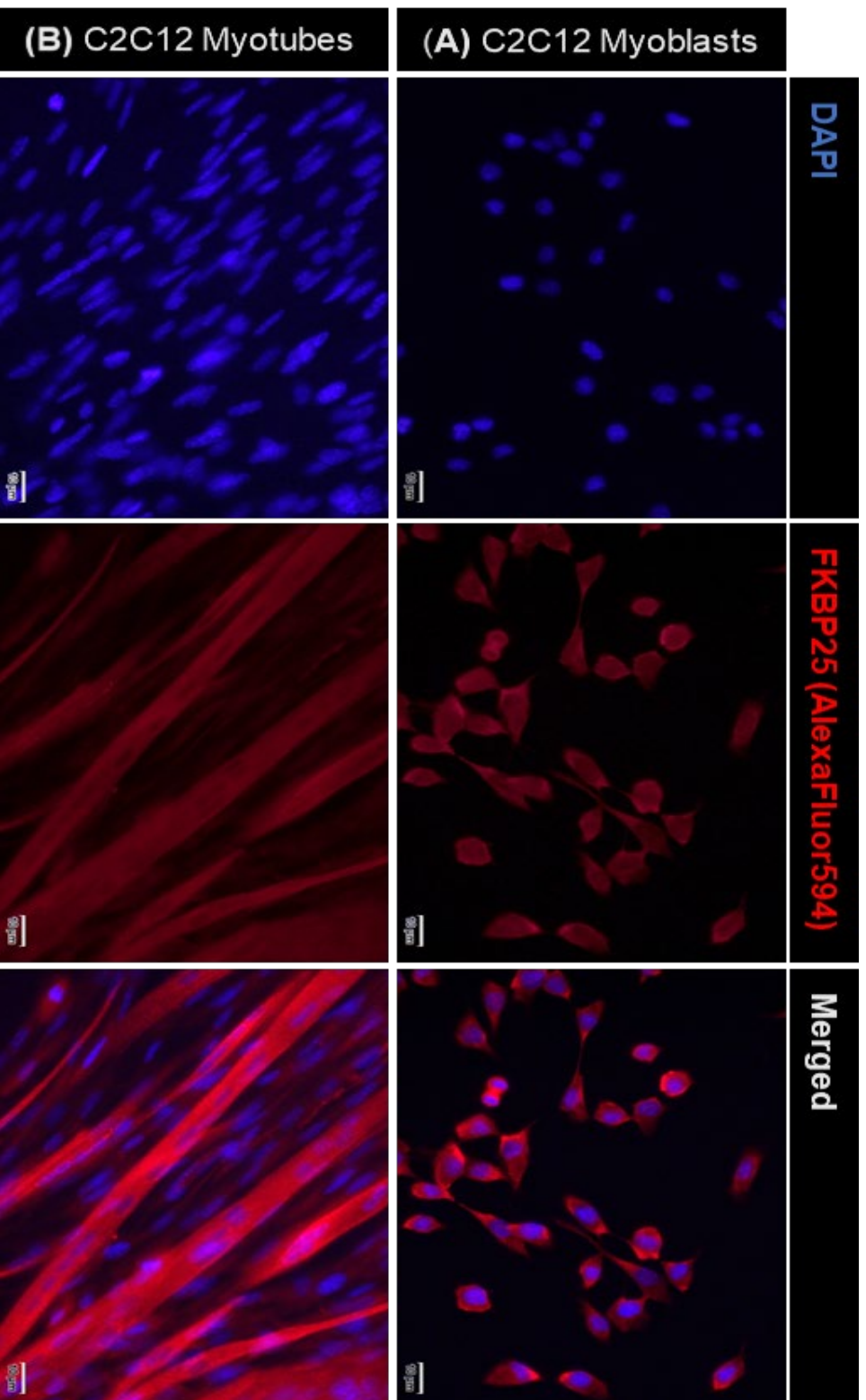


**Figure 4.6: Localisation of FKBP25 in C2C12 myoblasts and myotubes**  
 FFkBP25 is localised in the cytoplasm of C2C12 myoblasts (A) and myotubes (B). Scale bar = 10µm, n=3

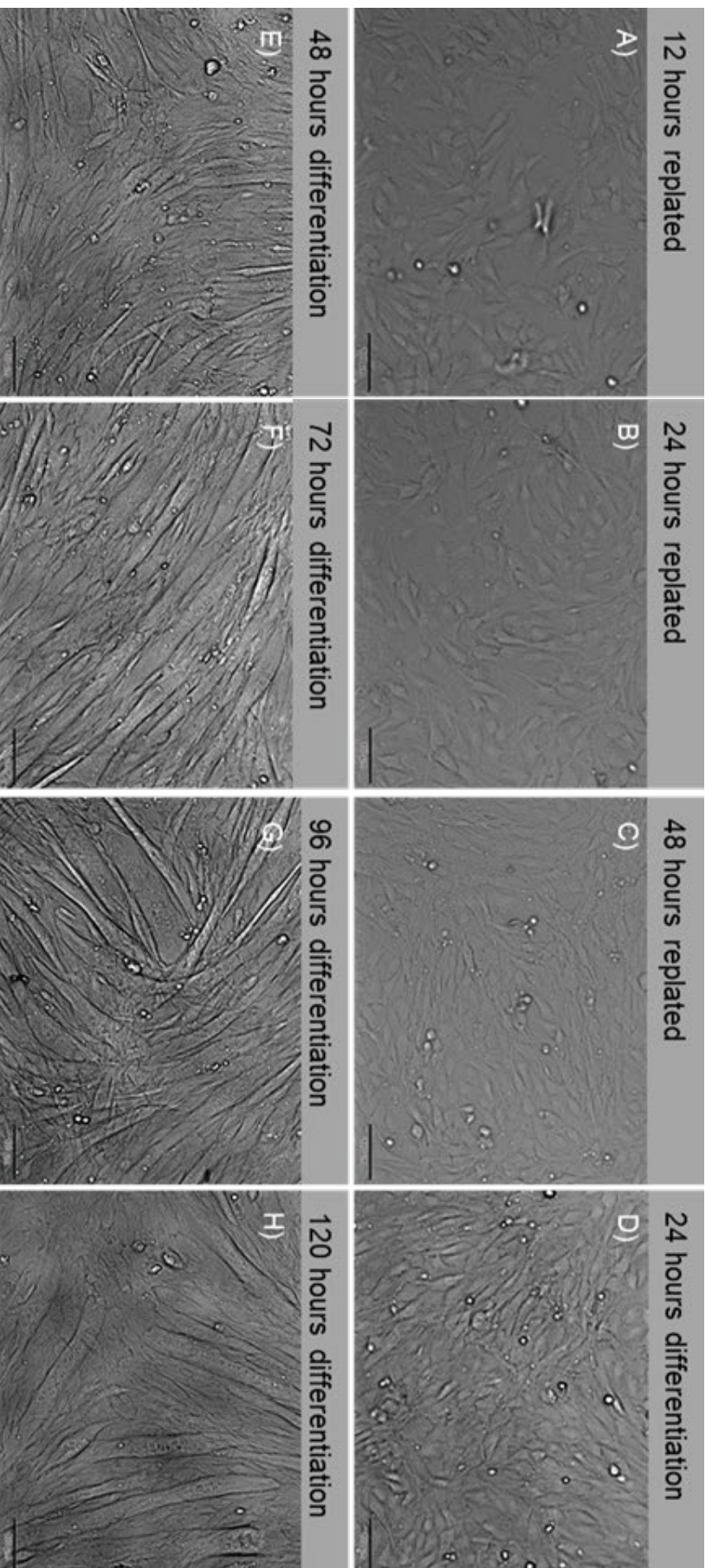


**Figure 4.7: Morphology of synchronous myoblasts following quiescence induction and subsequent differentiation**

A-C) Synchronous myoblasts replated for 12-48 hours following suspension in a semi solid medium. D-H) Differentiating myoblasts/myotubes over 120 hours show no morphological changes to asynchronous differentiation. Scale bar = 100µm. Data presented as mean  $\pm$  SD of n=3, \* = p $\leq$ 0.05

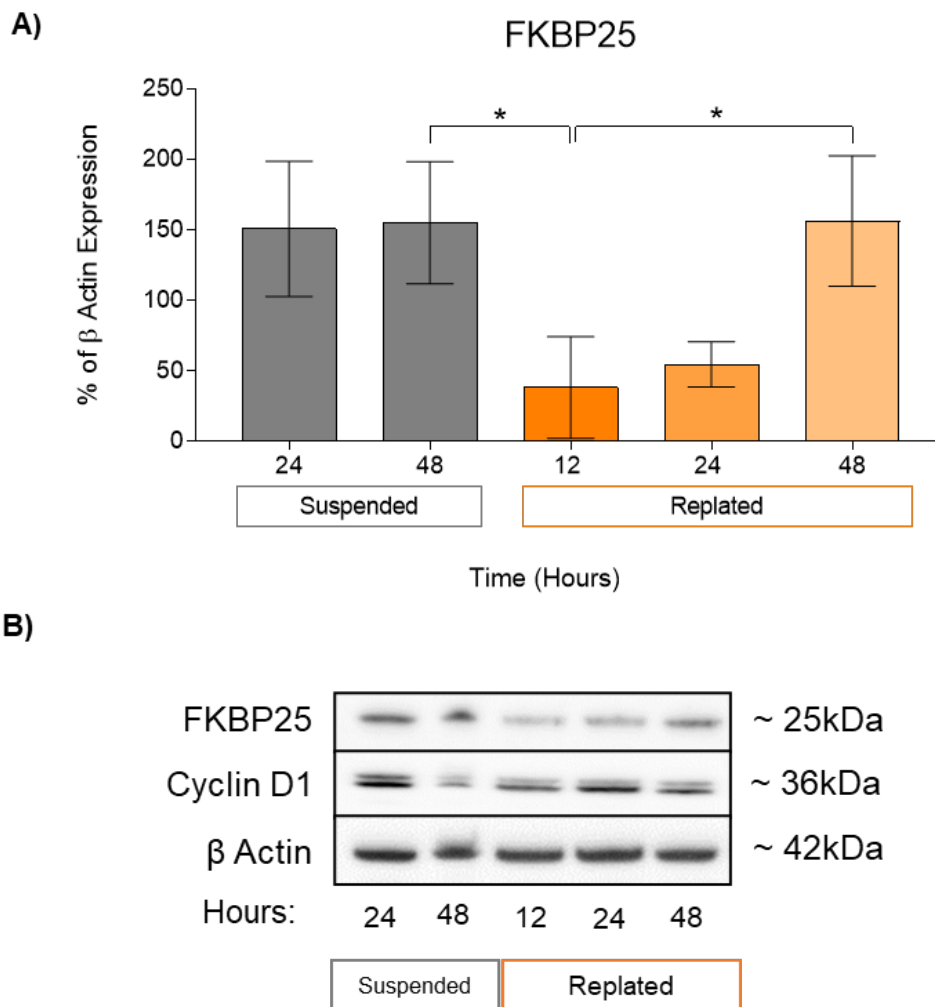


**Figure 4.8: FKBP25 expression in synchronous, quiescent, and differentiated C2C12 myoblasts**

**A)** FKBP25 expression is indifferent in suspended quiescent cells, however, decreases once replated and allowed to re-enter the cell cycle. This is seen by an increase in Cyclin D expression. **B)** Representative blots. Data presented as mean  $\pm$  SD of n=3, \* =  $p \leq 0.05$

#### 4.2.2 FKBP25 expression is increased in differentiated primary RMS cells but not differentiated primary myoblasts.

To further explore the role of FKBP25 in myogenesis differentiation of human primary myoblasts (MBA-135) and human RMS cells (Rh30) were examined. The RMS cell line, Rh30, was of particular interest considering their characteristic mutations (Pax3/7-FOXO1 and MyoD1) that prevents differentiation. Thus, to adequately contrast this model to a healthy model, a human primary cell line was also examined. To begin this study, localisation experiments were performed where it was identified that FKBP25 is expressed ubiquitously throughout MDA-135 myoblasts and myotubes (**Fig 4.9**), however, FKBP25 appears to be less concentrated in the nucleus. While Rh30 myoblasts express FKBP25 ubiquitously throughout the cell, there appeared to be a greater concentration localised to the nucleus (**Fig 4.10 A**), which dispersed upon treated with differentiation medium (**Fig 4.10 B**, note that these cells do not form myotubes).

To examine the impact of myoblast differentiation on FKBP25 expression, MBA-135 primary myoblasts were differentiated into myotubes (**Fig 4.11 A**) and confirmed the expression of a series of myogenic factors described in 3.2.4 (**Fig 4.11 B**). Upon differentiation of MDA-135 cells, it was found that FKBP25 expression remains unchanged (**Fig 4.11 C**). Interestingly, attempted differentiation of Rh30 cells (**Fig 4.12 A**, note lack of myoblast fusion) despite expression of myogenic factors, myogenin and MyoD, there is no expression of myosin heavy chain (**Fig 4.12 B**), however, there is a significant increase in FKBP25 expression (**Fig 4.12 C**). Intriguingly, these results contradict the results that were found in C2C12 mouse myoblasts, where it was found that FKBP25 protein expression increases upon differentiation (**Fig 4.4**). To determine if the presence of growth factors in the primary cell growth medium resulted in MBA-

135 myoblast expressing high levels of FKBP25, the impact of EGF, on C2C12 myoblasts was assessed. However, it was observed that there was no impact on FKBP25 protein expression (**Fig 4.13 and B**), or morphology (**4.13 C**) upon EGF treatment. These results indicate that perhaps the accumulation of FKBP25 in C2C12 myoblasts may be a cell type specific occurrence. The involvement of FKBP25 in myogenesis must be further examined through knockdown studies to comprehensively describe any possible role.

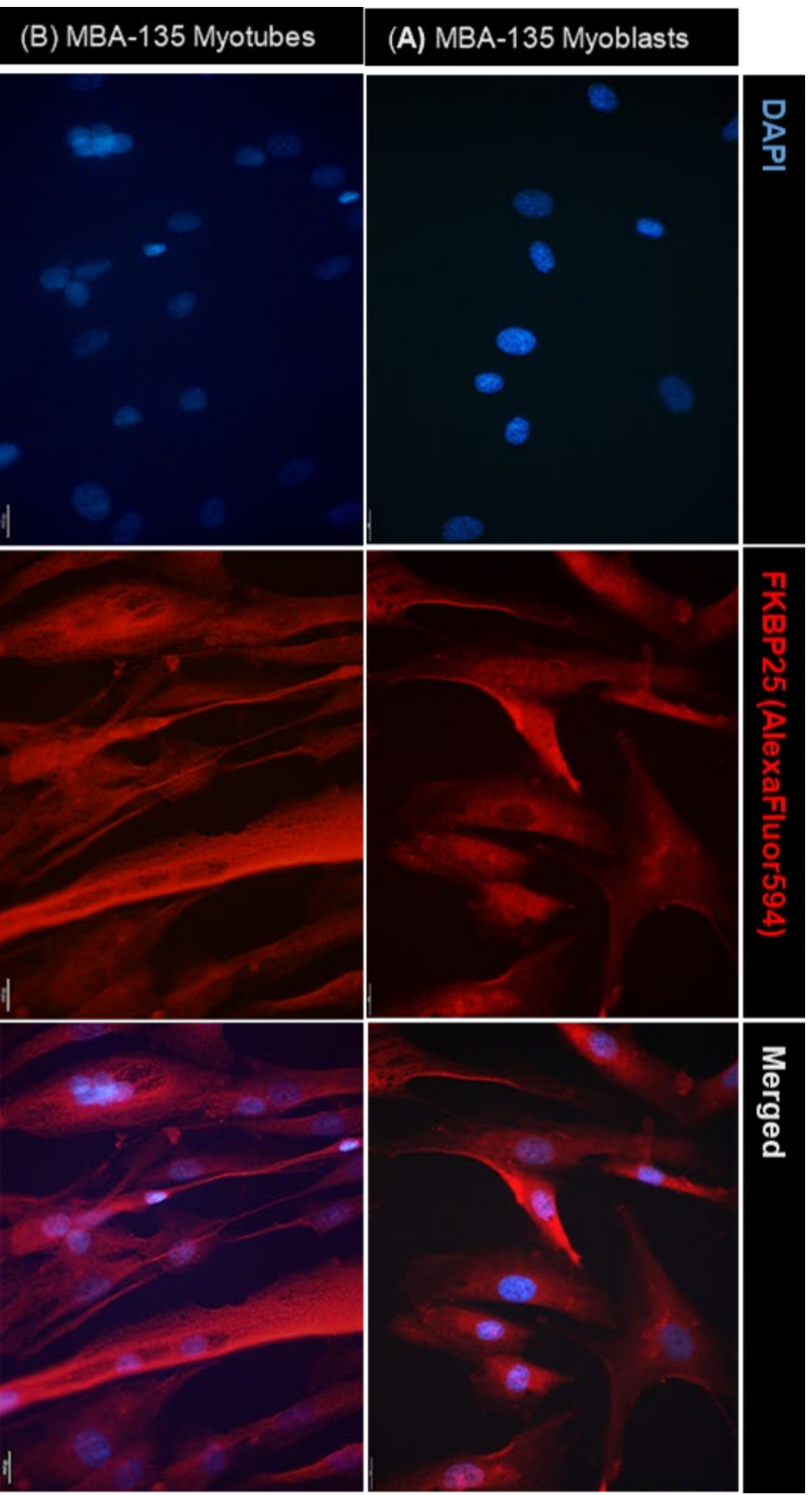


**Figure 4.9: Localisation of FKBP25 in human primary myoblast cell line MBA-135**  
 FKBP25 is ubiquitously throughout the cell of MBA-135 cells, in both myoblasts (A) and myotubes (B). Scale bar = 10µm.  
 Data presented as mean ± SD of n=3

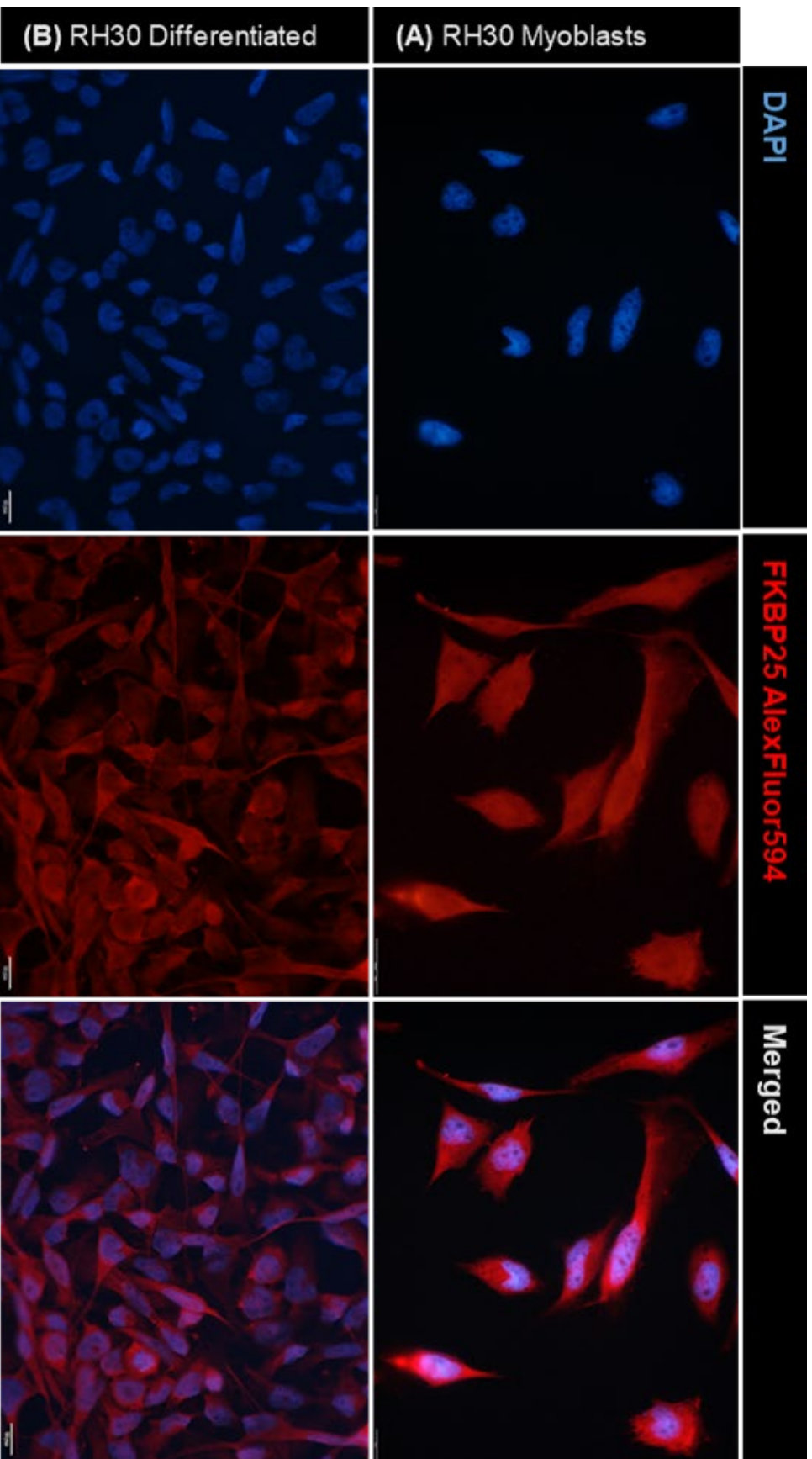


**Figure 4.10: Localisation of FKBP25 in rhabdomyosarcoma cell line Rh30**  
**A)** FKBP25 is ubiquitously throughout the cell of Rh30 cells, in both myoblasts (Scale bar = 10µm). **B)** Rh30 cells treated with differentiation media (Scale bar = 100µm). Data presented as mean ± SD of n=3

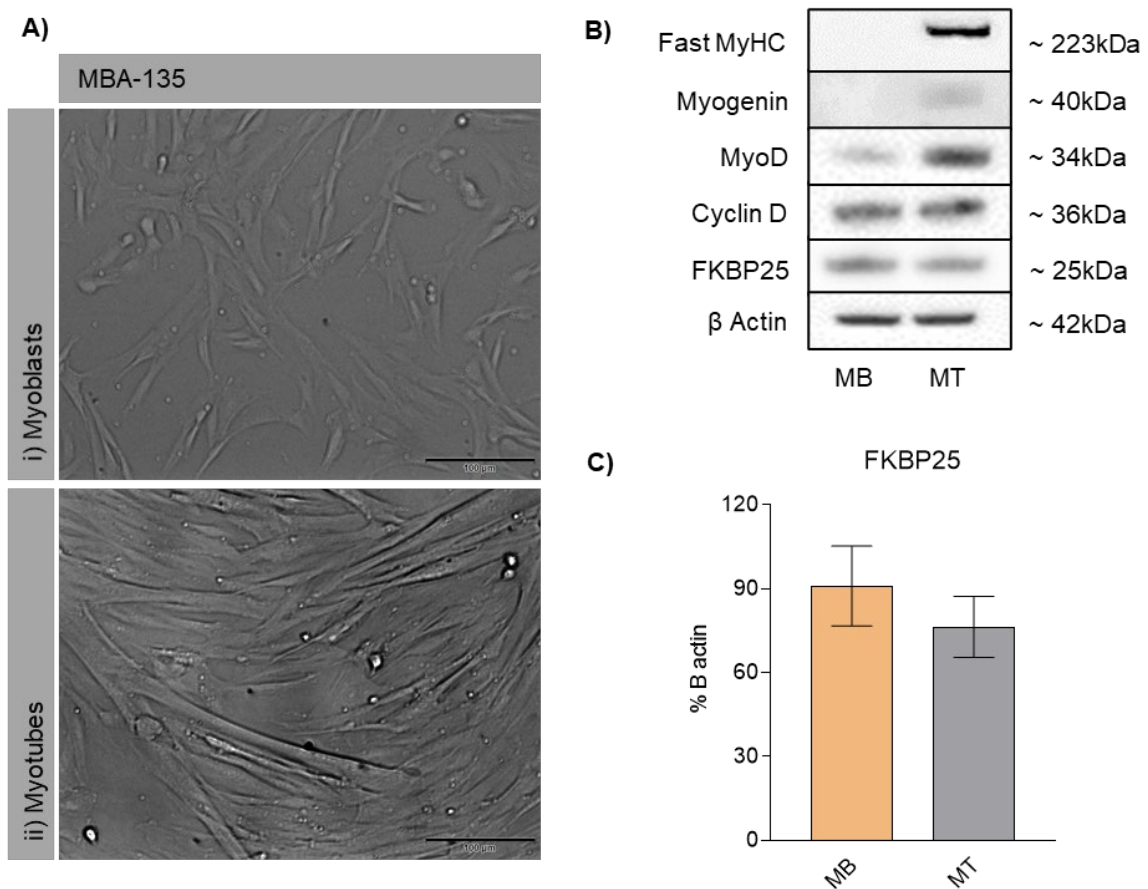


**Figure 4.11: FKBP25 expression is not altered in MBA-135 human primary myoblasts and differentiated myotubes**

**A)** Phase contrast images of MDA-135 myoblasts (i) and myotubes (ii). **B)** Expression of myogenic factors, proliferation markers and FKBP25 upon MBA-135 differentiation. **C)** FKBP25 expression is unchanged with differentiation. Scale bar = 100μm. Data presented as mean ± SD of n=3, \* = p≤0.05

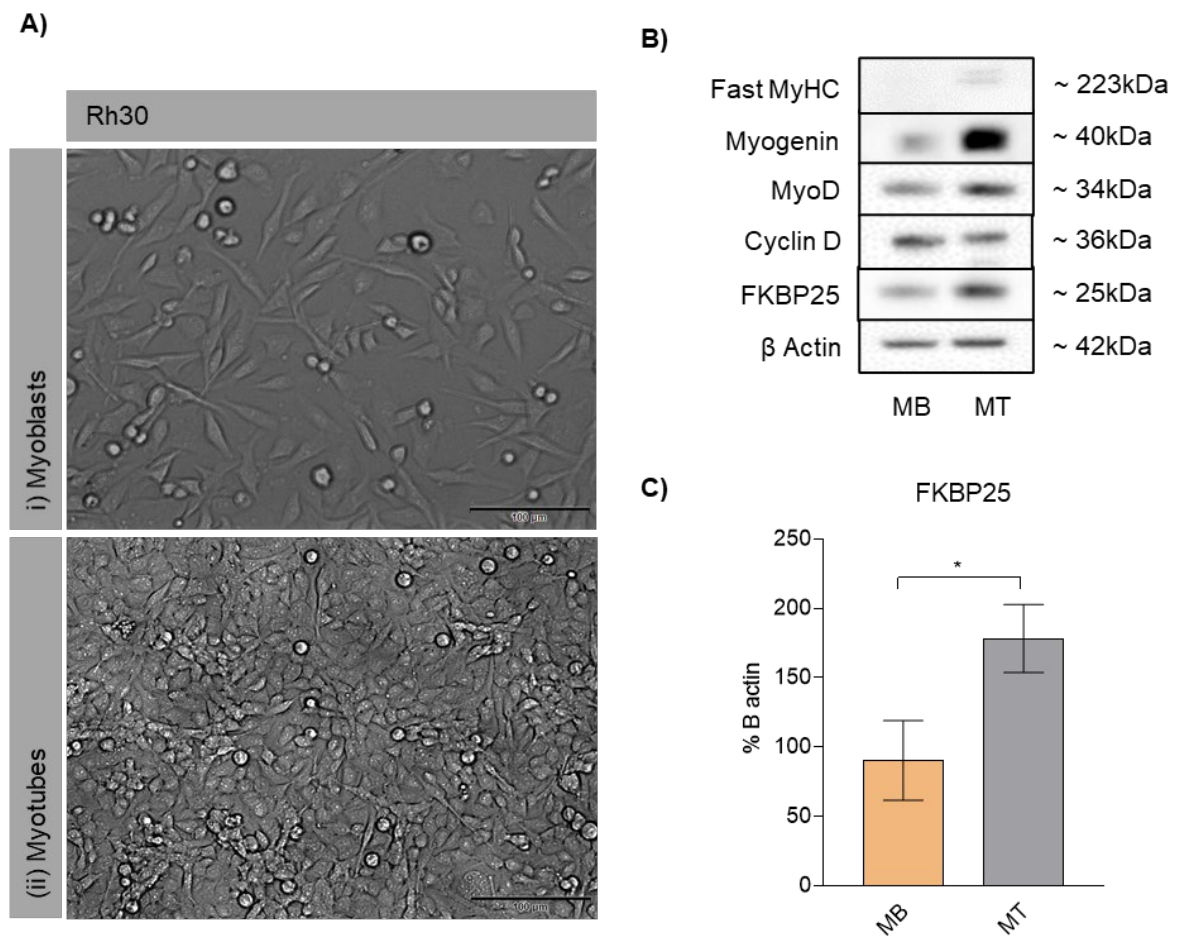


**Figure 4.12: FKBP25 expression is increased in differentiated human rhabdomyosarcoma cells**

**A)** Phase contrast images of Rh30 myoblasts (i) and differentiated Rh30 cells which do not form fused myotubes (ii). **B)** Expression of myogenic factors, proliferation markers and FKBP25 upon Rh30 differentiation. **C)** FKBP25 expression is increased with differentiation. Scale bar = 100μm. Data presented as mean ± SD of n=3, \* = p≤0.05

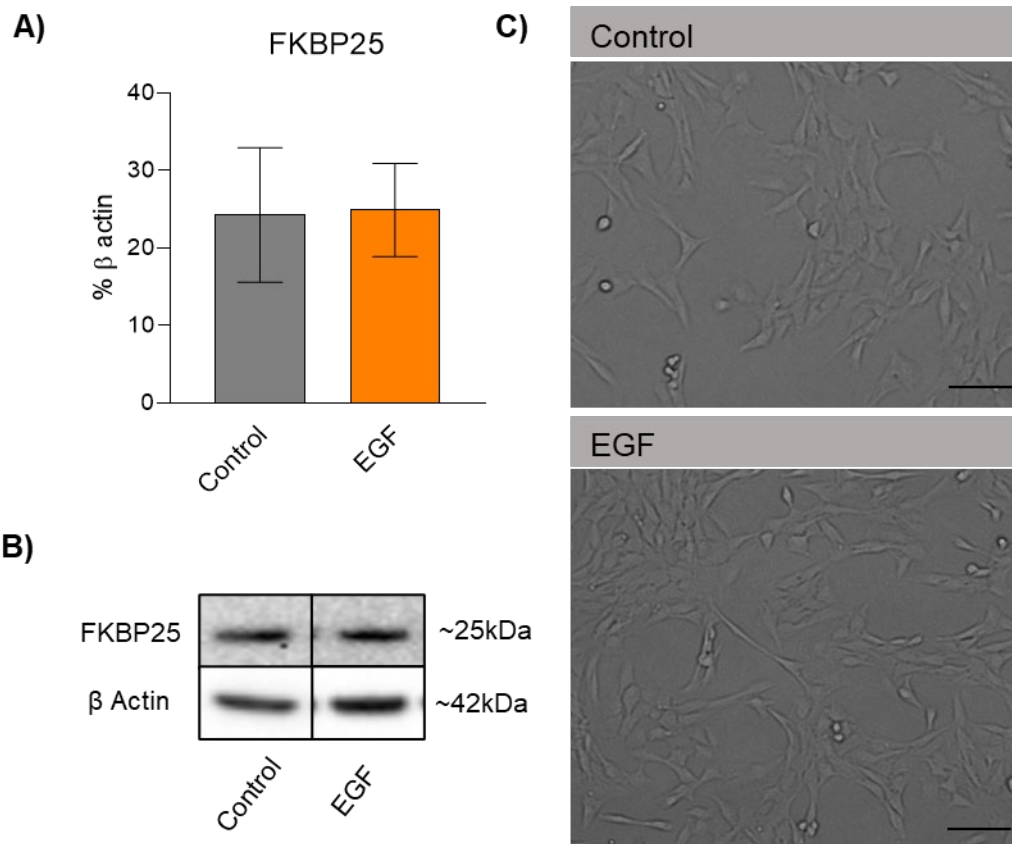


**Figure 4.13 FKBP25 protein expression is not altered by EGF treatment in C2C12 myoblasts**

**A)** FKBP25 protein expression is not altered upon treatment with 50ng/ml EGF for 72 hours. **B)** Representative blots. **C)** Control and EGF treated myoblasts do not exhibit morphological changes. All data is presented as mean  $\pm$  SD, n=3, \* = p $\leq$ 0.05. Scale bar = 100 $\mu$ m.

### 4.2.3 FKBP25 expression is increased in *in vivo* models of skeletal muscle hypertrophy and reduced in some models of atrophy.

To further investigate the role of FKBP25 in models of proliferation and differentiation several models of *in vivo* skeletal muscle plasticity were assessed to determine the impact on FKBP25 expression. These models include, chronic mechanical loading, murine Duchenne muscular dystrophy (mdx), denervation and food deprivation. These models can be divided further into two categories of skeletal muscle hypertrophy or atrophy. Muscle hypertrophy refers to increase in the size or number of muscle cells resulting in an increase in muscle mass, while atrophy refers to a decrease in the size of these cells resulting in loss of muscle mass.

The first model of skeletal muscle hypertrophy that was examined was chronic mechanical loading (CML). In this model of hypertrophy, two specific models, myotectomy (MTE) and synergist ablation (SA) were examined. These two models involve surgical interventions to remove part or all of the gastrocnemius muscle, forcing the synergist muscles (plantaris and soleus) to hypertrophy as they take over the role of the primary plantar flexor muscle. The MTE procedure involved removal of the achilles tendon, leaving the soleus muscle intact (338). While the SA involved removal of the soleus and distal half of the gastrocnemius, leaving only the plantaris (226). As such, MTE is a milder form of the SA resulting in less damage and regeneration of tissue. It has previously been demonstrated that these forms of CML result in increased muscle weight, increased RNA content, and increased protein synthesis after 14 days (227). Upon CML there is an increase in FKBP25 with both MTE and SA (**Fig 4.14**). Next, FKBP25 expression was examined in mdx muscle. DMD is a severe type of muscular dystrophy in which there is complete deletion of the dystrophin gene (339, 340). The pathogenesis of DMD in humans presents as

progressive muscle weakness and wasting resulting in impaired muscle function, and ultimately premature death from respiratory complications. Dystrophin is an essential anchoring protein which connects the cytoskeleton on the muscle fibres to the extracellular matrix through a variety of protein complexes (dystroglycan complex) (341). The absence of the dystrophin protein leads to a variety of pathologies that lead to muscle damage, including fibrosis, increased susceptibility to mechanical stress, amplified calcium signalling, pseudohypertrophy, and increased reactive oxygen species production and inflammation (342-344).

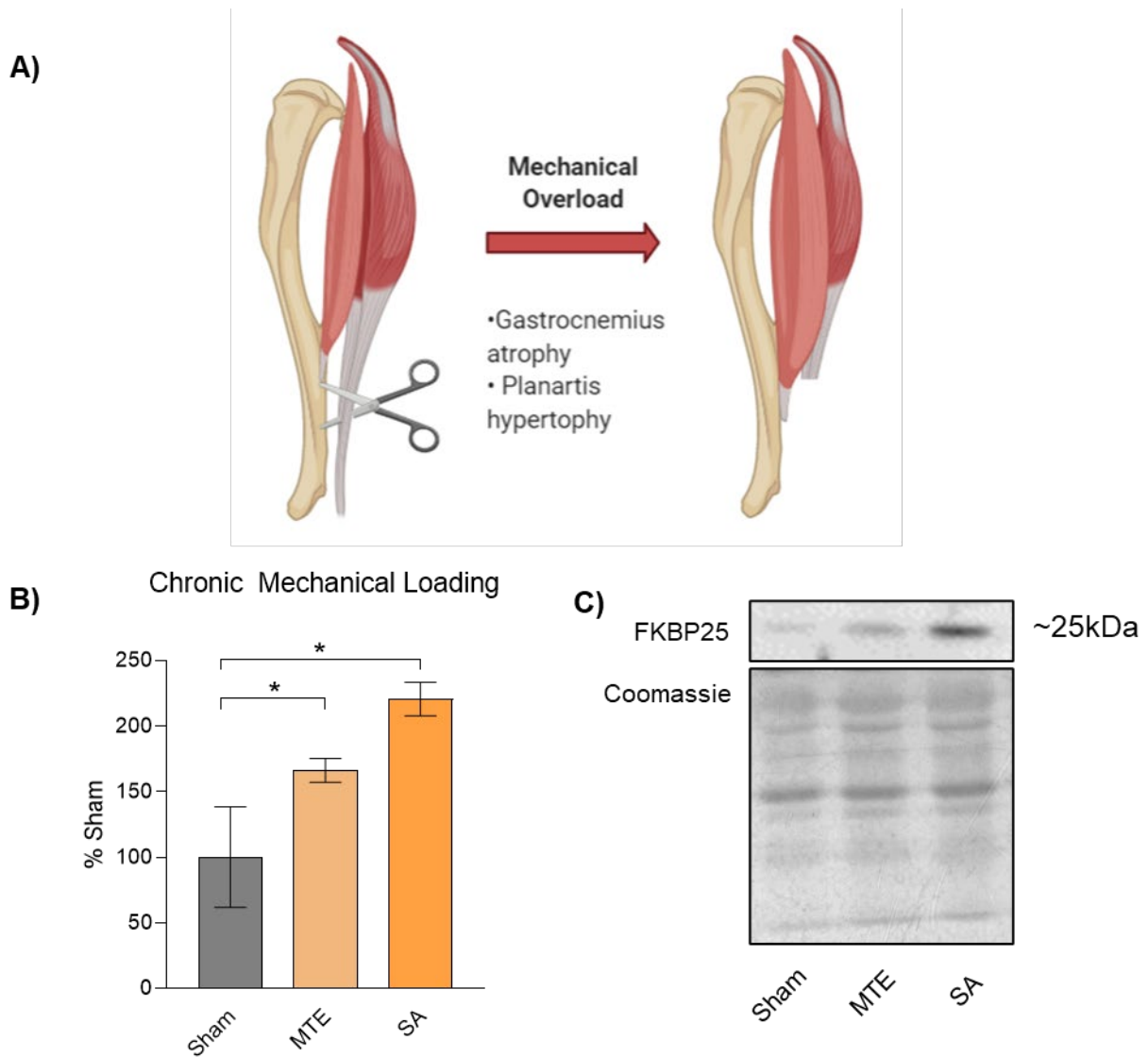


**Figure 4.14: FKBP25 protein expression is increased upon chronic mechanical overload**

**A)** Upon chronic mechanical loading (CML) through one of myotomectomy (MTE, severance of the Achilles tendon) or synergist ablation (SA, complete removal of the plantar flexor muscle - Gastrocnemius). Made with Biorender.com. **B)** Compared to Sham conditions, both MTE and SA result in a significant increase in FKBP25 protein expression. **C)** Representative blots. All data is presented as mean $\pm$ SD, n=3, p $\leq$ 0.05.

It was identified that FKBP25 expression was increased in mdx tissue compared to WT control (**Fig 4.15**). The samples that were examined in this study were obtained from 8-week-old mdx mice. The mdx pathology is well described and follows a known pattern of damage and regeneration (345). The disease phenotype onset begins at approximately 2.5 weeks of age and reaches peak damage onset by 3 weeks of age (346). After this peak period, the muscle fibres undergo necrosis and become highly inflammatory (347). Following the inflammation period there is a regeneration phase which enables the surviving muscle fibres to grow and hypertrophy (346). It is hypothesised that this increase in FKBP25 expression is a result of either hypertrophy of surviving muscle (348, 349), or extensive remodelling and density of the tubulin cytoskeleton (350). In contrast, upon examination of a denervation model of muscle atrophy, it was identified that FKBP25 expression is reduced compared to sham controls (**Fig 4.16**). Denervation is a widely used experimental model used to study skeletal muscle atrophy. This model requires severance of the common sciatic/peroneal nerve which innervates the anterior and lateral lower limb compartments (351). The disruption of innervation to the lower limb results in a progressive decline in fibre cross sectional area, muscle mass loss, and reduced contractile function (352). A second model of muscle atrophy using food deprivation was also examined. In this model the mice are deprived of food access for 48 hours which has previously been shown to reduce muscle mass (353) It was found that FKBP25 expression was not altered upon food deprivation (**Fig 4.17**). These studies have demonstrated that FKBP25 expression is altered in some models of skeletal muscle hypertrophy and atrophy. This suggests that in addition to proliferation and differentiation, FKBP25 may have a role in skeletal muscle plasticity in vivo.

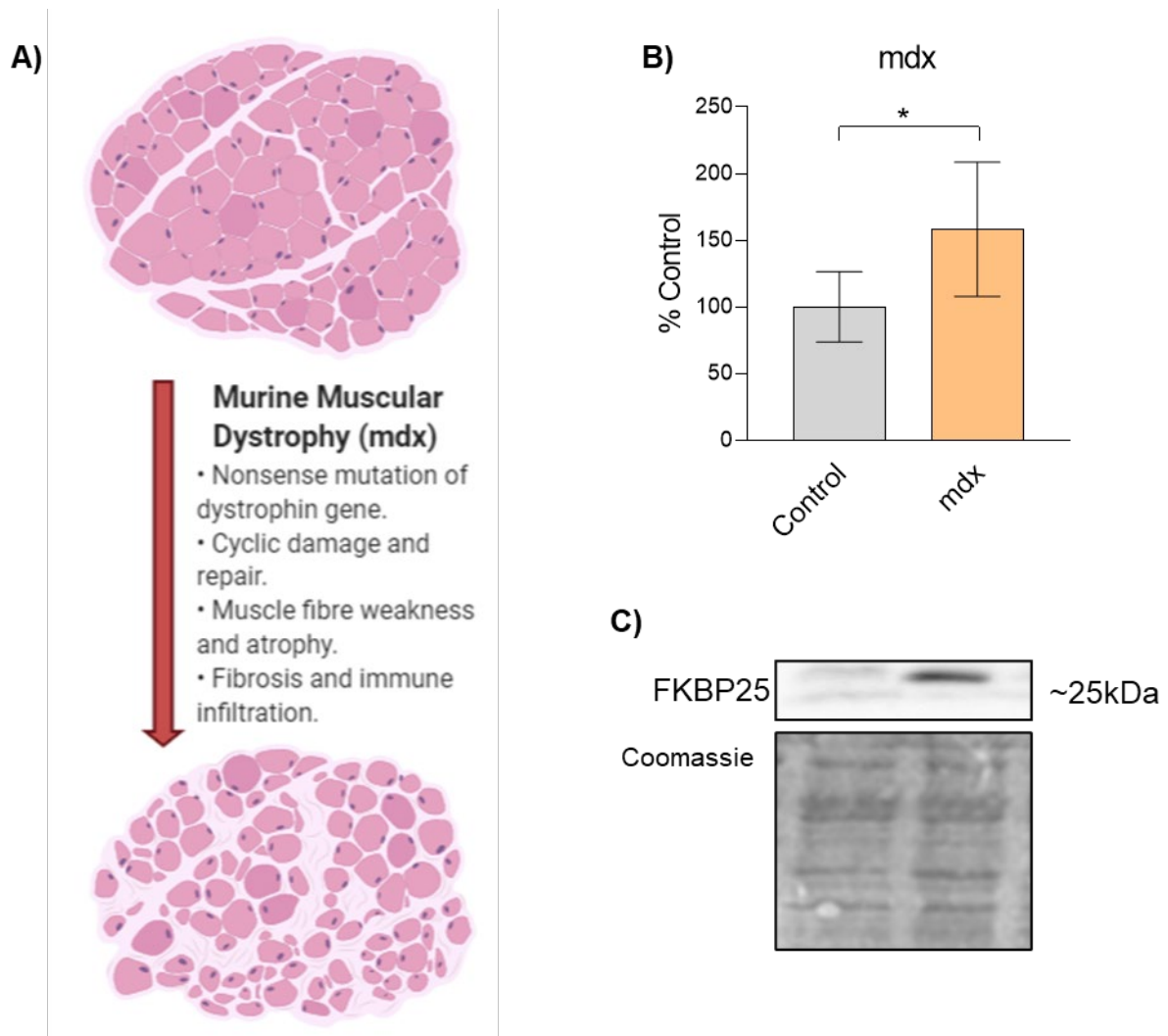


**Figure 4.15: FKBP25 protein expression is increased in a model of murine muscular dystrophy (mdx)**

**A)** Mdx is a murine pathology that mimics that of human Duchenne muscular dystrophy (DMD). The presence of a premature nonsense mutation in the dystrophin gene results in progressive muscular atrophy and fibrosis. Made with Biorender.com **B)** FKBP25 expression was increased in mdx muscle compared to control. **C)** Representative blot. All data is presented as mean  $\pm$  SD,  $n=3$ , \* =  $p \leq 0.05$ .

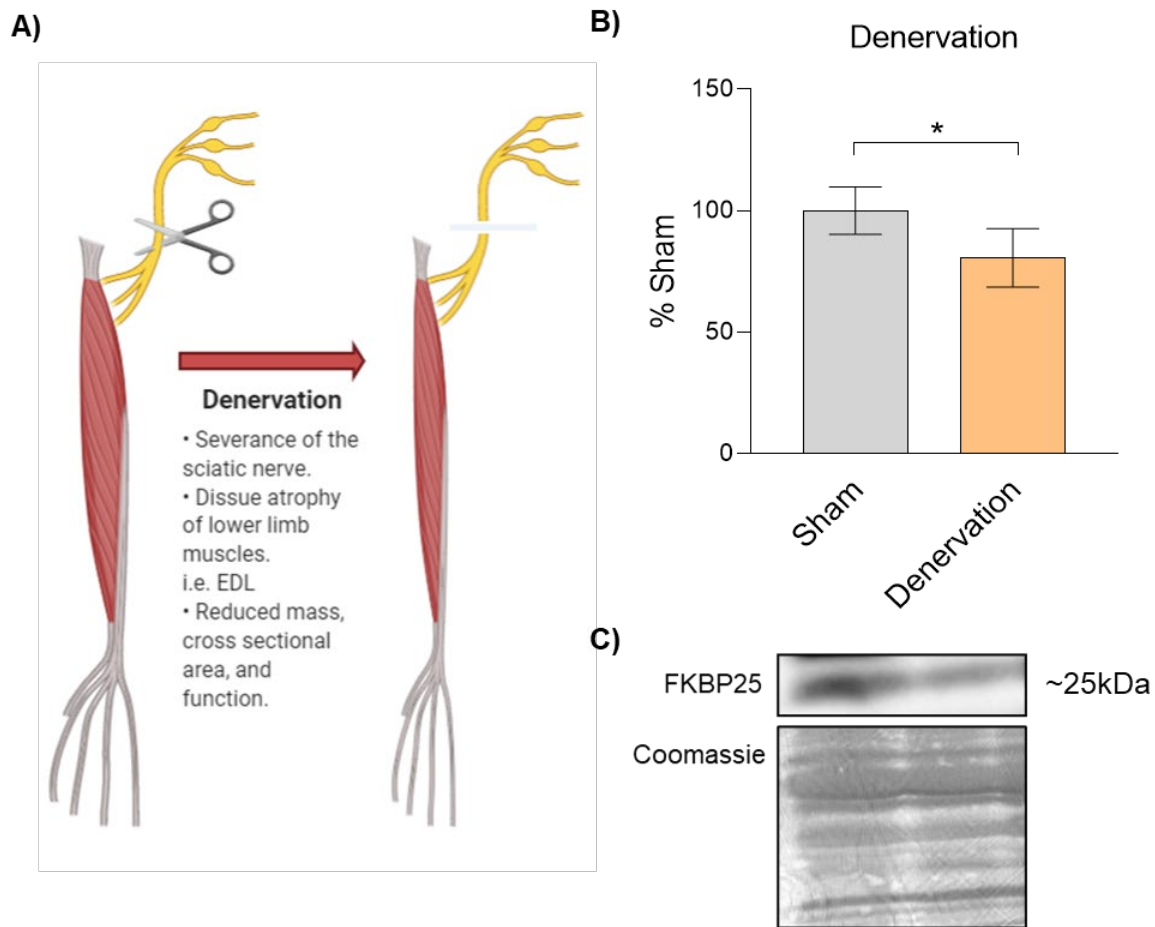


**Figure 4.16: FKBP25 protein expression is reduced upon hindlimb denervation**

**A)** Diagram depiction of denervation as a model of skeletal muscle atrophy. Denervation (severing of the sciatic nerve) is used to prevent use of the lower limb resulting in disuse atrophy, **B)** in this condition it was found that FKBP25 protein expression was reduced. **C)** Representative blot. All data is presented as mean  $\pm$  SD,  $n=3$ , \* =  $p \leq 0.05$ .

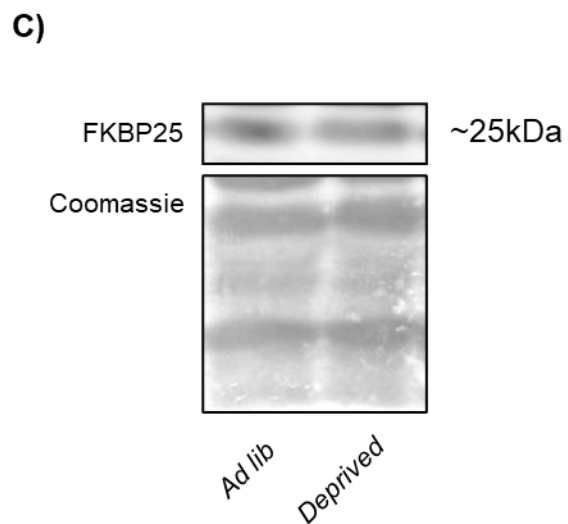
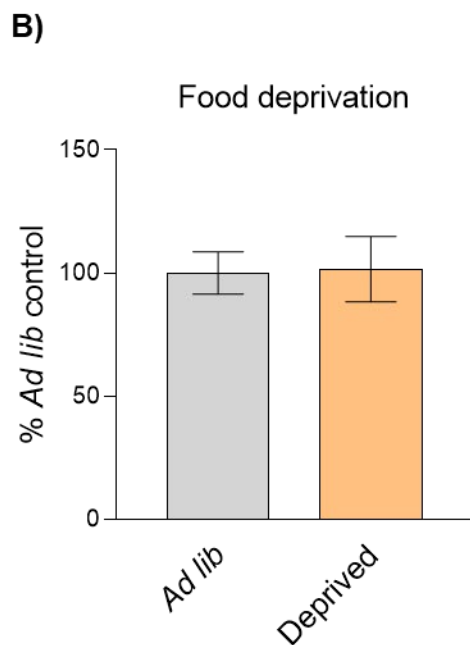
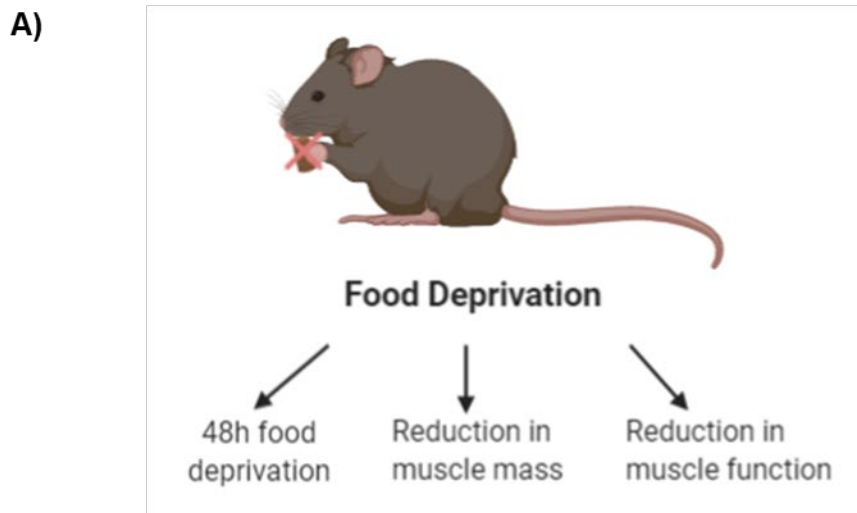


**Figure 4.17: FKBP25 protein expression is unaltered in a model of food deprivation induced skeletal muscle atrophy**

**A)** Mice were deprived of food for 48 hours to induce skeletal muscle atrophy. **B)** No change to FKBP25 protein expression was detected compared to ad libitum food access controls. **C)** Representative blot. All data is presented as mean  $\pm$  SD, n=3, \* =  $p \leq 0.05$

## 4.3 Discussion

### 4.3.1 FKBP25 expression is increased upon C2C12 differentiation and induction of quiescence.

Our previous studies have focused on the role of FKBP25 in EMT and models of breast cancer cell de-differentiation. Throughout this investigation it was questioned how FKBP25 would be expressed in models of physiological differentiation, specifically, would the opposite phenomena occur. It was hypothesised that, in the case of physiological differentiation, proliferative progenitor cells would express low levels of FKBP25 compared to mature or post mitotic non-proliferating cells. To examine this hypothesis, the C2C12 myoblast model of myogenesis was utilised. To date, there has been limited research in the role of FKBP25 in myogenesis or mature skeletal muscle. One major finding regarding FKBP25 in mature skeletal muscle physiology was that FKBP25 is expressed in the top 10% of the skeletal muscle proteome, suggesting that FKBP25 may play an essential role in maintaining muscle structure or function (225). Considering the hypothesis that was established earlier (**Fig 4.5**), whereby FKBP25 expression is reduced to facilitate a mesenchymal phenotype, described as proliferative and migratory, here it was hypothesised that myoblast cells would display a similar mesenchymal, or dedifferentiated, phenotype and consequently express low levels of FKBP25.

Upon examination of C2C12 myoblast differentiation in 24-hour intervals until complete differentiation to myotubes (96 hours), it was identified that C2C12 myotubes express significantly higher levels of FKBP25 than proliferating myoblasts (**Fig 4.4**). Here it was observed that throughout differentiation there are incremental increases in FKBP25 that corresponds with both myogenic commitment and cessation of

proliferation (indicated by the decline in cyclin D, **Fig 4.4 B**). This trend of FKBP25 expression being low in proliferative, de-differentiated cells and increased in polarised, differentiated cells is evident in C2C12 myogenesis, similarly to what was described earlier in MDA-MB-468 EGF-mediated EMT (**Fig 3.9**).

Next, the localisation of FKBP25 in myoblasts and myotubes was examined. As previously identified in breast cancer cell lines, FKBP25 was primarily located in the cytoplasm of both myoblasts and myotubes (**Fig. 4.6**). Upon differentiation it is noticeable that the content of FKBP25 is increased as the myoblasts fuse and form multinucleated myotubes. An essential structural feature of mature myotubes is a complex network of MTs to maintain the integrity of the fibre, as well as interact with contractile proteins (354). Structural changes to the MT network are indispensable for myogenesis and myoblast fusion, such that loss of end binding protein 1 (EB1; a MT plus end tracking protein) results in prevention of fusion, elongation, and expression of MRFs (355). Myoblasts contain an unstable MT network that must become stabilised to adequately differentiate (356). Interestingly, this coincides with FKBP25 lowest expression in de-differentiated myoblasts. As the myoblasts begin to differentiate and subsequently begin to stabilize the MT network, there is a consequent increase in FKBP25.

To further describe the role of FKBP25 in myogenesis, a model of skeletal muscle progenitor cells, satellite cells, was assessed by inducing quiescence in C2C12 myoblasts. This technique involved suspending the myoblasts in a viscous medium for a period of 48 hours to induce quiescence, or growth arrest, where there is no proliferation of cells (357). Upon induction of quiescence (at 48 hours) it was found that levels of FKBP25 are elevated compared to myoblasts that have been replated and allowed to re-enter the cell cycle (**Fig 4.8**, See **4.8 B**, Cyclin D). Notably, here it

was found that C2C12 myoblasts that have de-differentiated per se but are non-proliferative express greater levels of FKBP25 than actively proliferating myoblasts. In this model we were able to demonstrate that throughout C2C12 differentiation there are significant increases in FKBP25 protein expression. Together these data suggest that FKBP25 expression levels may be linked to proliferation status of the cells. Such that actively cycling myoblasts express low levels compared post mitotic myotubes which expressed high levels of FKBP25. Additionally there were no notable changes in differentiation morphology of previously quiescent cells (**Fig 4.7**) It has been previously established that FKBP25 is a microtubule associated protein that facilitates microtubule stability. As such, to aid in faster proliferation a decrease in FKBP25 expression may facilitate an increase in microtubule instability. Conversely, in the myotube, it would be of benefit for structural integrity and generation of the vast microtubule network to have increased FKBP25 expression. To further examine the potential role for FKBP25 in C2C12 structure and function FKBP25 loss of function must be explored in future studies.

#### 4.3.2 FKBP25 expression is increased in differentiated primary RMS cells but not differentiated primary myoblasts.

After investigating the impact on FKBP25 in C2C12 myoblast differentiation a second model was selected to test the hypothesis that FKBP25 is expressed highly in differentiated cells. Using human skeletal muscle myoblast cell line MBA-135 it was identified that FKBP25 expression is not altered in this model of differentiation (**Fig 4.9 and 4.11**). While it is confirmed that both MBA-135 and C2C12 cells have undergone differentiation to mature myotubes, the growth conditions of these two cell types are different. MBA-135, a primary cell line, require supplementation with growth factor fibroblast growth factor (FGF-b), while immortalised C2C12 myoblasts do not require

addition of growth factors. Interestingly, in our previous studies MCF10A cells with constitutively active Ras, it was identified that FKBP25 expression is elevated (See **Fig 3.5**; MCF10A Ras mutation). This suggests that stimulation of this growth factor pathway impacts upon FKBP25 expression, at least in non-cancer cells. Furthermore, it has been identified that FGF appears to have a longer lasting impact on Ras signalling than EGF (358). Considering the presence of FGF-b in the growth medium for these cells, it may be that there is an increased basal level of FKBP25 via growth factor signalling. Resulting in no obvious increase in FKBP25 upon differentiation. Next, the RMS cell line, Rh30, was examined where it was identified that upon differentiation, FKBP25 expression was increased (**Fig 4.10 and 4.12**). Unlike MDA-135 cells, the Rh30 cells do not form myotubes, which is due to p53 mutation (p53<sup>R373C</sup>, functionally identical to p53<sup>R273H</sup> mutation (359); described in Section 3.2.2) impairing the withdrawal from the cell cycle and the function of myogenic factors (360). This results in an inability to differentiate and produce the contractile protein, myosin heavy chain (See **Fig 4.12 B**). Again, this event was identified in MCF10A p53 mutant breast cancer cells, where FKBP25 was found to be increased in p53<sup>R273H</sup> MCF10A cells (See **Fig 3.6**; MCF10A p53 mutation panel). Interestingly, this p53 mutation is also found in MDA-MB-468 breast cancer cells which have notably high levels of FKBP25 expression (**Fig 3.3**). However, examination of the effect of EGF stimulation on C2C12 myoblasts demonstrated that there was no impact on FKBP25 protein expression (**Fig 4.13**). While it was observed this occurrence in differentiating C2C12 myoblasts, this event may not occur in human primary myoblasts. Alternatively, MDA-135 cells should be cultured in the absence of FGF-b in the growth medium to determine if this is causative to the increased FKBP25 expression in MDA-135 myoblasts.

### 4.3.3 FKBP25 expression is increased in in vivo models of skeletal muscle hypertrophy and reduced in some models of atrophy

To build on our previous in vitro studies in C2C12 myoblasts, it was aimed to examine the impact of skeletal muscle hypertrophy and atrophy conditions on the expression of FKBP25. To date, there are limited studies that have examined the roles of FKBP25 in the absence of exogenous ligands, including FK506 and rapamycin. Earlier, in section 3.2.4, it was revealed for the first time that FKBP25 protein expression is reduced in proliferating, de-differentiated myoblasts and throughout differentiation and commitment to a post mitotic phenotype there is an increase in FKBP25 protein expression (**Fig 4.5**). One such feature of myogenic differentiation of interest that may be related to FKBP25 is the remodelling of the MT cytoskeleton. As such, next it was aimed to investigate some in vivo models of muscle remodelling. These include atrophy, hypertrophy, and disease models to describe the impact of the changes of FKBP25 expression in these remodelling conditions.

The first model of skeletal muscle remodelling that was examined was chronic mechanical loading (CML), a model of skeletal muscle hypertrophy. Here it was hypothesised that, as demonstrated in our C2C12 model, as the fibres undergo overload-induced hypertrophy there will be an increase in FKBP25 expression. Upon examination of the tissues, it was identified that there was, in fact, an increase in FKBP25 protein expression with mechanical overload compared to sham control muscles (**Fig 4.14**). Interestingly, it has been identified that the synergist ablation model of mechanical overload results in increased satellite cell content and activation in the skeletal muscle (361). In our C2C12 model of quiescence it was seen that there is an increase in FKBP25 protein expression in quiescent cells compared to proliferating myoblasts (**Fig 4.8**). Which is in fact the opposite of what is observed in

the mechanical overload where FKBP25 protein expression is increased. This may indicate that the increase in FKBP25 protein expression is related to cytoskeletal remodelling of regenerated tissue. An important role of the MT network in skeletal muscle is to transduce mechanical signals to facilitate movement and contraction (362). In a model of skeletal muscle regeneration following chemical damage, it was found that there is significant remodelling of the MT network, resembling that of mdx pathology (350). Considering these roles of MT remodelling in regeneration, and FKBP25s role in stabilising the MT cytoskeleton (109), this may be why FKBP25 protein expression is elevated in overloaded muscles that have undergone regeneration and hypertrophy.

Next, a second model of skeletal muscle damage and regeneration was examined, the mouse model of Duchenne muscular dystrophy (DMD/mdx). In the mdx model of DMD there is an acute onset of the pathology including increased damage/necrosis at around 3 weeks of age, which reduces to a more chronic, lower level of damage by 8 weeks which persists throughout life (363). This chronic damage is persisted by recurring damage and regeneration cycles caused by physical activity resulting in inflammation (364). Dystrophin is an essential component of the transmembrane network known as the dystrophin-glycoprotein complex (DGC) (365). Dystrophin binds to the DGC component  $\beta$ -dystroglycan forming a link between the cytoskeleton and extracellular matrix (366). The loss of dystrophin protein from the sarcolemma membrane disrupts the protein complexes that convey mechano-transduction signals, and ultimately resulting in structural damage to the sarcolemma (367). The damage to the sarcolemma allows an influx of cytosolic  $\text{Ca}^{2+}$  and subsequent induction of reactive oxygen species (333, 368). Collectively these events manifest as loss of muscle strength and diminished muscle function (369). Interestingly, it has been demonstrated

that upon loss of dystrophin in the mdx phenotype results in significantly increased MT network compared to WT mice (370). It was proposed by Nelson et al., that this intense remodelling of the MT network in mdx muscle is an attempt to stabilise the damaged sarcolemma caused by the loss of dystrophin. This was supported by exogenous expression of mini-dystrophin molecules resulting return to baseline levels of MT content (370). Considering this feature of mdx pathology, it was hypothesised that FKBP25 may be upregulated in response to increased microtubule network remodelling. Upon examination of control and mdx skeletal muscle samples, it was found that mdx muscle has significantly increased expression of FKBP25 compared to control (**Fig 4.15**). The samples that were assessed were collected from 8-week-old mdx mice, meaning that the pathology was in a post regeneration state and likely to have undergone extensive MT network remodelling. The increased MT network would require increased microtubule stabilising proteins to maintain stability of MT polymers, such as FKBP25 – a known MT stabilising molecule.

Following out assessment of models of skeletal muscle hypertrophy and regeneration, next a skeletal muscle atrophy model was examined. As described in section 3.2.6, denervation involved severance of the common sciatic/peroneal nerve which innervates the anterior and lateral lower limb compartments (351). This procedure is well described and known to result in disuse atrophy of hindlimb muscles (371-373). Upon denervation there is a shift in microtubule organisation (332, 374). Interestingly, as described in regeneration models, there is an increase in the density of the MT network (332). This attribute of atrophied skeletal muscle is thought to be a protective mechanism to overcome mechanical stress (332). In microtubule associated protein 6 (MAP6; a microtubule stabilising molecule) knockout mouse model it was observed that there was an atrophy phenotype, characterised by reduced muscle cross sectional

area, reduced muscle mass, and muscle dysfunction (334). Importantly, there was a significant increase in MT network density reported. However, in this model we have observed a reduction in FKBP25 protein expression alongside skeletal muscle atrophy (**Fig 4.16**). In conjunction with the results observed in CML and mdx models, it appears that FKBP25 protein expression is synonymous with cytoskeletal remodelling associated with muscle regeneration.

Finally, a short-term model of skeletal muscle atrophy was examined. This model involved a 48-hour food deprivation period in which the mice still had ad libitum access to water (227). Upon food deprivation it has previously been demonstrated that protein synthesis becomes reduced and protein degradation becomes increased, ultimately resulting in a reduction in mass (353). Specifically, where reduced nutrient availability reduces signalling via PI3K/Akt, resulting in lowered activation of mTORC1, ultimately impairing p70S6K phosphorylation leading to a reduction in protein synthesis (375). In addition to this, a reduction in Akt phosphorylation can also activate Forkhead box protein 01 (FOXO1) transcription factors that transcribes E3 ubiquitin ligases, MURF-1, and atrogin-1, which control atrophy-induced muscle mass changes (376).

Similar to the denervation model, it was hypothesised that FKBP25 expression would be impacted by either reduced caloric intake impairing protein synthesis, or the remodelling that would be associated with muscle wasting. However, it was found that there was no change to FKBP25 expression following the food deprivation period (**Fig 4.17**). While food deprivation and denervation are both models of atrophy, the key difference in these two models is that the denervated animals are left for 7 days to induce the wasting phenotype. Comparatively, in the food deprivation model the animals are deprived for 48 hours, and the samples were collected immediately after the starvation period. The absence of the regeneration window may be the factor that

results in no change to FKBP25 protein levels. Nelson et al., propose that it takes between 5-10 days for regeneration of damaged mdx tissue to become re-stabilised by exogenous dystrophin molecules (370). In future studies it should be considered to include a recovery period following food deprivation to observe the potential changes in MT organisation and FKBP25 protein expression.

#### **4.4 Conclusions**

This chapter has described the role of FKBP25 in models of myogenesis and skeletal muscle plasticity. In line with our hypothesis that low levels of FKBP25 is required for a proliferative phenotype, it was observed that C2C12 myoblasts express low levels of FKBP25 which accumulates throughout myogenic differentiation. This was further supported by an increase in FKBP25 in quiescent myoblasts compared to proliferating myoblasts. Interestingly, this trend was not observed in human primary myoblasts which suggests that this hypothesis is not universally linked to myogenesis. Upon examination of *in vivo* models of skeletal muscle plasticity increases in FKBP25 protein expression were observed upon chronic mechanical loading and the regeneration phase of mdx pathology. In both of these models there is extensive regeneration to muscle fibres, and integration of activated satellite cells which is known to increase MT network density. Considering the role of FKBP25 as a MT stabiliser, it is hypothesised that the observed increase in FKBP25 expression has resulted from these changes in MT density. However, in a denervation model of skeletal muscle atrophy a reduction of FKBP25 protein expression was observed and no change in a food deprivation model. To fully describe the involvement of FKBP25 in mature muscle structure and function *in vivo* knockdown studies should be undertaken.

---

## Chapter 5: The impact of FKBP25 knockdown on cell biology and function

---

### 5.1 Introduction

To date there has been limited research surrounding the role of FKBP25 in cell biology and function. There are a diverse range of cellular functions that have implicated FKBP25, including proliferation, microtubule dynamics, p53 regulation and DNA damage repair (109, 112, 119). However, these functions have been examined in a limited context. Here it is aimed to examine the role of FKBP25 in physiological and pathological models of differentiation and de-differentiation. Many biological processes are required for differentiation and de-differentiation in various cellular models including TNBC EMT and in C2C12 myogenesis. These two processes effectively operate in the opposite direction, such that EMT begins with a differentiated cell type that becomes increasingly plastic and mesenchymal. In contrast, C2C12 myogenesis may be referred to as a MET. This occurs when a less differentiated progenitor cell commits to a cell lineage, in this case myogenic lineage, and differentiates into a committed myotube. Each of these processes require an assortment of biological processes to be completed including, but not limited to, cell proliferation, migration, anchorage dependent, and independent growth.

#### 5.1.1 The cell cycle

Cell proliferation is an essential process in which a mother cell grows and divides to produce two identical daughter cells (**Fig 5.1**). An abundance of events regulates the cell cycle to ensure that proliferation can occur without any abnormalities. In brief, when a cell enters the cell cycle, the cell will enter the first phase of growth (G1) where the cell is required to grow, that is increase its protein and organelle content to prepare

for mitosis (377). Next, the cell will enter the synthesis phase (S phase) where the DNA will be replicated and end with 2N chromosomes (378). S phase is then followed by a second growth phase (G2) in which the cell physically prepares for mitosis by increasing cell growth and assembling microtubule spindles. Importantly, there are several checkpoints that the cells must pass before being allowed to progress through the cell cycle, these are mediated by cyclins (G1) and p53 (G2) (379). Finally, after interphase is complete, the cell is able to undergo mitosis and cytokinesis and produce two daughter cells. Disruptions to the cell cycle or its checkpoints can have detrimental effects on the production of normal daughter cells. It is well described that excessive proliferation of abnormal cells results in the development of cancer (Reviewed in (380)). As such it is important to identify molecules that may impact upon appropriate cell proliferation. FKBP25 may impact upon cell proliferation in a number of ways, including inadequate formation of the mitotic spindle resulting in abnormal chromosome separation. Also, considering the role of FKBP25 in MT stability, loss of FKBP25 could result in increased dynamic instability of the MT network. Alternatively, FKBP25 may dysregulate p53 via its role as a regulator of p53's repressor MDM2 (119). Together these factors can lead to excessive and dysregulated proliferation that can progress EMT.

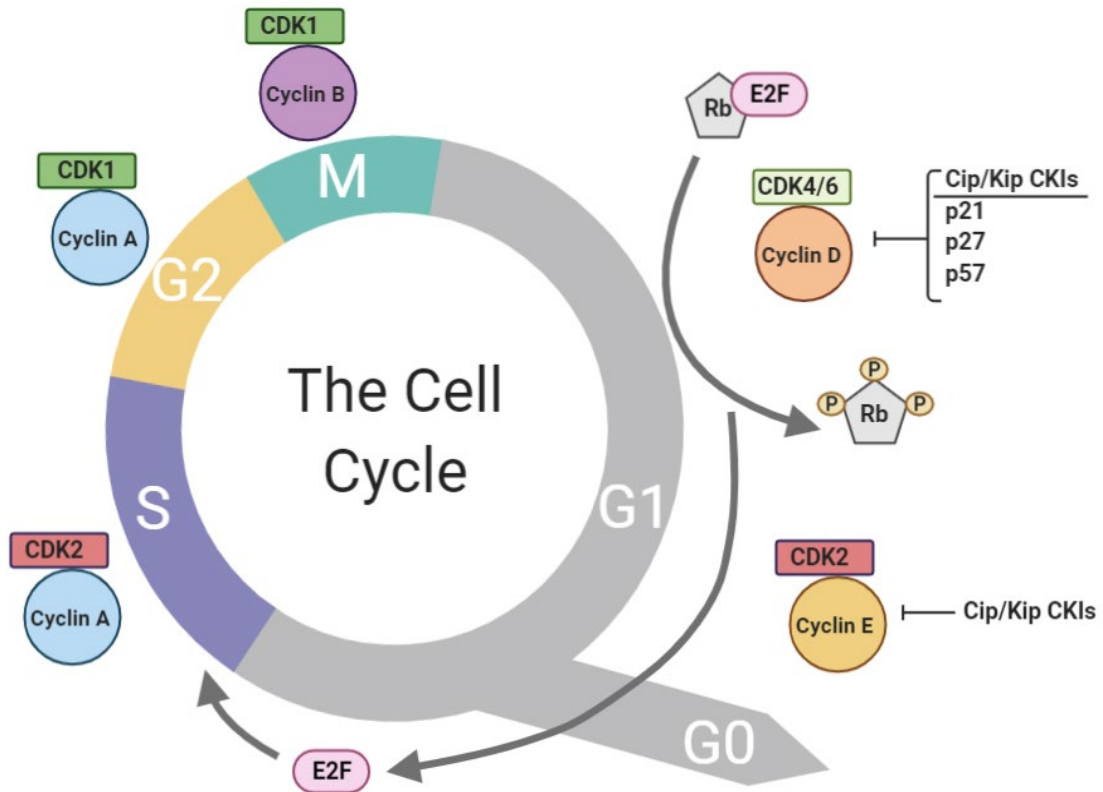


**Figure 5.1: The cell cycle**

The cell cycle is composed of 4 phases, growth (G1), synthesis (S), second growth (G2), and mitosis (M). Each of these phases is associated with different cyclin and cyclin-dependent kinases (CDK) that enable the cell to progress through the phase. G1 is governed by hyper-phosphorylation of retinoblastoma protein (Rb; by cyclin D/CDK4/6 complex) causing its dissociation from E2F. E2F initiates expression of S phase related genes, including Cyclin E, to allow S phase progression. Cyclin A binds to CDK2 to initiate S phase, and upon binding to CDK1 instigates nuclear envelope degradation in G2 phase to prepare for mitosis. CDK1 becomes bound to cyclin B to progress through M phase and complete the cell cycle. Made with Biorender.com.

Following G1, phase there are several outcomes for the cell including, progression to S phase, become arrested in G1 and not progress, or be removed from the cell cycle and enter a quiescent state (G0) (381). In relation to myogenesis, it is essential that cells enter G0 to stop proliferation and commit to terminal differentiation. Upon entry into G0, there are a variety of processes that occur to initiate myogenic differentiation

including, induction of myogenic regulatory factors (MyoD, Myf5, myogenin) which are essential for cessation of proliferation and fusion (382, 383). These myogenic factors can be directly induced by repression of cyclin dependent kinases (CDKs). For example, CDK4 has been demonstrated to bind to MyoD and prevent its transcriptional program (384). Thus, once withdrawn from the cell cycle, myogenic commitment can occur. The role of FKBP25 has not been investigated in the process of myogenesis or proliferation. Considering our previous findings in chapter 3, it is hypothesised that FKBP25 is a negative regulator of the cell cycle. As such, it is thought that the accumulation of FKBP25 protein throughout differentiation is required to halt proliferation.

### 5.1.2 Cell movement

Cell migration is an important biological process for cells in both physiological and pathological processes. In normal physiology, some cell types, including activated satellite cells and myoblasts, must migrate from the basement membrane into the damage site. Conversely, cancer cells acquire the ability to migrate either toward a chemoattractant or growth stimulus at a secondary site. In either case, the process of migration is identical and consists of a cycle of steps to facilitate movement (**Fig 5.2**). These steps include, actin driven extension of the leading edge, integrin mediated focal adhesion to the ECM, contraction of the cytoplasm resulting in forward movement of the cell body, and release from contact sites (385, 386). Importantly a cascade of molecular events facilitates this movement. In short this occurs via

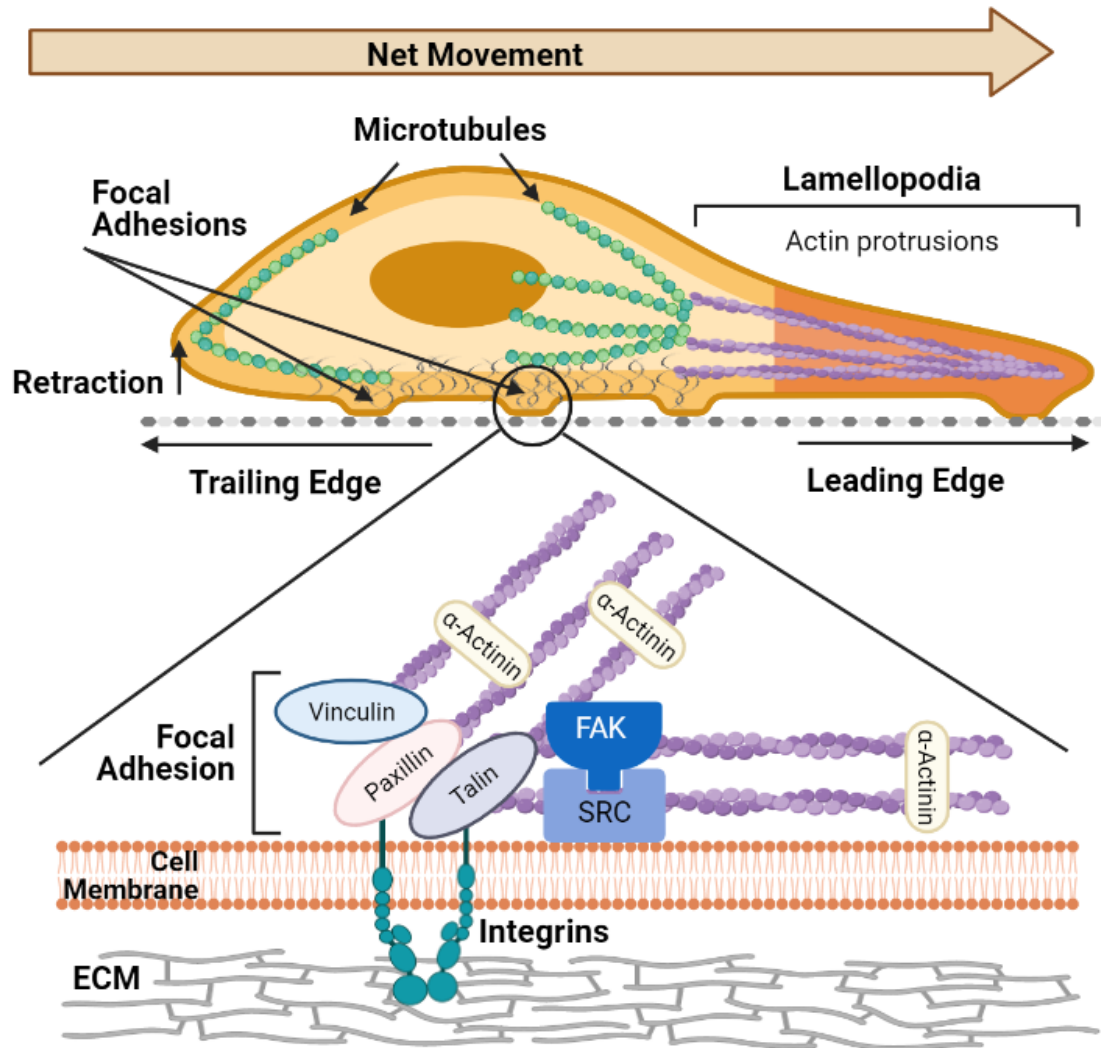


**Figure 5.2: Cell migration and principles of focal adhesion**

A migrating cell can be divided into two poles, the leading edge (at the direction of movement) and the trailing edge (behind the direction of movement). The microtubule network is essential to maintain the directionality of cell movement. The cell is anchored to the ECM by focal adhesions at which actin fibres protrude to polarise the cell (at both focal adhesions and leading edge). The focal adhesion is anchored to the ECM via integrin dimers which interact with a series of adhesion-related proteins (including, actin, vinculin, paxillin, talin, focal adhesion kinase (FAK), Src). Phosphorylation of FAK (by Src) initiates its focal adhesion engagement with the ECM. (Adapted from Katoh, *Cells*, 2020). Made with Biorender.com.

interactions between the cellular integrins and ECM via ligands (including fibronectin, vitronectin, and collagen). The formation of these cell adhesions regulates focal adhesion kinases (FAK) and Src kinases to activate substrates that will instigate adhesion of the actin cytoskeleton to these anchorage points – referred to as focal adhesions (387). In addition to the role of the actin cytoskeleton in migration, the MT cytoskeleton plays an integral role in cell migration. The formation of the trailing edge is facilitated by the protrusion of stabilised MTs and acts as a guide for the cell movement. Crucially, impairment of MT dynamic instability has been shown to impair cell migration *in vitro* (388). It has been previously established that FKBP25 has a role in regulating MT stability and, as such, may be implicated in regulating cell migration.

#### 5.1.4 Anchorage dependence and cell growth

Anchorage dependence is a feature of all tissue derived cells, except for those cells derived from hematopoietic lineage and selected transformed cancer cells. Anchorage-dependent cells require adhesion to a solid substratum, such as the ECM or tissue culture treated plastics. Adhesion has previously been shown to induce expression of cyclin D1, Rb phosphorylation, and activation of cyclin E/CDK2 (389). It has also been demonstrated that binding to ECM strata, including fibronectin, induces cyclin A and associated CDK activity (390). These features are relied upon less as cells undergo tumorigenic transformations, as seen in the EMT process. Anchorage-independent growth refers to the ability of cells to proliferate independently of adhesion to a solid substratum. This feature of cancer cells can occur as cells develop an increasing number of mutations, namely to oncogenes including c-Myc, v-Src, H-ras (391). H-ras oncogenic mutations have been shown to induce uncontrolled cyclin D-dependent kinases (CDK4/6), leading to proliferation independent of adhesion (392). Other studies have demonstrated that overexpression of integrin-linked kinases (ILKs)

in cells grown in suspension cultures improved cell cycle progression by upregulating cyclin D1 and cyclin E and reducing associated CDKI expression (393). FKBP25 has not been directly associated with cell cycle regulators, however, its association with MT stability may again be at play. The role of FKBP25 as a MT stabiliser may impact upon mitotic spindle assembly and dynamics in transformed cells to facilitate loss of anchorage dependence.

### 5.1.3 Implications for EMT and MET

The processes of proliferation, migration, and cell growth are essential for differentiation and de-differentiation of cells in both of EMT and MET. The EMT programme relies on loss of epithelial characteristics and gain of mesenchymal attributes. These include the loss of cell polarity and cell to cell adhesion, increased proliferation, and gain of invasion and migratory capabilities (Reviewed in (288)). As previously discussed, it appears that FKBP25 may play a role in cell proliferation and migration via p53 regulation, or tubulin dynamics which may occur in a cumulative or independent manner. For example, as cells acquire p53 mutations, which are associated with highly proliferative phenotype, there is a net reduction of FKBP25 to allow faster progression through the cell cycle. Alternatively, it could be that the reduction of FKBP25 results from other EMT pathways, such as abhorrent tyrosine kinase signalling. This would result in increased proliferation via Ras signalling and again result in dampened FKBP25 expression to maintain increased proliferative capacity. This was previously demonstrated in chapter 3, section 3.2.6, where release from quiescence resulted in a reduction in FKBP25 expression (**Fig 4.8**). Proliferation may also be influenced by microtubule stability, another function of FKBP25 (**Fig 5.3**). FKBP25 is a known microtubule stabiliser, notably being demonstrated to play a role adequate mitotic spindle formation (109).

In EMT, plasticity of the mitotic spindle demonstrates some positive features, including reducing the time required for the spindle to disassemble and reassemble for the next round of division (394). Conversely, it has been shown that loss of FKBP25 results in an increase of chromosomal abnormalities in osteosarcoma cells (109). Interestingly, FKBP25 has also been discovered to be involved in double stranded DNA break repair (111). This function could be linked to FKBP25 role in MT stability as stable MTs are required for transport of DNA damage repair proteins (395). Additionally, FKBP25 itself

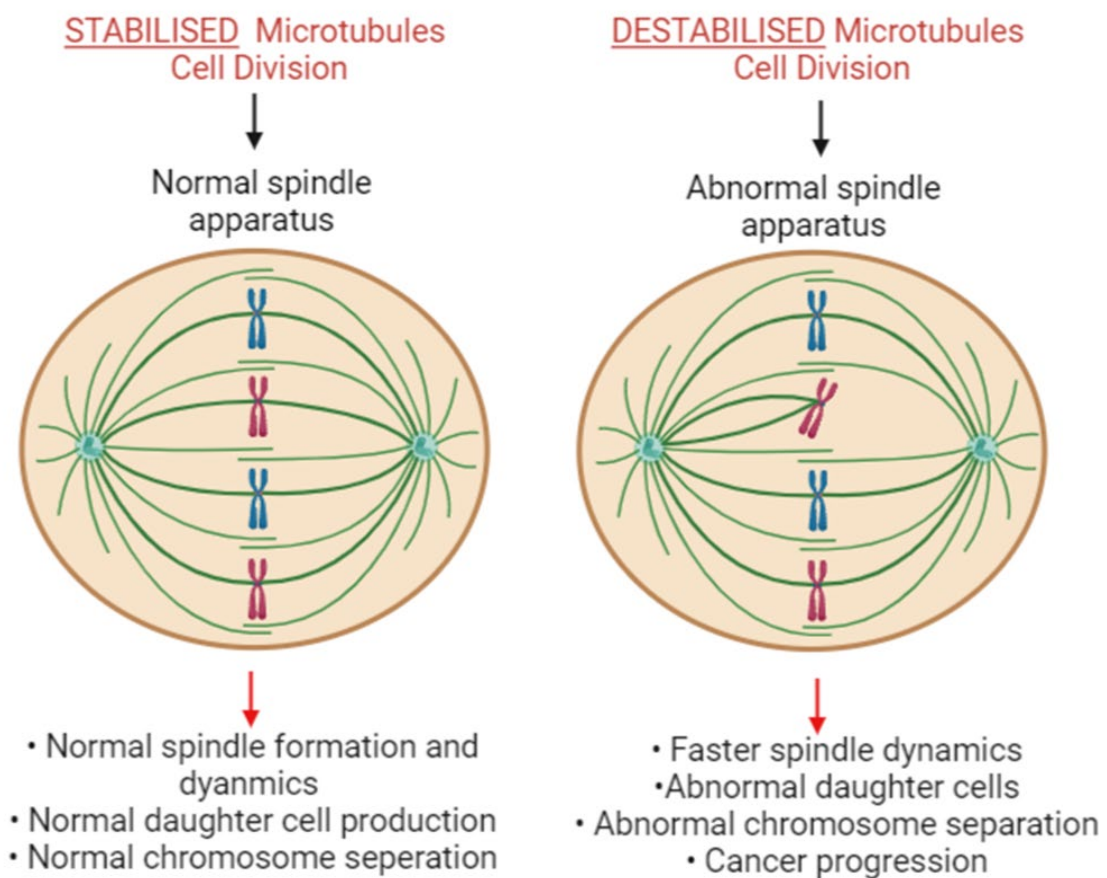


**Figure 5.3: The role of microtubule stability in cell division**

Stabilised microtubules (MT) are required for formation and maintenance of the mitotic spindle during cell division (Left). Destabilisation of the MT and mitotic spindle is known to result in weakening of the spindle apparatus resulting in abnormal chromosome separation (Right), Abnormal chromosome separation results in acquisition of somatic mutations that may impact upon cancer progression. Made with Biorender.com.

has been shown to interact with DNA, however, post translational modification to FKBP25 led to dissociation of FKBP25 from the MT apparatus (109). These functions suggest that FKBP25 may have an important role in MT formation, adequate cell cycle progression and accumulation of genomic mutations.

Conversely in MET, or cell differentiation in our myogenesis model, it was observed an increase in FKBP25 expression. Interestingly, in comparison to EMT, there are many opposing features, such as a cessation of proliferation and return of cell polarity (396). In this model of myogenic differentiation, it is hypothesised that as the maturing myoblasts withdraw from the cell cycle to enter a post mitotic state there is an accumulation of FKBP25 which acts as a positive feedback mechanism to halt cell cycle re-entry. Commitment to myogenic differentiation requires complete termination of the cell cycle to adequately induce myogenic factors including MyoD, myogenin, Myf-5, and Myf-6 (397-399). This results in an interplay between cell cycle inhibitors, cyclin dependent kinase inhibitors (CDKI), and retinoblastoma protein (Rb) and induction of myogenic factors, namely MyoD (382, 400). MyoD has been shown to bind to CDKI (including p21, p27, p57) resulting in ensuing inhibition of CDKs (401). Additionally, MyoD has been demonstrated to impair Rb phosphorylation, which would normally allow cells to progress through the cell cycle, thus impairing cell cycle advancement (402). Interestingly, the FKBP25 promoter region contains a MyoD binding site (Signalling Pathways Project 2017-2020) indicating that there may be a positive feedback loop operating. Myogenic commitment induces MyoD expression which may, in turn, promote MyoD-induced FKBP25 expression. The combination of MyoD and FKBP25 may cooperate to dampen proliferation signals and improve myogenic differentiation. The role of FKBP25 in microtubule dynamics may differ in this MET model. It is hypothesised that the sheer complexity and stability of the

microtubule network of mature myotubes is another feature that requires FKBP25 accumulation. An example of this was described in chapter 3, section 3.2.6, where models of muscle atrophy and regeneration, known to involve extensive remodelling of MT structure, also exhibited increased levels of FKBP25 (**Figs 4.13 - 4.16**) (350, 403). Considering these observations, the regulation of proliferation and MT stability are crucial regulators of FKBP25 content in MET and EMT.

The role of FKBP25 in cell biology to date has been poorly described. Here it is hypothesised a variety of roles for FKBP25 in cell biology and function including proliferation, migration, and anchorage-dependent growth. These roles have implications for both physiological and pathological models of differentiation and de-differentiation.

#### 5.1.4 Chapter Aims

This chapter aims to examine the impact of FKBP25 knockdown on cell biology and function of MDA-MB-468 breast cancer cells and C2C12 myoblasts.

##### **Specific aims:**

7. Generation of doxycycline-inducible shRNA knockdown of FKBP25 in MDA-MB-468 and C2C12 cell lines.
8. Examining the impact of FKBP25 knockdown on cell proliferation.
9. Examining the impact of FKBP25 knockdown on cell migration.
10. Examining the impact of FKBP25 knockdown on anchorage-dependent growth and invasion outgrowth in MDA-MB-468 cells.
11. Examining the impact of FKBP25 knockdown on C2C12 differentiation.
12. Examining the impact of FKBP25 knockdown epithelial to mesenchymal transition of MDA-MB-468 cells.

## 5.2 Results

### 5.2.1 Generation of doxycycline-inducible shRNA knockdown of FKBP25 in MDA-MB-468 and C2C12 cell lines.

Our previous data identified that FKBP25 expression is related to the degree of differentiation, or lack thereof in myogenic differentiation and EMT, respectively. It was identified that as the cells committed to differentiation, there is a substantial increase in FKBP25 protein expression, while loss of differentiation was associated with loss of FKBP25 protein expression. It is hypothesised that there may be at least two consequential factors that are attributing to the expression change in relation to the differentiated or de-differentiated phenotype. It is known that FKBP25 is a MT stabiliser and, as such, alteration of FKBP25 protein expression may have some impact upon MT stability. This impact of MT stability may manifest in many ways, however. In terms of differentiation, the focus is on alterations to proliferation as a measurable outcome. To adequately assess the impact that FKBP25 expression has on cell function, it is aimed to knockdown FKBP25 in MDA-MB-468 and C2C12 cell lines.

FKBP25 expression was found to be increased in the MDA-MB-468 breast cancer cell line compared to other TNBC cell lines (**Fig 3.3**). This data was further supported in an EGF-mediated model of EMT in MDA-MB-468 cells where FKBP25 protein was reduced upon de-differentiation and EMT induction (**Fig 3.9**). Conversely in the C2C12 differentiation model, it was identified that upon differentiation there is an accumulation of FKBP25 expression over time (**Fig 4.4**). In an attempt to model de-differentiation in these cells, C2C12 cells were grown in a suspension culture to induce quiescence. Here we were given crucial insight into the function of FKBP25 in relation to the working hypothesis. Upon induction of quiescence, it was found that there was some

reduction in FKBP25 expression, however, FKBP25 expression was more intricately linked to proliferation and re-entry to the cell cycle (**Fig 4.8**). With these results in mind, it was aimed to functionally assess the impact of FKBP25 KD on cell biology and function.

To examine the impact of FKBP25 loss of function on cell biology and function 25KD cell lines were developed in MDA-MB-468 and C2C12 cell lines. To develop these cell lines doxycycline (dox)-inducible short hairpin RNA vectors (shRNA; SMARTvector, Dharmacon, CO, USA) were lentivirally transduced into the cells of interest. Two 25KD vectors that transcribe two respective micro RNAs (Mir; Mir2 and Mir3) upon activation with dox (0.5µg/ml) were utilised for development of these cell lines. However, despite the homology of human and mouse FKBP25, Mir 3 was not adequate to induce FKBP25 knockdown in C2C12 myoblasts and, as such, C2C12 studies utilise only one mir. A non-targeting (NT) Mir was utilised to control for transfection related effects. All transduced cells were selected based on puromycin resistance encoded on the 25KD SMARTvectors. Following antibiotic selection, the cells were examined to visualise the red fluorescent protein (RFP) reporter that is expressed in concurrently with the shRNA (**Figs 5.4 and 5.5**). Upon confirmation of RFP expression, FKBP25 knockdown was confirmed via western blot. It was determined that upon treatment with dox there was an observable 70% reduction in FKBP25 protein expression in both MDA-MB-468 (**Fig 5.6**) and C2C12 (**Fig 5.7**) compared to their non-dox treated controls. Following the generation of these inducible cell lines *in vitro* functional and biochemical assays could be assessed

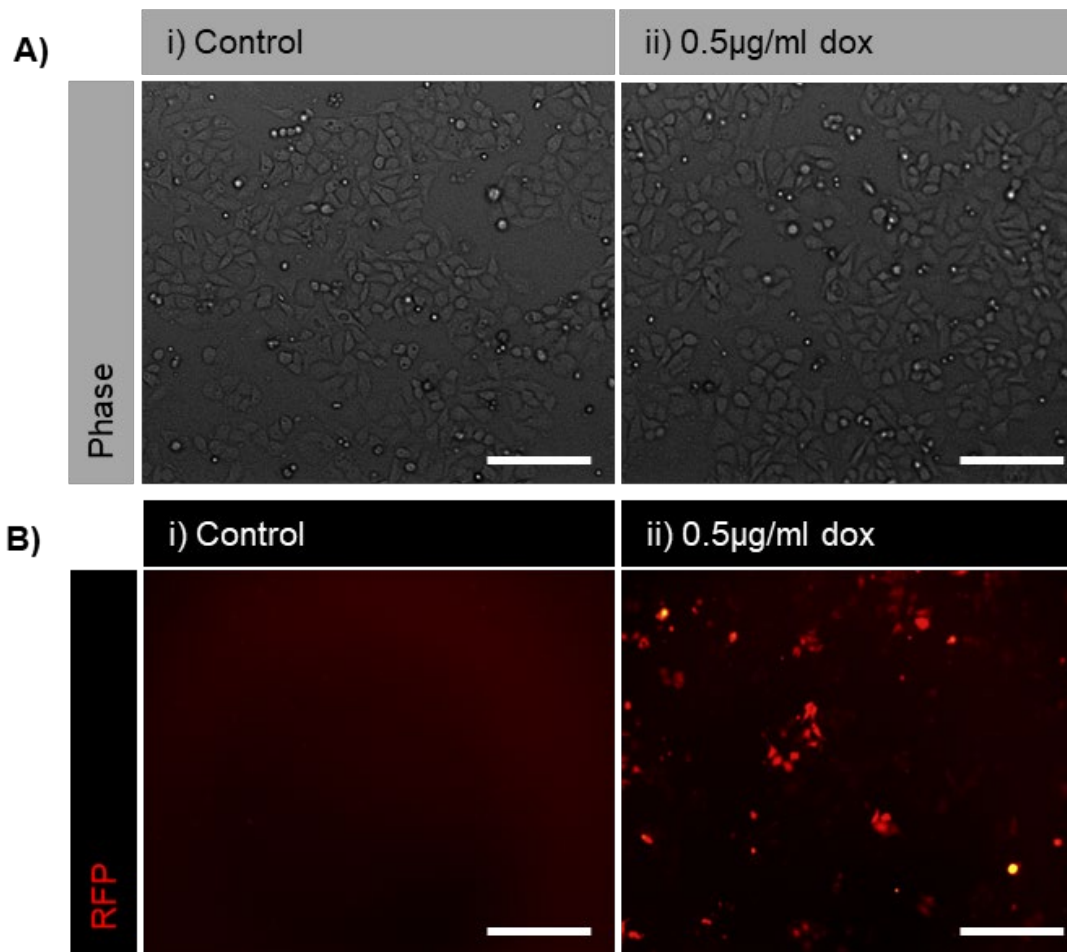


**Figure 5.4: Generation of a doxycycline inducible shRNA knockdown of FKBP25 in MDA-MB-468 breast cancer cells**

**A)** Phase contrast images of FKBP25 knockdown cells. **B)** Red fluorescence protein (RFP) expression in MDA-MB-468 cells upon 72 hours of doxycycline treatment. Scale bar = 100µm. Data presented as mean ± SD of n=3, \* =

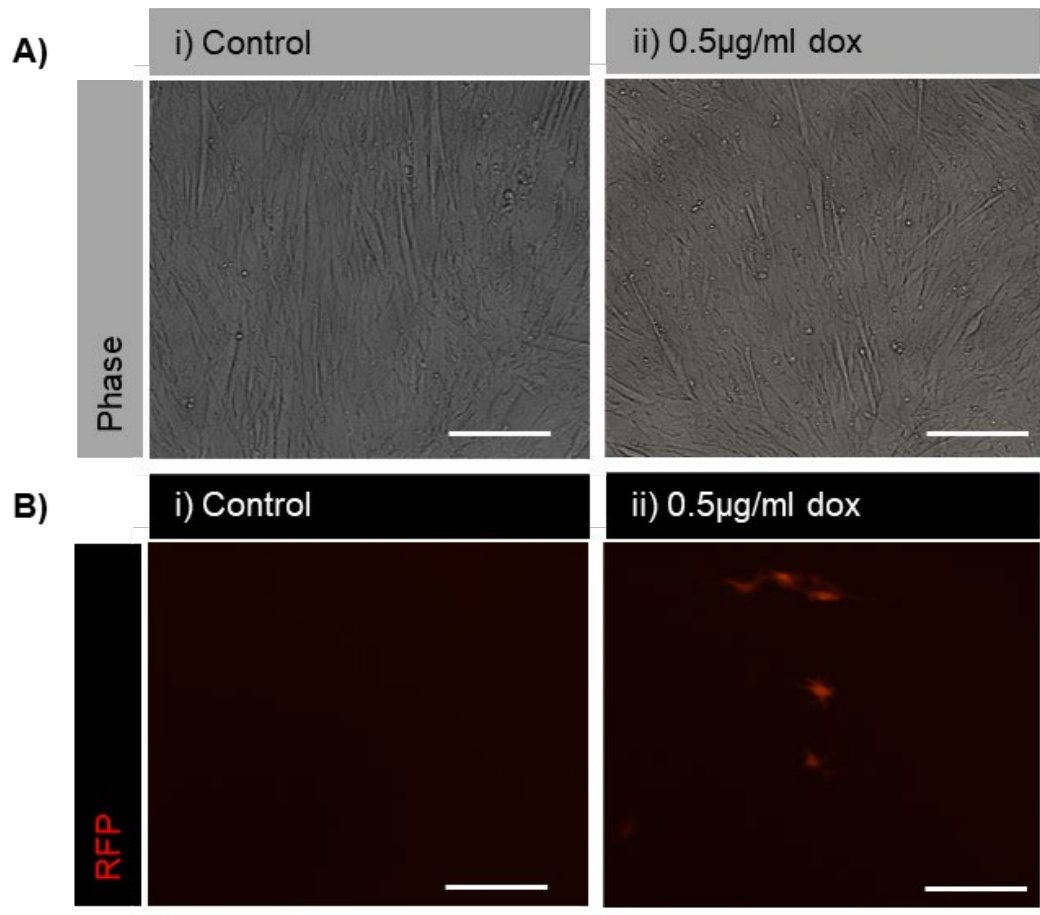


**Figure 5.5: Generation of a doxycycline inducible shRNA knockdown of FKBP25 in C2C12 myoblasts**

**A)** Phase contrast images of control (i) and induced (ii) knockdown C2C12 myoblasts. **B)** Red fluorescence protein (RFP) images of control (i) and induced (ii) knockdown C2C12 myoblasts. Scale bar = 100µm. Data presented as mean  $\pm$  SD of n=3, \* =  $p \leq 0.05$

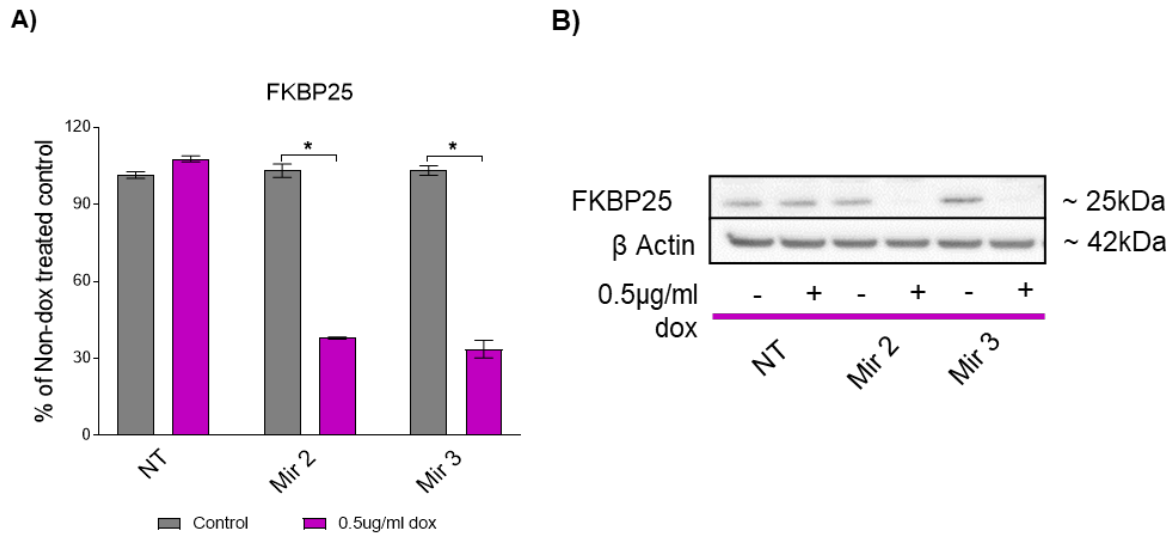


**Figure 5.6: Confirmation of FKBP25 inducible knockdown in MDA-MB-468 breast cancer cell line**

**A)** FKBP25 was knocked down in MDA-MB-468 cells using SMARTvector doxycycline inducible shRNA constructs, Mir 2 and Mir 3, and a non-targeting (NT) control. **B)** Representative blots. Data presented as mean  $\pm$  SD of  $n=3$ , \* =  $p \leq 0.05$

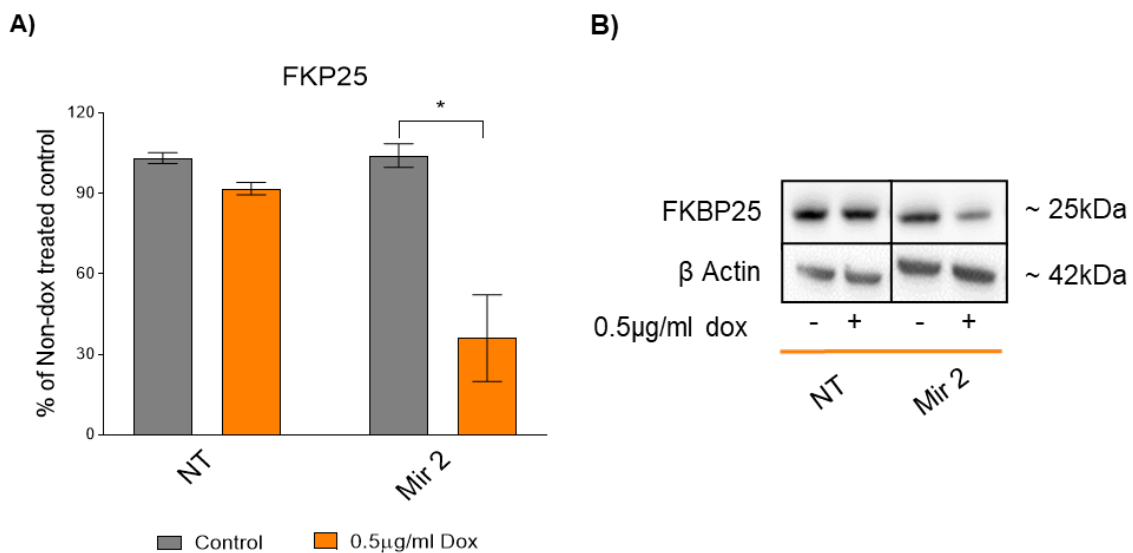


**Figure 5.7: Confirmation of FKBP25 knockdown in C2C12 myoblasts**

**A)** FKBP25 was knocked down in C2C12 myoblasts using doxycycline inducible SMARTvector shRNA constructs (Mir 2) and a NT control. **B)** Representative blots. Data presented as mean  $\pm$  SD of  $n=3$ , \* =  $p \leq 0.05$

### 5.2.2 FKBP25 knockdown increases cell viability and density over time indicating increased proliferation.

To examine the impact of 25KD on cell proliferation, a combination of biochemical assays was utilised. Resazurin (Sigma Aldrich, MO, USA) is a non-fluorescent substrate that can be reduced by oxidoreductases in the mitochondria to produce the highly fluorescent product, resorufin (404). Measurement of this conversion is an indicator of mitochondrial viability which is reflective of the content of living cells in a population, however, it does not distinguish dividing and non-dividing cells. Resazurin-based assays were measured daily for a period of 5 days to track cell viability of 25KD compared to NT control and non-dox treated controls. In conjunction with cell viability, cell accumulation was observed using Diff-Quick stain (Histolabs, Australia). After staining, the plates were scanned, and density was quantified. Here it was hypothesised that 25KD, based on the assumption that FKBP25 would impair MT stability, would lead to increased cell division.

It was found that over the five-day period there was a significant increase in cell viability and density for both MDA-MB-468 (**Fig 5.8**) and C2C12 (**Fig 5.9**). (109) MDA-MB-468 active Mirs 2 and 3 display significantly increased cell viability measurements compared to NT and non-dox treated controls (**Fig 5.8 A**). Furthermore, this is supported by an increase in cell accumulation measured by staining intensity of cells at the assay end point (**Fig 5.8 B and C**). In combination, these data indicate that there is an increase in proliferation in response to 25KD. Similarly, the same trend was identified in C2C12 myoblasts where the active Mir2 displayed an increase in cell viability measurements compared to controls (**Fig 5.9 A**). This was supported by an increase in cell accumulation density staining (**Fig 5.9 B and C**). This data supports

the hypothesis that loss of FKBP25 expression is associated with a proliferative phenotype.

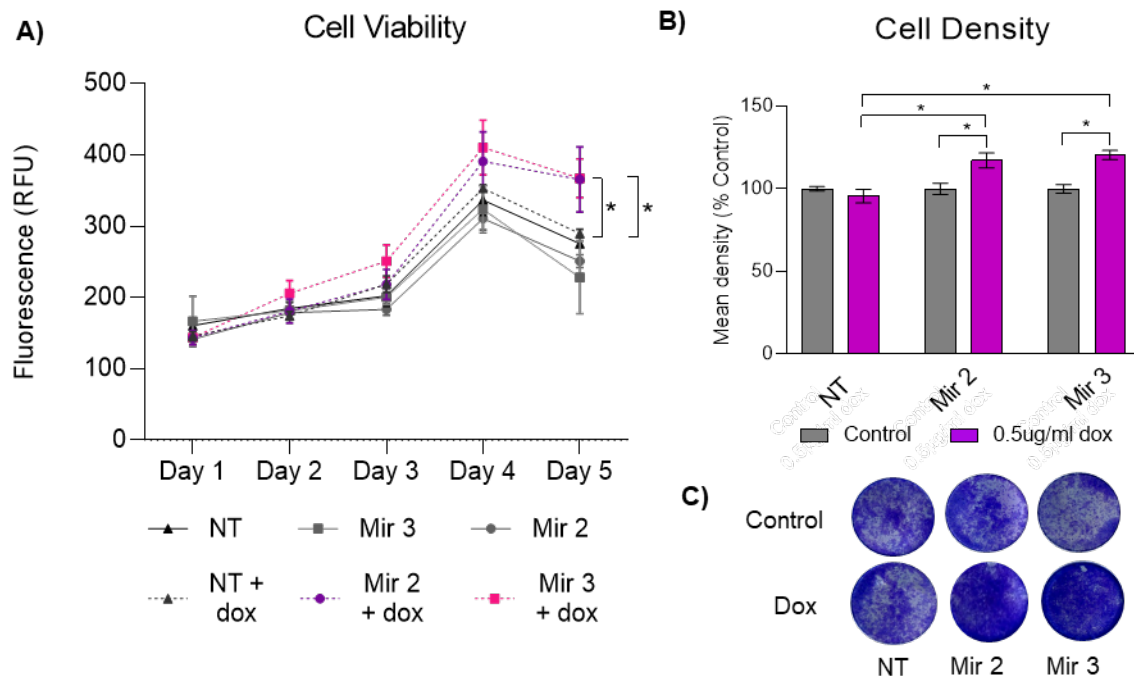


**Figure 5.8: FKBP25 knockdown increases cell viability and cell accumulation over time in MDA-MB-468 breast cancer cells**  
**A)** Cell viability measured using Resazurin dye demonstrates that FKBP25 knockdown (Mir 2 and 3) is increased compared to the non-targeting Mir. **B)** Measured staining density of cells following a 5-day growth period indicating that the active knockdown increases the number of cells over time. **C)** Representative cell density staining. Data presented as mean  $\pm$  SD of n=3, \* =  $p \leq 0.05$

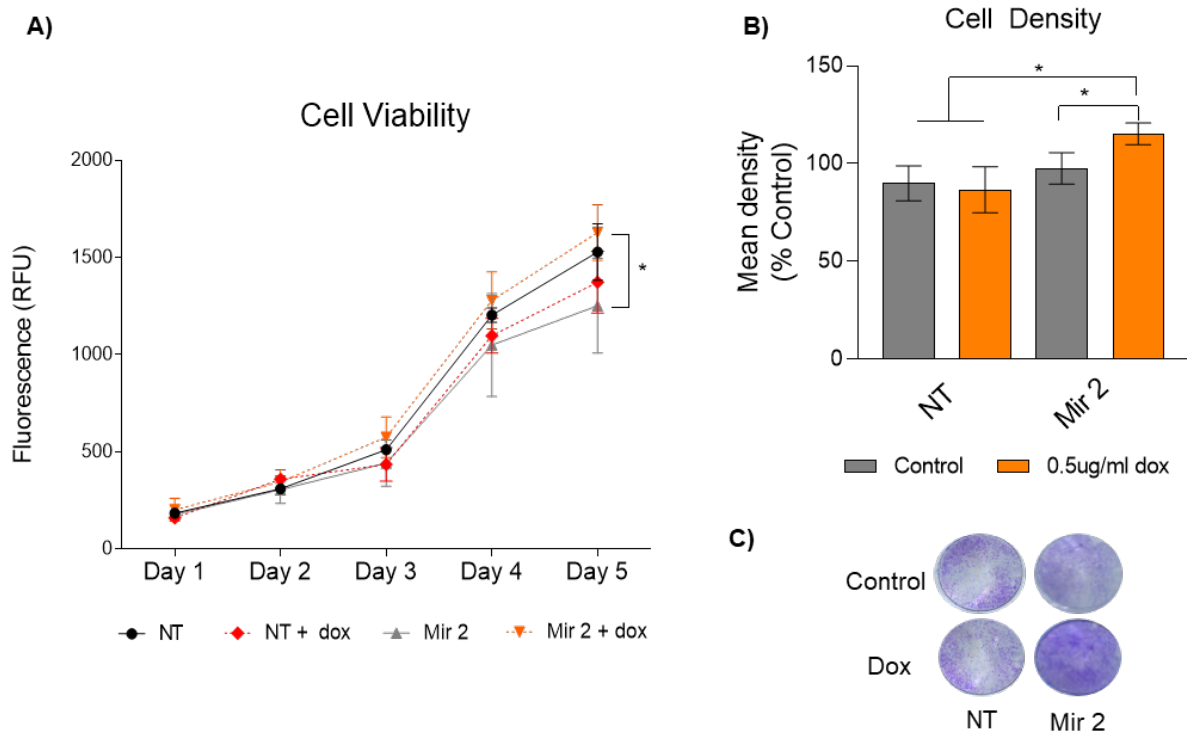


**Figure 5.9: FKBP25 knockdown increases cell viability and cell accumulation over time in C2C12 myoblasts**

**A)** Cell viability measured using AlamarBlue demonstrates that FKBP25 knockdown (Mir 2) is increased compared to the non-targeting Mir in C2C12 myoblasts **B)** Measured staining density of cells following a 5-day growth period indicating that the active knockdown increases the number of cells over time. **C)** Representative cell density staining. All data is presented as mean  $\pm$  SD,  $n=3$ , \* =  $p \leq 0.05$ .

### 5.2.3 FKBP25 knockdown enhances C2C12 myoblast wound healing but not chemotactic migration of MDA-MB-468 cells.

The second cell function to be assessed with 25KD was cell migration. To accurately assess the behaviours of the two cell lines of interest, it was appropriate to utilise two separate models of migrations, including chemotactic migration and wound healing. Chemotactic migration is a process in which cells are attracted to a chemical attractant (chemoattractant) and proceed to migrate toward such attraction. Both normal and cancer cells have the capability to carry out chemotaxis, however, certain genomic mutations (including PTEN) are associated with increased propensity to perform chemotaxis (405). It is well established that cancer cells migrate via chemotaxis toward sites that contain high concentrations of chemoattractant, such as growth factors (EGF, FGF, VEGF, outlined in (406)). MDA-MB-468 cells were examined using chemotactic migration assays, also referred to as a Boyden's chamber assay. This method of migration was selected to measure cancer cell migration, as it most closely represents the fashion in which cancer cells would migrate from one site to another. Cells were plated into the top chamber of a two-chamber apparatus separated by a porous membrane (8µm polycarbonate membrane coated in collagen 4). The bottom chamber contained the chemoattractant (either 10ng/ml EGF, or fibroblast conditioned medium), after assay completion the membrane was fixed and stained to allow the migrated cells to be counted (as described in (407)). It was determined that 25KD did not alter chemotactic migration of MDA-MB-468 cells toward either EGF (**Fig 5.10**) or fibroblast conditioned medium (**Fig 5.11**). Further studies should examine other methods of MDA-MB-468 migration.

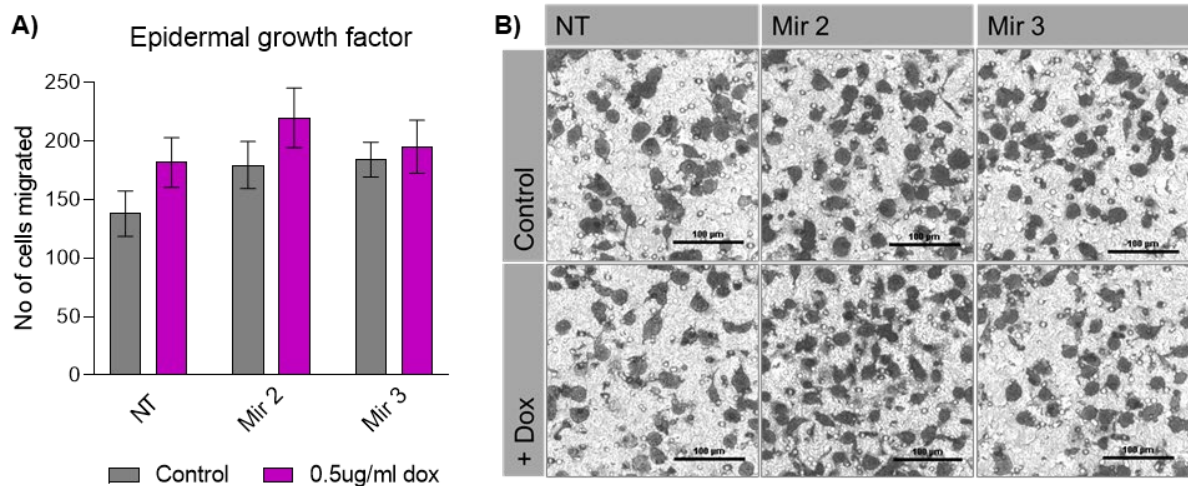


**Figure 5.10: FKBP25 knockdown does not impact upon chemotactic migration toward epidermal growth factor (EGF)**

**A)** Following FKBP25 knockdown MDA-MB-468 cells did not show any difference in chemotactic migration toward epidermal growth factor. **B)** Representative phase contrast images of migrated FKBP25 knockdown MDA-MB-468 cells. Scale bar = 100µm. Data presented as mean ± SD of n=3, \* = p≤0.05

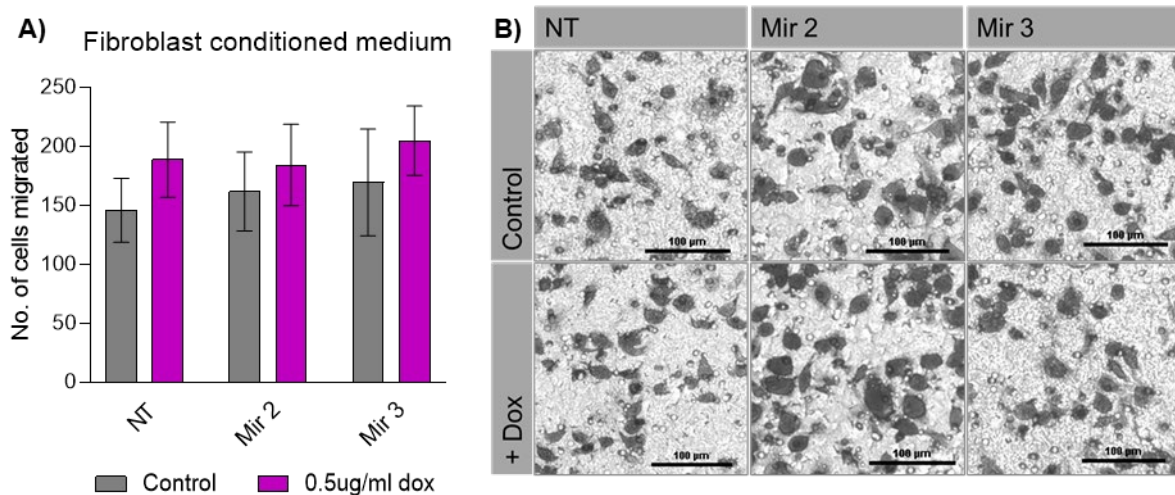


**Figure 5.11: FKBP25 knockdown does not impact upon chemotactic migration toward fibroblast conditioned medium**

**A)** Following FKBP25 knockdown MDA-MB-468 cells did not show any difference in chemotactic migration toward fibroblast conditioned medium. **B)** Representative phase contrast images of migrated FKBP25 knockdown MDA-MB-468 cells. Scale bar = 100µm. Data presented as mean ± SD of n=3, \* = p≤0.05

In contrast, C2C12 migration was examined using a wound healing assay. This assay was selected to measure myoblast migration as it is similar to the manner in which myoblasts would migrate to regenerate damaged muscle tissue (408). Wound healing assays are used to analyse collective migration, a process by which a monolayer of cells move communally as wounded edge becomes polarised and leads the cell movement (409, 410). This method of migration is characteristic of non-cancer cells. During this assay, confluent C2C12 myoblasts were scratched to create a wound within the cell monolayer. Live imaging was used to take images at regular intervals and produce a time lapse video to analyse cell migration. It was determined that C2C12 cells containing active 25KD Mir2 were able to close the ~400µm wound while the control cells remained unclosed (**Fig 5.12 A**). Upon quantification, it was found that 25KD improves wound closure time by 20% (**Fig 5.12 B**, difference between controls ~80% closure when active Mir2 reaches 100% closure). Thus, in addition to C2C12 proliferation, 25KD improves C2C12 wound healing migration. Further studies could add to this finding and observe the impact of 25KD on other modes of migration, including chemotactic migration in C2C12 myoblasts.

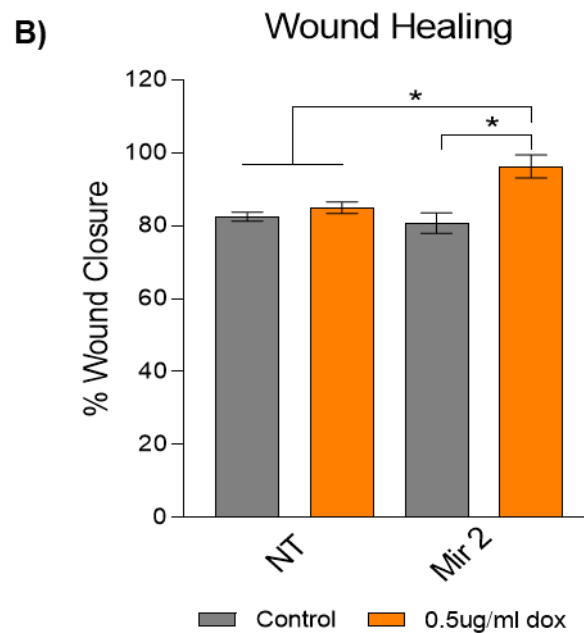
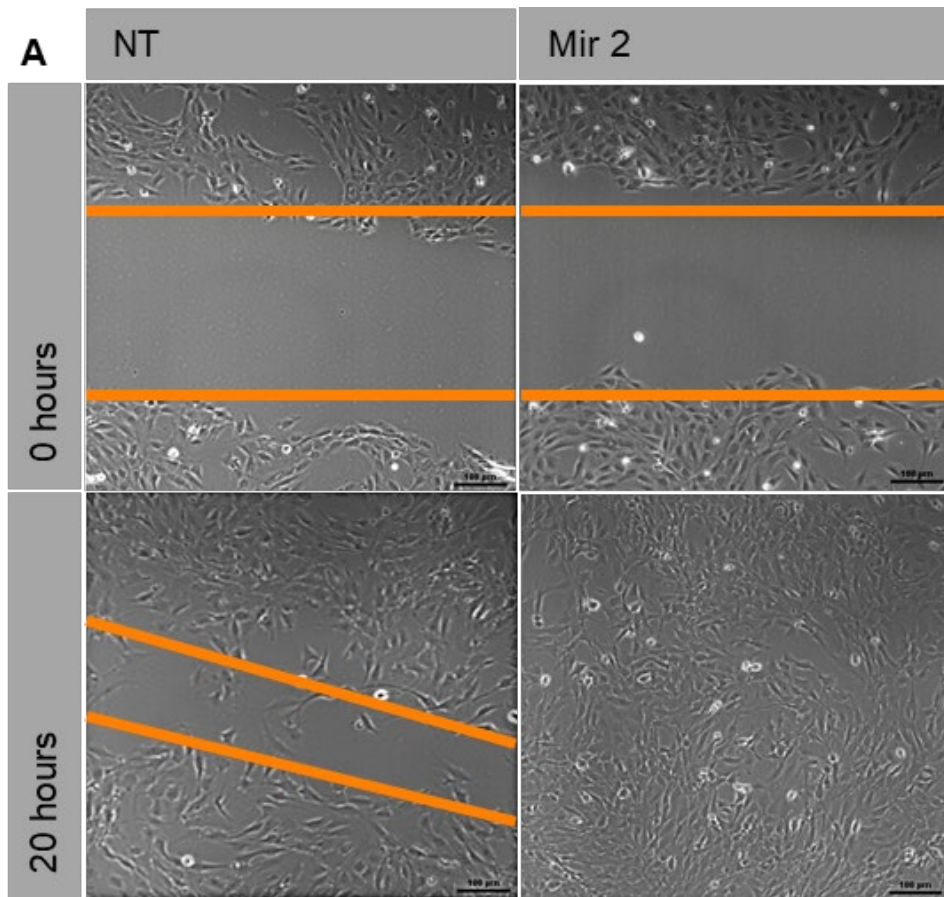


**Figure 5.12: FKBP25 knockdown increases wound healing migration of C2C12 myoblasts**

**A)** After 20 hours of migration cells containing Mir 2 FKBP25 knockdown can fully close the wound, while the NT control closes ~80%. **B)** Quantified wound closure. All data is presented as mean  $\pm$  SD, n=3, \* = p<0.05.

#### 5.2.4 FKBP25 knockdown reduces anchorage-dependent growth of MDA-MB-468 cells but not invasion outgrowth.

After comparing the biology of C2C12 and MDA-MB-468 cells containing 25KD, next it was aimed to evaluate the impact of cell-specific functions of these cell models. In the first instance, MDA-MB-468 cells were examined to assess their ability to form anchorage-dependent and -independent colonies *in vitro* with 25KD. The formation of both anchorage-dependent and -independent colonies is indicative of cell survival capacity and metastatic potential, respectively (391). Anchorage-dependent growth is required for normal proliferation and cell growth. In a cancer cell, while cells may not be dependent on anchorage for growth, this feature is required for colonisation at a secondary site. When cells metastasise, there are few cells that are able to survive the harsh process and, as a result, single cells often colonise to form a secondary tumour (411). This process is measured using the anchorage-dependent growth assay. To assess anchorage-dependent growth, FKBP25 knockdown cells were plated at very low confluence, either  $1 \times 10^3$  or  $5 \times 10^3$  cells per well and allowed to colonise for 14 days. It was determined that there is a significant decrease of anchorage-dependent colony formation of MDA-MB-468 25KD cells at both low (**Fig 5.13 A**) and high density (**Fig 5.13 B**) compared to their respective controls. This result suggests that 25KD is not beneficial for anchorage-dependent growth, which may be a result of altered adhesion properties. Analysis of substrata adhesion should be considered as part of future studies.

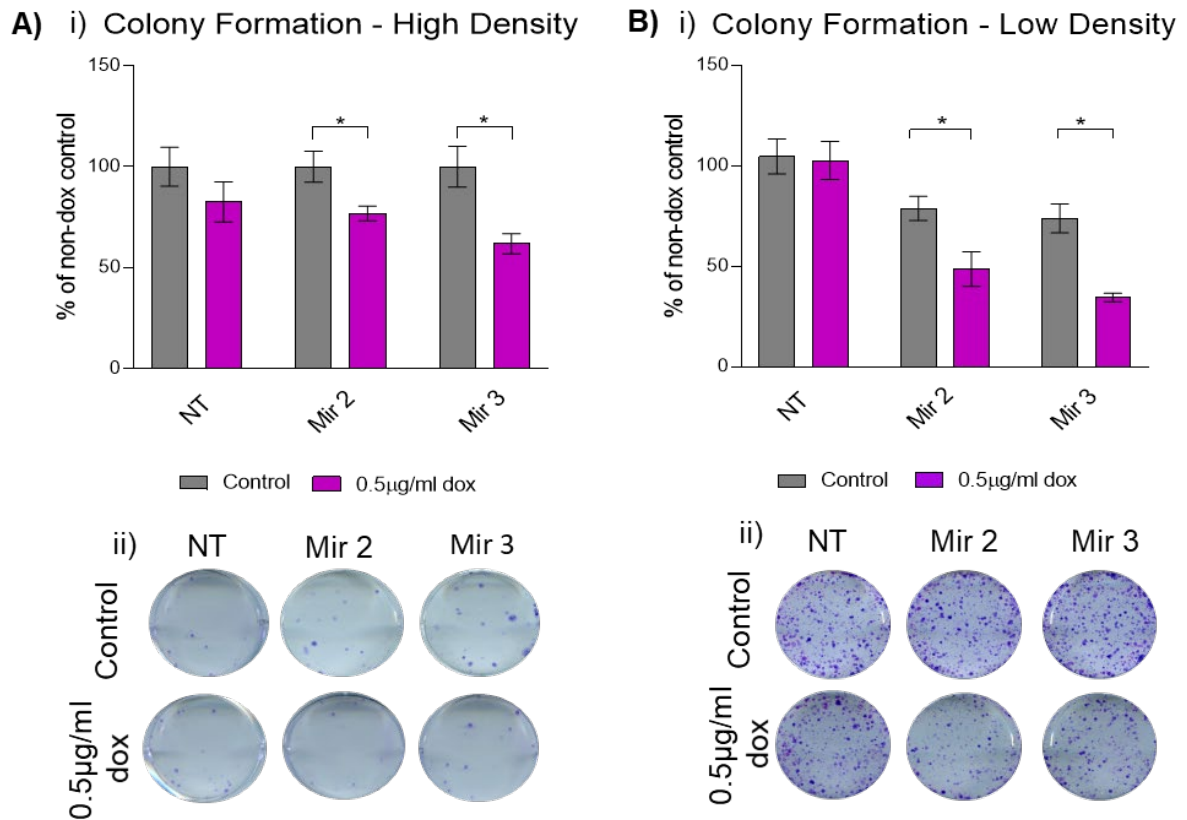


**Figure 5.13: FKBP25 knockdown results in decreased ability to form anchorage dependent colonies at both low and high seeding density**  
**A)** At low seeding density ( $1 \times 10^3$  cells per well) FKBP25 knockdown (mir 2 and 3) forms less colonies than the NT control. **B)** At high seeding density ( $5 \times 10^3$  cells per well) FKBP25 knockdown forms less colonies than the NT control. Data presented as mean  $\pm$  SD of  $n=3$ , \* =  $p \leq 0.05$

The invasive properties of a cell line can be assessed using a variety of *in vitro* methods. The Matrigel invasion-outgrowth assay assesses the ability of cancer cells to form colonies within the substrata, degrade and invade the matrix (412). Next, invasion out-growth was examined in MDA-MB-468 25KD cells. This was achieved by culturing  $1 \times 10^4$  cells on top of a Matrigel ECM base layer to mimic cell growth in the presence of a basement membrane. It was found that 25KD did not alter the ability of MDA-MB-468 cells to invade the Matrigel (**Fig 5.14**). The addition of an exogenous stress, such as serum deprivation, may have pushed the cells further to determine if they were able to survive in high stress conditions and further elucidated if FKBP25 is required for invasion out-growth. A potential limitation of this assay is that MDA-MB-468 cells have weak metastatic propensity compared to other breast cancer cells. It was hypothesised that 25KD would increase their metastatic propensity, but this assay was possibly too great of a challenge on their phenotype (discussed in (413)). Overall, 25KD induced a cell growth change that is present in both MDA-MB-468 and C2C12 cell lines, however, this was not carried over into measures of the metastatic phenotype of MDA-MB-468 cells.

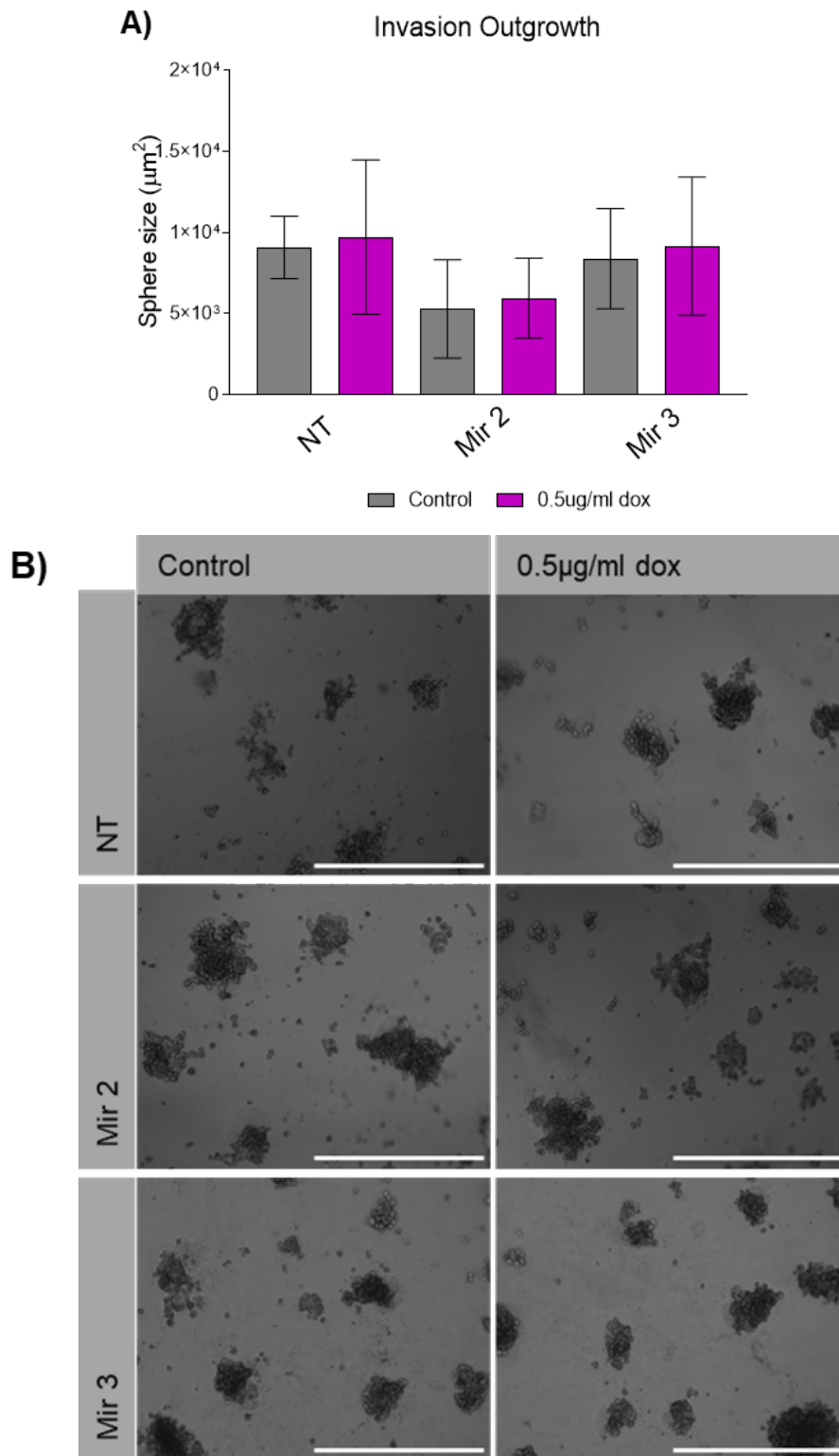


**Figure 5.14: FKBP25 knockdown does not impact upon invasion out-growth**  
**A)** Following 5 days of invasion outgrowth in Matrigel FKBP25 knockdown MDA-MB-468 spheres were measured using Olympus CellSens software, **B)** Representative phase contrast images of FKBP25 knockdown MDA-MB-468 cells. Scale bar = 50µm. All data is presented as mean ± SD, n=3, \* = p≤0.05.

### 5.2.5 FKBP25 knockdown does not impair markers of myogenesis or fibre size of differentiated C2C12 myotubes.

Following the functional assessment of 25KD on MDA-MB-468 cell function, next it was aimed to assess the impact of 25KD on C2C12 myogenesis. To examine the impact on myogenesis, first, the impact of 25KD on myoblasts alone must be observed. Upon 25KD, it was found that there was a significant reduction in FKBP25 protein expression (**Fig 5.15 A**), but no changes to myogenin or MyoD (**Fig 5.15 B and C**).

Interestingly, there was no reduction in MyoD expression in 25KD myoblasts (**Fig 5.15 C and D**). A reduction in MyoD suggests that there is still active proliferation occurring and cells remain active in the cell cycle, consistent with our finding that there was an increase in cell proliferation (**Fig 5.9**). Next, it was endeavoured to explore the effects of 25KD on C2C12 differentiation. Using this doxycycline-inducible model posed some issues surrounding myoblast differentiation. Upon investigating the issue, it became apparent that C2C12 differentiation is inhibited by the presence of doxycycline (45). This issue was overcome by treating the myoblasts with doxycycline to induce 25KD prior to initiation of differentiation. Here it was found that 25KD was able to be maintained for 120 hours during the differentiation period (**Fig 5.16 A**).

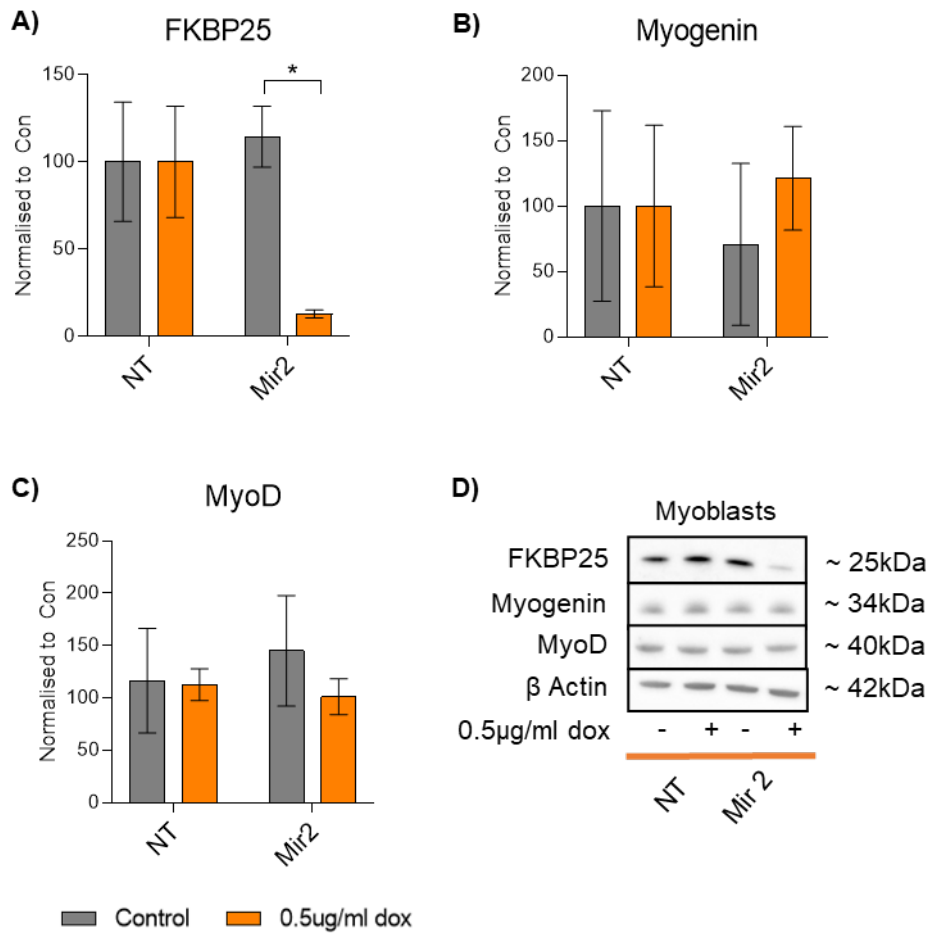


**Figure 4.15: Impact upon myogenic factors following FKBP25 knockdown in C2C12 myoblasts**

**A)** 25KD is induced upon treatment with doxycycline. **B)** There are no observed changes to myogenin expression in myoblasts. **C)** MyoD expression is unchanged in myoblasts. **D)** Representative blots. All data is presented as mean  $\pm$  SD, n=3, \* =  $p \leq 0.05$ .

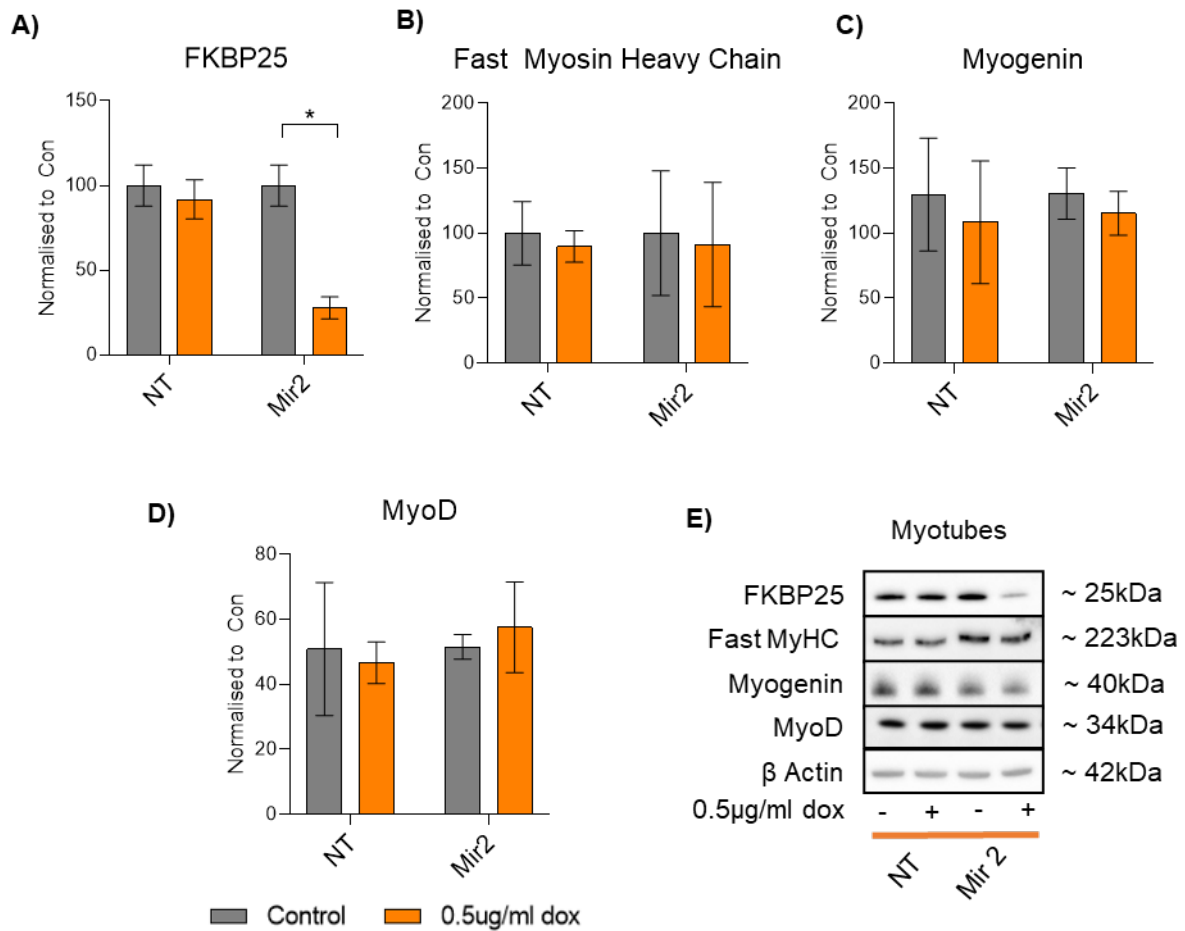


**Figure 5.16: FKBP25 knockdown does not impact upon features of myogenic differentiation or myogenic regulatory factors**

**A)** 25KD knockdown was maintained throughout C2C12 differentiation. **B) – E)** 25KD did not impact upon fast myosin heavy chain, myogenin, or MyoD protein expression in differentiated C2C12 myotubes. All data is presented as mean ± SD, n=3, \* = p ≤ 0.05.

Here it was observed no differences to fast myosin heavy chain, indicating that there were no changes to myotube formation (**Fig 5.16 B**). Following examination of other myogenic factors, myogenin and MyoD, no changes were observed (**Fig 5.16 C and D**). To further describe the impact of 25KD on myogenesis, myotube formation was investigated. While there were some changes in the expression of myogenic factors, upon examination of myotube measurement, it was found that there were no differences in myotube diameter (**Fig 5.17**). Considering the changes observed in 25KD cells, next it was hypothesised that while there was no net change in myotube formation there could be alterations to the number of cells that form a single myotube – known as fusion index. This hypothesis was further supported by increased proliferation and migration (described in sections 5.2.2 and 5.2.3) observed with 25KD. To assess fusion index, 25KD cells were differentiated and stained with myosin heavy chain and nuclear stain, DAPI. Fusion index was calculated by counting the number of nuclei in myosin heavy chain positive myotubes as a proportion of total nuclei (**Fig 5.18 A**). However, upon quantification it was found that there were no differences in fusion index of 25KD myotubes (**Fig 5.18 B**). Together, these results suggest that 25KD in C2C12 myoblasts does not alter myotube fusion or terminal differentiation *in vitro*.

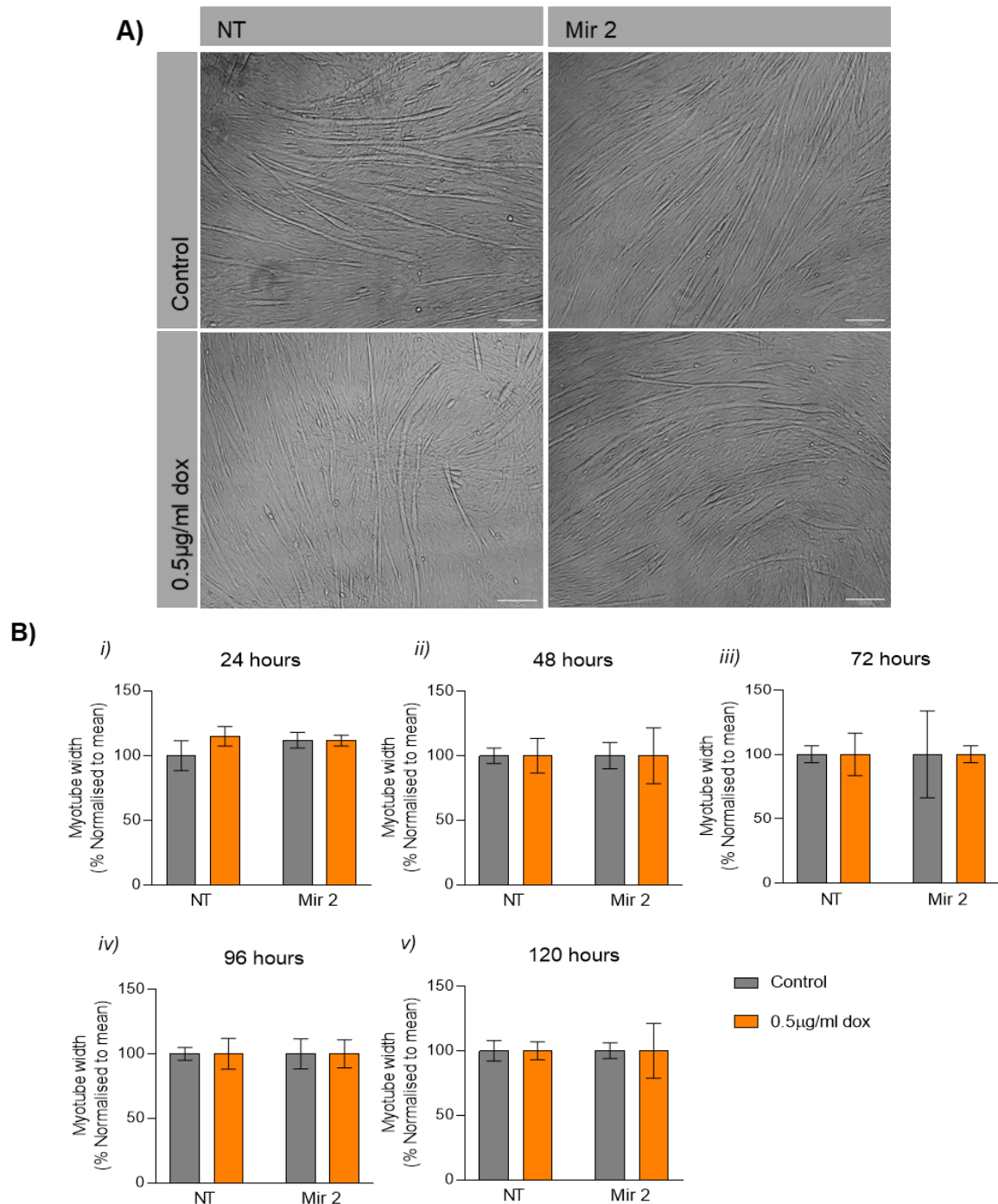


**Figure 5.17: FKBP25 knockdown does not impair myotube formation *in vitro***

**A)** Myotube formation after 120 hours of differentiation post FKBP25 knockdown resulted in no morphological alterations compared to NT control. **B)** Myotube diameter (i-v) was measured at 24 to 120-hour timepoints, from phase contrast microscopy. These measurements were not found differ upon FKBP25 knockdown. All data is presented as mean  $\pm$  SD, n=3, \* =  $p \leq 0.05$ .

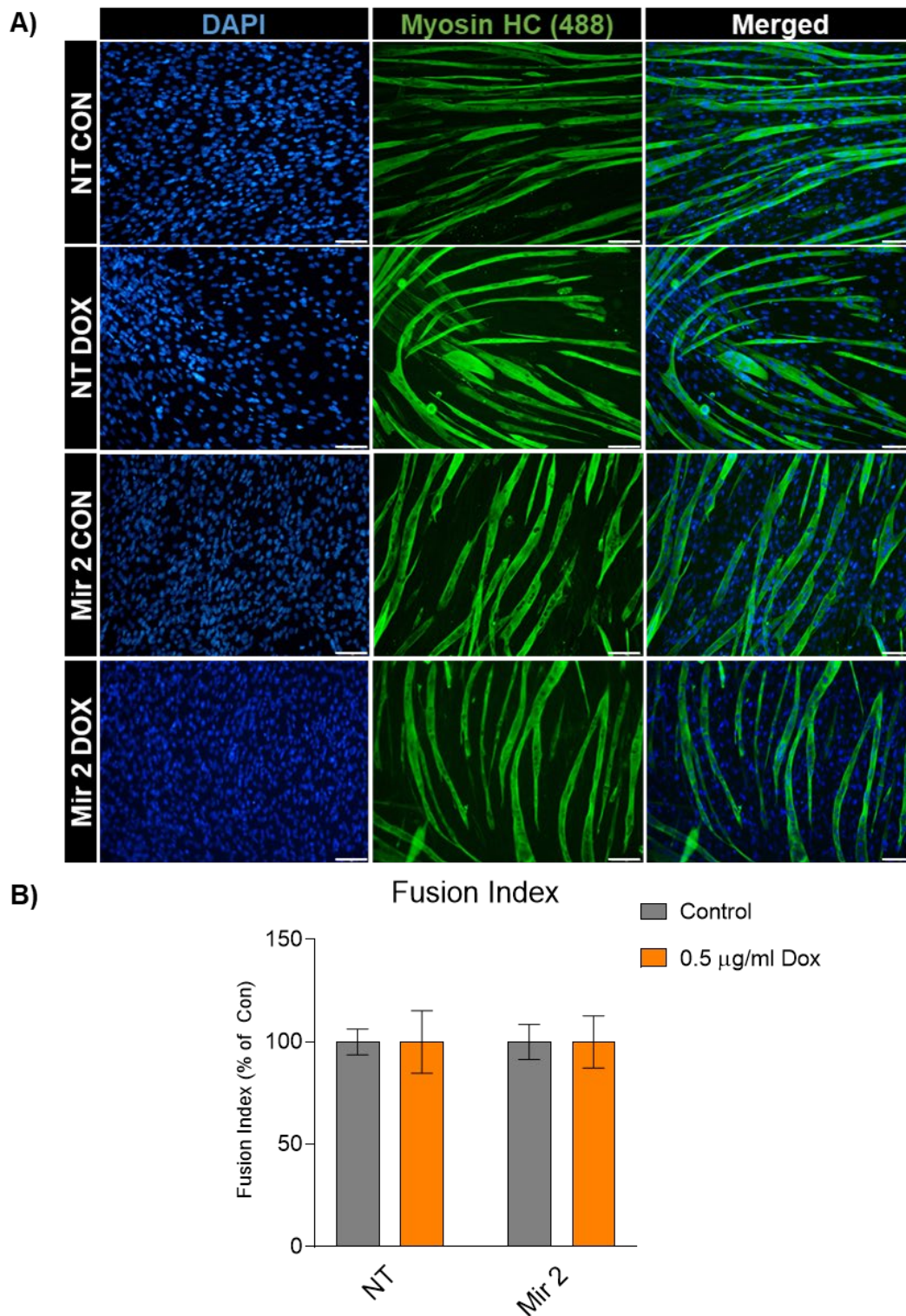


**Figure 5.18: FKBP25 knockdown does not impair myoblast fusion index**  
**A)** Staining of DAPI and Myosin heavy chain (MyHC) were used to determine the number of nuclei per MyHC positive fibre to calculate the number of myoblasts that have fused to form a myofibre. **B)** Quantification of nuclei per MyHC positive fibre revealed that there are no alteration to fusion index upon 25KD. Representative images of n=3, scale bar 100µm.

### 5.2.6 FKBP25 knockdown increases susceptibility to EGF mediated EMT by increasing markers E cadherin and vimentin.

Finally, to examine the impact of FKBP25 on EMT, EMT was induced in the presence of 25KD and measured associated morphology and molecular markers. To include this phenotype, cells were cultured as described in *section 2.2.4*. In brief, cells were plated at low confluence in the presence of dox to induce 25KD, following 24h of dox treatment, cells were serum deprived overnight followed by treatment with 50ng/ml of EGF for 72h. As previously observed in *section 3.2.3*, MDA-MB-468 cells undergo a morphological change upon treatment with EGF. The current study has replicated that finding, and further described that the addition of 25KD does not exacerbate these morphological changes (**Fig 5.19**). Upon molecular investigation, quantification of markers of EMT, including E cadherin and vimentin, revealed that there was a significant increase in vimentin expression in the active Mirs (2 and 3) with 25KD (**Fig 5.20 A**). However, this change was not different between EGF only and EGF with dox treated groups, indicating that the change was not caused by 25KD (**Fig 5.20 B**). Interestingly, quantification of E cadherin demonstrated that there was in fact a cumulative decrease in expression facilitated by 25KD in addition to EMT (**Fig 5.20 C**). Interestingly, this reduction in E cadherin upon 25KD is reflective of the low levels of FKBP25 in mesenchymal breast cancer cell line MDA-MB-231, which does not express E cadherin.

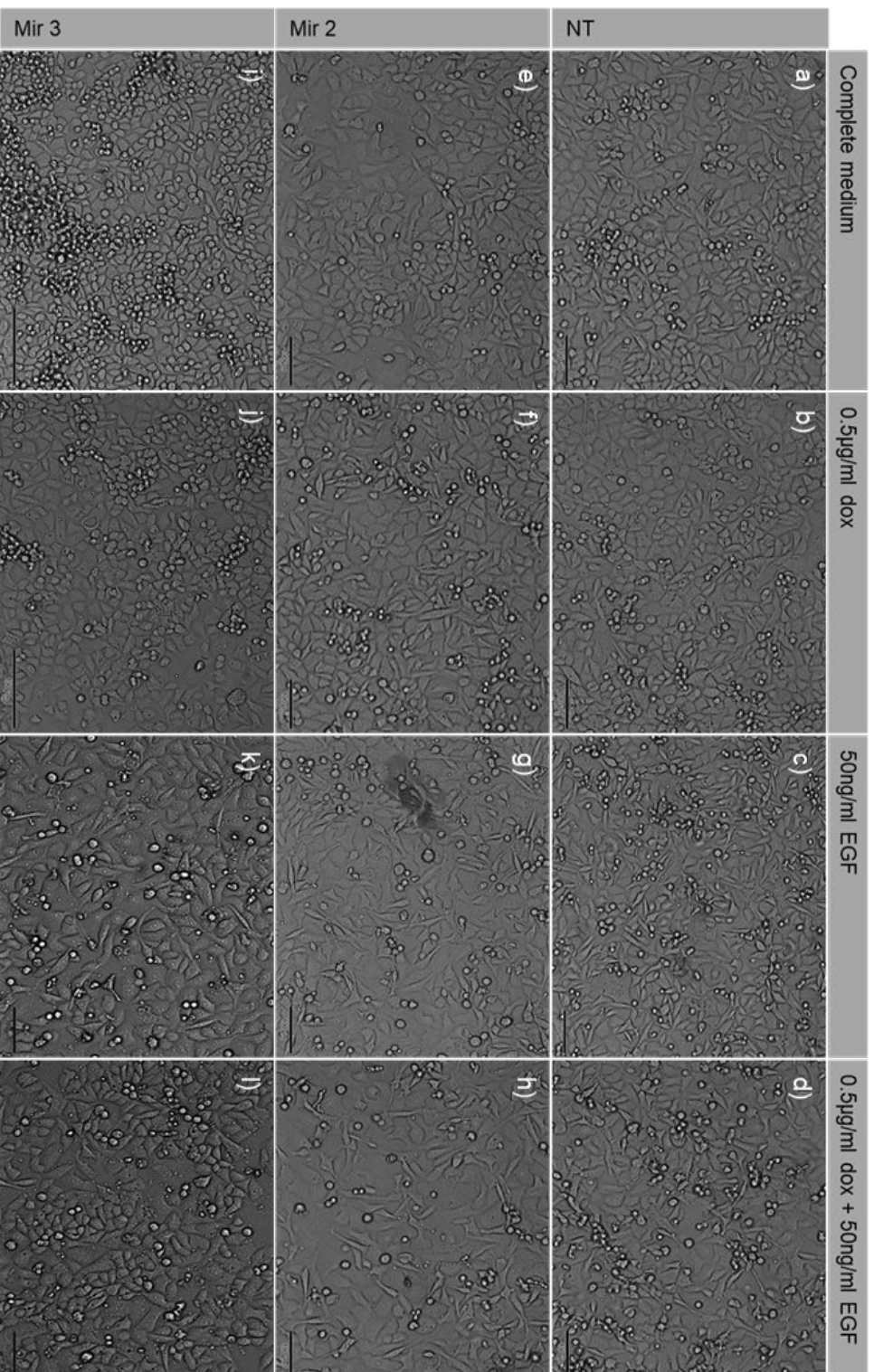


**Figure 5.19: FKBP25 knockdown in addition to EGF mediated EMT does not induce further morphological change**  
**a-d)** NT Mir, **e-h)** Mir 2 and **i-l)** Mir 3 with either complete medium, 0.5µg/ml dox, 50ng/ml EGF, or both dox and EGF. No morphological changes are noted between Mirs for each treatment group. Scale bar = 100µm. All data is presented as mean ± SD, n=3, \* = p≤0.05.

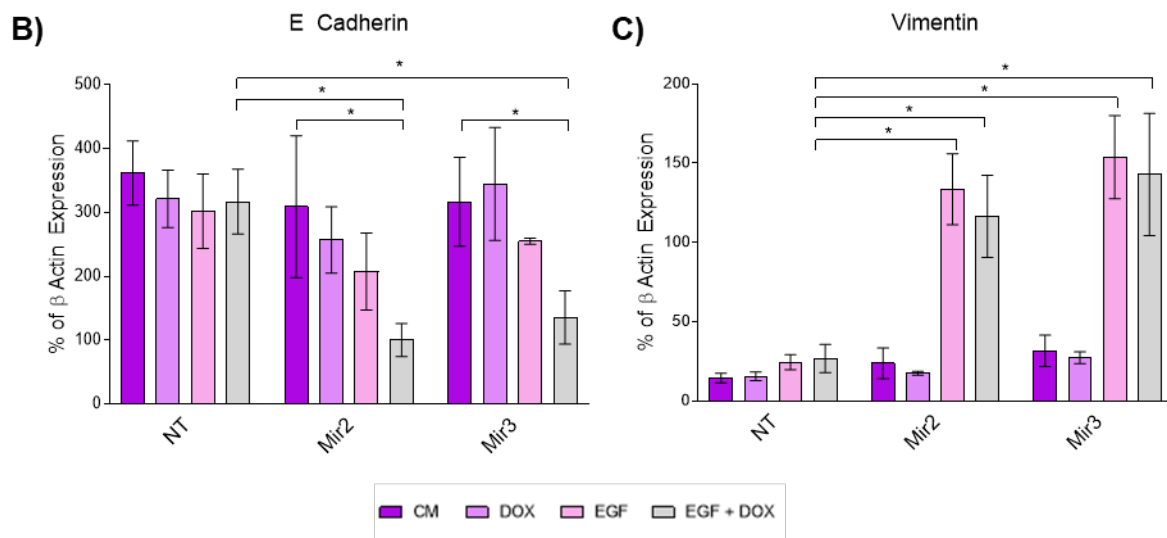
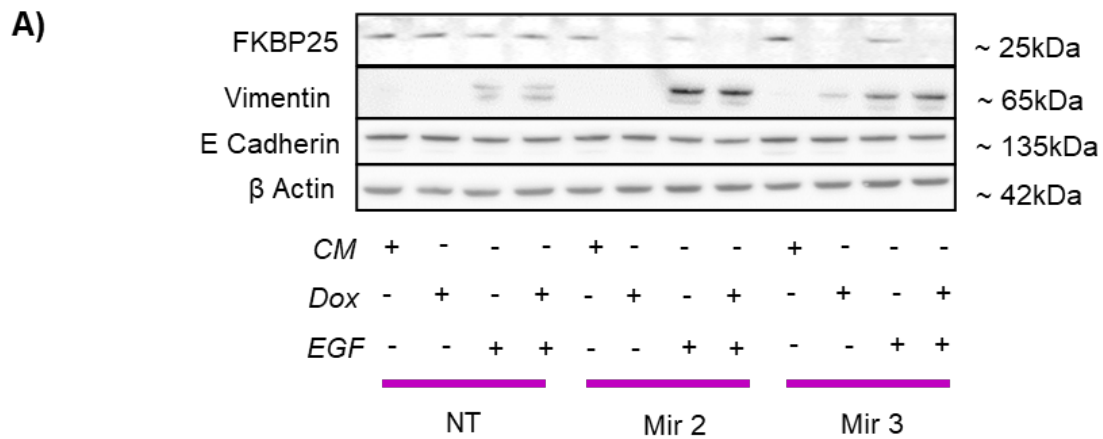


**Figure 5.20: FKBP25 knockdown exacerbates EMT markers E cadherin and vimentin upon EGF mediated EMT induction**

**A)** Representative blot of EGF mediated EMT in FKBP25 knockdown cell lines treated with dox to induce knockdown, and/or EGF to mediate EMT. **B)** Vimentin is significantly further increased in Mir 3 compared to NT. **C)** E cadherin is further decreased in both Mir 2 and 3 compared to NT upon FKBP25 knockdown with EGF mediated EMT. All data is presented as mean  $\pm$  SD, n=3, \* =  $p \leq 0.05$ .

To assess the impact of 25KD on EGF signalling, we have interrogated downstream targets, including Akt and MAPK phosphorylation (**Fig 5.21**). Upon EGF binding to the EGFR, a cascade of events leads to EMT-related signalling. One such pathway that is affected is the MAPK pathway. Binding to tyrosine kinase receptors leads to activation of the RAS/MEK/ERK-MAPK signalling cascade, which results in proliferation signalling stimulus to the cell. Over stimulation of this pathway is known to result in excessive proliferation as Ras is a well described oncogene (Reviewed in (414)). Erk-MAPK kinase activity is required for cell cycle entry and suppression of negative regulators of the cell cycle (415). Additionally, Erk signalling is essential in activating transcription factors, including c-Myc, which, in turn, play a role in activation of the cell cycle (14). As such, aberrant EGFR signalling results in oncogenic Erk signalling. The PI3K-Akt pathway is also impacted upon by EGFR signalling. Hyperactivation of this pathway results in altered cell metabolism, proliferation, and survival. Akt phosphorylation can occur at two sites, Thr308 and Ser473, which will activate the kinase properties of Akt. Each of these phosphorylation sites are facilitated by different kinases, Thr308 by PI3K, and Ser473 by mTORC2 (416). Here we have treated MDA-MB-468 25KD cells with EGF at 10ng/ml over a 30-minute time course. Upon quantification of EGFR downstream targets, it was found that there are no changes to Akt phosphorylation at Ser473 (**Fig 5.22**), or Erk at Thr202/Tyr204 (**Fig 5.23**). These results indicate that the changes that were found in 25KD EMT may be the result of longer EGF stimulation to induce EMT-related factors.

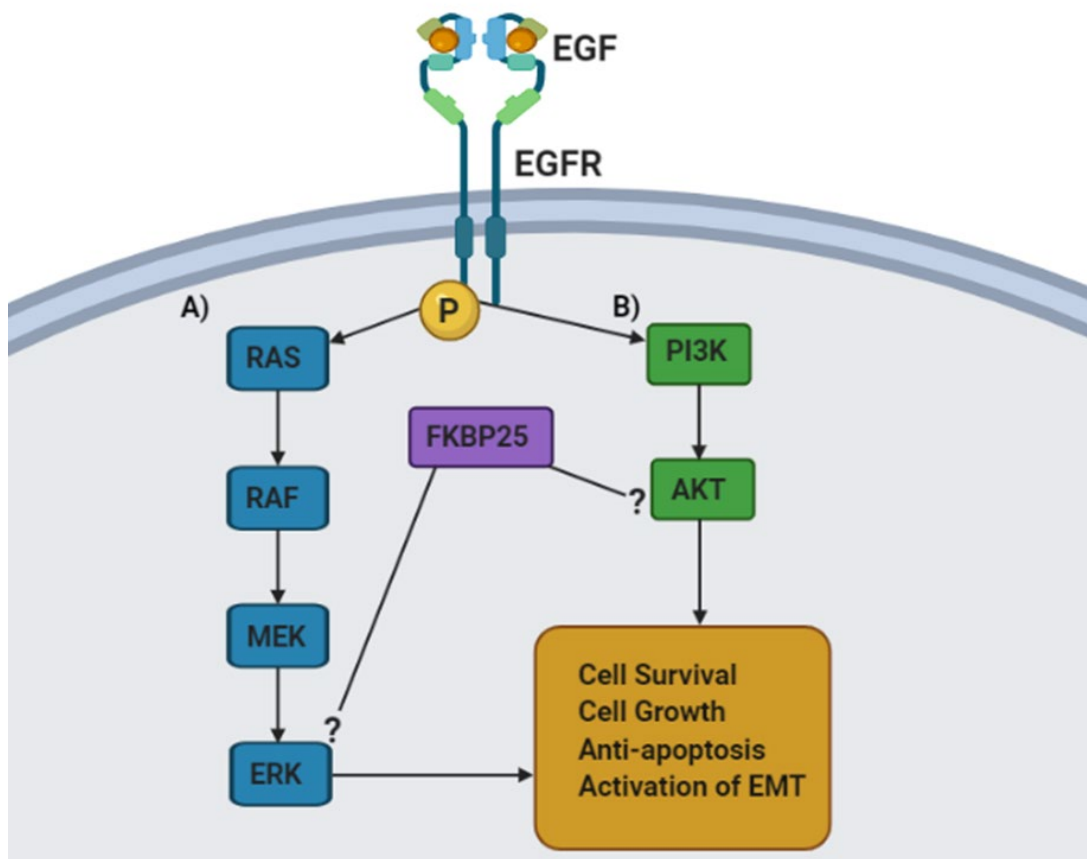


**Figure 5.21: Epidermal growth factor receptor (EGFR) signalling**  
 Upon EGF ligand binding to the EGFR there is activation of both Erk (**A**) and Akt (**B**) signalling pathways. Both pathways result in a series of cell survival, growth, anti-apoptotic, and EMT signals. Made with Biorender.com.

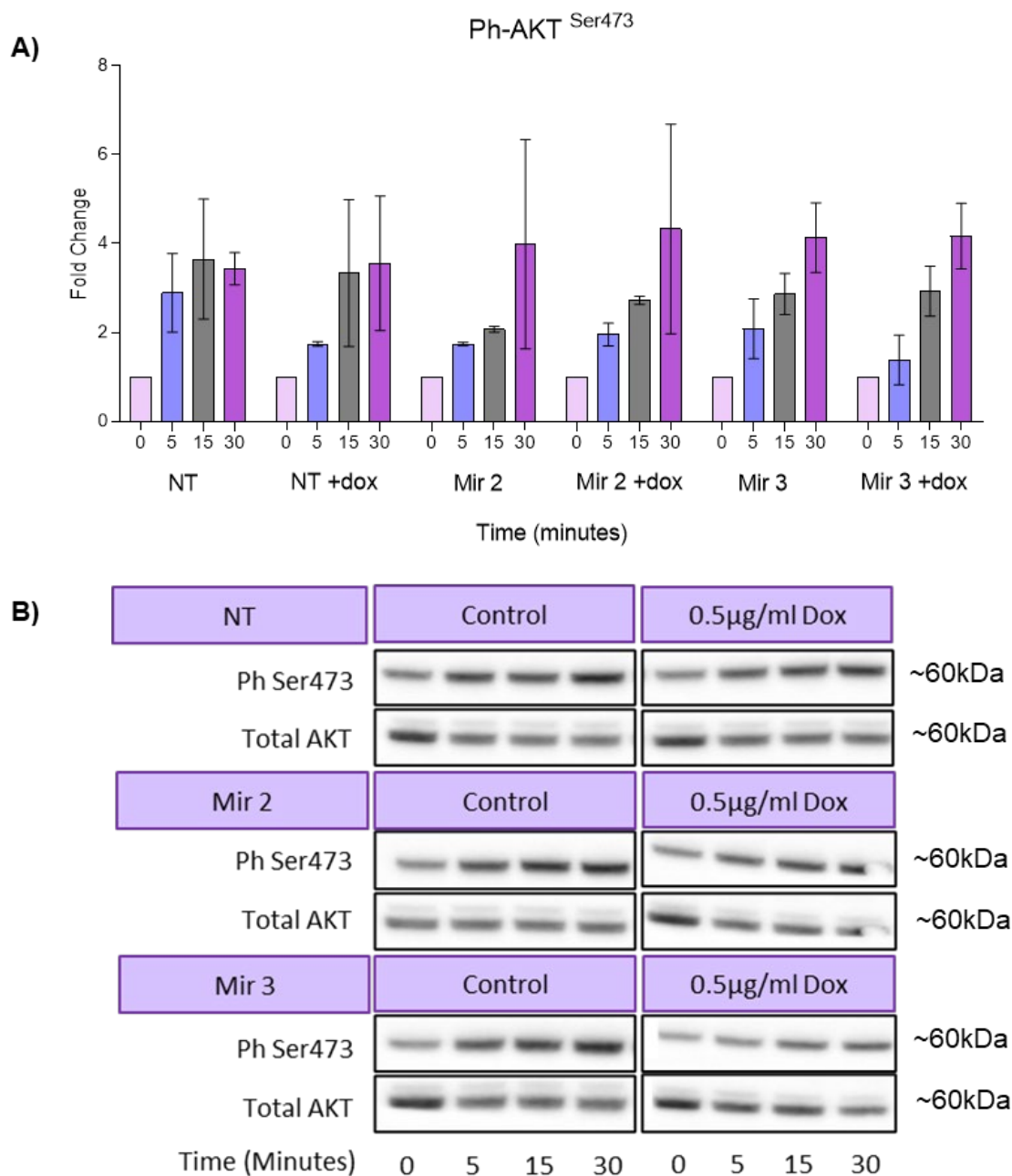


**Figure 5.22: FKBP25 knockdown does not alter Akt signaling in response to EGF stimulation**

**A)** Upon stimulation with EGF there are no significant changes to AKT phosphorylation in MDA-MB-468 cells with 25KD. **B)** Representative blots. Data presented as mean  $\pm$  SD of n=3, \* =  $p \leq 0.05$

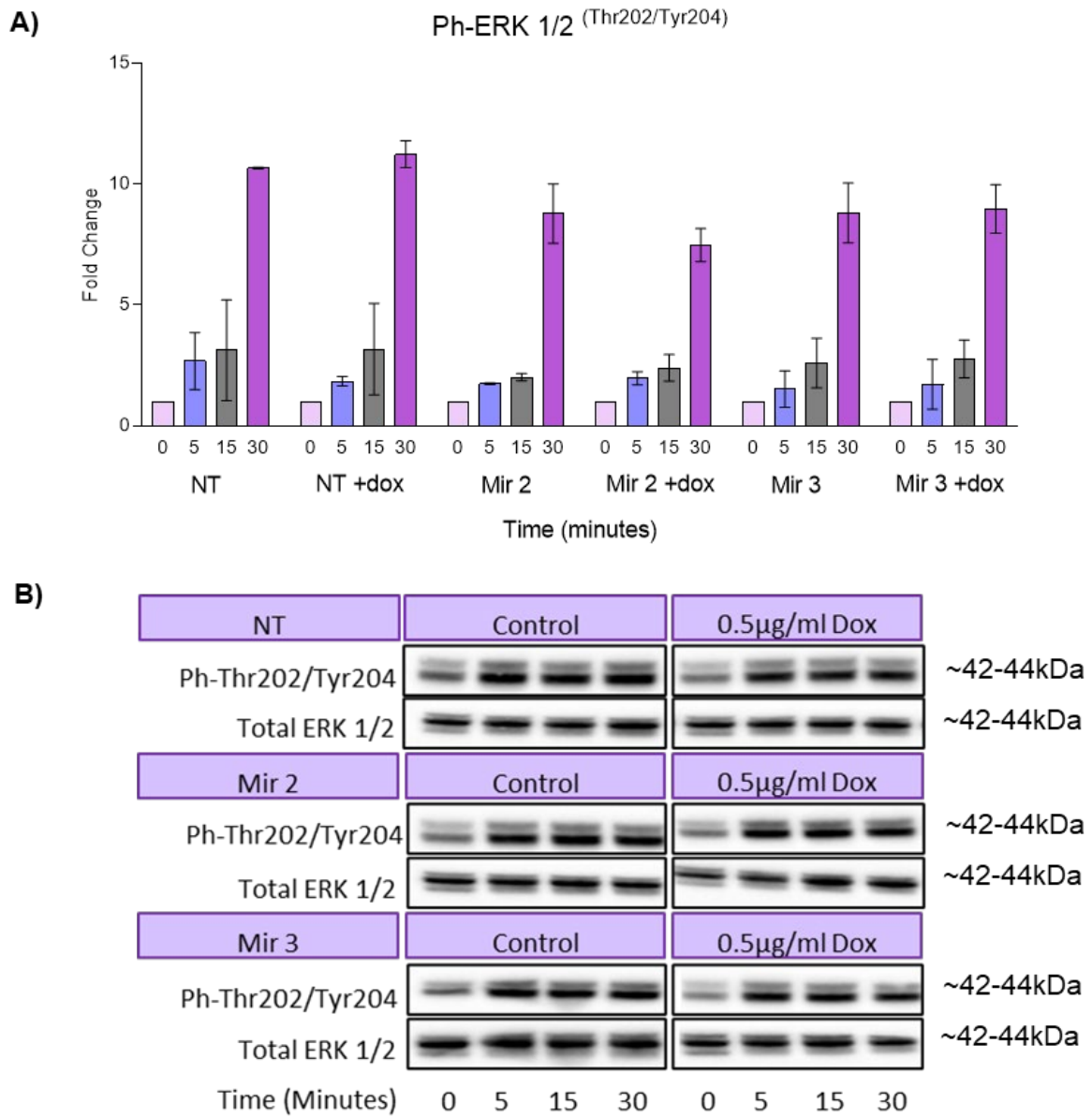


**Figure 5.23: FKBP25 knockdown does not alter Erk signaling in response to EGF stimulation**

**A)** Upon stimulation with EGF there are no significant changes to ERK phosphorylation in MDA-MB-468 cells with 25KD. **B)** Representative blots. Data presented as mean  $\pm$  SD of n=3, \* = p<0.05

### 5.2.7 FKBP25 knockdown does not impact upon tubulin post-translational modifications, or microtubule regulating protein stathmin

One of the known functions of FKBP25 is its ability to bind to and stabilise microtubule (MT) polymers (109). Upon examination of a variety of functional studies throughout this chapter, it was hypothesised that the impact of 25KD would result in a reduction of MT stability. This reduction in MT stability would give cells a proliferation advantage due to increased MT plasticity, specifically in the context of mitotic spindle formation. Here we have examined the impact of 25KD on two tubulin post translation modifications (PTM), acetylation and detyrosination. Tubulin acetylation is a PTM that is associated with increased MT stability that is facilitated by alpha tubulin acetyltransferase 1 ( $\alpha$ TAT1) (417). Similarly, tubulin detyrosination is also associated with polymerised MTs as it is required to form the bond between monomers (418). Previously, we had identified that 25KD in C2C12 myoblasts resulted in changes to proliferation and migration (*section 5.2.2 and 5.2.3*) which were attributed to hypothesised alterations in tubulin stability. Here we have found that tubulin acetylation is unaffected by 25KD (**Fig 5.24 A and D**), which was also observed in relation to tubulin detyrosination (**Fig 5.24 B and D**). Conversely, in MDA-MB-468 cells, where 25KD was found to induce increased proliferation (*see section 4.2.2*), no alterations to tubulin PTMs were identified (**Fig 5.25**). It appears that this phenomenon may be exclusive to normal cells, while cancer cells remain unaffected.

Next, the expression of a MT destabilising molecule, known as Stathmin, was assessed. Stathmin binds to MT polymers and sequesters tubulin heterodimers to induce catastrophe (419). Stathmin is post-translationally modified by serine phosphorylation to prevent tubulin binding and this encourages MT polymerisation (420). Here we have examined total stathmin in both C2C12 myoblasts (**Fig 5.24 C**

**and D)** and MDA-MB-468 (**Fig 5.25 C and D**) where it was found that while there was no change to stathmin expression. To further analyse the impact of 25KD on MT stability, next we examine the proportion of free and polymerised tubulin.

One of the fundamental roles of FKBP25 is its function as a MT stabilising molecule. To assess this role a series of MT polymerisation assays were completed in which the soluble (free tubulin) and insoluble (polymerised MT) were fractioned by high-speed ultracentrifugation. Cells were collected under two conditions, control condition in complete growth medium, or in the presence of paclitaxel (1 $\mu$ m for 1 hour). Paclitaxel treatment forces the maximal amount of MT polymerisation to be undertaken in the absence of FKBP25. First, we examined C2C12 25KD cells and found that under both control (**Fig 5.26**) and paclitaxel treated (**Fig 5.27**) there are no significant differences to the proportion of polymerised tubulin. Similarly, in MDA-MB-468 cells, there are no observed differences in either control (**Fig 5.28**) or paclitaxel treated (**Fig 5.29**). These results suggest that FKBP25 is potentially not an indispensable MT stabilising molecule, such that its loss is not substantial to impair MT polymerisation.

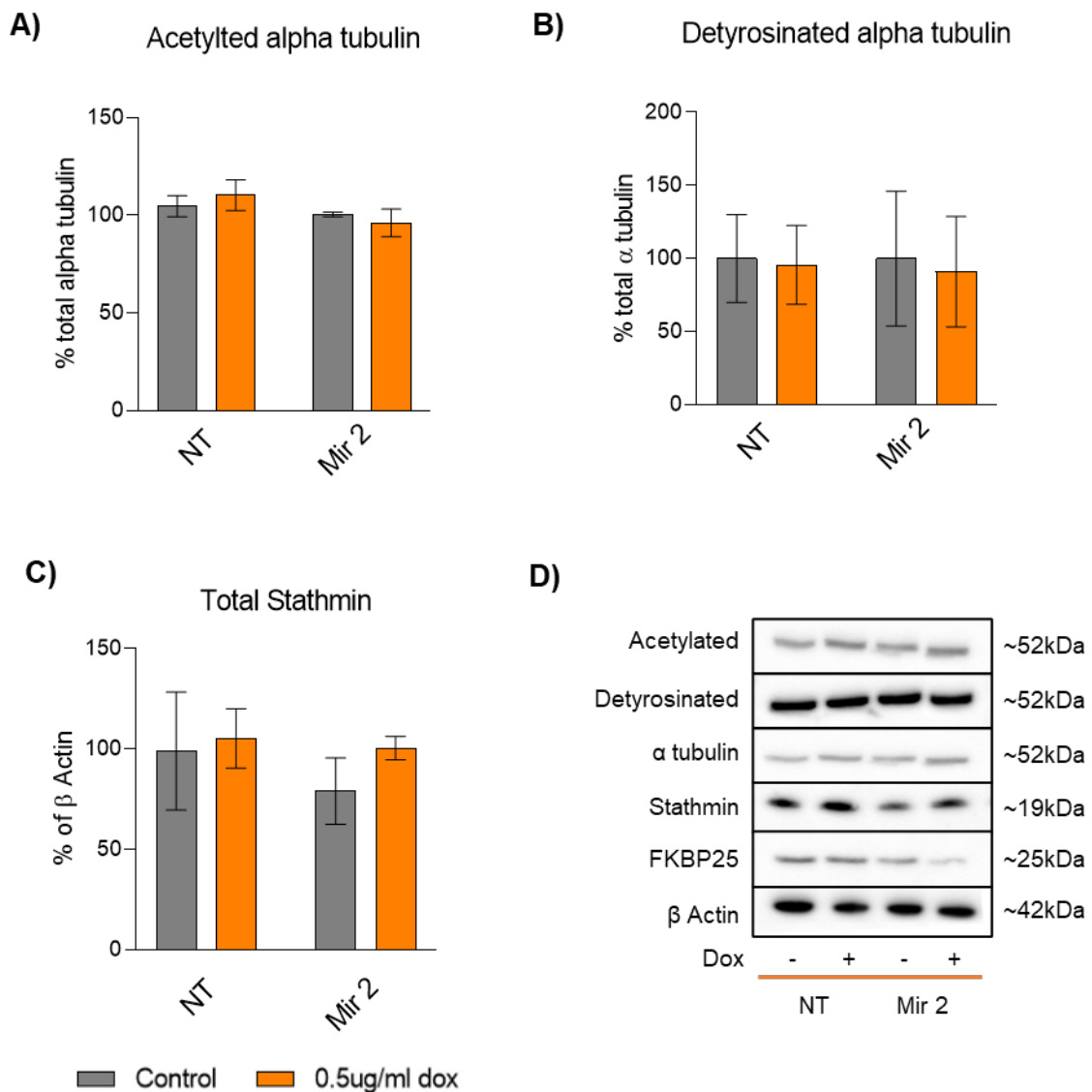


**Figure 5.24: FKBP25 knockdown in C2C12 myoblasts does not affect tubulin modifications associated with microtubule stability**  
**A)** FKBP25 knockdown does not impair tubulin acetylation. **B)** or tubulin detyrosination. **C)** Total Stathmin-1 expression is unchanged. **D)** Representative blots. All data is presented as mean  $\pm$  SD, n=3, \* =  $p \leq 0.05$

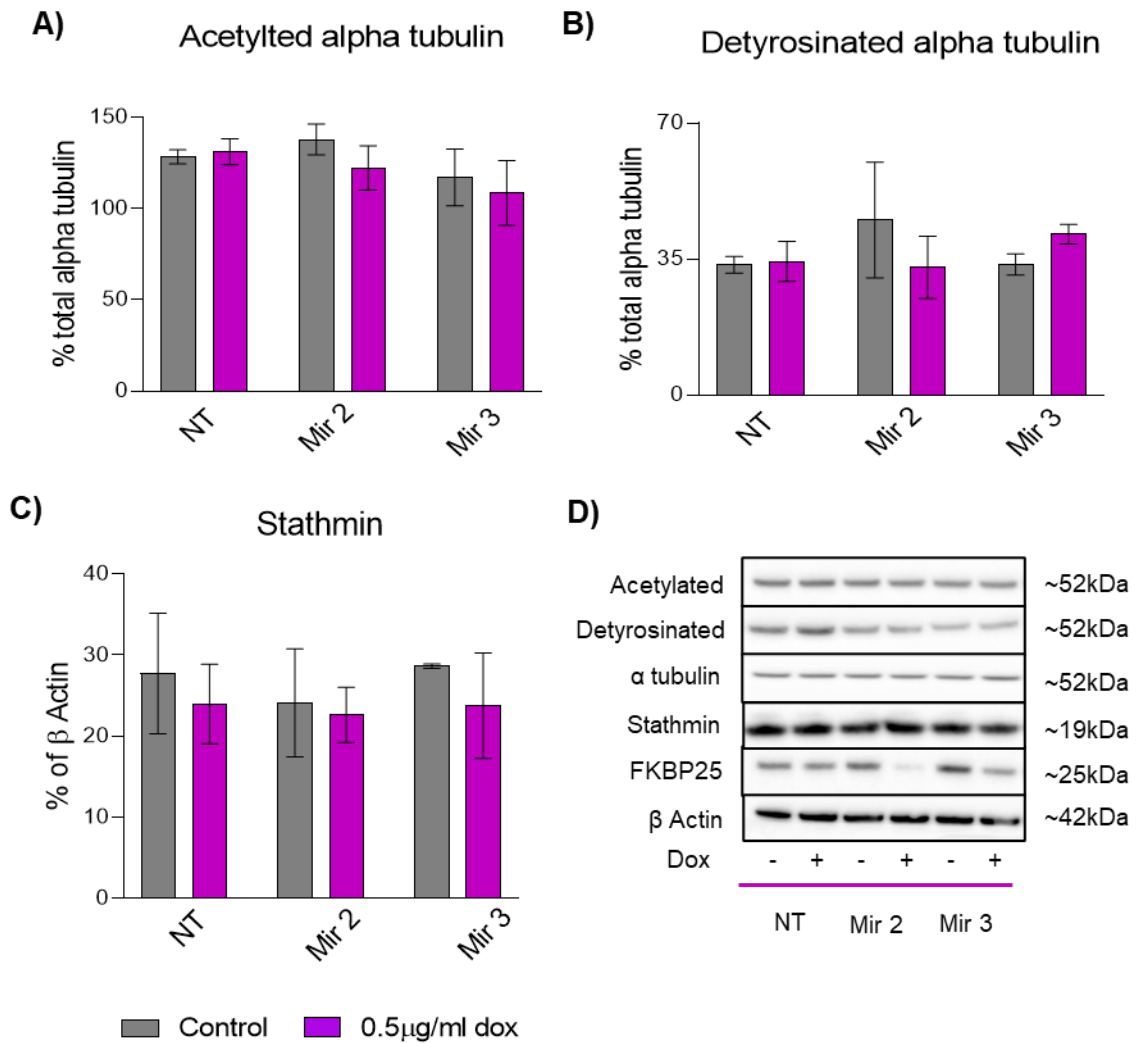


**Figure 5.25: FKBP25 knockdown in MDA-MB-468 cells does not affect tubulin modifications associated with microtubule stability**

**A)** FKBP25 knockdown does not impair tubulin acetylation. **B)** FKBP25 knockdown does not impair detyrosinated tubulin. **C)** Total Stathmin-1 expression is unchanged upon 25KD. **D)** Representative blots. All data is presented as mean  $\pm$  SD, n=3, \* = p $\leq$ 0.05

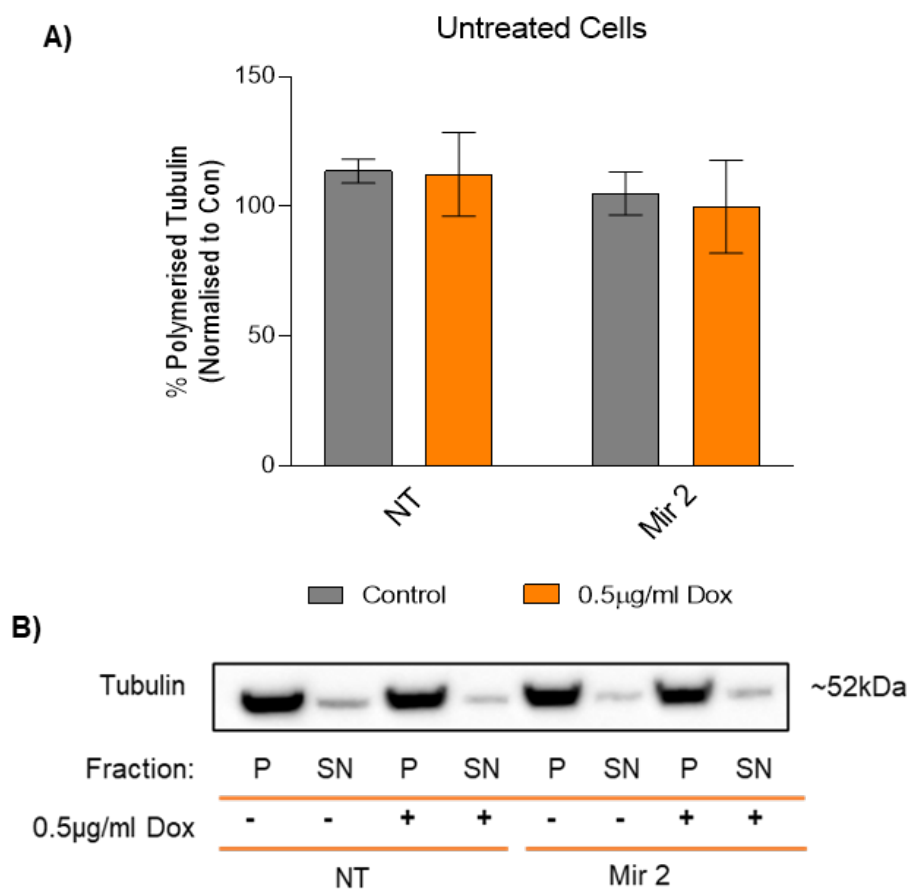


**Figure 5.26: FKBP25 knockdown is not sufficient to alter the proportion of polymerised tubulin in C2C12 cells**

**A)** FKBP25 KD does not alter MT polymerisation under control conditions (i.e., complete medium). **B)** Representative blot (SN = Supernatant/soluble free tubulin monomers, P= Pellet/Polymerised MT filaments). All data is presented as mean  $\pm$  SD, n=3, \* = p $\leq$ 0.05.

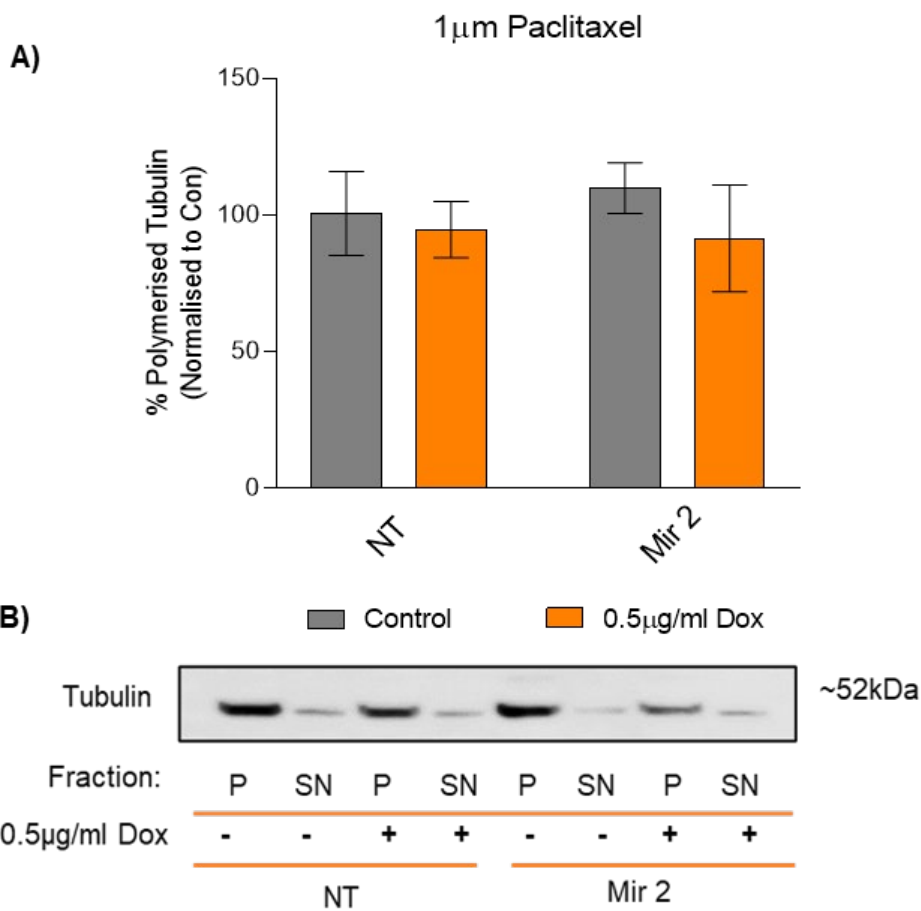


**Figure 5.27: FKBP25 knockdown is not sufficient to alter the proportion of polymerised tubulin in C2C12 cells pre-treated with paclitaxel**

**A)** FKBP25 KD does not alter MT polymerisation in the presence of paclitaxel (i.e., MT stabilising drug). **B)** Representative blot (SN = Supernatant/soluble free tubulin monomers, P= Pellet/Polymerised MT filaments). Representative blot. All data is presented as mean  $\pm$  SD, n=3, \* =  $p \leq 0.05$ .

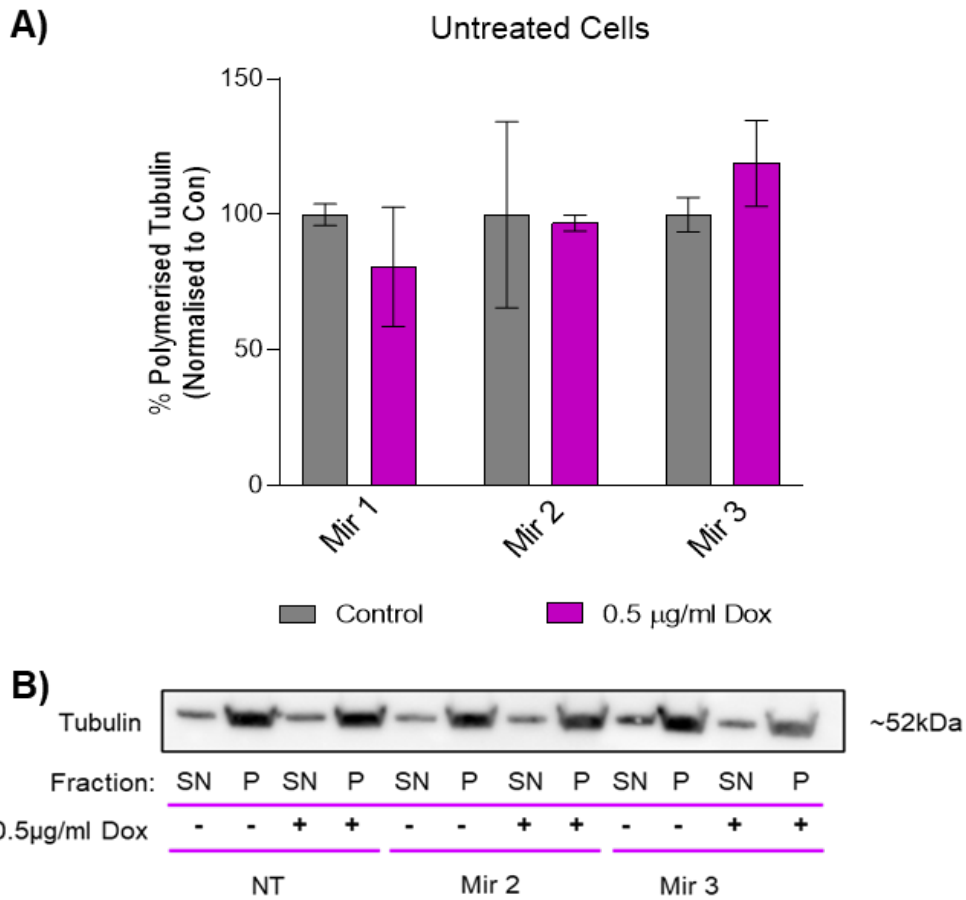


**Figure 5.28: FKBP25 knockdown is not sufficient to alter the proportion of polymerised tubulin in MDA-MB-468 cells**

**A)** FKBP25 KD does not alter MT polymerisation under control conditions (i.e., complete medium). **B)** Representative blot (SN = Supernatant/soluble free tubulin monomers, P= Pellet/Polymerised MT filaments). All data is presented as mean  $\pm$  SD, n=3, \* =  $p \leq 0.05$ .

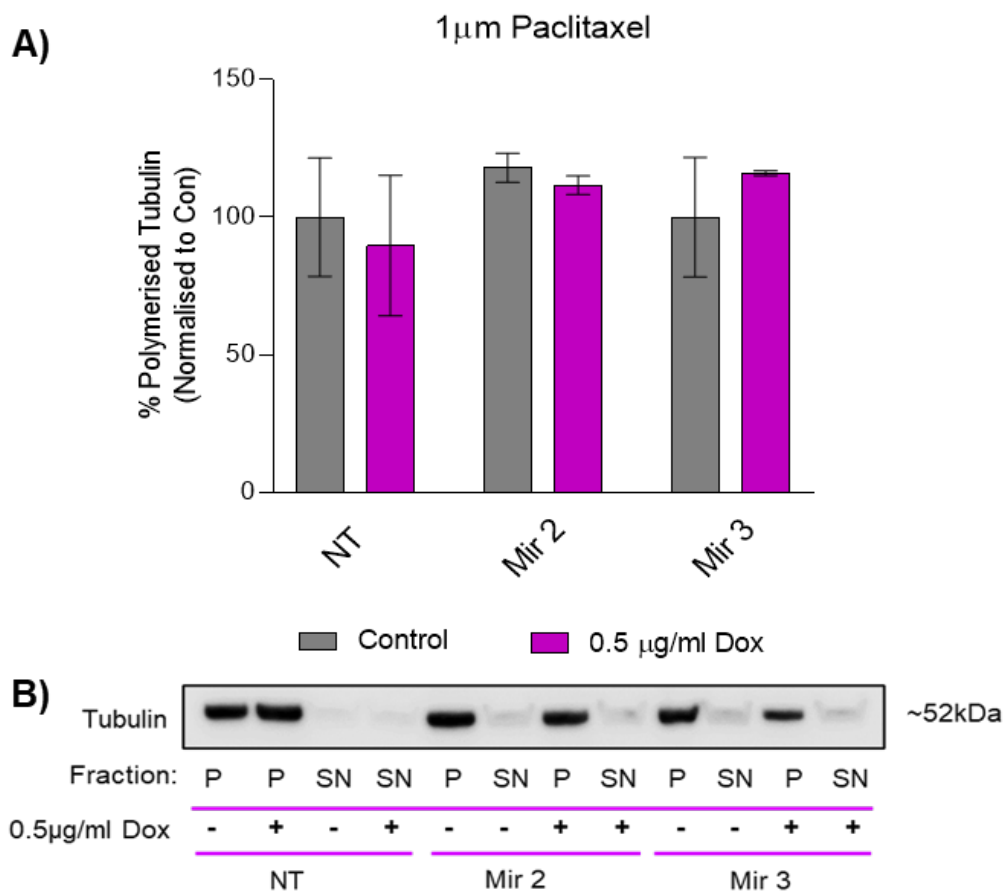


**Figure 5.29: FKBP25 knockdown is not sufficient to alter the proportion of polymerised tubulin in MDA-MB-468 cells pre-treated with paclitaxel**  
**A)** FKBP25 KD does not alter MT polymerisation in the presence of paclitaxel (i.e., MT stabilising drug). **B)** Representative blot (SN = Supernatant/soluble free tubulin monomers, P= Pellet/Polymerised MT filaments). Representative blot. All data is presented as mean  $\pm$  SD, n=3, \* =  $p \leq 0.05$ .

## 5.3 Discussion

### 5.3.1 FKBP25 knockdown increases cell viability and density over time indicating increased proliferation.

The roles of FKBP25 have been briefly described in the literature in a small sample of cell types. To date, it has been determined that FKBP25 functions as a MT stabiliser, nucleic acid binding protein, and a mediator of DNA repair (109, 111, 112). These functions have only been examined in selected cell lines, not specifically in the context of cancer cell function, or a physiological process such as cell differentiation. To assess the role of FKBP25 in these processes, 25KD was induced in two cell lines, MDA-MB-468 (Figs 5.4 and 5.6) and C2C12 (Figs 5.5 and 5.7). Here we have shown for the first time that 25KD resulted in an increase in cell viability and cell accumulation of both MDA-MB-468 (Fig 5.8) and C2C12 cells (Fig 5.9). These findings contradict the current literature which suggests that 25KD would result in a reduction in proliferation (109). Considering these factors, it may be that short term 25KD results in an increase in proliferation, while over time insufficiency overtakes and reduces net proliferation. To further elucidate the impact of 25KD on cell proliferation a more direct assay, such as a bromodeoxyuridine (BrdU) incorporation assay, could be used to accurately measure DNA synthesis as an indicator of proliferation is needed.

It is also important to consider the role of FKBP25 in cell proliferation as a MT stabiliser. In the absence of MT stabilisation, the cells MT may be more dynamic. This could improve the ability of the cells to undergo mitosis hence the increase in proliferation that we have observed. This may be a double-edged sword, as the MT are potentially less stable increasing the error margin in chromosome separation potentially resulting in an accumulation of somatic mutations (109, 421). In the context

of normal cells, in this case myoblasts, there could be an increase in regenerative capacity in the absence of FKBP25 that results in increased proliferation. This finding may hold more translational merit in regeneration of skeletal muscle myoblasts (or satellite cells) for damage repair. It is established that loss of the satellite cell pool results in reduced regenerative capacity (319). It is hypothesised that a reduction in FKBP25 in satellite cells may transiently increase their proliferation and result in an increase in the satellite cell pool. This increase in cells may consequently increase the capacity of regeneration of skeletal muscle. Further research is required to consolidate these hypotheses.

### 5.3.2 FKBP25 knockdown improves C2C12 myoblast wound healing but not chemotactic migration of MDA-MB-468 cells.

To adequately examine the impact of 25KD on the two cell lines of interest, separate migration assays were utilised. MDA-MB-468 cells were examined using a two-chamber chemotactic migration assay which is more representative of how cancer cells would migrate (422). Comparatively, C2C12 cells were assessed with a wound healing assay which would more accurately measure adherent migration that myoblasts would undertake (423). Here it was found that while 25KD had no impact upon MDA-MB-468 chemotactic migration (toward EGF or FbCM, **Fig 5.10 and 5.11**), there was a significant increase in migration in 25KD C2C12 cells (**Fig 5.12**).

It is important to remember the characteristics of the cell types being examined. MDA-MB-468 are an epithelial-like breast cancer cell, which behave similarly to epithelial cells, such that they maintain polarity and cell to cell adhesions. Compared to other breast cancer cell lines, MDA-MB-468 cells have a relatively low invasive and migratory potential as reflected by a series of markers, including integrins and

adhesion molecules (424). Considering this, it may be a cell line-dependent finding and measuring migration/chemotaxis may be difficult in MDA-MB-468 cell line. Similarly, it is typical of cancer cells to adapt quickly to alterations in their environment. It is possible that upon 25KD, MDA-MB-468 cells are able to acclimate to this event better than normal healthy cells, such as C2C12 cells. For example, 25KD results in increased migration ability in normal C2C12 cells but not breast cancer cells, likely due to the plethora of factors and pathways that are implicated in cell migration (425). Future studies should consider examining migration in additional breast cancer cell lines.

### 5.3.3 FKBP25 knockdown reduces anchorage-dependent growth of MDA-MB-468 cells but not invasion outgrowth.

Upon progression of cells to mesenchymal phenotype they lose their requirement for anchorage-dependent growth and gain an ability for anchorage-independent growth (426). This is largely facilitated by the cell's ability to adapt and overcome the requirement for anchorage to mediate cell cycle progression. Under normal conditions the binding of cell integrins to the ECM elicits a cascade of events that result in cell cycle progression (427). However, upon mesenchymal progression, these signalling events occur in the absence of integrin binding and anchorage – resulting in anchorage-independent growth. Anchorage-independent growth refers to the ability of mesenchymal cancer cells to grow without being anchored to an ECM (428). This event allows metastatic cells to grow in a secondary site where they would otherwise not survive (429). Additional assays can be utilised to assess the invasiveness of a particular cell line by culturing cells on a basement membrane preparation (412). Considering the previous findings that we have identified linking FKBP25 and EMT, we hypothesised that 25KD would be beneficial to the EMT program. Specifically, that

25KD would benefit both anchorage-dependent growth and invasion out-growth *in vitro*. Contrary to our hypothesis, it was found that 25 KD compromised anchorage-dependent growth. Considering that MDA-MB-468 cells are not mesenchymal cells, we found that at low density ( $1 \times 10^3$  cells, **Fig 5.13 A**) there was a significant reduction in colony formation. This was replicated at high density ( $5 \times 10^3$  cells, **Fig 5.13 B**) where the same significant reduction in colony formation was observed. Additionally, the invasion out-growth assay results suggested that 25KD had no effect on colony formation in Matrigel (**Fig 5.14**). Considering the non-mesenchymal phenotype of MDA-MB-468 cells, these assays may have been too stringent to see the hypothesised functional changes. Alternatively, these assays could be performed on EGF-mediated EMT MDA-MB-468 cells to overcome the limitations of using a basal breast cancer cell type.

#### 4.5.3.4 FKBP25 knockdown does not impair markers of myogenesis or myotube size of differentiated C2C12 myotubes.

To functionally assess the role of FKBP25 in myogenesis we have examined the impact of 25KD on induction of myogenic regulatory factors and myotube size. Myogenesis is the process of myoblast fusion to form mature myotubes which is regulated by a series of myogenic regulatory factors, including MyoD1 and myogenin (Discussed in chapter 4). The expression of myosin heavy chain (MyHC) is an essential component of the contractile apparatus of myotubes that distinguishes them from myoblasts. As such, a comprehensive examination of these molecular markers of myogenesis was required to examine the impact of 25KD. Upon induction of 25KD (0.5 $\mu$ g/ml dox for 72h prior to differentiation induction, described in *section 2.2.1*, for 120 hours or 5 days). It was found that C2C12 myotubes were able to maintain 25KD through the differentiation period equivalent to the 25KD achieved in myoblasts (**Fig 5.15 A-C**). Despite maintenance of 25KD, it was identified that there were no

significant changes to myogenin or MyoD in myoblasts. An anticipated reduction in MyoD may have explain the increase in proliferation that were observed in 25KD cells, however, this was not the case. It has been demonstrated that there may be a feedback loop acting in myogenic differentiation implicating MDM2 (a repressor of FKBP25) and MyoD. This feedback loop suggests that MDM2 prevents MyoD promotor binding to the MyoD response elements to initiate withdrawal from the cell cycle (430). Concurrent with unchanged myogenic factors in 25KD myoblasts there was no observable change to fast myosin heavy chain expression in 25KD myotubes (**Fig 5.16 A and B**) Interestingly, it has been shown that transcription factor YY1 becomes reduced upon C2C12 differentiation (431), and it has previously been identified that FKBP25 interacts with YY1 (173). These findings contradict our original hypothesis that 25KD would reduce myogenesis and induction of myogenic factors.

Next, we considered the impact of 25KD on myotube size and myoblast fusion. Here it was hypothesised that 25KD would impair myotube size and myoblast fusion due to the increased dynamic instability of the MT network. However, it was found that there were no differences in myotube size (**Fig 5.17**). Post-translational modifications to tubulin result in modifications to the stability of the MT polymers, with deetyrosination of tubulin monomers resulting in increased stability. It has previously been identified that MT stability is a factor in myogenesis and disruption to MT stability impairs myogenesis (432). While myotube size was not directly impacted, we hypothesised that there may be some impact upon the number of myoblasts required to form mature myotubes considering the changes to migration observed in 25KD myoblasts (**Fig 5.12**). Following fusion index analysis, it was confirmed that 25KD had no impact on myoblast fusion (**Fig 5.18**). Together, this data may indicate that in terms of regeneration, a reduction in FKBP25 may be important for increasing the proliferative

and migratory capacity of myoblasts only, while not having an impact upon terminal differentiation and fusion. Examining the influence of 25KD in myogenesis in other models, including human myoblasts may provide further insights into the role of FKBP25 in cell differentiation.

### 5.3.5 FKBP25 knockdown increases markers of epithelial to mesenchymal transition in MDA-MB-468 cells

To further elucidate the impact of FKBP25 on the EMT process we induced EMT in 25KD cells using EGF (as described in 3.2.3). It was found that upon 25KD there were no obvious morphological changes (**Fig 5.19**). Nevertheless, we have observed a 25KD effect on E cadherin reduction (**Fig 5.20 A and B**), however, this effect was not seen with vimentin expression (**Fig 5.20 A and C**). EGF signalling is an essential pathway in the facilitation of EMT, namely the signalling cascade activates Snail and Slug transcriptional pathways (433). These transcription factors are required for inhibition of E cadherin expression and induction of intermediate filament switching to vimentin (434, 435). To date, there is no research that has investigated the link between FKBP25, EGF signalling, or EMT. EGFR signalling is intricately linked to EMT as it is overactivated in many epithelial cancers and is closely associated with poor patient outcomes (436, 437). EGFR signalling activates an abundance of molecular mediators including PI3K, Akt, Erk, and nuclear factor- $\kappa$ B (438-441). Here we have focused on the roles of Akt and Erk signalling in EMT. The role of Akt in cancer progression and EMT is largely associated with pro survival and anti-apoptotic signalling, including suppression of pro-apoptotic factor Bcl-2 associated death promoter (BAD) and cAMP response element-binding protein (CREB) associated survival genes (442, 443). However, in our models we were unable to identify changes

to Akt phosphorylation upon EGF stimulation (**Fig 5.22**). Likewise, Erk signalling was unaffected in our 25KD models (**Fig 5.23**). In contrast to Akt signalling, Erk signalling is principally linked to the cell cycle and its progression (444, 445). This study could be optimised by inducing EMT in 25KD cells prior to stimulation with EGF to observe if there is a change in the signalling activation compared to normal conditions. While there are no current studies that proposed any link between FKBP25 and signalling molecules, we have shown that upon EGF mediated EMT there is a reduction in FKBP25 expression. However, our previous study demonstrated that upon treatment with small molecule inhibitors there were no alterations to FKBP25 protein expression (**Fig 3.10**). Together this data suggests that FKBP25 protein expression in EMT may not be occurring through signalling events caused by EGF stimulation directly.

#### 5.3.6 FKBP25 knockdown does not alter tubulin post translational modifications associated with tubulin polymer stability in C2C12 myoblasts but not MDA-MB-468 cells.

The final aspect of this study involved examining the impact of 25KD on tubulin polymerisation and stability in both MDA-MB-468 and C2C12 cells. FKBP25 is a known MT associated protein that acts to promote MT polymer stability (See **Fig 5.3**). The stability of the MT network of a cell is integral for many cell functions including mechanical support, cytoplasmic organisation, cytoplasmic cargo transport, cell movement, and chromosome separation (reviewed in (160)). MT dynamics are described as dynamically instable, which refers to the coexistence of both polymerisation and depolymerisation of a single MT. The growing end of the MT is referred to as the 'plus end' which can be capped by end binding proteins (EB family of proteins). During plus end growth of the MT, tubulin monomers are in a GTP-bound

state which acts as a structural stability modification. Hydrolyzation of this GTP bound state results in GDP-bound monomers, subsequently causing depolymerisation. MT's are able to be post -translationally modified to enhance their stability. Common PTM's of MTs include acetylation, detyrosination, and phosphorylation (446). Tubulin acetylation is associated with MTs that have been formed for an extended period of time, such as structural filaments (447). Detyrosination of the MT plus end refers to the removal of a tyrosine residue on the C terminal of the polymer to expose a glutamine residue. Detyrosinated MTs have a longer half-life and are less dynamic compared to Glu-MTs (448). To assess the impact of 25KD on MT stability first we have examined detyrosination and acetylation PTM's. Here it was found that in C2C12 myoblasts there were no changes to acetylation (**Fig 5.24 A and D**), or detyrosinated alpha tubulin (**Fig 5.24 B and D**). Suggesting that 25KD was insufficient to impact upon tubulin modifications *in vitro*. Similarly, in MDA-MB-468 cells there was no change to tubulin acetylation (**Fig 5.25 A and D**), although there were no changes to tubulin detyrosination (**Fig 5.25 B and D**). One such explanation for the differences in tubulin detyrosination between the two cell lines may be confluence of the cultures upon sample collection (449). To avoid differentiation of C2C12 myoblasts the cultures must remain highly sub confluent (~70% confluence). While MDA-MB-468 cells tend to grow in clusters despite their malignant phenotype these cells maintain some epithelial characteristics, namely anchorage-dependent growth. Considering this, it is likely that as the MDA-MB-468 cells became increasingly confluent, the pool of detyrosinated MTs may have become saturated in 25KD cells. Next, we studied the expression of stathmin, a molecule that is involved in promoting MT depolymerisation (450). Here it was identified that 25KD in C2C12 myoblasts did not affect stathmin expression (**Fig 5.24 C and D**). Similarly, in MDA-MB-468 cells there were no

observed changes in stathmin levels (**Fig 5.25 C and D**). To further examine the role of 25KD on MT stability future studies should consider examining more markers of tubulin stability and different culture conditions, such as confluence.

To assess the impact of 25KD on MT polymerisation the soluble and insoluble proportions of tubulin were fractioned from both C2C12 and MDA-MB-468 cells. Upon gel electrophoresis the proportions of tubulin fractions were assessed, and it was revealed that there were no significant differences in polymerised MT content in either cell line (**Figs 5.26 to 5.29**). Interestingly, a previous publication from Dilworth et al., established that in their hands FKBP25 knockdown resulted in an approximate 4-fold reduction in polymerised MT fraction compared to the non-targeting control (109). Additionally, it was reported that further to the reduction in MT proportion, there were faults in mitotic spindle formation and consequential micro and binucleation of daughter cells. Furthermore, cells were shown to be resistant to Taxol (up to 10nM for 24 hours). In our models, no statistical differences were observed which may be reflective of cell type choices. MT dynamics are regulated in vastly different manners in various cell types, such as epithelial fibroblastic/mesenchymal. It has been reported that epithelial cell MTs have a half-life of 4 minutes, while fibroblastic cell MTs have a half-life of 18 minutes at 37°C (451). It is likely that small temperature changes can rapidly shift the MT polymer proportion of cells and thus confound the results of polymerisation assays. Further experiments would be required to assess if changes in temperature were the cause of variability. Finally, to sufficiently analyse the impact of 25KD on MT stability, more cell types must be examined to make an appropriate conclusion.

## 5.4 Conclusions

These studies have investigated the role of FKBP25 in cell biology and function of both C2C12 myoblasts and MDA-MB-468 breast cancer cells. Here we have revealed that upon 25KD there is an increase in both cell viability and cell accumulation of both C2C12 and MDA-MB-468 cells over time. This data indicates that there is a net increase in proliferation resulting from 25KD. Further to this finding, it was identified that 25KD facilitates an increase of ~20% in wound healing migration of C2C12 myoblasts compared to controls. However, upon measuring chemotactic migration MDA-MB-468 cells there were no differences measured in migration toward either EGF or fibroblast conditioned medium. This may be a limitation of utilising this basal-like cell line as they are less prone to migrate than other subtypes. Considering our previous data that demonstrated that EGF-mediated EMT alone reduced FKBP25 and caused an increase in EMT markers, future studies should examine migration of MDA-MB-468 cells that have undergone EGF-mediated EMT. Upon measurement of anchorage-dependent growth of MDA-MB-468 cells, it was shown that there was a reduction in colony formation under both high and low seeding density. This data demonstrated that independent of confluence 25KD reduced the ability of MDA-MB-468 cells to form and survive in colonies. It was hypothesised that this was due to impaired MT stability resulting from 25KD. Conversely, it was found that 25KD did not affect invasion-outgrowth. Assessment of the functional impact of 25KD on C2C12 myoblasts differentiation revealed no alterations to myogenic regulatory factors were observed. Measurement of both myotube diameter and fusion index contradict the proposed hypothesis. Further examination of 25KD in EGF-mediated EMT revealed that 25KD resulted in a cumulative reduction in E cadherin expression but not vimentin, suggesting that 25KD may be involved in the loss of epithelial characteristics rather

than the transition to mesenchymal characteristics. The final study of this chapter aimed to investigate the influence of 25KD on MT stability and dynamics. It was shown that 25KD in both MDA-MB-468 and C2C12 did not alter MT modifications or MT regulating proteins. Finally, upon fractionation of free and polymerised tubulin it was shown that 25KD did not alter polymerised tubulin content in either C2C12 or MDA-MB-468 cells. To further elucidate the role of FKBP25 in MT dynamics further studies should examine alternative methods that are less temperature sensitive and prone to error. In conclusion, this study determined that the loss of FKBP25 largely impacted upon proliferation, rather than other functional measures. However, upon examination of a molecular reason for this alteration, specifically tubulin stability, no link able to be determined. This study lays foundational research that indicates that FKBP25 protein expression can be utilised as a measurement of proliferation in both cancer and muscle progenitor cells.

---

## Chapter 6: General discussion

---

### 6.1 FKBP25 in breast cancer cell de-differentiation

FK506 binding proteins are a diverse family of immunophilin molecules that are involved in a variety of cell functions. While some FKBP25s have been extensively researched in the context of cancer progression and de-differentiation, there has been limited research regarding FKBP25. Current literature has identified that FKBP25 is a nucleic acid binding protein that is able to shuttle between the nucleus and the cytoplasm, where it can perform protein interactions. In the cytoplasm, FKBP25 is able to facilitate protein folding, cytoskeletal dynamics, dsRNA binding, interactions with the pre-ribosome, and respond to cell stress responses. Despite these known functions, there is no current research that has implicated FKBP25 in cell differentiation or cancer pathogenesis. To address these questions, the current study first assessed FKBP25 protein expression in a panel of breast cancer cell lines of different classifications. Here it was identified that FKBP25 was highly expressed in epithelial-like subtypes, including luminal (T47D) and basal (MDA-MB-468), compared to mesenchymal subtypes (BT-549, Hs578t, MDA-MB-231). Interestingly, similar research recently revealed that FKBP25 mRNA levels are increased in mesenchymal breast cancer cell line MDA-MB-231 and murine breast cancer cell line 4T1 (452). Considering that the present study has uncovered the opposite findings, it may appear that FKBP25 mRNA is degraded and not translated in mesenchymal subtypes. The loss of FKBP25 protein may have several beneficial roles to a de-differentiated cancer phenotype, which could include increased propensity to proliferate, increased cytoskeletal plasticity, and stabilisation of EMT-related mRNA.

To further elucidate this finding, the current study examined oncogenic mutations that are commonly found in malignant transformation, such as Ras and p53 mutants. Surprisingly, it was demonstrated that in these models there were significant increases in FKBP25 protein expression, which contradicts the previous data from the breast cancer subtype panel. While these models are a valuable representation of the behaviours of de-differentiated cancer cells, it is important to remember that a single somatic mutation does not transform otherwise normal mammary epithelium. This indicates that the presence of multiple mutations may be required for loss of FKBP25 expression to benefit malignant progression. To assess this hypothesis, MDA-MB-468 cells were utilised to develop an EGF-mediated EMT model. This model of basal breast cancer cell EMT was confirmed by both morphological alterations and protein expression of EMT markers E cadherin and vimentin. This model demonstrated that cells that had already undergone some level of transformation, such as basal subtype breast cancer cells (with high levels of FKBP25 expression), could undergo EMT and subsequently reduce FKBP25 protein expression. This study demonstrated that epithelial-like breast cancer cell subtypes express increased levels of FKBP25 and loss of FKBP25 may be due to multiple mutations and a progressed phenotype.

## **6.2 The involvement of FKBP25 in myogenesis**

After examining FKBP25 in models of cancer pathogenesis, a hypothesis was developed suggesting that epithelial-like cells express high levels of FKBP25, while mesenchymal-like cells express lower levels of FKBP25. To further examine this hypothesis, the current study assessed the MET-like model of C2C12 myogenesis. This study revealed that proliferative, mesenchymal-like myoblasts express low levels of FKBP25 protein compared to post-mitotic, epithelial-like myotubes. Furthermore, it was demonstrated that upon induction of quiescence, a model of undifferentiated but

non-proliferative cells, it was identified that quiescent myoblasts expressed greater levels of FKBP25 than proliferative myoblasts. This finding supports the hypothesis that loss of FKBP25 is associated with a proliferative, mesenchymal-like phenotype. However, this hypothesis did not hold true in human primary myoblasts which displayed increased FKBP25 protein expression. This may be explained by the presence of growth factors that are present in the growth medium. Interestingly, FKBP25 was also found to be increased in MCF10A Ras<sup>V12</sup> transformed cells (**Fig3.5**) which mimics constant stimulation with growth factors, such as EGF. Thus the presence of fibroblast growth factor in the growth medium of MBA-135 cells may be involved in upregulating FKBP25 in these cells. Conversely, Rh30 RMS myoblasts express low levels of FKBP25 which is consistent with their proliferative, mesenchymal-like phenotype. Upon differentiation, or rather treatment with differentiation medium as RMS cells do not differentiate, there was a significant increase in FKBP25 protein expression.

Unlike the primary myoblasts, RH30 myoblasts treatment with differentiation medium results in a clear increase in myogenin, which is also noted upon C2C12 differentiation indicating commitment to myogenin. Myogenin is required for commitment to myogenesis and initiates transcription of other myogenic factors. Which suggests that these cells have undergone some level of MET, and potentially become more epithelial-like, and less proliferative. Additionally, the p53 mutation status of RMS cells may impact upon FKBP25 expression. RMS cells were cultured in the same growth medium as primary myoblasts containing growth factors, however, the presence of somatic mutations associated with RMS may have a reverse effect to the EMT effect that was observed in MDA-MB-468 cells, such that the removal of growth factors from transitioning to differentiation medium has resulted in an MET-like effect. These

hypotheses should be examined in future studies to establish the impact of growth factors on FKBP25 expression. Furthermore, loss of function studies were able to demonstrate that FKBP25 KD did not impact upon C2C12 myogenesis, indicating the role of FKBP25 is associated with proliferative cell types. Together, this study has further demonstrated that FKBP25 is expressed at low levels in proliferative, mesenchymal-like cells, and expressed highly in epithelial-like, differentiated cells.

### **6.3 FKBP25 in mature muscle plasticity**

FKBP25 is the most abundantly expressed FKBP in the skeletal muscle proteome (225). As such, the current study aimed to assess the impact of a range of models of skeletal muscle plasticity on FKBP25 protein expression. Here, models of chronic mechanical loading and mdx regeneration both exhibited significant increases in FKBP25 expression. Both of these models are known to undergo extensive structural remodelling, satellite cell activation and regeneration, and subsequent cytoskeletal remodelling (453-456). Upon these remodelling events, MT and MT organising centres are formed, and stabilised, to reorganise the location of newly fused nuclei and arrange organelles accordingly (456). Considering that FKBP25 is a known MT stabilising molecule, it is hypothesised that these reorganisation events rely on increased expression of MT stabilising proteins, which may not be limited to FKBP25. It has previously been demonstrated that the loss of microtubule associated proteins, such as MAP6, results in loss of MT organisation and impaired muscle function (334). This suggests that adequate stabilisation of the MTs is required for muscle function. Upon damage to skeletal muscle, from either mechanical loading or pathology (such as mdx) extensive MT remodelling is an adaptation to prevent dysfunction. Conversely, in a model of skeletal muscle denervation-induced atrophy, there was an observed reduction in FKBP25 expression. Similar to the previously described

regeneration models, atrophy models are also known to undergo extensive MT reorganisation (332). Interestingly, in the food deprivation study, it was identified that FKBP25 protein expression was unaltered. In this atrophy model, it was anticipated that there would be a reduction in FKBP25 as the muscle fibres waste. It seems that while the 48-hour food deprivation time frame is adequate to induce wasting, this short-term model may not allow for sufficient remodelling that must occur to detect observable differences in FKBP25 protein expression. Conversely, the other models that were examined in the present study were collected 7-days post intervention (CML and denervation), or at 8-weeks of age for MDX dystrophic mice after a severe damage period which peaks at around 3 weeks of age. Thus, in all of these cases there was adequate time for muscle regeneration, and importantly, MT reorganisation. Previous studies have demonstrated that it takes approximately 3 days to detect observable changes in MT network, and at 5-10 days to see MT organising centres forming around centrally located nuclei for repositioning in mature fibres (332). Overall, this study has demonstrated that FKBP25 expression is increased in models of muscle regeneration and decreased in a model of skeletal muscle atrophy, which is likely to result from extensive MT remodelleling. Due to time constraints and the impact of COVID-19 pandemic, we were unable to peruse this line of investigation any further. As such, further studies should consider examination of the impacts FKBP25 knockdown, and overexpression, on skeletal muscle structure and function *in vivo*.

#### **6.4 FKBP25 in cell biology and function**

FKBP25 knockdown (25KD) models were generated in MDA-MB-468 and C2C12 cell lines to examine the impact of FKBP25 on cell biology and function. 25KD cell lines that were generated resulted in an approximate 75% reduction in FKBP25 protein being expression. It was revealed in the current study that 25KD resulted in increased

in cell viability and cell accumulation, which indicated a net increase in proliferation of both cell lines. However, upon examination of cell migration it was revealed that 25D MDA-MB-468 cells did not have altered propensity to migrate toward a chemoattractant. While 25KD C2C12 myoblasts displayed a significant increase in wound healing migration compared to NT controls. The differences in migration may be related to the difference in cell type, such that MDA-MB-468 cells are a cancer cell line. Considering that these cells already contain many somatic mutations, the addition of 25KD alone was not sufficient to induce a phenotypic change. Furthermore, MDA-MB-468 25KD cells were shown to display a significant reduction in anchorage-dependent growth suggesting that 25KD reduces the capacity of these cells to successfully colonise at low confluency, which is a key behaviour of metastatic cells. However, it was demonstrated that 25KD had no effect on *in vitro* invasion out-growth. Interestingly, the sole function that 25KD impacted upon in MDA-MB-468 cells was proliferation. Previous studies have demonstrated that FKBP25 is required for mitotic spindle formation and subsequent stabilisation of the spindle apparatus (109, 121). As such, 25KD in this case is suspected to cause destabilisation of the mitotic spindle and allow for increased MT dynamics, however, this feature is likely to promote the accumulation of chromosomal abnormalities which can contribute to cancer progression and EMT (457).

To further elucidate the role of FKBP25 in EMT, an EGF-mediated EMT model was utilised containing 25KD. It was found that there were cumulative reductions in E cadherin upon 25KD compared to untreated controls. This data suggests that loss of FKBP25 may prime breast cancer cells for EMT and initiation of malignant transformation. However it was demonstrated that this occurrence does not occur as a result of EGF signalling. Further exploration of the role of FKBP25 in breast cancer

using *in vivo* models could reveal more regarding the potential implications of FKBP25 in cancer progression and EMT.

Upon assessment of 25KD in C2C12 myoblasts and myotubes revealed that there were no alterations to myogenic regulatory factor expression. This was supported by no observed changes to measures of differentiation, including myotube size and fusion index. Together, the current study suggests that 25KD may be impacting upon C2C12 myoblasts, specifically through proliferation and migration. However, 25KD alone is not sufficient to impair mature myotube formation. The role of FKBP25 in myogenesis and muscle function would benefit from additional *in vivo* studies to examine the impact of 25KD on skeletal muscle structure, function, and regeneration.

## **6.5 FKBP25 on MT polymerisation**

An important role of FKBP25 that has been hypothesised throughout these studies is its ability to stabilise the MTs and the consequences of this function on cell biology and function. Initially, the expression of MT stabilising post-translational modifications, including tubulin acetylation and detyrosination were assessed in both MDA-MB-468 and C2C12 25KD cell lines. There were no observed changes to acetylated or detyrosinated tubulin in MDA-MB-468 or C2C12 25KD cells. Similarly, no changes were observed to stathmin, a known MT depolymerising protein (458). To comprehensively assess the impact of 25KD on MT polymerisation, MT content was measured in each cell line using a cell fractionation method. Cells were examined with the presence or absence of paclitaxel to induce maximal polymerisation. Here it was revealed that neither C2C12 nor MDA-MB-468 25KD cells displayed a significant reduction in MT content. In these studies, it is noted that there is a high level of variability in the final datasets, which is likely to have resulted from slight temperature

changes that cause MT polymers to depolymerise. Ultimately causing variance in biological replicates. Future studies should consider implementing methods that enable a more consistent temperature to prevent these confounding variables.

## **6.6 Summary of the main findings of the thesis**

- FKBP25 protein expression is increased in luminal and basal breast cancer cell types compared to mesenchymal types.
- FKBP25 protein expression increased throughout C2C12 myogenesis
- FKBP25 protein expression increased following suspension culture of C2C12 myoblasts to model quiescence.
- FKBP25 protein is increased in models of skeletal muscle plasticity that are associated with extensive MT remodelling.
- FKBP25 knockdown increased proliferation and cell accumulation in both C2C12 myoblasts and MDA-MB-468 breast cancer cells.
- FKBP25 knockdown reduced anchorage dependent growth in MDA-MB-468 breast cancer cells compared to non-targeting controls.
- FKBP25 knockdown increased wound healing cell migration in C2C12 myoblasts compared to non-targeting control.
- FKBP25 knockdown did not have any impact upon C2C12 myogenesis, fusion index, or expression of myogenic factors.
- FKBP25 knockdown did not have any impact upon MT stabilisation or polymerisation in either C2C12 myoblasts or MDA-MB-468 breast cancer cells.

In conclusion, it was determined that low levels of FKBP25 protein was associated with a proliferative and mesenchymal phenotype. Contrary to the initial hypothesis,

FKBP25 protein expression was not found to be related to differentiation *per se*, however, it was identified that FKBP25 protein expression was consistently downregulated in response to EGF-mediated EMT/de-differentiation of MDA-MB-468 breast cancer cells. Additionally, it was found that a reduction in FKBP25 resulted in an increase in wound healing ability of C2C12 myoblasts. *In vivo* models of skeletal muscle plasticity illustrated that there was an increase in FKBP25 protein expression. Further studies should examine the exact mechanism that resulted in this increase in FKBP25 expression. It was speculated that these changes occurred from significant cytoskeletal remodelling associated with these conditions. It was hypothesised that these features occurred due to alterations in MT dynamics caused by loss of FKBP25, a MT stabilising protein, however, this was unable to be demonstrated by this study. The studies contained in this thesis have contributed to understanding the biological roles of FKBP25 in models of cell proliferation and differentiation.

## **6.7 Limitations of the study**

While these studies have contributed to describing and understanding the role of FKBP25 in a variety of *in vitro* and *in vivo* models, there are some limitations to the outcomes. First, many of these studies have been undertaken in *in vitro* models which have limitations to *in vivo* translation ability. A second limitation of the study is the use of MDA-MB-468 cell line for measuring invasive capacity. As a basal breast cancer subtype, MDA-MB-468 cells are known to be less invasive and less successful at the types of *in vitro* assays that they were used for in the current study. The use of a different breast cancer cell line or future studies could reveal more regarding the functional changes associated with 25KD. Additionally, it is also possible that the presence of 25KD in conjunction with other somatic mutation in cancer cell lines is not

sufficient to induce functional changes, compared to a 'normal' cell line, such as C2C12. Throughout the study there were more functional differences observed in C2C12 cells, these findings should be confirmed in another myoblast cell line to confirm that they are not species specific. Finally, the current study utilised a doxycycline-inducible knockdown model which is an important tool for studying the short-term effects of gene knockdown, however, in the current study it was observed, that C2C12 cell specifically, were prone to off target effects. Namely, it was identified that in the presence of doxycycline C2C12 myoblasts could not differentiate. Fortunately, cells were able to maintain 25KD for 96h post doxycycline treatment and differentiation studies were undertaken. Conversely, a constitutive knockdown could cause additional issues, such as overcoming the knockdown by compensating with overexpression of another protein. Nonetheless, the current study has appropriately examined the role of FKBP25 in cell differentiation and proliferation.

## **6.8 Future directions**

Future studies should consider examining the impact of FKBP25 overexpression and mutagenesis to elucidate how FKBP25 contributes to EMT and MET-like differentiation. It was initially planned that this study would develop FKBP25 overexpressing cell lines, expressing one of wild type, FKBP25 N-terminal mutant (FKBP25<sup>K22M/K23M</sup>; resulting in disruption to DNA binding functions) or FKBP25 C-terminal mutant (FKBP25<sup>Y198F</sup>; resulting in impaired PPlase function and MT binding ability). These vectors were aimed to be transfected into cell lines that express low levels of FKBP25 (such as MDA-MB-213) to assess if overexpression could impair invasive progression, and importantly, which domain is responsible for this outcome. Additionally, these vectors were going to be utilised to examine the impact of FKBP25 overexpression could increase myogenic differentiation, and again, which domain is

required for this function. To add to the current study, it would be exciting to synthetically rescue 25KD in MDA-MB-468 cells with WT, K22M/K23M, or Y198F mutants to determine how the 25KD results in the changes that were previously observed. These rescue studies would add to the understanding of the roles of the functional domains of FKBP25 in its biological function and would build on the current findings in this thesis. Additionally, this would allow the studies to be expanded into additional cell lines to assess the impact on EMT in cell types that are already mesenchymal to see if FKBP25 can regress the phenotype. Also to examine if FKBP25 over expression in skeletal could potentially have a protective role in muscle structure or function with age and disease states.

## References:

1. Rahfeld JU, Schierhorn A, Mann K, Fischer G. A novel peptidyl-prolyl cis/trans isomerase from *Escherichia coli*. *FEBS Lett.* 1994;343(1):65-9.
2. Pan CQ, Liou YC, Low BC. Active Mek2 as a regulatory scaffold that promotes Pin1 binding to BPGAP1 to suppress BPGAP1-induced acute Erk activation and cell migration. *J Cell Sci.* 2010;123(Pt 6):903-16.
3. Cheng CW, Leong KW, Ng YM, Kwong YL, Tse E. The peptidyl-prolyl isomerase PIN1 relieves cyclin-dependent kinase 2 (CDK2) inhibition by the CDK inhibitor p27. *J Biol Chem.* 2017;292(52):21431-41.
4. Estey MP, Di Ciano-Oliveira C, Froese CD, Fung KYY, Steels JD, Litchfield DW, et al. Mitotic regulation of SEPT9 protein by cyclin-dependent kinase 1 (Cdk1) and Pin1 protein is important for the completion of cytokinesis. *J Biol Chem.* 2013;288(42):30075-86.
5. So KY, Oh SH. Prolyl isomerase Pin1 regulates cadmium-induced autophagy via ubiquitin-mediated post-translational stabilization of phospho-Ser GSK3 $\alpha\beta$  in human hepatocellular carcinoma cells. *Biochem Pharmacol.* 2015;98(3):511-21.
6. Liou YC, Ryo A, Huang HK, Lu PJ, Bronson R, Fujimori F, et al. Loss of Pin1 function in the mouse causes phenotypes resembling cyclin D1-null phenotypes. *Proc Natl Acad Sci U S A.* 2002;99(3):1335-40.
7. Rizzolio F, Lucchetti C, Caligiuri I, Marchesi I, Caputo M, Klein-Szanto AJ, et al. Retinoblastoma tumor-suppressor protein phosphorylation and inactivation depend on direct interaction with Pin1. *Cell Death Differ.* 2012;19(7):1152-61.
8. Zheng H, You H, Zhou XZ, Murray SA, Uchida T, Wulf G, et al. The prolyl isomerase Pin1 is a regulator of p53 in genotoxic response. *Nature.* 2002;419(6909):849-53.
9. Yeh ES, Lew BO, Means AR. The loss of PIN1 deregulates cyclin E and sensitizes mouse embryo fibroblasts to genomic instability. *J Biol Chem.* 2006;281(1):241-51.
10. Crenshaw DG, Yang J, Means AR, Kornbluth S. The mitotic peptidyl-prolyl isomerase, Pin1, interacts with Cdc25 and Plx1. *Embo j.* 1998;17(5):1315-27.
11. Ryo A, Liou YC, Wulf G, Nakamura M, Lee SW, Lu KP. PIN1 is an E2F target gene essential for Neu/Ras-induced transformation of mammary epithelial cells. *Mol Cell Biol.* 2002;22(15):5281-95.
12. Zannini A, Rustighi A, Campaner E, Del Sal G. Oncogenic Hijacking of the PIN1 Signaling Network. *Frontiers in oncology.* 2019;9:94-.
13. Kim G, Bhattarai PY, Choi HS. Peptidyl-prolyl cis/trans isomerase NIMA-interacting 1 as a molecular target in breast cancer: a therapeutic perspective of gynecological cancer. *Archives of pharmacal research.* 2019.
14. Yeh E, Cunningham M, Arnold H, Chasse D, Monteith T, Ivaldi G, et al. A signalling pathway controlling c-Myc degradation that impacts oncogenic transformation of human cells. *Nature Cell Biology.* 2004;6(4):308-18.
15. Uchida T, Fujimori F, Tradler T, Fischer G, Rahfeld J-U. Identification and characterization of a 14 kDa human protein as a novel parvulin-like peptidyl prolyl cis/trans isomerase. *FEBS Letters.* 1999;446(2-3):278-82.
16. Fujiyama-Nakamura S, Yoshikawa H, Homma K, Hayano T, Tsujimura-Takahashi T, Izumikawa K, et al. Parvulin (Par14), a Peptidyl-Prolyl Isomerase, Is a Novel rRNA Processing Factor That Evolved in the Metazoan Lineage. *Molecular & Cellular Proteomics.* 2009;8(7):1552-65.

17. Thiele A, Krentzlin K, Erdmann F, Rauh D, Hause G, Zerweck J, et al. Parvulin 17 Promotes Microtubule Assembly by Its Peptidyl-Prolyl Cis/Trans Isomerase Activity. *Journal of molecular biology*. 2011;411(4):896-909.
18. Surmacz TA, Bayer E, Rahfeld J-U, Fischer G, Bayer P. The N-terminal Basic Domain of Human Parvulin hPar14 is Responsible for the Entry to the Nucleus and High-affinity DNA-binding. *Journal of molecular biology*. 2002;321(2):235-47.
19. Saningong AD, Bayer P. Human DNA-binding peptidyl-prolyl cis/trans isomerase Par14 is cell cycle dependently expressed and associates with chromatin in vivo. *BMC biochemistry*. 2015;16:4.
20. Uchida T, Takamiya M, Takahashi M, Miyashita H, Ikeda H, Terada T, et al. Pin1 and Par14 peptidyl prolyl isomerase inhibitors block cell proliferation. *Chem Biol*. 2003;10(1):15-24.
21. Walsh CT, Zydowsky LD, McKeon FD. Cyclosporin A, the cyclophilin class of peptidylprolyl isomerases, and blockade of T cell signal transduction. *J Biol Chem*. 1992;267(19):13115-8.
22. Steinmann B, Bruckner P, Superti-Furga A. Cyclosporin A slows collagen triple-helix formation in vivo: indirect evidence for a physiologic role of peptidyl-prolyl cis-trans-isomerase. *J Biol Chem*. 1991;266(2):1299-303.
23. Helekar SA, Patrick J. Peptidyl prolyl cis-trans isomerase activity of cyclophilin A in functional homo-oligomeric receptor expression. *Proc Natl Acad Sci U S A*. 1997;94(10):5432-7.
24. Pan H, Luo C, Li R, Qiao A, Zhang L, Mines M, et al. Cyclophilin A is required for CXCR4-mediated nuclear export of heterogeneous nuclear ribonucleoprotein A2, activation and nuclear translocation of ERK1/2, and chemotactic cell migration. *J Biol Chem*. 2008;283(1):623-37.
25. Wei Y, Jinchuan Y, Yi L, Jun W, Zhongqun W, Cuiping W. Antiapoptotic and Proapoptotic Signaling of Cyclophilin A in Endothelial Cells. *Inflammation*. 2013;36(3):567-72.
26. Jin ZG, Melaragno MG, Liao DF, Yan C, Haendeler J, Suh YA, et al. Cyclophilin A is a secreted growth factor induced by oxidative stress. *Circ Res*. 2000;87(9):789-96.
27. Qi YJ, He QY, Ma YF, Du YW, Liu GC, Li YJ, et al. Proteomic identification of malignant transformation-related proteins in esophageal squamous cell carcinoma. *J Cell Biochem*. 2008;104(5):1625-35.
28. Yang H, Chen J, Yang J, Qiao S, Zhao S, Yu L. Cyclophilin A is upregulated in small cell lung cancer and activates ERK1/2 signal. *Biochem Biophys Res Commun*. 2007;361(3):763-7.
29. Obchoei S, Weakley SM, Wongkham S, Wongkham C, Sawanyawisuth K, Yao Q, et al. Cyclophilin A enhances cell proliferation and tumor growth of liver fluke-associated cholangiocarcinoma. *Molecular Cancer*. 2011;10(1):102.
30. Bannon JH, O'Donovan DS, Kennelly SM, Mc Gee MM. The peptidyl prolyl isomerase cyclophilin A localizes at the centrosome and the midbody and is required for cytokinesis. *Cell Cycle*. 2012;11(7):1340-53.
31. Choi KJ, Piao YJ, Lim MJ, Kim JH, Ha J, Choe W, et al. Overexpressed cyclophilin A in cancer cells renders resistance to hypoxia- and cisplatin-induced cell death. *Cancer Res*. 2007;67(8):3654-62.
32. Yu X, Harris SL, Levine AJ. The Regulation of Exosome Secretion: a Novel Function of the p53 Protein. *Cancer Research*. 2006;66(9):4795.
33. Howard BA, Furumai R, Campa MJ, Rabbani ZN, Vujaskovic Z, Wang X-F, et al. Stable RNA Interference-Mediated Suppression of Cyclophilin A Diminishes

Non-Small-Cell Lung Tumor Growth & In vivo. *Cancer Research*. 2005;65(19):8853.

34. Li Z, Zhao X, Bai S, Wang Z, Chen L, Wei Y, et al. Proteomics identification of cyclophilin a as a potential prognostic factor and therapeutic target in endometrial carcinoma. *Mol Cell Proteomics*. 2008;7(10):1810-23.

35. Li J, Xie H, Yi M, Peng L, Lei D, Chen X, et al. Expression of cyclophilin A and CD147 during skin aging. *Zhong nan da xue xue bao Yi xue ban = Journal of Central South University Medical sciences*. 2011;36(3):203-11.

36. Gromov P, Skovgaard GL, Palsdottir H, Gromova I, Østergaard M, Celis JE. Protein profiling of the human epidermis from the elderly reveals up-regulation of a signature of interferon-gamma-induced polypeptides that includes manganese-superoxide dismutase and the p85beta subunit of phosphatidylinositol 3-kinase. *Mol Cell Proteomics*. 2003;2(2):70-84.

37. Boraldi F, Bini L, Liberatori S, Armini A, Pallini V, Tiozzo R, et al. Proteome analysis of dermal fibroblasts cultured in vitro from human healthy subjects of different ages. *Proteomics*. 2003;3(6):917-29.

38. Mayer AD, Dmitrewski J, Squifflet J-P, Besse T, Grabensee B, Klein B, et al. Multicenter randomized trial comparing tacrolimus (FK506) and cyclosporine in the prevention of renal allograft rejection: a report of the European Tacrolimus Multicenter Renal Study Group. *Transplantation*. 1997;64(3).

39. Brown EJ, Albers MW, Bum Shin T, Ichikawa K, Keith CT, Lane WS, et al. A mammalian protein targeted by G1-arresting rapamycin-receptor complex. *Nature*. 1994;369(6483):756-8.

40. Kang CB, Hong Y, Dhe-Paganon S, Yoon HS. FKBP family proteins: immunophilins with versatile biological functions. *Neurosignals*. 2008;16(4):318-25.

41. Jayaraman T, Brillantes AM, Timerman AP, Fleischer S, Erdjument-Bromage H, Tempst P, et al. FK506 binding protein associated with the calcium release channel (ryanodine receptor). *J Biol Chem*. 1992;267(14):9474-7.

42. Brillantes AB, Ondrias K, Scott A, Kobrinsky E, Ondriasová E, Moschella MC, et al. Stabilization of calcium release channel (ryanodine receptor) function by FK506-binding protein. *Cell*. 1994;77(4):513-23.

43. Tang W, Ingalls CP, Durham WJ, Snider J, Reid MB, Wu G, et al. Altered excitation-contraction coupling with skeletal muscle specific FKBP12 deficiency. *FASEB journal : official publication of the Federation of American Societies for Experimental Biology*. 2004;18(13):1597-9.

44. Zissimopoulos S, Lai FA. Interaction of FKBP12.6 with the cardiac ryanodine receptor C-terminal domain. *J Biol Chem*. 2005;280(7):5475-85.

45. Xin H-B, Rogers K, Qi Y, Kanematsu T, Fleischer S. Three Amino Acid Residues Determine Selective Binding of FK506-binding Protein 12.6 to the Cardiac Ryanodine Receptor. *The Journal of biological chemistry*. 1999;274:15315-9.

46. Galfré E, Pitt SJ, Venturi E, Sitsapesan M, Zaccai NR, Tsaneva-Atanasova K, et al. FKBP12 activates the cardiac ryanodine receptor Ca<sup>2+</sup>-release channel and is antagonised by FKBP12.6. *PLoS One*. 2012;7(2):e31956.

47. Derynck R, Zhang YE. Smad-dependent and Smad-independent pathways in TGF- $\beta$  family signalling. *Nature*. 2003;425(6958):577-84.

48. Ye-Guang Chen FLJM. Mechanism of TGF $\beta$  receptor inhibition by FKBP12. *The EMBO Journal*. 1997;16(13):3866-76.

49. Aghdasi, Keqiang Ye, Adam Resnick, Alex Huang, Hyo Chol Ha, Xin Guo, et al. FKBP12, the 12-kDa FK506-binding protein, is a physiologic regulator of the cell cycle. *PNAS*. 2001;98(5):2425-30.

50. Liu T, Xiong J, Yi S, Zhang H, Zhou S, Gu L, et al. FKBP12 enhances sensitivity to chemotherapy-induced cancer cell apoptosis by inhibiting MDM2. *Oncogene*. 2017;36(12):1678-86.
51. Linke K, Mace PD, Smith CA, Vaux DL, Silke J, Day CL. Structure of the MDM2/MDMX RING domain heterodimer reveals dimerization is required for their ubiquitylation in trans. *Cell Death & Differentiation*. 2008;15(5):841-8.
52. Li J, McQuade T, Siemer AB, Napetschnig J, Moriwaki K, Hsiao YS, et al. The RIP1/RIP3 necrosome forms a functional amyloid signaling complex required for programmed necrosis. *Cell*. 2012;150(2):339-50.
53. Galluzzi L, Kepp O, Kroemer G. MLKL regulates necrotic plasma membrane permeabilization. *Cell Res*. 2014;24(2):139-40.
54. Zicheng Wang JF, Jiyun Yu, Guozhu Chen. FKBP12 mediates necroptosis by initiating RIPK1/RIPK3/MLKL signal transduction in response to TNF receptor 1 ligation. *Journal of Cell Science*. 2019;132.
55. Li P, Ding Y, Wu B, Shu C, Shen B, Rao Z. Structure of the N-terminal domain of human FKBP52. *Acta crystallographica Section D, Biological crystallography*. 2003;59(Pt 1):16-22.
56. Chambraud B, Rouvière-Fourmy N, Radanyi C, Hsiao K, Peattie DA, Livingston DJ, et al. Overexpression of p59-HBI (FKBP59), full length and domains, and characterization of PPlase activity. *Biochem Biophys Res Commun*. 1993;196(1):160-6.
57. Miyata Y, Chambraud B, Radanyi C, Leclerc J, Lebeau M-C, Renoir J-M, et al. Phosphorylation of the immunosuppressant FK506-binding protein FKBP52 by casein kinase II: Regulation of HSP90-binding activity of FKBP52. *Proceedings of the National Academy of Sciences*. 1997;94(26):14500-5.
58. Radanyi C, Chambraud B, Baulieu EE. The ability of the immunophilin FKBP59-HBI to interact with the 90-kDa heat shock protein is encoded by its tetratricopeptide repeat domain. *Proceedings of the National Academy of Sciences*. 1994;91(23):11197-201.
59. Ning YM, Sánchez ER. In vivo evidence for the generation of a glucocorticoid receptor-heat shock protein-90 complex incapable of binding hormone by the calmodulin antagonist phenoxybenzamine. *Molecular Endocrinology*. 1996;10(1):14-23.
60. Banerjee A, Periyasamy S, Wolf IM, Hinds TD, Jr., Yong W, Shou W, et al. Control of glucocorticoid and progesterone receptor subcellular localization by the ligand-binding domain is mediated by distinct interactions with tetratricopeptide repeat proteins. *Biochemistry*. 2008;47(39):10471-80.
61. Tai PKK, Maeda Y, Nakao K, Wakim NG, Duhring JL, Faber LE. A 59-kilodalton protein associated with progesterin, estrogen, androgen, and glucocorticoid receptors. *Biochemistry*. 1986;25(18):5269-75.
62. Galigniana MD, Echeverria PC, Erlejman AG, Piwien-Pilipuk G. Role of molecular chaperones and TPR-domain proteins in the cytoplasmic transport of steroid receptors and their passage through the nuclear pore. *Nucleus*. 2010;1(4):299-308.
63. Timmermans S, Souffriau J, Libert C. A General Introduction to Glucocorticoid Biology. *Frontiers in Immunology*. 2019;10.
64. Galigniana MD, Harrell JM, Murphy PJM, Chinkers M, Radanyi C, Renoir J-M, et al. Binding of hsp90-Associated Immunophilins to Cytoplasmic Dynein: Direct Binding and in Vivo Evidence that the Peptidylprolyl Isomerase Domain Is a Dynein Interaction Domain. *Biochemistry*. 2002;41(46):13602-10.

65. Chambraud B, Belabes H, Fontaine-Lenoir V, Fellous A, Baulieu EE. The immunophilin FKBP52 specifically binds to tubulin and prevents microtubule formation. *FASEB journal : official publication of the Federation of American Societies for Experimental Biology*. 2007;21(11):2787-97.
66. Perrot-Appianat M, Cibert C, Geraud G, Renoir JM, Baulieu EE. The 59 kDa FK506-binding protein, a 90 kDa heat shock protein binding immunophilin (FKBP59-HBI), is associated with the nucleus, the cytoskeleton and mitotic apparatus. *Journal of Cell Science*. 1995;108(5):2037.
67. Ward BK, Mark PJ, Ingram DM, Minchin RF, Ratajczak T. Expression of the estrogen receptor-associated immunophilins, cyclophilin 40 and FKBP52, in breast cancer. *Breast Cancer Research and Treatment*. 1999;58(3):265-78.
68. Pan Z, Tan H. Autocrine regulation of cell proliferation by ER $\alpha$  in breast cancer cells. *Cancer Research*. 2008;68(9 Supplement):3040.
69. Fanelli MA, Vargas-Roig LM, Gago FE, Tello O, De Angelis RL, Ciocca DR. Estrogen receptors, progesterone receptors, and cell proliferation in human breast cancer. *Breast Cancer Research and Treatment*. 1996;37(3):217-28.
70. Ward BK, Mark PJ, Ingram DM, Minchin RF, Ratajczak T. Expression of the estrogen receptor-associated immunophilins, cyclophilin 40 and FKBP52, in breast cancer. *Breast Cancer Res Treat*. 1999;58(3):267-80.
71. Kumar P, Mark PJ, Ward BK, Minchin RF, Ratajczak T. Estradiol-regulated expression of the immunophilins cyclophilin 40 and FKBP52 in MCF-7 breast cancer cells. *Biochem Biophys Res Commun*. 2001;284(1):219-25.
72. Yang WS, Moon HG, Kim HS, Choi EJ, Yu MH, Noh DY, et al. Proteomic approach reveals FKBP4 and S100A9 as potential prediction markers of therapeutic response to neoadjuvant chemotherapy in patients with breast cancer. *J Proteome Res*. 2012;11(2):1078-88.
73. Hong C, Li T, Zhang F, Wu X, Chen X, Cui X, et al. Elevated FKBP52 expression indicates a poor outcome in patients with breast cancer. *Oncol Lett*. 2017;14(5):5379-85.
74. Scheufler C, Brinker A, Bourenkov G, Pegoraro S, Moroder L, Bartunik H, et al. Structure of TPR Domain–Peptide Complexes: Critical Elements in the Assembly of the Hsp70–Hsp90 Multichaperone Machine. *Cell*. 2000;101(2):199-210.
75. Barent RL, Nair SC, Carr DC, Ruan Y, Rimerman RA, Fulton J, et al. Analysis of FKBP51/FKBP52 chimeras and mutants for Hsp90 binding and association with progesterone receptor complexes. *Mol Endocrinol*. 1998;12(3):342-54.
76. Davies TH, Ning Y-M, Sánchez ER. A New First Step in Activation of Steroid Receptors: HORMONE-INDUCED SWITCHING OF FKBP51 AND FKBP52 IMMUNOPHILINS. *Journal of Biological Chemistry*. 2002;277(7):4597-600.
77. Wochnik GM, Ruegg J, Abel GA, Schmidt U, Holsboer F, Rein T. FK506-binding proteins 51 and 52 differentially regulate dynein interaction and nuclear translocation of the glucocorticoid receptor in mammalian cells. *J Biol Chem*. 2005;280(6):4609-16.
78. Vermeer H, Hendriks-Stegeman BI, van der Burg B, van Buul-Offers SC, Jansen M. Glucocorticoid-induced increase in lymphocytic FKBP51 messenger ribonucleic acid expression: a potential marker for glucocorticoid sensitivity, potency, and bioavailability. *The Journal of clinical endocrinology and metabolism*. 2003;88(1):277-84.
79. Zhang X, Clark AF, Yorio T. FK506-Binding Protein 51 Regulates Nuclear Transport of the Glucocorticoid Receptor  $\beta$  and Glucocorticoid Responsiveness. *Investigative Ophthalmology & Visual Science*. 2008;49(3):1037-47.

80. Qiu B, Xu Y, Wang J, Liu M, Dou L, Deng R, et al. Loss of FKBP5 Affects Neuron Synaptic Plasticity: An Electrophysiology Insight. *Neuroscience*. 2019;402:23-36.
81. Ni L, Yang CS, Gioeli D, Frierson H, Toft DO, Paschal BM. FKBP51 promotes assembly of the Hsp90 chaperone complex and regulates androgen receptor signaling in prostate cancer cells. *Mol Cell Biol*. 2010;30(5):1243-53.
82. Periyasamy S, Hinds T, Jr., Shemshedini L, Shou W, Sanchez ER. FKBP51 and Cyp40 are positive regulators of androgen-dependent prostate cancer cell growth and the targets of FK506 and cyclosporin A. *Oncogene*. 2010;29(11):1691-701.
83. Magee JA, Chang L-w, Stormo GD, Milbrandt J. Direct, Androgen Receptor-Mediated Regulation of the FKBP5 Gene via a Distal Enhancer Element. *Endocrinology*. 2006;147(1):590-8.
84. Febbo PG, Lowenberg M, Thorner AR, Brown M, Loda M, Golub TR. Androgen mediated regulation and functional implications of fkbp51 expression in prostate cancer. *The Journal of urology*. 2005;173(5):1772-7.
85. Perkins ND. Integrating cell-signalling pathways with NF- $\kappa$ B and IKK function. *Nature Reviews Molecular Cell Biology*. 2007;8(1):49-62.
86. Lawrence T. The nuclear factor NF-kappaB pathway in inflammation. *Cold Spring Harb Perspect Biol*. 2009;1(6):a001651.
87. Bouwmeester T, Bauch A, Ruffner H, Angrand PO, Bergamini G, Croughton K, et al. A physical and functional map of the human TNF-alpha/NF-kappa B signal transduction pathway. *Nat Cell Biol*. 2004;6(2):97-105.
88. Avellino R, Romano S, Parasole R, Bisogni R, Lamberti A, Poggi V, et al. Rapamycin stimulates apoptosis of childhood acute lymphoblastic leukemia cells. *Blood*. 2005;106(4):1400-6.
89. Romano MF, Avellino R, Petrella A, Bisogni R, Romano S, Venuta S. Rapamycin inhibits doxorubicin-induced NF-kappaB/Rel nuclear activity and enhances the apoptosis of melanoma cells. *Eur J Cancer*. 2004;40(18):2829-36.
90. Gasparian AV, Yao YJ, Kowalczyk D, Lyakh LA, Karseladze A, Slaga TJ, et al. The role of IKK in constitutive activation of NF-kappaB transcription factor in prostate carcinoma cells. *J Cell Sci*. 2002;115(Pt 1):141-51.
91. Pei H, Li L, Fridley BL, Jenkins GD, Kalari KR, Lingle W, et al. FKBP51 affects cancer cell response to chemotherapy by negatively regulating Akt. *Cancer Cell*. 2009;16(3):259-66.
92. Shang Z, Yu J, Sun L, Tian J, Zhu S, Zhang B, et al. LncRNA PCAT1 activates AKT and NF- $\kappa$ B signaling in castration-resistant prostate cancer by regulating the PHLPP/FKBP51/IKK $\alpha$  complex. *Nucleic Acids Res*. 2019;47(8):4211-25.
93. Banasavadi-Siddegowda YK, Mai J, Fan Y, Bhattacharya S, Giovannucci DR, Sanchez ER, et al. FKBP38 peptidylprolyl isomerase promotes the folding of cystic fibrosis transmembrane conductance regulator in the endoplasmic reticulum. *The Journal of biological chemistry*. 2011;286(50):43071-80.
94. Walker VE, Atanasiu R, Lam H, Shrier A. Co-chaperone FKBP38 promotes HERG trafficking. *J Biol Chem*. 2007;282(32):23509-16.
95. Wang X, Venable J, LaPointe P, Hutt DM, Koulov AV, Coppinger J, et al. Hsp90 cochaperone Aha1 downregulation rescues misfolding of CFTR in cystic fibrosis. *Cell*. 2006;127(4):803-15.
96. Misaka T, Murakawa T, Nishida K, Omori Y, Taneike M, Omiya S, et al. FKBP8 protects the heart from hemodynamic stress by preventing the accumulation

of misfolded proteins and endoplasmic reticulum-associated apoptosis in mice. *J Mol Cell Cardiol.* 2018;114:93-104.

97. Shirane M, Nakayama KI. Inherent calcineurin inhibitor FKBP38 targets Bcl-2 to mitochondria and inhibits apoptosis. *Nat Cell Biol.* 2003;5(1):28-37.

98. Hockenbery D, Nuñez G, Millman C, Schreiber RD, Korsmeyer SJ. Bcl-2 is an inner mitochondrial membrane protein that blocks programmed cell death. *Nature.* 1990;348(6299):334-6.

99. Itakura E, Mizushima N. Characterization of autophagosome formation site by a hierarchical analysis of mammalian Atg proteins. *Autophagy.* 2010;6(6):764-76.

100. Bhujabal Z, Birgisdottir Á B, Sjøttem E, Brenne HB, Øvervatn A, Habisov S, et al. FKBP8 recruits LC3A to mediate Parkin-independent mitophagy. *EMBO Rep.* 2017;18(6):947-61.

101. Shirane-Kitsuji M, Nakayama KI. Mitochondria: FKBP38 and mitochondrial degradation. *The International Journal of Biochemistry & Cell Biology.* 2014;51:19-22.

102. Rosner M, Hofer K, Kubista M, Hengstschlager M. Cell size regulation by the human TSC tumor suppressor proteins depends on PI3K and FKBP38. *Oncogene.* 2003;22(31):4786-98.

103. Bai X, Ma D, Liu A, Shen X, Wang QJ, Liu Y, et al. Rheb activates mTOR by antagonizing its endogenous inhibitor, FKBP38. *Science.* 2007;318(5852):977-80.

104. Fu YT, Zheng X, He Q, Jia XY, Guo ZX, Yao RY, et al. Silencing FKBP38 gene by siRNA induces activation of mTOR signaling in goat fetal fibroblasts. *Genet Mol Res.* 2015;14(3):9675-82.

105. Yoon MS, Sun Y, Arauz E, Jiang Y, Chen J. Phosphatidic Acid Activates Mammalian Target of Rapamycin Complex 1 (mTORC1) Kinase by Displacing FK506 Binding Protein 38 (FKBP38) and Exerting an Allosteric Effect. *The Journal of biological chemistry.* 2011;286(34):29568-74.

106. Zou H, Lai Y, Zhao X, Yan G, Ma D, Cardenas N, et al. Regulation of mammalian target of rapamycin complex 1 by Bcl-2 and Bcl-XL proteins. *J Biol Chem.* 2013;288(40):28824-30.

107. Jin YJ, Burakoff SJ, Bierer BE. Molecular cloning of a 25-kDa high affinity rapamycin binding protein, FKBP25. *J Biol Chem.* 1992;267(16):10942-5.

108. Prakash A, Shin J, Rajan S, Yoon HS. Structural basis of nucleic acid recognition by FK506-binding protein 25 (FKBP25), a nuclear immunophilin. *Nucleic Acids Res.* 2016;44(6):2909-25.

109. Dilworth D, Gudavicius G, Xu X, Boyce AKJ, O'Sullivan C, Serpa JJ, et al. The prolyl isomerase FKBP25 regulates microtubule polymerization impacting cell cycle progression and genomic stability. *Nucleic Acids Res.* 2018.

110. Gudavicius G, Dilworth D, Serpa JJ, Sessler N, Petrotchenko EV, Borchers CH, et al. The prolyl isomerase, FKBP25, interacts with RNA-engaged nucleolin and the pre-60S ribosomal subunit. *RNA.* 2014;20(7):1014-22.

111. David Dilworth FG, Kyle Miller, and Christopher J Nelson. FKBP25 participates in DNA double-strand break repair. *Biochemistry and Cell Biology.* 2019.

112. Dilworth D, Upadhyay SK, Bonnafous P, Edoe AB, Bourbigot S, Pesek-Jardim F, et al. The basic tilted helix bundle domain of the prolyl isomerase FKBP25 is a novel double-stranded RNA binding module. *Nucleic Acids Res.* 2017.

113. Jiang Q, Wu G, Yang L, Lu YP, Liu XX, Han F, et al. Elucidation of the FKBP25-60S Ribosomal Protein L7a Stress Response Signaling During Ischemic Injury. *Cellular physiology and biochemistry : international journal of experimental cellular physiology, biochemistry, and pharmacology.* 2018;47(5):2018-30.

114. Erard MS, Belenguer P, Caizergues-Ferrer M, Pantaloni A, Amalric F. A major nucleolar protein, nucleolin, induces chromatin decondensation by binding to histone H1. *European journal of biochemistry*. 1988;175(3):525-30.
115. Thacker J. Homologous Recombination Repair. In: Schwab M, editor. *Encyclopedia of Cancer*. Berlin, Heidelberg: Springer Berlin Heidelberg; 2011. p. 1725-9.
116. Rothenberg E, Grimme JM, Spies M, Ha T. Human Rad52-mediated homology search and annealing occurs by continuous interactions between overlapping nucleoprotein complexes. *Proc Natl Acad Sci U S A*. 2008;105(51):20274-9.
117. Deniz M, Romashova T, Kostezka S, Faul A, Gundelach T, Moreno-Villanueva M, et al. Increased single-strand annealing rather than non-homologous end-joining predicts hereditary ovarian carcinoma. *Oncotarget*. 2017;8(58):98660-76.
118. Ceccaldi R, Rondinelli B, D'Andrea AD. Repair Pathway Choices and Consequences at the Double-Strand Break. *Trends in cell biology*. 2016;26(1):52-64.
119. Ochocka AM, Kampanis P, Nicol S, Allende-Vega N, Cox M, Marcar L, et al. FKBP25, a novel regulator of the p53 pathway, induces the degradation of MDM2 and activation of p53. *FEBS Lett*. 2009;583(4):621-6.
120. Ahn J, Murphy M, Kratowicz S, Wang A, Levine AJ, George DL. Down-regulation of the stathmin/Op18 and FKBP25 genes following p53 induction. *Oncogene*. 1999;18(43):5954-8.
121. Wang D, Sun H, Zhang J, Huang Z, Li C, Han L, et al. FKBP25 Regulates Meiotic Apparatus During Mouse Oocyte Maturation. *Front Cell Dev Biol*. 2021;9:625805.
122. Zgajnar NR, De Leo SA, Lotufo CM, Erlejman AG, Piwien-Pilipuk G, Galigniana MD. Biological Actions of the Hsp90-binding Immunophilins FKBP51 and FKBP52. *Biomolecules*. 2019;9(2):52.
123. Gougelet A, Bouclier C, Marsaud V, Maillard S, Mueller SO, Korach KS, et al. Estrogen receptor alpha and beta subtype expression and transactivation capacity are differentially affected by receptor-, hsp90- and immunophilin-ligands in human breast cancer cells. *J Steroid Biochem Mol Biol*. 2005;94(1-3):71-81.
124. Cariou S, Donovan JCH, Flanagan WM, Milic A, Bhattacharya N, Slingerland JM. Down-regulation of p21WAF1/CIP1 or p27Kip1 abrogates antiestrogen-mediated cell cycle arrest in human breast cancer cells. *Proceedings of the National Academy of Sciences*. 2000;97(16):9042-6.
125. Li Y, Wang JP, Santen RJ, Kim TH, Park H, Fan P, et al. Estrogen stimulation of cell migration involves multiple signaling pathway interactions. *Endocrinology*. 2010;151(11):5146-56.
126. Yong W, Yang Z, Periyasamy S, Chen H, Yucel S, Li W, et al. Essential role for Co-chaperone Fkbp52 but not Fkbp51 in androgen receptor-mediated signaling and physiology. *J Biol Chem*. 2007;282(7):5026-36.
127. De Leon JT, Iwai A, Feau C, Garcia Y, Balsiger HA, Storer CL, et al. Targeting the regulation of androgen receptor signaling by the heat shock protein 90 cochaperone FKBP52 in prostate cancer cells. *Proc Natl Acad Sci U S A*. 2011;108(29):11878-83.
128. Riggs DL, Cox MB, Tardif HL, Hessling M, Buchner J, Smith DF. Noncatalytic role of the FKBP52 peptidyl-prolyl isomerase domain in the regulation of steroid hormone signaling. *Molecular and cellular biology*. 2007;27(24):8658-69.
129. Hanahan D, Weinberg RA. The hallmarks of cancer. *Cell*. 2000;100.

130. Westphal D, Kluck RM, Dewson G. Building blocks of the apoptotic pore: how Bax and Bak are activated and oligomerize during apoptosis. *Cell Death Differ.* 2014;21(2):196-205.
131. Uğuz AC, Nazıroğlu M, Espino J, Bejarano I, González D, Rodríguez AB, et al. Selenium Modulates Oxidative Stress-Induced Cell Apoptosis in Human Myeloid HL-60 Cells Through Regulation of Calcium Release and Caspase-3 and -9 Activities. *Journal of Membrane Biology.* 2009;232(1):15.
132. Xie Z, Klionsky DJ. Autophagosome formation: core machinery and adaptations. *Nature Cell Biology.* 2007;9(10):1102-9.
133. Bhujabal Z, Birgisdottir AB, Sjøttem E, Brenne HB, Overvatn A, Habisov S, et al. FKBP8 recruits LC3A to mediate Parkin-independent mitophagy. *EMBO Rep.* 2017;18(6):947-61.
134. Saita S, Shirane M, Nakayama KI. Selective escape of proteins from the mitochondria during mitophagy. *Nature Communications.* 2013;4(1):1410.
135. Kang CB, Feng L, Chia J, Yoon HS. Molecular characterization of FK-506 binding protein 38 and its potential regulatory role on the anti-apoptotic protein Bcl-2. *Biochem Biophys Res Commun.* 2005;337(1):30-8.
136. Qin X, Ma D, Tan Y-x, Wang H-y, Cai Z. The role of necroptosis in cancer: A double-edged sword? *Biochimica et Biophysica Acta (BBA) - Reviews on Cancer.* 2019;1871(2):259-66.
137. Seifert L, Werba G, Tiwari S, Giao Ly NN, Alothman S, Alqunaibit D, et al. The necrosome promotes pancreatic oncogenesis via CXCL1 and Mincle-induced immune suppression. *Nature.* 2016;532(7598):245-9.
138. Ruan J, Mei L, Zhu Q, Shi G, Wang H. Mixed lineage kinase domain-like protein is a prognostic biomarker for cervical squamous cell cancer. *Int J Clin Exp Pathol.* 2015;8(11):15035-8.
139. He L, Peng K, Liu Y, Xiong J, Zhu F-F. Low expression of mixed lineage kinase domain-like protein is associated with poor prognosis in ovarian cancer patients. *OncoTargets and therapy.* 2013;6:1539-43.
140. de Martel C, Franceschi S. Infections and cancer: Established associations and new hypotheses. *Critical Reviews in Oncology/Hematology.* 2009;70(3):183-94.
141. Karin M. Nuclear factor- $\kappa$ B in cancer development and progression. *Nature.* 2006;441(7092):431-6.
142. Stoll G, Ma Y, Yang H, Kepp O, Zitvogel L, Kroemer G. Pro-necrotic molecules impact local immunosurveillance in human breast cancer. *Oncolmmunology.* 2017;6(4):e1299302.
143. Soria G, Ofri-Shahak M, Haas I, Yaal-Hahoshen N, Leider-Trejo L, Leibovich-Rivkin T, et al. Inflammatory mediators in breast cancer: coordinated expression of TNF $\alpha$  & IL-1 $\beta$  with CCL2 & CCL5 and effects on epithelial-to-mesenchymal transition. *BMC Cancer.* 2011;11:130.
144. Fletcher DA, Mullins RD. Cell mechanics and the cytoskeleton. *Nature.* 2010;463(7280):485-92.
145. Hohmann T, Dehghani F. The Cytoskeleton-A Complex Interacting Meshwork. *Cells.* 2019;8(4).
146. Wang W, Goswami S, Lapidus K, Wells AL, Wyckoff JB, Sahai E, et al. Identification and testing of a gene expression signature of invasive carcinoma cells within primary mammary tumors. *Cancer Res.* 2004;64(23):8585-94.
147. Haynes J, Srivastava J, Madson N, Wittmann T, Barber DL. Dynamic actin remodeling during epithelial-mesenchymal transition depends on increased moesin expression. *Molecular biology of the cell.* 2011;22(24):4750-64.

148. Bhowmick NA, Ghiassi M, Bakin A, Aakre M, Lundquist CA, Engel ME, et al. Transforming growth factor-beta1 mediates epithelial to mesenchymal transdifferentiation through a RhoA-dependent mechanism. *Mol Biol Cell*. 2001;12.
149. Yamasaki T, Seki N, Yamada Y, Yoshino H, Hidaka H, Chiyomaru T, et al. Tumor suppressive microRNA-138 contributes to cell migration and invasion through its targeting of vimentin in renal cell carcinoma. *Int J Oncol*. 2012;41(3):805-17.
150. Herrmann H, Bär H, Kreplak L, Strelkov SV, Aebi U. Intermediate filaments: from cell architecture to nanomechanics. *Nature Reviews Molecular Cell Biology*. 2007;8(7):562-73.
151. Szeverenyi I, Cassidy AJ, Chung CW, Lee BT, Common JE, Ogg SC, et al. The Human Intermediate Filament Database: comprehensive information on a gene family involved in many human diseases. *Hum Mutat*. 2008;29(3):351-60.
152. Johnen N, Francart ME, Thelen N, Cloes M, Thiry M. Evidence for a partial epithelial-mesenchymal transition in postnatal stages of rat auditory organ morphogenesis. *Histochem Cell Biol*. 2012;138(3):477-88.
153. Sutoh Yoneyama M, Hatakeyama S, Habuchi T, Inoue T, Nakamura T, Funyu T, et al. Vimentin intermediate filament and plectin provide a scaffold for invadopodia, facilitating cancer cell invasion and extravasation for metastasis. *European journal of cell biology*. 2014;93(4):157-69.
154. Eckes B, Colucci-Guyon E, Smola H, Nodder S, Babinet C, Krieg T, et al. Impaired wound healing in embryonic and adult mice lacking vimentin. *J Cell Sci*. 2000;113 ( Pt 13):2455-62.
155. Eckes B, Dogic D, Colucci-Guyon E, Wang N, Maniotis A, Ingber D, et al. Impaired mechanical stability, migration and contractile capacity in vimentin-deficient fibroblasts. *J Cell Sci*. 1998;111 ( Pt 13):1897-907.
156. Yoon S, Leube RE. Keratin intermediate filaments: intermediaries of epithelial cell migration. *Essays in biochemistry*. 2019;63(5):521-33.
157. Mendez MG, Kojima S-I, Goldman RD. Vimentin induces changes in cell shape, motility, and adhesion during the epithelial to mesenchymal transition. *FASEB journal : official publication of the Federation of American Societies for Experimental Biology*. 2010;24(6):1838-51.
158. Tsuruta D, Jones JC. The vimentin cytoskeleton regulates focal contact size and adhesion of endothelial cells subjected to shear stress. *J Cell Sci*. 2003;116(Pt 24):4977-84.
159. Weisenberg RC. Microtubule Formation in vitro in Solutions Containing Low Calcium Concentrations. *Science*. 1972;177(4054):1104-5.
160. Janke C, Magiera MM. The tubulin code and its role in controlling microtubule properties and functions. *Nat Rev Mol Cell Biol*. 2020.
161. Mitchison T, Kirschner M. Dynamic instability of microtubule growth. *Nature*. 1984;312(5991):237-42.
162. Weaver BA. How Taxol/paclitaxel kills cancer cells. *Molecular Biology of the Cell*. 2014;25(18):2677-81.
163. Jordan MA. Mechanism of Action of Antitumor Drugs that Interact with Microtubules and Tubulin. *Current Medicinal Chemistry - Anti-Cancer Agents*. 2002;2(1):1-17.
164. Schiff PB, Horwitz SB. Taxol stabilizes microtubules in mouse fibroblast cells. *Proc Natl Acad Sci U S A*. 1980;77(3):1561-5.
165. Himes RH, Kersey RN, Heller-Bettinger I, Samson FE. Action of the vinca alkaloids vincristine, vinblastine, and desacetyl vinblastine amide on microtubules in vitro. *Cancer Res*. 1976;36(10):3798-802.

166. Tanaka S, Nohara T, Iwamoto M, Sumiyoshi K, Kimura K, Takahashi Y, et al. Tau expression and efficacy of paclitaxel treatment in metastatic breast cancer. *Cancer Chemother Pharmacol*. 2009;64(2):341-6.
167. Tan MH, De S, Bebek G, Orloff MS, Wesolowski R, Downs-Kelly E, et al. Specific kinesin expression profiles associated with taxane resistance in basal-like breast cancer. *Breast Cancer Res Treat*. 2012;131(3):849-58.
168. Zhao W, Song Y, Xu B, Zhan Q. Overexpression of centrosomal protein Nlp confers breast carcinoma resistance to paclitaxel. *Cancer Biol Ther*. 2012;13(3):156-63.
169. Chambrud B, Belabes H, Fontaine-Lenoir V, Fellous A, Baulieu EE. The immunophilin FKBP52 specifically binds to tubulin and prevents microtubule formation. *The FASEB Journal*. 2007;21(11):2787-97.
170. Waldeck K. Characterisation of the role of FKBP52 in breast cancer: Monash University; 2008.
171. Qi W-X, Shen Z, Lin F, Sun Y-j, Min D-l, Tang L-N, et al. Paclitaxel-based versus docetaxel-based regimens in metastatic breast cancer: a systematic review and meta-analysis of randomized controlled trials. *Current Medical Research and Opinion*. 2013;29(2):117-25.
172. Yao YL, Liang YC, Huang HH, Yang WM. FKBP52 in chromatin modification and cancer. *Curr Opin Pharmacol*. 2011;11(4):301-7.
173. Yang Y, Seto. The FK506-binding protein 25 functionally associates with histone deacetylases and with transcription factor YY1. *The European Molecular Biology Organization Journal*. 2001;20(17):4814-25.
174. Bushmeyer S, Park K, Atchison ML. Characterization of functional domains within the multifunctional transcription factor, YY1. *J Biol Chem*. 1995;270(50):30213-20.
175. Gao Y, Sun L, Wu Z, Xuan C, Zhang J, You Y, et al. miR-218 inhibits the proliferation of human glioma cells through downregulation of Yin Yang 1. *Mol Med Rep*. 2018;17(1):1926-32.
176. Wan M, Huang W, Kute TE, Miller LD, Zhang Q, Hatcher H, et al. Yin Yang 1 plays an essential role in breast cancer and negatively regulates p27. *Am J Pathol*. 2012;180(5):2120-33.
177. Gao L, Cueto MA, Asselbergs F, Atadja P. Cloning and Functional Characterization of HDAC11, a Novel Member of the Human Histone Deacetylase Family\*. *Journal of Biological Chemistry*. 2002;277(28):25748-55.
178. Thorne AW, Kmiciek D, Mitchelson K, Sautiere P, Crane-Robinson C. Patterns of histone acetylation. *European journal of biochemistry*. 1990;193(3):701-13.
179. Huang BH, Laban M, Leung CH, Lee L, Lee CK, Salto-Tellez M, et al. Inhibition of histone deacetylase 2 increases apoptosis and p21Cip1/WAF1 expression, independent of histone deacetylase 1. *Cell Death Differ*. 2005;12(4):395-404.
180. Draney C, Austin MC, Leifer AH, Smith CJ, Kener KB, Aitken TJ, et al. HDAC1 overexpression enhances  $\beta$ -cell proliferation by down-regulating Cdkn1b/p27. *Biochem J*. 2018;475(24):3997-4010.
181. Peinado H, Ballestar E, Esteller M, Cano A. Snail mediates E-cadherin repression by the recruitment of the Sin3A/histone deacetylase 1 (HDAC1)/HDAC2 complex. *Mol Cell Biol*. 2004;24(1):306-19.

182. Kim MS, Kwon HJ, Lee YM, Baek JH, Jang JE, Lee SW, et al. Histone deacetylases induce angiogenesis by negative regulation of tumor suppressor genes. *Nat Med.* 2001;7(4):437-43.
183. Scroggins BT, Robzyk K, Wang D, Marcu MG, Tsutsumi S, Beebe K, et al. An acetylation site in the middle domain of Hsp90 regulates chaperone function. *Mol Cell.* 2007;25(1):151-9.
184. Shan X, Xue Z, Mélése T. Yeast NPI46 encodes a novel prolyl cis-trans isomerase that is located in the nucleolus. *Journal of Cell Biology.* 1994;126(4):853-62.
185. Dingwall C, Robbins J, Dilworth SM, Roberts B, Richardson WD. The nucleoplasmic nuclear location sequence is larger and more complex than that of SV-40 large T antigen. *Journal of Cell Biology.* 1988;107(3):841-9.
186. Grelet S, Link LA, Howley B, Obellianne C, Palanisamy V, Gangaraju VK, et al. A regulated PNUTS mRNA to lncRNA splice switch mediates EMT and tumour progression. *Nat Cell Biol.* 2017;19(9):1105-15.
187. Chaudhury A, Hussey GS, Ray PS, Jin G, Fox PL, Howe PH. TGF-beta-mediated phosphorylation of hnRNP E1 induces EMT via transcript-selective translational induction of Dab2 and ILEI. *Nat Cell Biol.* 2010;12(3):286-93.
188. Preca BT, Bajdak K, Mock K, Sundararajan V, Pfannstiel J, Maurer J, et al. A self-enforcing CD44s/ZEB1 feedback loop maintains EMT and stemness properties in cancer cells. *Int J Cancer.* 2015;137(11):2566-77.
189. Ge Z, Quek BL, Beemon KL, Hogg JR. Polypyrimidine tract binding protein 1 protects mRNAs from recognition by the nonsense-mediated mRNA decay pathway. *eLife.* 2016;5.
190. Hou P, Li L, Chen F, Chen Y, Liu H, Li J, et al. PTBP3-Mediated Regulation of ZEB1 mRNA Stability Promotes Epithelial-Mesenchymal Transition in Breast Cancer. *Cancer Res.* 2018;78(2):387-98.
191. Lu W, Ning H, Gu L, Peng H, Wang Q, Hou R, et al. MCPIP1 Selectively Destabilizes Transcripts Associated with an Antiapoptotic Gene Expression Program in Breast Cancer Cells That Can Elicit Complete Tumor Regression. *Cancer Res.* 2016;76(6):1429-40.
192. Gutschner T, Hämmerle M, Pazaitis N, Bley N, Fiskin E, Uckelmann H, et al. Insulin-like growth factor 2 mRNA-binding protein 1 (IGF2BP1) is an important protumorigenic factor in hepatocellular carcinoma. *Hepatology (Baltimore, Md).* 2014;59(5):1900-11.
193. Stöhr N, Köhn M, Lederer M, Glass M, Reinke C, Singer RH, et al. IGF2BP1 promotes cell migration by regulating MK5 and PTEN signaling. *Genes Dev.* 2012;26(2):176-89.
194. Guo X, Connick MC, Vanderhoof J, Ishak MA, Hartley RS. MicroRNA-16 modulates HuR regulation of cyclin E1 in breast cancer cells. *Int J Mol Sci.* 2015;16(4):7112-32.
195. Shao R, Scully SJ, Jr., Yan W, Bentley B, Mueller J, Brown C, et al. The novel lupus antigen related protein acheron enhances the development of human breast cancer. *Int J Cancer.* 2012;130(3):544-54.
196. Manojlovic Z, Blackmon J, Stefanovic B. Tacrolimus (FK506) prevents early stages of ethanol induced hepatic fibrosis by targeting LARP6 dependent mechanism of collagen synthesis. *PLoS One.* 2013;8(6):e65897.
197. Thiery JP, Acloque H, Huang RY, Nieto MA. Epithelial-mesenchymal transitions in development and disease. *Cell.* 2009;139(5):871-90.

198. Thiery JP. Epithelial-mesenchymal transitions in tumour progression. *Nat Rev Cancer*. 2002;2.
199. Dillekås H, Rogers MS, Straume O. Are 90% of deaths from cancer caused by metastases? *Cancer Med*. 2019;8(12):5574-6.
200. Qiu WZ, Huang PY, Shi JL, Xia HQ, Zhao C, Cao KJ. Neoadjuvant chemotherapy plus intensity-modulated radiotherapy versus concurrent chemoradiotherapy plus adjuvant chemotherapy for the treatment of locoregionally advanced nasopharyngeal carcinoma: a retrospective controlled study. *Chinese journal of cancer*. 2016;35:2.
201. Al-Ejeh F, Shi W, Miranda M, Simpson PT, Vargas AC, Song S, et al. Treatment of triple-negative breast cancer using anti-EGFR-directed radioimmunotherapy combined with radiosensitizing chemotherapy and PARP inhibitor. *Journal of nuclear medicine : official publication, Society of Nuclear Medicine*. 2013;54(6):913-21.
202. Fabi A, Merola R, Ferretti G, Di Benedetto A, Antoniani B, Ercolani C, et al. Epidermal growth factor receptor gene copy number may predict lapatinib sensitivity in HER2-positive metastatic breast cancer. *Expert opinion on pharmacotherapy*. 2013;14(6):699-706.
203. Stommel JM, Wahl GM. Accelerated MDM2 auto-degradation induced by DNA-damage kinases is required for p53 activation. *The EMBO Journal*. 2004;23(7):1547-56.
204. Palmer MB, Majumder P, Cooper JC, Yoon H, Wade PA, Boss JM. Yin yang 1 regulates the expression of snail through a distal enhancer. *Mol Cancer Res*. 2009;7(2):221-9.
205. Cho AA, Bonavida B. Targeting the Overexpressed YY1 in Cancer Inhibits EMT and Metastasis. *Crit Rev Oncog*. 2017;22(1-2):49-61.
206. Zhu W, Li Z, Xiong L, Yu X, Chen X, Lin Q. FKBP3 Promotes Proliferation of Non-Small Cell Lung Cancer Cells through Regulating Sp1/HDAC2/p27. *Theranostics*. 2017;7(12):3078-89.
207. Tong J, Shen Y, Chen X, Wang R, Hu Y, Zhang X, et al. FKBP3 mediates oxaliplatin resistance in colorectal cancer cells by regulating HDAC2 expression. *Oncology reports*. 2019.
208. Ruscetti M, Dadashian EL, Guo W, Quach B, Mulholland DJ, Park JW, et al. HDAC inhibition impedes epithelial-mesenchymal plasticity and suppresses metastatic, castration-resistant prostate cancer. *Oncogene*. 2016;35(29):3781-95.
209. SJ JYaB. The 25-kDa FK506-binding protein is localized in the nucleus and associates with casein kinase II and nucleolin. *Proc Natl Acad Sci U S A*. 1993;90(16):7769-73.
210. Pichiorri F, Palmieri D, De Luca L, Consiglio J, You J, Rocci A, et al. In vivo NCL targeting affects breast cancer aggressiveness through miRNA regulation. *Journal of Experimental Medicine*. 2013;210(5):951-68.
211. Pustovalova M, Alhaddad L, Blokhina T, Smetanina N, Chigasova A, Chuprova-Netochin R, et al. The CD44<sup>high</sup> Subpopulation of Multifraction Irradiation-Surviving NSCLC Cells Exhibits Partial EMT-Program Activation and DNA Damage Response Depending on Their p53 Status. *International journal of molecular sciences*. 2021;22(5):2369.
212. Ghatak D, Das Ghosh D, Roychoudhury S. Cancer Stemness: p53 at the Wheel. *Frontiers in oncology*. 2021;10:604124-.

213. Surget S, Khoury MP, Bourdon JC. Uncovering the role of p53 splice variants in human malignancy: a clinical perspective. *OncoTargets and therapy*. 2013;7:57-68.
214. Hanel W, Moll UM. Links between mutant p53 and genomic instability. *J Cell Biochem*. 2012;113(2):433-9.
215. Cano A, Pérez-Moreno MA, Rodrigo I, Locascio A, Blanco MJ, del Barrio MG, et al. The transcription factor snail controls epithelial-mesenchymal transitions by repressing E-cadherin expression. *Nat Cell Biol*. 2000;2(2):76-83.
216. Casas E, Kim J, Bendesky A, Ohno-Machado L, Wolfe CJ, Yang J. Snail2 is an Essential Mediator of Twist1-Induced Epithelial Mesenchymal Transition and Metastasis. *Cancer Research*. 2011;71(1):245.
217. Lai W, Zhu W, Li X, Han Y, Wang Y, Leng Q, et al. GTSE1 promotes prostate cancer cell proliferation via the SP1/FOXM1 signaling pathway. *Lab Invest*. 2020.
218. Yang H, Salz T, Zajac-Kaye M, Liao D, Huang S, Qiu Y. Overexpression of histone deacetylases in cancer cells is controlled by interplay of transcription factors and epigenetic modulators. *The FASEB Journal*. 2014;28(10):4265-79.
219. Bayfield MA, Maraia RJ. Precursor-product discrimination by La protein during tRNA metabolism. *Nature structural & molecular biology*. 2009;16(4):430-7.
220. Farazi TA, Horlings HM, Ten Hoeve JJ, Mihailovic A, Halfwerk H, Morozov P, et al. MicroRNA sequence and expression analysis in breast tumors by deep sequencing. *Cancer Res*. 2011;71(13):4443-53.
221. Pickering BF, Yu D, Van Dyke MW. Nucleolin protein interacts with microprocessor complex to affect biogenesis of microRNAs 15a and 16. *J Biol Chem*. 2011;286(51):44095-103.
222. Stark JM, Pierce AJ, Oh J, Pastink A, Jasin M. Genetic Steps of Mammalian Homologous Repair with Distinct Mutagenic Consequences. *Molecular and Cellular Biology*. 2004;24(21):9305.
223. Pei D, Shu X, Gassama-Diagne A, Thiery JP. Mesenchymal–epithelial transition in development and reprogramming. *Nature Cell Biology*. 2019;21(1):44-53.
224. Wood WM, Etemad S, Yamamoto M, Goldhamer DJ. MyoD-expressing progenitors are essential for skeletal myogenesis and satellite cell development. *Dev Biol*. 2013;384(1):114-27.
225. Potts GK, McNally RM, Blanco R, You JS, Hebert AS, Westphall MS, et al. A map of the phosphoproteomic alterations that occur after a bout of maximal-intensity contractions. *J Physiol*. 2017;595(15):5209-26.
226. Goodman CA, Dietz JM, Jacobs BL, McNally RM, You J-S, Hornberger TA. Yes-Associated Protein is up-regulated by mechanical overload and is sufficient to induce skeletal muscle hypertrophy. *FEBS letters*. 2015;589(13):1491-7.
227. Goodman CA, Mabrey DM, Frey JW, Miu MH, Schmidt EK, Pierre P, et al. Novel insights into the regulation of skeletal muscle protein synthesis as revealed by a new nonradioactive in vivo technique. *FASEB journal : official publication of the Federation of American Societies for Experimental Biology*. 2011;25(3):1028-39.
228. Timpani CA, Goodman CA, Stathis CG, White JD, Mamchaoui K, Butler-Browne G, et al. Adenylosuccinic acid therapy ameliorates murine Duchenne Muscular Dystrophy. *Sci Rep*. 2020;10(1):1125.
229. Watt KI, Goodman CA, Hornberger TA, Gregorevic P. The Hippo Signaling Pathway in the Regulation of Skeletal Muscle Mass and Function. *Exerc Sport Sci Rev*. 2018;46(2):92-6.

230. AIHW. Breast cancer in Australia: An overview. Australian Institute of Health and Welfare; 2017.

231. World Cancer Day:

Breast cancer overtakes lung cancer as leading cause of cancer worldwide.

IARC showcases key research projects to address breast cancer [press release]. Lyon, France: IARC Communications 2021.

232. Neve RM, Chin K, Fridlyand J, Yeh J, Baehner FL, Fevr T, et al. A collection of breast cancer cell lines for the study of functionally distinct cancer subtypes. *Cancer Cell*. 2006;10.

233. Thaler S, Schmidt M, Robetawag S, Thiede G, Schad A, Sleeman JP. Proteasome inhibitors prevent bi-directional HER2/estrogen-receptor cross-talk leading to cell death in endocrine and lapatinib-resistant HER2+/ER+ breast cancer cells. *Oncotarget*. 2017;8(42):72281-301.

234. Anders CK, Carey LA. Biology, metastatic patterns, and treatment of patients with triple-negative breast cancer. *Clin Breast Cancer*. 2009;9 Suppl 2:S73-81.

235. Mani SA, Guo W, Liao MJ, Eaton EN, Ayyanan A, Zhou AY, et al. The epithelial-mesenchymal transition generates cells with properties of stem cells. *Cell*. 2008;133(4):704-15.

236. Morel AP, Lièvre M, Thomas C, Hinkal G, Ansieau S, Puisieux A. Generation of breast cancer stem cells through epithelial-mesenchymal transition. *PLoS One*. 2008;3(8):e2888.

237. Dilworth D, Gong F, Miller K, Nelson CJ. FKBP25 participates in DNA double-strand break repair (1). *Biochem Cell Biol*. 2019:1-8.

238. Kalluri R, Weinberg RA. The basics of epithelial-mesenchymal transition. *J Clin Invest*. 2009;119(6):1420-8.

239. Villarejo A, Cortés-Cabrera A, Molina-Ortiz P, Portillo F, Cano A. Differential role of Snail1 and Snail2 zinc fingers in E-cadherin repression and epithelial to mesenchymal transition. *The Journal of biological chemistry*. 2014;289(2):930-41.

240. Peinado H, Olmeda D, Cano A. Snail, Zeb and bHLH factors in tumour progression: an alliance against the epithelial phenotype? *Nature Reviews Cancer*. 2007;7(6):415-28.

241. Orford K, Orford CC, Byers SW. Exogenous expression of beta-catenin regulates contact inhibition, anchorage-independent growth, anoikis, and radiation-induced cell cycle arrest. *The Journal of cell biology*. 1999;146(4):855-68.

242. Goessling W, North TE, Loewer S, Lord AM, Lee S, Stoick-Cooper CL, et al. Genetic interaction of PGE2 and Wnt signaling regulates developmental specification of stem cells and regeneration. *Cell*. 2009;136(6):1136-47.

243. Poodineh J, Sirati-Sabet M, Rajabibazl M, Mohammadi-Yeganeh S. MiR-130a-3p blocks Wnt signaling cascade in the triple-negative breast cancer by targeting the key players at multiple points. *Heliyon*. 2020;6(11):e05434.

244. Thrasivoulou C, Millar M, Ahmed A. Activation of intracellular calcium by multiple Wnt ligands and translocation of  $\beta$ -catenin into the nucleus: a convergent model of Wnt/Ca<sup>2+</sup> and Wnt/ $\beta$ -catenin pathways. *J Biol Chem*. 2013;288(50):35651-9.

245. Stanisavljevic J, Porta-de-la-Riva M, Batlle R, de Herreros AG, Baulida J. The p65 subunit of NF- $\kappa$ B and PARP1 assist Snail1 in activating fibronectin transcription. *J Cell Sci*. 2011;124(Pt 24):4161-71.

246. Zhao Y, Yan Q, Long X, Chen X, Wang Y. Vimentin affects the mobility and invasiveness of prostate cancer cells. *Cell biochemistry and function*. 2008;26(5):571-7.
247. Vuoriluoto K, Haugen H, Kiviluoto S, Mpindi JP, Nevo J, Gjerdrum C, et al. Vimentin regulates EMT induction by Slug and oncogenic H-Ras and migration by governing Axl expression in breast cancer. *Oncogene*. 2011;30(12):1436-48.
248. Kast K, Link T, Friedrich K, Petzold A, Niedostatek A, Schoffer O, et al. Impact of breast cancer subtypes and patterns of metastasis on outcome. *Breast Cancer Res Treat*. 2015;150(3):621-9.
249. Scheel C, Weinberg RA. Phenotypic plasticity and epithelial-mesenchymal transitions in cancer and normal stem cells? *Int J Cancer*. 2011;129(10):2310-4.
250. Konen J, Summerbell E, Dwivedi B, Galior K, Hou Y, Rusnak L, et al. Image-guided genomics of phenotypically heterogeneous populations reveals vascular signalling during symbiotic collective cancer invasion. *Nat Commun*. 2017;8:15078.
251. Cheung KJ, Gabrielson E, Werb Z, Ewald AJ. Collective invasion in breast cancer requires a conserved basal epithelial program. *Cell*. 2013;155(7):1639-51.
252. Bryan BB, Schnitt SJ, Collins LC. Ductal carcinoma in situ with basal-like phenotype: a possible precursor to invasive basal-like breast cancer. *Mod Pathol*. 2006;19(5):617-21.
253. Peng J, Wang X, Ran L, Song J, Luo R, Wang Y. Hypoxia-Inducible Factor 1 $\alpha$  Regulates the Transforming Growth Factor  $\beta$ 1/SMAD Family Member 3 Pathway to Promote Breast Cancer Progression. *J Breast Cancer*. 2018;21(3):259-66.
254. Hong T, Watanabe K, Ta CH, Villarreal-Ponce A, Nie Q, Dai X. An *Ovol2-Zeb1* Mutual Inhibitory Circuit Governs Bidirectional and Multi-step Transition between Epithelial and Mesenchymal States. *PLOS Computational Biology*. 2015;11(11):e1004569.
255. Bocci F, Tripathi SC, Vilchez Mercedes SA, George JT, Casabar JP, Wong PK, et al. NRF2 activates a partial epithelial-mesenchymal transition and is maximally present in a hybrid epithelial/mesenchymal phenotype. *Integrative Biology*. 2019;11(6):251-63.
256. Mooney SM, Talebian V, Jolly MK, Jia D, Gromala M, Levine H, et al. The GRHL2/ZEB Feedback Loop—A Key Axis in the Regulation of EMT in Breast Cancer. *Journal of Cellular Biochemistry*. 2017;118(9):2559-70.
257. Bocci F, Jolly MK, Tripathi SC, Aguilar M, Hanash SM, Levine H, et al. Numb prevents a complete epithelial-mesenchymal transition by modulating Notch signalling. *Journal of the Royal Society, Interface*. 2017;14(136).
258. Gould R, Bassen DM, Chakrabarti A, Varner JD, Butcher J. Population Heterogeneity in the Epithelial to Mesenchymal Transition Is Controlled by NFAT and Phosphorylated Sp1. *PLoS Comput Biol*. 2016;12(12):e1005251.
259. Dong P, Tada M, Hamada J, Nakamura A, Moriuchi T, Sakuragi N. p53 dominant-negative mutant R273H promotes invasion and migration of human endometrial cancer HHUA cells. *Clin Exp Metastasis*. 2007;24(6):471-83.
260. Nguyen CH, Lang BJ, Chai RC, Vieusseux JL, Kouspou MM, Price JT. Heat-shock factor 1 both positively and negatively affects cellular clonogenic growth depending on p53 status. *Biochem J*. 2013;452(2):321-9.
261. Benvenuti S, Sartore-Bianchi A, Di Nicolantonio F, Zanon C, Moroni M, Veronese S, et al. Oncogenic activation of the RAS/RAF signaling pathway impairs the response of metastatic colorectal cancers to anti-epidermal growth factor receptor antibody therapies. *Cancer Res*. 2007;67(6):2643-8.

262. Gialeli C, Theocharis AD, Karamanos NK. Roles of matrix metalloproteinases in cancer progression and their pharmacological targeting. *FEBS J.* 2011;278(1):16-27.
263. John T. Price TT, Anurag Agarwal, Daniel Djakiew, and Erik W. Thompson. Epidermal Growth Factor Promotes MDA-MB-231 Breast Cancer Cell Migration through a Phosphatidylinositol 3'-Kinase and Phospholipase C-dependent Mechanism. *Cancer Research.* 1999;59:5475–8.
264. Davis FM, Kenny PA, Soo ET, van Denderen BJ, Thompson EW, Cabot PJ, et al. Remodeling of purinergic receptor-mediated Ca<sup>2+</sup> signaling as a consequence of EGF-induced epithelial-mesenchymal transition in breast cancer cells. *PLoS One.* 2011;6(8):e23464.
265. Davis FM, Azimi I, Faville RA, Peters AA, Jalink K, Putney JW, Jr., et al. Induction of epithelial-mesenchymal transition (EMT) in breast cancer cells is calcium signal dependent. *Oncogene.* 2014;33(18):2307-16.
266. Davis FM, Peters AA, Grice DM, Cabot PJ, Parat MO, Roberts-Thomson SJ, et al. Non-stimulated, agonist-stimulated and store-operated Ca<sup>2+</sup> influx in MDA-MB-468 breast cancer cells and the effect of EGF-induced EMT on calcium entry. *PLoS One.* 2012;7(5):e36923.
267. Kokkinos MI, Wafai R, Wong MK, Newgreen DF, Thompson EW, Waltham M. Vimentin and epithelial-mesenchymal transition in human breast cancer--observations in vitro and in vivo. *Cells Tissues Organs.* 2007;185(1-3):191-203.
268. Bonnomet A, Brysse A, Tachsidis A, Waltham M, Thompson EW, Polette M, et al. Epithelial-to-mesenchymal transitions and circulating tumor cells. *J Mammary Gland Biol Neoplasia.* 2010;15(2):261-73.
269. Bonnomet A, Syne L, Brysse A, Feyereisen E, Thompson EW, Noel A, et al. A dynamic in vivo model of epithelial-to-mesenchymal transitions in circulating tumor cells and metastases of breast cancer. *Oncogene.* 2012;31(33):3741-53.
270. Patel NA, Patel PS, Vora HH. Role of PRL-3, Snail, Cytokeratin and Vimentin expression in epithelial mesenchymal transition in breast carcinoma. *Breast Dis.* 2015;35(2):113-27.
271. Lombaerts M, van Wezel T, Philippo K, Dierssen JW, Zimmerman RM, Oosting J, et al. E-cadherin transcriptional downregulation by promoter methylation but not mutation is related to epithelial-to-mesenchymal transition in breast cancer cell lines. *Br J Cancer.* 2006;94(5):661-71.
272. Scimeca M, Antonacci C, Colombo D, Bonfiglio R, Buonomo OC, Bonanno E. Emerging prognostic markers related to mesenchymal characteristics of poorly differentiated breast cancers. *Tumour Biol.* 2016;37(4):5427-35.
273. Dilworth D, Gudavicius G, Xu X, Boyce AKJ, O'Sullivan C, Serpa JJ, et al. GFOLD. *Nucleic Acids Res.* 2018;46(5):2459-78.
274. Hernandez P, Tirnauer JS. Tumor suppressor interactions with microtubules: keeping cell polarity and cell division on track. *Dis Model Mech.* 2010;3(5-6):304-15.
275. Masliah G, Barraud P, Allain FH. RNA recognition by double-stranded RNA binding domains: a matter of shape and sequence. *Cell Mol Life Sci.* 2013;70(11):1875-95.
276. Li H, Zhang J, Tong JHM, Chan AWH, Yu J, Kang W, et al. Targeting the Oncogenic p53 Mutants in Colorectal Cancer and Other Solid Tumors. *Int J Mol Sci.* 2019;20(23).
277. Castellano E, Downward J. RAS Interaction with PI3K: More Than Just Another Effector Pathway. *Genes Cancer.* 2011;2(3):261-74.

278. Chang MT, Asthana S, Gao SP, Lee BH, Chapman JS, Kandoth C, et al. Identifying recurrent mutations in cancer reveals widespread lineage diversity and mutational specificity. *Nat Biotechnol.* 2016;34(2):155-63.
279. Prior IA, Lewis PD, Mattos C. A comprehensive survey of Ras mutations in cancer. *Cancer research.* 2012;72(10):2457-67.
280. Young A, Lou D, McCormick F. Oncogenic and wild-type Ras play divergent roles in the regulation of mitogen-activated protein kinase signaling. *Cancer Discov.* 2013;3(1):112-23.
281. Debnath J, Muthuswamy SK, Brugge JS. Morphogenesis and oncogenesis of MCF-10A mammary epithelial acini grown in three-dimensional basement membrane cultures. *Methods (San Diego, Calif).* 2003;30(3):256-68.
282. Oh H, Eliassen AH, Beck AH, Rosner B, Schnitt SJ, Collins LC, et al. Breast cancer risk factors in relation to estrogen receptor, progesterone receptor, insulin-like growth factor-1 receptor, and Ki67 expression in normal breast tissue. *NPJ Breast Cancer.* 2017;3:39.
283. Zhang X, Gureasko J, Shen K, Cole PA, Kuriyan J. An allosteric mechanism for activation of the kinase domain of epidermal growth factor receptor. *Cell.* 2006;125(6):1137-49.
284. McBryan J, Howlin J, Napoletano S, Martin F. Amphiregulin: role in mammary gland development and breast cancer. *J Mammary Gland Biol Neoplasia.* 2008;13(2):159-69.
285. Liu X, Wang P, Zhang C, Ma Z. Epidermal growth factor receptor (EGFR): A rising star in the era of precision medicine of lung cancer. *Oncotarget.* 2017;8(30):50209-20.
286. Jeong Y, Bae SY, You D, Jung SP, Choi HJ, Kim I, et al. EGFR is a Therapeutic Target in Hormone Receptor-Positive Breast Cancer. *Cellular physiology and biochemistry : international journal of experimental cellular physiology, biochemistry, and pharmacology.* 2019;53(5):805-19.
287. Ackland ML, Newgreen DF, Fridman M, Waltham MC, Arvanitis A, Minichiello J, et al. Epidermal Growth Factor-Induced Epithelio-Mesenchymal Transition in Human Breast Carcinoma Cells. *Laboratory Investigation.* 2003;83(3):435-48.
288. De Craene B, Berx G. Regulatory networks defining EMT during cancer initiation and progression. *Nat Rev Cancer.* 2013;13(2):97-110.
289. Diaz VM, Vinas-Castells R, Garcia de Herreros A. Regulation of the protein stability of EMT transcription factors. *Cell Adh Migr.* 2014;8(4):418-28.
290. Huang RY, Guilford P, Thiery JP. Early events in cell adhesion and polarity during epithelial-mesenchymal transition. *J Cell Sci.* 2012;125(Pt 19):4417-22.
291. Mathea S, Li S, Schierhorn A, Jahreis G, Schiene-Fischer C. Suppression of EGFR autophosphorylation by FKBP12. *Biochemistry.* 2011;50(50):10844-50.
292. Chen YG, Liu F, Massague J. Mechanism of TGFbeta receptor inhibition by FKBP12. *The EMBO journal.* 1997;16(13):3866-76.
293. Shin DW, Pan Z, Bandyopadhyay A, Bhat MB, Kim DH, Ma J. Ca(2+)-dependent interaction between FKBP12 and calcineurin regulates activity of the Ca(2+) release channel in skeletal muscle. *Biophysical journal.* 2002;83(5):2539-49.
294. Ghartey-Kwansah G, Li Z, Feng R, Wang L, Zhou X, Chen FZ, et al. Comparative analysis of FKBP family protein: evaluation, structure, and function in mammals and *Drosophila melanogaster*. *BMC developmental biology.* 2018;18(1):7-.
295. Lo HW, Hsu SC, Xia W, Cao X, Shih JY, Wei Y, et al. Epidermal growth factor receptor cooperates with signal transducer and activator of transcription 3 to induce

- epithelial-mesenchymal transition in cancer cells via up-regulation of TWIST gene expression. *Cancer Res.* 2007;67(19):9066-76.
296. Lopez E, Berna-Erro A, Salido GM, Rosado JA, Redondo PC. FKBP25 and FKBP38 regulate non-capacitative calcium entry through TRPC6. *Biochim Biophys Acta.* 2015;1853(10 Pt A):2684-96.
297. Lodish H BA, Zipursky SL, et al. *Microtubule Dynamics and Motor Proteins during Mitosis.* Molecular Cell Biology. New York, USA: W. H. Freeman and Company; 2000.
298. Hanahan D, Weinberg RA. Hallmarks of cancer: the next generation. *Cell.* 2011;144(5):646-74.
299. Gros J, Manceau M, Thome V, Marcelle C. A common somitic origin for embryonic muscle progenitors and satellite cells. *Nature.* 2005;435(7044):954-8.
300. Li J, Wang Y, Wang Y, Yan Y, Tong H, Li S. Fibronectin type III domain containing four promotes differentiation of C2C12 through the Wnt/ $\beta$ -catenin signaling pathway. *FASEB journal : official publication of the Federation of American Societies for Experimental Biology.* 2020.
301. Comai G, Tajbakhsh S. Chapter One - Molecular and Cellular Regulation of Skeletal Myogenesis. In: Taneja R, editor. *Current Topics in Developmental Biology.* 110: Academic Press; 2014. p. 1-73.
302. Liu X, Wang Y, Zhao S, Li X. Fibroblast Growth Factor 21 Promotes C2C12 Cells Myogenic Differentiation by Enhancing Cell Cycle Exit. *Biomed Res Int.* 2017;2017:1648715.
303. Daneshvar N, Tatsumi R, Peeler J, Anderson JE. Premature satellite cell activation before injury accelerates myogenesis and disrupts neuromuscular junction maturation in regenerating muscle. *Am J Physiol Cell Physiol.* 2020.
304. Relaix F, Rocancourt D, Mansouri A, Buckingham M. A Pax3/Pax7-dependent population of skeletal muscle progenitor cells. *Nature.* 2005;435(7044):948-53.
305. Seale P, Poleskaya A, Rudnicki MA. Adult Stem Cell Specification by Wnt Signaling in Muscle Regeneration. *Cell Cycle.* 2003;2(5):417-8.
306. Arndt CA, Rose PS, Folpe AL, Laack NN. Common musculoskeletal tumors of childhood and adolescence. *Mayo Clinic proceedings.* 2012;87(5):475-87.
307. Newton WA, Jr., Gehan EA, Webber BL, Marsden HB, van Unnik AJ, Hamoudi AB, et al. Classification of rhabdomyosarcomas and related sarcomas. Pathologic aspects and proposal for a new classification--an Intergroup Rhabdomyosarcoma Study. *Cancer.* 1995;76(6):1073-85.
308. Barr FG, Galili N, Holick J, Biegel JA, Rovera G, Emanuel BS. Rearrangement of the PAX3 paired box gene in the paediatric solid tumour alveolar rhabdomyosarcoma. *Nat Genet.* 1993;3(2):113-7.
309. Davis RJ, D'Cruz CM, Lovell MA, Biegel JA, Barr FG. Fusion of PAX7 to FKHR by the Variant t(1;13)(p36;q14) Translocation in Alveolar Rhabdomyosarcoma. *Cancer Research.* 1994;54(11):2869-72.
310. Gryder BE, Yohe ME, Chou H-C, Zhang X, Marques J, Wachtel M, et al. PAX3-FOXO1 Establishes Myogenic Super Enhancers and Confers BET Bromodomain Vulnerability. *Cancer Discovery.* 2017;7(8):884.
311. Seki M, Nishimura R, Yoshida K, Shimamura T, Shiraishi Y, Sato Y, et al. Integrated genetic and epigenetic analysis defines novel molecular subgroups in rhabdomyosarcoma. *Nature Communications.* 2015;6(1):7557.
312. Martinelli S, McDowell HP, Vigne SD, Kokai G, Uccini S, Tartaglia M, et al. RAS signaling dysregulation in human embryonal Rhabdomyosarcoma. *Genes, chromosomes & cancer.* 2009;48(11):975-82.

313. Zhang M, Linardic CM, Kirsch DG. RAS and ROS in rhabdomyosarcoma. *Cancer cell*. 2013;24(6):689-91.
314. Yohe ME, Gryder BE, Shern JF, Song YK, Chou H-C, Sindiri S, et al. MEK inhibition induces MYOG and remodels super-enhancers in RAS-driven rhabdomyosarcoma. *Science translational medicine*. 2018;10(448):eaan4470.
315. Schultz E. Satellite Cell Proliferative Compartments in Growing Skeletal Muscles. *Developmental Biology*. 1996;175(1):84-94.
316. Mauro A. SATELLITE CELL OF SKELETAL MUSCLE FIBERS. *The Journal of Biophysical and Biochemical Cytology*. 1961;9(2):493-5.
317. Dumont NA, Bentzinger CF, Sincennes MC, Rudnicki MA. Satellite Cells and Skeletal Muscle Regeneration. *Comprehensive Physiology*. 2015;5(3):1027-59.
318. Halevy O, Piestun Y, Allouh MZ, Rosser BWC, Rinkevich Y, Reshef R, et al. Pattern of Pax7 expression during myogenesis in the posthatch chicken establishes a model for satellite cell differentiation and renewal. *Developmental Dynamics*. 2004;231(3):489-502.
319. Shefer G, Van de Mark DP, Richardson JB, Yablonka-Reuveni Z. Satellite-cell pool size does matter: defining the myogenic potency of aging skeletal muscle. *Dev Biol*. 2006;294(1):50-66.
320. Mourkioti F, Rosenthal N. IGF-1, inflammation and stem cells: interactions during muscle regeneration. *Trends in immunology*. 2005;26(10):535-42.
321. Alfaro LA, Dick SA, Siegel AL, Anonuevo AS, McNagny KM, Megeney LA, et al. CD34 promotes satellite cell motility and entry into proliferation to facilitate efficient skeletal muscle regeneration. *Stem Cells*. 2011;29(12):2030-41.
322. Mylona E, Jones KA, Mills ST, Pavlath GK. CD44 regulates myoblast migration and differentiation. *Journal of cellular physiology*. 2006;209(2):314-21.
323. Kaar JL, Li Y, Blair HC, Asche G, Koepsel RR, Huard J, et al. Matrix metalloproteinase-1 treatment of muscle fibrosis. *Acta biomaterialia*. 2008;4(5):1411-20.
324. Kherif S, Lafuma C, Dehaupas M, Lachkar S, Fournier JG, Verdière-Sahuqué M, et al. Expression of matrix metalloproteinases 2 and 9 in regenerating skeletal muscle: a study in experimentally injured and mdx muscles. *Dev Biol*. 1999;205(1):158-70.
325. Tidball JG, Villalta SA. Regulatory interactions between muscle and the immune system during muscle regeneration. *American journal of physiology Regulatory, integrative and comparative physiology*. 2010;298(5):R1173-87.
326. Yablonka-Reuveni Z, Rivera AJ. Influence of PDGF-BB on proliferation and transition through the MyoD-myogenin-MEF2A expression program during myogenesis in mouse C2 myoblasts. *Growth Factors*. 1997;15(1):1-27.
327. Kaufmann U, Kirsch J, Irintchev A, Wernig A, Starzinski-Powitz A. The M-cadherin catenin complex interacts with microtubules in skeletal muscle cells: implications for the fusion of myoblasts. *Journal of Cell Science*. 1999;112(1):55.
328. Gundersen GG, Worman HJ. Nuclear positioning. *Cell*. 2013;152(6):1376-89.
329. Metzger T, Gache V, Xu M, Cadot B, Folker ES, Richardson BE, et al. MAP and kinesin-dependent nuclear positioning is required for skeletal muscle function. *Nature*. 2012;484(7392):120-4.
330. Holy TE, Dogterom M, Yurke B, Leibler S. Assembly and positioning of microtubule asters in microfabricated chambers. *Proceedings of the National Academy of Sciences*. 1997;94(12):6228-31.

331. Cadot B, Gache V, Vasyutina E, Falcone S, Birchmeier C, Gomes ER. Nuclear movement during myotube formation is microtubule and dynein dependent and is regulated by Cdc42, Par6 and Par3. *EMBO reports*. 2012;13(8):741-9.
332. Boudriau S, Cote CH, Vincent M, Houle P, Tremblay RR, Rogers PA. Remodeling of the cytoskeletal lattice in denervated skeletal muscle. *Muscle Nerve*. 1996;19(11):1383-90.
333. Khairallah RJ, Shi G, Sbrana F, Prosser BL, Borroto C, Mazaitis MJ, et al. Microtubules underlie dysfunction in duchenne muscular dystrophy. *Science signaling*. 2012;5(236):ra56.
334. Sébastien M, Giannesini B, Aubin P, Brocard J, Chivet M, Pietrangelo L, et al. Deletion of the microtubule-associated protein 6 (MAP6) results in skeletal muscle dysfunction. *Skeletal Muscle*. 2018;8(1):30.
335. Wilson MH, Holzbaur ELF. Opposing microtubule motors drive robust nuclear dynamics in developing muscle cells. *Journal of Cell Science*. 2012;125(17):4158.
336. Koutalios D, Koutsoulidou A, Mastrogiannopoulos NP, Furling D, Phylactou LA. MyoD transcription factor induces myogenesis by inhibiting Twist-1 through miR-206. *J Cell Sci*. 2015;128(19):3631-45.
337. Pavlidou T, Rosina M, Fuoco C, Gerini G, Gargioli C, Castagnoli L, et al. Regulation of myoblast differentiation by metabolic perturbations induced by metformin. *PLoS One*. 2017;12(8):e0182475.
338. You JS, McNally RM, Jacobs BL, Privett RE, Gundermann DM, Lin KH, et al. The role of raptor in the mechanical load-induced regulation of mTOR signaling, protein synthesis, and skeletal muscle hypertrophy. *FASEB journal : official publication of the Federation of American Societies for Experimental Biology*. 2019;33(3):4021-34.
339. Hoffman EP, Brown RH, Jr., Kunkel LM. Dystrophin: the protein product of the Duchenne muscular dystrophy locus. *Cell*. 1987;51(6):919-28.
340. Pons F, Augier N, Heilig R, Leger J, Mornet D, Leger JJ. Isolated dystrophin molecules as seen by electron microscopy. *Proc Natl Acad Sci U S A*. 1990;87(20):7851-5.
341. Murphy S, Ohlendieck K. Mass spectrometric identification of dystrophin, the protein product of the Duchenne muscular dystrophy gene, in distinct muscle surface membranes. *Int J Mol Med*. 2017;40(4):1078-88.
342. Hughes KJ, Rodriguez A, Flatt KM, Ray S, Schuler A, Rodemoyer B, et al. Physical exertion exacerbates decline in the musculature of an animal model of Duchenne muscular dystrophy. *Proc Natl Acad Sci U S A*. 2019;116(9):3508-17.
343. Gaglianone RB, Bloise FF, Ortiga-Carvalho TM, Quirico-Santos T, Costa ML, Mermelstein C. Comparative study of calcium and calcium-related enzymes with differentiation markers in different ages and muscle types in mdx mice. *Histology and histopathology*. 2020;35(2):203-16.
344. Hori YS, Kuno A, Hosoda R, Tanno M, Miura T, Shimamoto K, et al. Resveratrol ameliorates muscular pathology in the dystrophic mdx mouse, a model for Duchenne muscular dystrophy. *The Journal of pharmacology and experimental therapeutics*. 2011;338(3):784-94.
345. Radley-Crabb HG, Marini JC, Sosa HA, Castillo LI, Grounds MD, Fiorotto ML. Dystroptology increases energy expenditure and protein turnover in the mdx mouse model of duchenne muscular dystrophy. *PLoS One*. 2014;9(2):e89277.
346. Grounds MD, Radley HG, Lynch GS, Nagaraju K, De Luca A. Towards developing standard operating procedures for pre-clinical testing in the mdx mouse model of Duchenne muscular dystrophy. *Neurobiol Dis*. 2008;31(1):1-19.

347. Evans NP, Misyak SA, Robertson JL, Bassaganya-Riera J, Grange RW. Dysregulated intracellular signaling and inflammatory gene expression during initial disease onset in Duchenne muscular dystrophy. *American journal of physical medicine & rehabilitation*. 2009;88(6):502-22.
348. Cros D, Harnden P, Pellissier JF, Serratrice G. Muscle hypertrophy in Duchenne muscular dystrophy. A pathological and morphometric study. *Journal of neurology*. 1989;236(1):43-7.
349. Gillis JM. Understanding dystrophinopathies: an inventory of the structural and functional consequences of the absence of dystrophin in muscles of the mdx mouse. *Journal of muscle research and cell motility*. 1999;20(7):605-25.
350. Randazzo D, Khalique U, Belanto JJ, Kenea A, Talsness DM, Olthoff JT, et al. Persistent upregulation of the  $\beta$ -tubulin tubb6, linked to muscle regeneration, is a source of microtubule disorganization in dystrophic muscle. *Hum Mol Genet*. 2019;28(7):1117-35.
351. Liu H, Thompson LV. Skeletal muscle denervation investigations: selecting an experimental control wisely. *Am J Physiol Cell Physiol*. 2019;316(3):C456-c61.
352. Midrio M. The denervated muscle: facts and hypotheses. A historical review. *Eur J Appl Physiol*. 2006;98(1):1-21.
353. Choi RH, McConahay A, Silvestre JG, Moriscot AS, Carson JA, Koh HJ. TRB3 regulates skeletal muscle mass in food deprivation-induced atrophy. *FASEB journal : official publication of the Federation of American Societies for Experimental Biology*. 2019;33(4):5654-66.
354. Oddoux S, Zaal KJ, Tate V, Kenea A, Nandkeolyar SA, Reid E, et al. Microtubules that form the stationary lattice of muscle fibers are dynamic and nucleated at Golgi elements. *J Cell Biol*. 2013;203(2):205-13.
355. Zhang T, Zaal KJ, Sheridan J, Mehta A, Gundersen GG, Ralston E. Microtubule plus-end binding protein EB1 is necessary for muscle cell differentiation, elongation and fusion. *J Cell Sci*. 2009;122(Pt 9):1401-9.
356. Mian I, Pierre-Louis WS, Dole N, Gilberti RM, Dodge-Kafka K, Tirnauer JS. LKB1 destabilizes microtubules in myoblasts and contributes to myoblast differentiation. *PLoS One*. 2012;7(2):e31583.
357. Subramaniam S, Sreenivas P, Cheedipudi S, Reddy VR, Shashidhara LS, Chilukoti RK, et al. Distinct transcriptional networks in quiescent myoblasts: a role for Wnt signaling in reversible vs. irreversible arrest. *PLoS One*. 2014;8(6):e65097.
358. Yamada S, Taketomi T, Yoshimura A. Model analysis of difference between EGF pathway and FGF pathway. *Biochem Biophys Res Commun*. 2004;314(4):1113-20.
359. Garg A, Hazra JP, Sannigrahi MK, Rakshit S, Sinha S. Variable Mutations at the p53-R273 Oncogenic Hotspot Position Leads to Altered Properties. *Biophysical journal*. 2020;118(3):720-8.
360. Cam H, Griesmann H, Beitzinger M, Hofmann L, Beinoraviciute-Kellner R, Sauer M, et al. p53 family members in myogenic differentiation and rhabdomyosarcoma development. *Cancer Cell*. 2006;10(4):281-93.
361. Murach KA, White SH, Wen Y, Ho A, Dupont-Versteegden EE, McCarthy JJ, et al. Differential requirement for satellite cells during overload-induced muscle hypertrophy in growing versus mature mice. *Skelet Muscle*. 2017;7(1):14.
362. Coleman AK, Joca HC, Shi G, Lederer WJ, Ward CW. Tubulin acetylation increases cytoskeletal stiffness to regulate mechanotransduction in striated muscle. *bioRxiv*. 2020:2020.06.10.144931.

363. McGeachie JK, Grounds MD, Partridge TA, Morgan JE. Age-related changes in replication of myogenic cells in mdx mice: quantitative autoradiographic studies. *Journal of the neurological sciences*. 1993;119(2):169-79.
364. Porter JD, Khanna S, Kaminski HJ, Rao JS, Merriam AP, Richmonds CR, et al. A chronic inflammatory response dominates the skeletal muscle molecular signature in dystrophin-deficient mdx mice. *Human Molecular Genetics*. 2002;11(3):263-72.
365. Ehmsen J, Poon E, Davies K. The dystrophin-associated protein complex. *J Cell Sci*. 2002;115(Pt 14):2801-3.
366. Jung D, Yang B, Meyer J, Chamberlain JS, Campbell KP. Identification and characterization of the dystrophin anchoring site on beta-dystroglycan. *J Biol Chem*. 1995;270(45):27305-10.
367. Kumar A, Khandelwal N, Malya R, Reid MB, Boriek AM. Loss of dystrophin causes aberrant mechanotransduction in skeletal muscle fibers. *FASEB journal : official publication of the Federation of American Societies for Experimental Biology*. 2004;18(1):102-13.
368. Yeung EW, Whitehead NP, Suchyna TM, Gottlieb PA, Sachs F, Allen DG. Effects of stretch-activated channel blockers on  $[Ca^{2+}]_i$  and muscle damage in the mdx mouse. *J Physiol*. 2005;562(Pt 2):367-80.
369. Lindsay A, Baumann CW, Rebbeck RT, Yuen SL, Southern WM, Hodges JS, et al. Mechanical factors tune the sensitivity of mdx muscle to eccentric strength loss and its protection by antioxidant and calcium modulators. *Skeletal Muscle*. 2020;10(1):3.
370. Nelson DM, Lindsay A, Judge LM, Duan D, Chamberlain JS, Lowe DA, et al. Variable rescue of microtubule and physiological phenotypes in mdx muscle expressing different miniaturized dystrophins. *Hum Mol Genet*. 2018;27(12):2090-100.
371. Goldspink DF. The effects of denervation on protein turnover of the soleus and extensor digitorum longus muscles of adult mice. *Comparative biochemistry and physiology B, Comparative biochemistry*. 1978;61(1):37-41.
372. Magnusson C, Svensson A, Christerson U, Tagerud S. Denervation-induced alterations in gene expression in mouse skeletal muscle. *The European journal of neuroscience*. 2005;21(2):577-80.
373. Baumann CW, Liu HM, Thompson LV. Denervation-Induced Activation of the Ubiquitin-Proteasome System Reduces Skeletal Muscle Quantity Not Quality. *PLoS One*. 2016;11(8):e0160839.
374. Ralston E, Lu Z, Ploug T. The organization of the Golgi complex and microtubules in skeletal muscle is fiber type-dependent. *The Journal of neuroscience : the official journal of the Society for Neuroscience*. 1999;19(24):10694-705.
375. Bodine SC, Stitt TN, Gonzalez M, Kline WO, Stover GL, Bauerlein R, et al. Akt/mTOR pathway is a crucial regulator of skeletal muscle hypertrophy and can prevent muscle atrophy in vivo. *Nat Cell Biol*. 2001;3(11):1014-9.
376. Brocca L, Toniolo L, Reggiani C, Bottinelli R, Sandri M, Pellegrino MA. FoxO-dependent atrogenes vary among catabolic conditions and play a key role in muscle atrophy induced by hindlimb suspension. *J Physiol*. 2017;595(4):1143-58.
377. Foster DA, Yellen P, Xu L, Saqcena M. Regulation of G1 Cell Cycle Progression: Distinguishing the Restriction Point from a Nutrient-Sensing Cell Growth Checkpoint(s). *Genes & cancer*. 2010;1(11):1124-31.

378. Bertoli C, Skotheim JM, de Bruin RAM. Control of cell cycle transcription during G1 and S phases. *Nature Reviews Molecular Cell Biology*. 2013;14(8):518-28.
379. Wang X, Simpson ER, Brown KA. p53: Protection against Tumor Growth beyond Effects on Cell Cycle and Apoptosis. *Cancer Research*. 2015;75(23):5001.
380. Feitelson MA, Arzumanyan A, Kulathinal RJ, Blain SW, Holcombe RF, Mahajna J, et al. Sustained proliferation in cancer: Mechanisms and novel therapeutic targets. *Seminars in cancer biology*. 2015;35 Suppl(Suppl):S25-S54.
381. Pardee AB. A restriction point for control of normal animal cell proliferation. *Proceedings of the National Academy of Sciences of the United States of America*. 1974;71(4):1286-90.
382. Guo K, Wang J, Andrés V, Smith RC, Walsh K. MyoD-induced expression of p21 inhibits cyclin-dependent kinase activity upon myocyte terminal differentiation. *Molecular and cellular biology*. 1995;15(7):3823-9.
383. Mastroiannopoulos NP, Nicolaou P, Anayasa M, Uney JB, Phylactou LA. Down-regulation of myogenin can reverse terminal muscle cell differentiation. *PLoS One*. 2012;7(1):e29896.
384. Zhang JM, Wei Q, Zhao X, Paterson BM. Coupling of the cell cycle and myogenesis through the cyclin D1-dependent interaction of MyoD with cdk4. *The EMBO journal*. 1999;18(4):926-33.
385. Friedl P, Wolf K. Proteolytic interstitial cell migration: a five-step process. *Cancer Metastasis Rev*. 2009;28(1-2):129-35.
386. Sheetz MP, Felsenfeld D, Galbraith CG, Choquet D. Cell migration as a five-step cycle. *Biochemical Society symposium*. 1999;65:233-43.
387. Keith Burridge CET, and Lewis H. Romerw. Tyrosine phosphorylation of paxillin and pp125FAK accompanies cell adhesion to extracellular matrix: a role in cytoskeletal assembly. *Journal of Cell Biology*. 1992;119(4):893-903.
388. Yang H, Ganguly A, Cabral F. Inhibition of cell migration and cell division correlates with distinct effects of microtubule inhibiting drugs. *J Biol Chem*. 2010;285(42):32242-50.
389. Zhu X, Ohtsubo M, Böhmer RM, Roberts JM, Assoian RK. Adhesion-dependent cell cycle progression linked to the expression of cyclin D1, activation of cyclin E-cdk2, and phosphorylation of the retinoblastoma protein. *J Cell Biol*. 1996;133(2):391-403.
390. Symington BE. Fibronectin receptor modulates cyclin-dependent kinase activity. *J Biol Chem*. 1992;267(36):25744-7.
391. Mori S, Chang JT, Andrechek ER, Matsumura N, Baba T, Yao G, et al. Anchorage-independent cell growth signature identifies tumors with metastatic potential. *Oncogene*. 2009;28(31):2796-805.
392. Kawada M, Yamagoe S, Murakami Y, Suzuki K, Mizuno S, Uehara Y. Induction of p27Kip1 degradation and anchorage independence by Ras through the MAP kinase signaling pathway. *Oncogene*. 1997;15(6):629-37.
393. Radeva G, Petrocelli T, Behrend E, Leung-Hagesteijn C, Filmus J, Slingerland J, et al. Overexpression of the integrin-linked kinase promotes anchorage-independent cell cycle progression. *J Biol Chem*. 1997;272(21):13937-44.
394. Holy TE, Leibler S. Dynamic instability of microtubules as an efficient way to search in space. *Proc Natl Acad Sci U S A*. 1994;91(12):5682-5.
395. Poruchynsky MS, Komlodi-Pasztor E, Trostel S, Wilkerson J, Regairaz M, Pommier Y, et al. Microtubule-targeting agents augment the toxicity of DNA-

damaging agents by disrupting intracellular trafficking of DNA repair proteins. *Proc Natl Acad Sci U S A*. 2015;112(5):1571-6.

396. Laprise P, Lau KM, Harris KP, Silva-Gagliardi NF, Paul SM, Beronja S, et al. Yurt, Coracle, Neurexin IV and the Na<sup>+</sup>,K<sup>+</sup>-ATPase form a novel group of epithelial polarity proteins. *Nature*. 2009;459(7250):1141-5.

397. Wright WE, Sassoon DA, Lin VK. Myogenin, a factor regulating myogenesis, has a domain homologous to MyoD. *Cell*. 1989;56(4):607-17.

398. Braun T, Buschhausen-Denker G, Bober E, Tannich E, Arnold HH. A novel human muscle factor related to but distinct from MyoD1 induces myogenic conversion in 10T1/2 fibroblasts. *The EMBO journal*. 1989;8(3):701-9.

399. Rhodes SJ, Konieczny SF. Identification of MRF4: a new member of the muscle regulatory factor gene family. *Genes Dev*. 1989;3(12b):2050-61.

400. Novitsch BG, Mulligan GJ, Jacks T, Lassar AB. Skeletal muscle cells lacking the retinoblastoma protein display defects in muscle gene expression and accumulate in S and G2 phases of the cell cycle. *J Cell Biol*. 1996;135(2):441-56.

401. Reynaud EG, Leibovitch MP, Tintignac LA, Pospel K, Guillier M, Leibovitch SA. Stabilization of MyoD by direct binding to p57(Kip2). *J Biol Chem*. 2000;275(25):18767-76.

402. Gu W, Schneider JW, Condorelli G, Kaushal S, Mahdavi V, Nadal-Ginard B. Interaction of myogenic factors and the retinoblastoma protein mediates muscle cell commitment and differentiation. *Cell*. 1993;72(3):309-24.

403. Kerr JP, Robison P, Shi G, Bogush AI, Kempema AM, Hexum JK, et al. Detyrosinated microtubules modulate mechanotransduction in heart and skeletal muscle. *Nature Communications*. 2015;6:8526.

404. Zhou M, Diwu Z, Panchuk-Voloshina N, Haugland RP. A stable nonfluorescent derivative of resorufin for the fluorometric determination of trace hydrogen peroxide: applications in detecting the activity of phagocyte NADPH oxidase and other oxidases. *Analytical biochemistry*. 1997;253(2):162-8.

405. Iijima M, Devreotes P. Tumor suppressor PTEN mediates sensing of chemoattractant gradients. *Cell*. 2002;109(5):599-610.

406. Roussos ET, Condeelis JS, Patsialou A. Chemotaxis in cancer. *Nature reviews Cancer*. 2011;11(8):573-87.

407. Kouspou MM, Price JT. Analysis of cellular migration using a two-chamber methodology. *Methods in molecular biology (Clifton, NJ)*. 2011;787:303-17.

408. Goetsch KP, Niesler CU. Optimization of the scratch assay for in vitro skeletal muscle wound healing analysis. *Analytical biochemistry*. 2011;411(1):158-60.

409. Grada A, Otero-Vinas M, Prieto-Castrillo F, Obagi Z, Falanga V. Research Techniques Made Simple: Analysis of Collective Cell Migration Using the Wound Healing Assay. *Journal of Investigative Dermatology*. 2017;137(2):e11-e6.

410. Ridley AJ, Schwartz MA, Burridge K, Firtel RA, Ginsberg MH, Borisy G, et al. Cell migration: integrating signals from front to back. *Science*. 2003;302(5651):1704-9.

411. Giampieri S, Manning C, Hooper S, Jones L, Hill CS, Sahai E. Localized and reversible TGFbeta signalling switches breast cancer cells from cohesive to single cell motility. *Nat Cell Biol*. 2009;11(11):1287-96.

412. Price JT, Thompson EW. Models for studying cellular invasion of basement membranes. *Methods in molecular biology (Clifton, NJ)*. 1999;129:231-49.

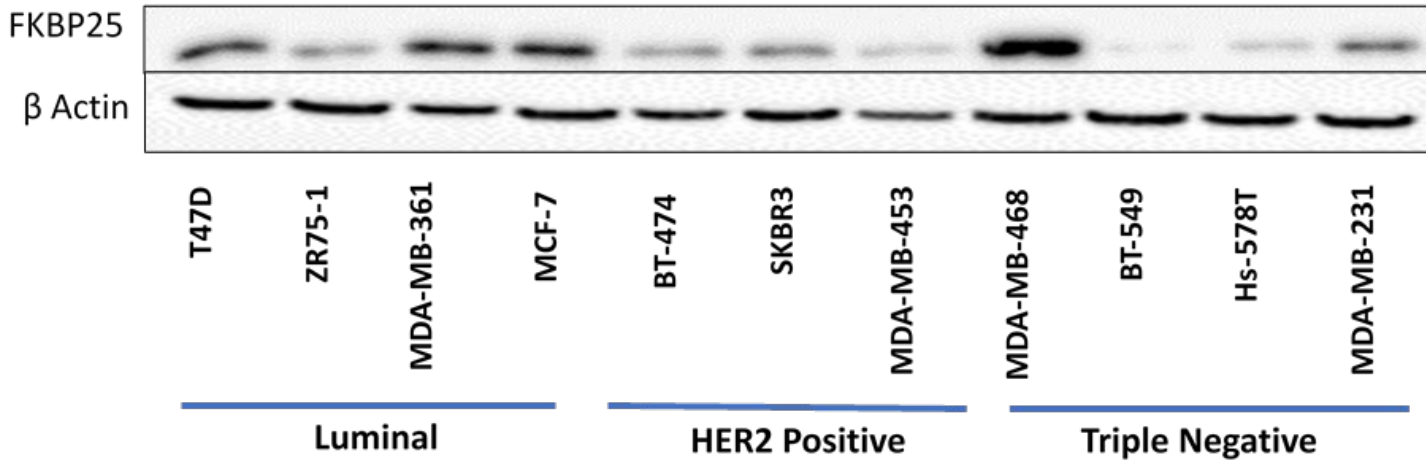
413. Baskaran JP, Weldy A, Guarin J, Munoz G, Shpilker PH, Kotlik M, et al. Cell shape, and not 2D migration, predicts extracellular matrix-driven 3D cell invasion in breast cancer. *APL Bioeng*. 2020;4(2):026105.

414. Murugan AK, Grieco M, Tsuchida N. RAS mutations in human cancers: Roles in precision medicine. *Semin Cancer Biol.* 2019;59:23-35.
415. Chambard JC, Lefloch R, Pouysségur J, Lenormand P. ERK implication in cell cycle regulation. *Biochim Biophys Acta.* 2007;1773(8):1299-310.
416. Berg M, Soreide K. EGFR and downstream genetic alterations in KRAS/BRAF and PI3K/AKT pathways in colorectal cancer: implications for targeted therapy. *Discovery medicine.* 2012;14(76):207-14.
417. Eshun-Wilson L, Zhang R, Portran D, Nachury MV, Toso DB, Löhr T, et al. Effects of  $\alpha$ -tubulin acetylation on microtubule structure and stability. *Proc Natl Acad Sci U S A.* 2019;116(21):10366-71.
418. Nieuwenhuis J, Brummelkamp TR. The Tubulin Detyrosination Cycle: Function and Enzymes. *Trends Cell Biol.* 2019;29(1):80-92.
419. Manna T, Thrower D, Miller HP, Curmi P, Wilson L. Stathmin Strongly Increases the Minus End Catastrophe Frequency and Induces Rapid Treadmilling of Bovine Brain Microtubules at Steady State in Vitro\*. *Journal of Biological Chemistry.* 2006;281(4):2071-8.
420. Di Paolo G, Antonsson B, Kassel D, Riederer BM, Grenningloh G. Phosphorylation regulates the microtubule-destabilizing activity of stathmin and its interaction with tubulin. *FEBS Letters.* 1997;416(2):149-52.
421. Tirnauer JS, Bierer BE. EB1 proteins regulate microtubule dynamics, cell polarity, and chromosome stability. *J Cell Biol.* 2000;149(4):761-6.
422. Justus CR, Leffler N, Ruiz-Echevarria M, Yang LV. In vitro cell migration and invasion assays. *Journal of visualized experiments : JoVE.* 2014(88):51046.
423. De Pascalis C, Etienne-Manneville S. Single and collective cell migration: the mechanics of adhesions. *Mol Biol Cell.* 2017;28(14):1833-46.
424. Gordon LA, Mulligan KT, Maxwell-Jones H, Adams M, Walker RA, Jones JL. Breast cell invasive potential relates to the myoepithelial phenotype. *International Journal of Cancer.* 2003;106(1):8-16.
425. Vicente-Manzanares M, Webb DJ, Horwitz AR. Cell migration at a glance. *Journal of Cell Science.* 2005;118(21):4917.
426. Carstens C-P, Krämer A, Fahl WE. Adhesion-Dependent Control of Cyclin E/cdk2 Activity and Cell Cycle Progression in Normal Cells but Not in Ha-rasTransformed NRK Cells. *Experimental Cell Research.* 1996;229(1):86-92.
427. Benecke BJ, Ben-Ze'ev A, Penman S. The control of mRNA production, translation and turnover in suspended and reattached anchorage-dependent fibroblasts. *Cell.* 1978;14(4):931-9.
428. Freedman VH, Shin SI. Cellular tumorigenicity in nude mice: correlation with cell growth in semi-solid medium. *Cell.* 1974;3(4):355-9.
429. Gassmann P, Haier J. The tumor cell-host organ interface in the early onset of metastatic organ colonisation. *Clin Exp Metastasis.* 2008;25(2):171-81.
430. Guo CS, Degnin C, Fiddler TA, Stauffer D, Thayer MJ. Regulation of MyoD activity and muscle cell differentiation by MDM2, pRb, and Sp1. *J Biol Chem.* 2003;278(25):22615-22.
431. Lee H, Hong Y, Kong G, Lee DH, Kim M, Tran Q, et al. Yin Yang 1 is required for PHD finger protein 20-mediated myogenic differentiation in vitro and in vivo. *Cell Death Differ.* 2020.
432. Zhu S, Goldschmidt-Clermont PJ, Dong C. Transforming growth factor-beta-induced inhibition of myogenesis is mediated through Smad pathway and is modulated by microtubule dynamic stability. *Circ Res.* 2004;94(5):617-25.

433. Smith BN, Burton LJ, Henderson V, Randle DD, Morton DJ, Smith BA, et al. Snail promotes epithelial mesenchymal transition in breast cancer cells in part via activation of nuclear ERK2. *PLoS one*. 2014;9(8):e104987-e.
434. Savagner P, Yamada KM, Thiery JP. The zinc-finger protein slug causes desmosome dissociation, an initial and necessary step for growth factor-induced epithelial-mesenchymal transition. *The Journal of cell biology*. 1997;137(6):1403-19.
435. Boyer B, Tucker GC, Vallés AM, Franke WW, Thiery JP. Rearrangements of desmosomal and cytoskeletal proteins during the transition from epithelial to fibroblastoid organization in cultured rat bladder carcinoma cells. *The Journal of cell biology*. 1989;109(4 Pt 1):1495-509.
436. Abhold EL, Kiang A, Rahimy E, Kuo SZ, Wang-Rodriguez J, Lopez JP, et al. EGFR kinase promotes acquisition of stem cell-like properties: a potential therapeutic target in head and neck squamous cell carcinoma stem cells. *PLoS One*. 2012;7(2):e32459.
437. Ardito CM, Grüner BM, Takeuchi KK, Lubeseder-Martellato C, Teichmann N, Mazur PK, et al. EGF receptor is required for KRAS-induced pancreatic tumorigenesis. *Cancer Cell*. 2012;22(3):304-17.
438. Nicholson KM, Anderson NG. The protein kinase B/Akt signalling pathway in human malignancy. *Cellular Signalling*. 2002;14(5):381-95.
439. Douziech N, Calvo E, Lainé J, Morisset J. Activation of MAP Kinases in Growth Responsive Pancreatic Cancer Cells. *Cellular Signalling*. 1999;11(8):591-602.
440. Perugini RA, McDade TP, Vittimberga FJ, Jr., Callery MP. Pancreatic cancer cell proliferation is phosphatidylinositol 3-kinase dependent. *The Journal of surgical research*. 2000;90(1):39-44.
441. Wang W, Abbruzzese JL, Evans DB, Larry L, Cleary KR, Chiao PJ. The nuclear factor-kappa B RelA transcription factor is constitutively activated in human pancreatic adenocarcinoma cells. *Clin Cancer Res*. 1999;5(1):119-27.
442. del Peso L, González-García M, Page C, Herrera R, Nuñez G. Interleukin-3-induced phosphorylation of BAD through the protein kinase Akt. *Science*. 1997;278(5338):687-9.
443. Du K, Montminy M. CREB is a regulatory target for the protein kinase Akt/PKB. *J Biol Chem*. 1998;273(49):32377-9.
444. Jia D, Zheng J, Yu J, Zhao N, Lu S, Hao D. Anticancer effects of ovatodioid on human prostate cancer cells involves cell cycle arrest, apoptosis and blocking of Ras/Raf/MEK/ERK signaling pathway. *Journal of BUON : official journal of the Balkan Union of Oncology*. 2020;25(5):2412-7.
445. Meloche S, Pouységur J. The ERK1/2 mitogen-activated protein kinase pathway as a master regulator of the G1- to S-phase transition. *Oncogene*. 2007;26(22):3227-39.
446. Garnham CP, Roll-Mecak A. The chemical complexity of cellular microtubules: Tubulin post-translational modification enzymes and their roles in tuning microtubule functions. *Cytoskeleton*. 2012;69(7):442-63.
447. Maruta H, Greer K, Rosenbaum JL. The acetylation of alpha-tubulin and its relationship to the assembly and disassembly of microtubules. *J Cell Biol*. 1986;103(2):571-9.
448. Webster DR, Gundersen GG, Bulinski JC, Borisy GG. Differential turnover of tyrosinated and detyrosinated microtubules. *Proc Natl Acad Sci U S A*. 1987;84(24):9040-4.

449. Bré M-H, Pepperkok R, Kreis TE, Karsenti E. Cellular interactions and tubulin deetyrosination in fibroblastic and epithelial cells. *Biology of the Cell*. 1991;71(1-2):149-60.
450. Rubin CI, Atweh GF. The role of stathmin in the regulation of the cell cycle. *J Cell Biochem*. 2004;93(2):242-50.
451. Wadsworth P, McGrail M. Interphase microtubule dynamics are cell type-specific. *Journal of Cell Science*. 1990;95(1):23.
452. Liu P, Xie X, Yang A, Kong Y, Allen-Gipson D, Tian Z, et al. Melatonin Regulates Breast Cancer Progression by the Inc010561/miR-30/FKBP3 Axis. *Mol Ther Nucleic Acids*. 2019;19:765-74.
453. Salaycik KJ, Fagerstrom CJ, Murthy K, Tulu US, Wadsworth P. Quantification of microtubule nucleation, growth and dynamics in wound-edge cells. *J Cell Sci*. 2005;118(Pt 18):4113-22.
454. Gallot YS, Straughn AR, Bohnert KR, Xiong G, Hindi SM, Kumar A. MyD88 is required for satellite cell-mediated myofiber regeneration in dystrophin-deficient mdx mice. *Hum Mol Genet*. 2018;27(19):3449-63.
455. Fukuda S, Kaneshige A, Kaji T, Noguchi Y-T, Takemoto Y, Zhang L, et al. Sustained expression of HeyL is critical for the proliferation of muscle stem cells in overloaded muscle. *eLife*. 2019;8:e48284.
456. Becker R, Leone M, Engel FB. Microtubule Organization in Striated Muscle Cells. *Cells*. 2020;9(6).
457. Singh D, Schmidt N, Müller F, Bange T, Bird AW. Destabilization of Long Astral Microtubules via Cdk1-Dependent Removal of GTSE1 from Their Plus Ends Facilitates Prometaphase Spindle Orientation. *Curr Biol*. 2021;31(4):766-81.e8.
458. Cassimeris L. The oncoprotein 18/stathmin family of microtubule destabilizers. *Current Opinion in Cell Biology*. 2002;14(1):18-24.

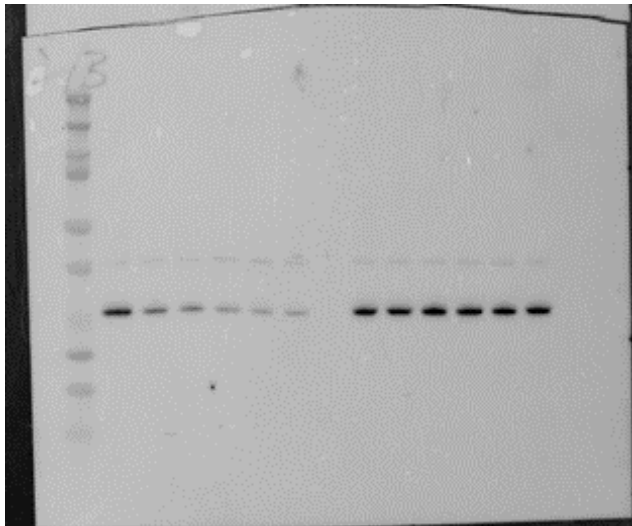
## Appendix 1: Complete breast cancer cell line panel



FKBP25 protein expression across full breast cancer panel that was examined in preliminary studies. Note: MDA-MB0468 is a basal breast cancer subtype, which is a subcategory of triple negative.

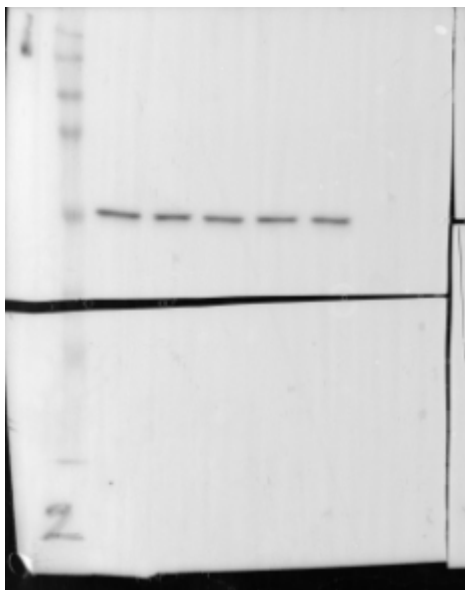
**Appendix 2: Full view of western blots with molecular weight marker.**

FKBP25 MAB2955 (FKBP25 Knockdown titration)



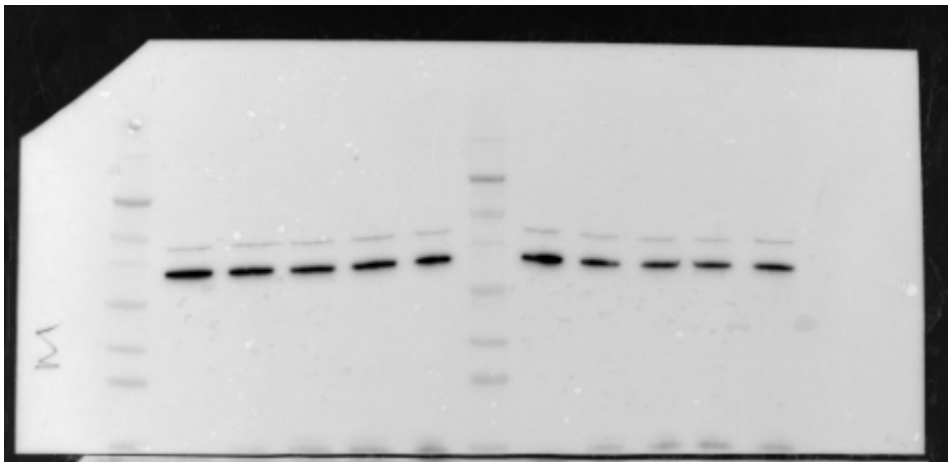
MW marker Amersham ECL Rainbow Molecular Weight Marker  
LEFT: FKBP25 Mir2 dox titration, RIGHT: FKBP25 NT Mir dox titration

B actin #4970 (C2C12 differentiation)



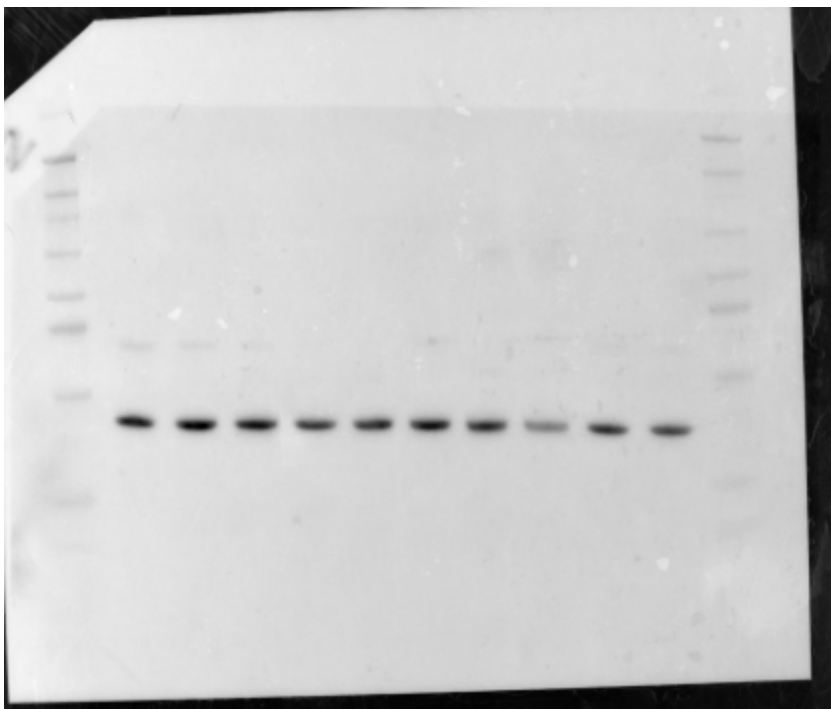
MW marker Amersham ECL Rainbow Molecular Weight Marker  
Lanes 1-5 C2C12 differentiation 24–96-hour samples

Myogenin ab124800 (C2C12 differentiation)



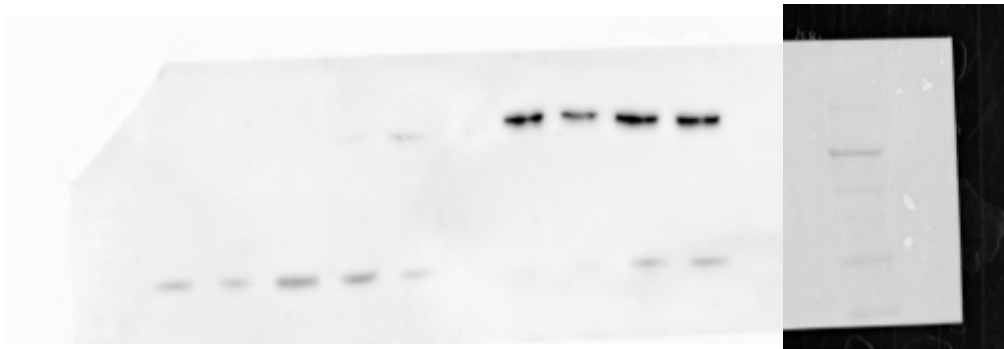
MW marker Novex™ Sharp Pre-stained Protein Standard  
Left and Right represent 2 biological replicates of C2C12 differentiation 24-96h samples

MyoD1 ab16148 (25KD and differentiation)



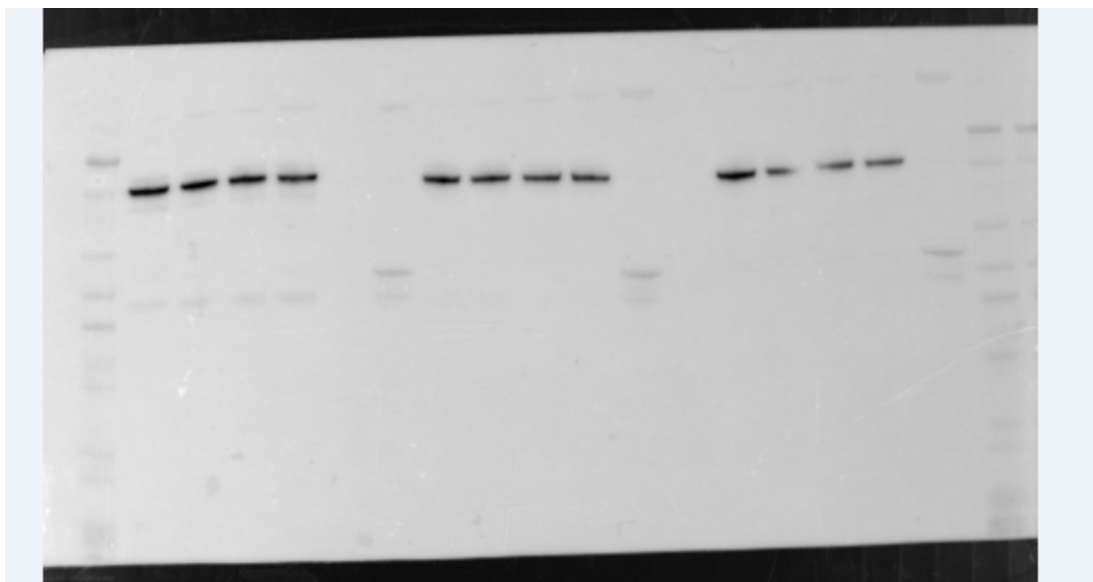
MW marker Novex™ Sharp Pre-stained Protein Standard  
C2C12 25KD differentiated myotube, treated with or without dox for 72h.

Fast myosin Heavy chain ab51263 (Differentiating C2C12)



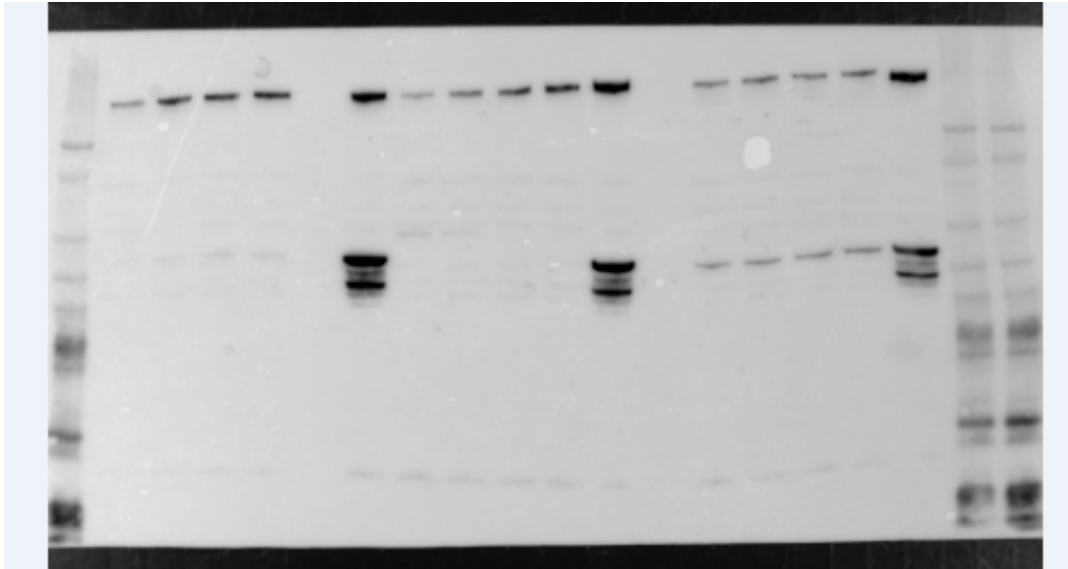
MW marker Novex™ Sharp Pre-stained Protein Standard  
C2C12 25KD differentiated myotube, treated with or without dox for 72h.

E Cadherin #3195 (EMT Induction titration; 5<sup>th</sup> lane negative control MDA-MB-231)



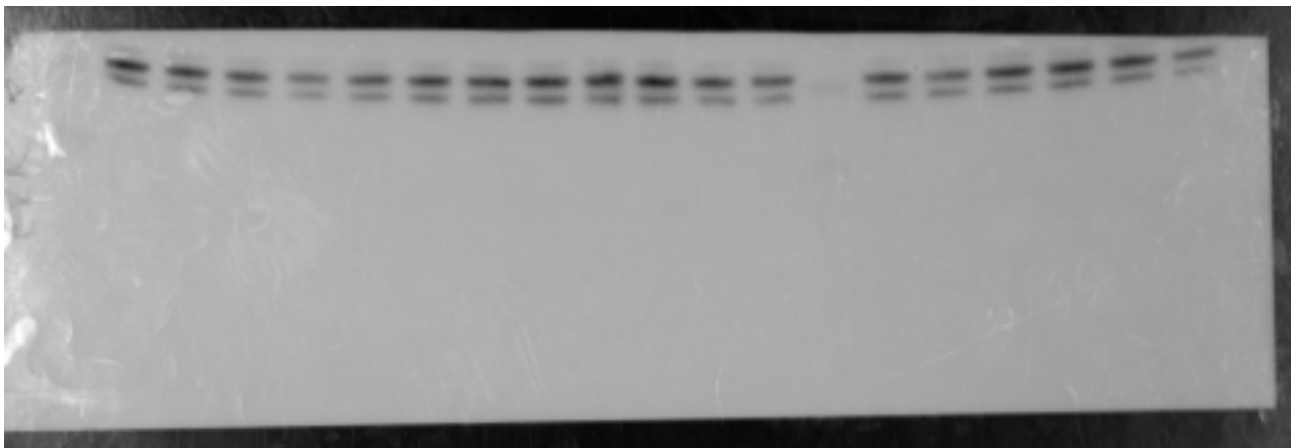
MW marker Novex™ Sharp Pre-stained Protein Standard  
Epidermal growth factor induced EMT titration; 5<sup>th</sup> lane in each group represents negative control for E cadherin MDA-MB-231)

Vimentin #5741 (EMT Induction titration)



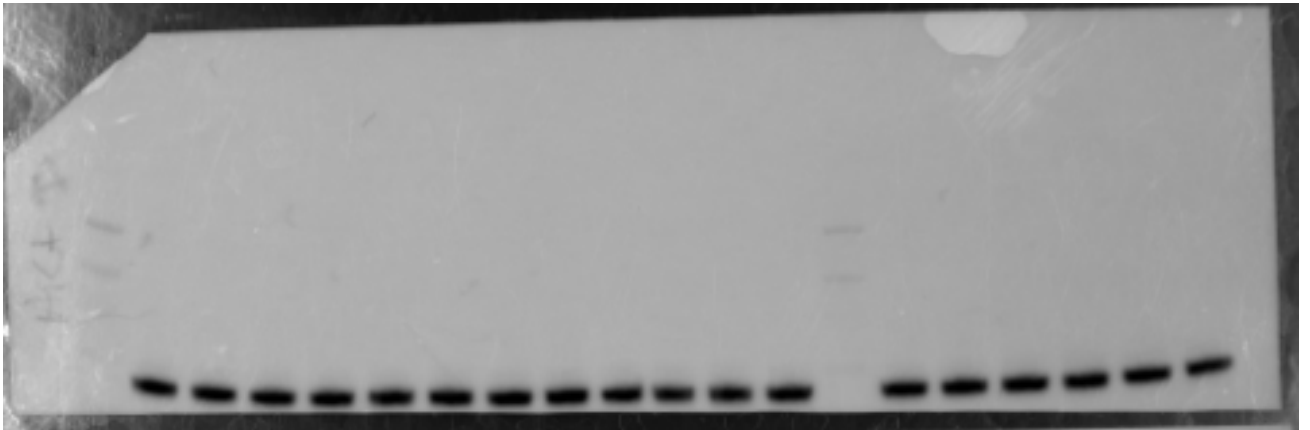
MW marker Novex™ Sharp Pre-stained Protein Standard  
Epidermal growth factor induced EMT titration; 5<sup>th</sup> lane in each group represents positive control for vimentin MDA-MB-231)

Erk #9102 (FKBP25 KD inhibitor titration)



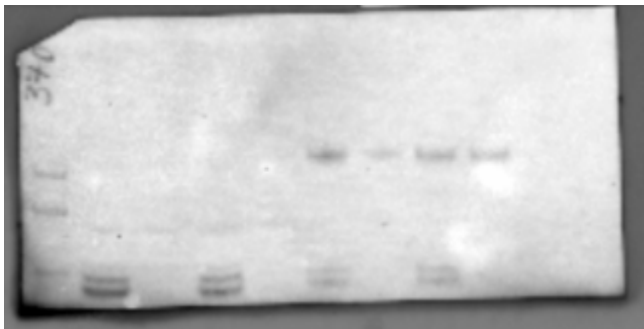
MW marker Novex™ Sharp Pre-stained Protein Standard  
Epidermal growth factor time-based titration 0-30 minutes on MDA-MB-468 cells.

Akt #4691 (FKBP25 KD inhibitor titration)



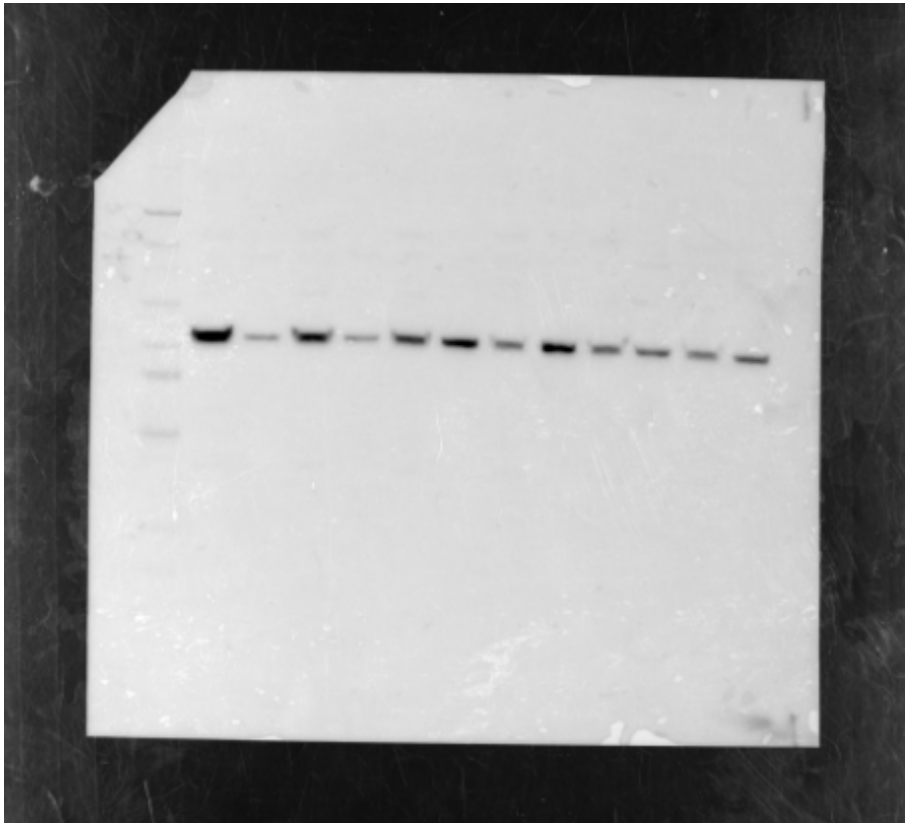
MW marker Novex™ Sharp Pre-stained Protein Standard  
Epidermal growth factor time-based titration 0-30 minutes on MDA-MB-468 cells.

P70s6 Kinase #2708 (FKBP25 KD inhibitor titration)



MW marker Novex™ Sharp Pre-stained Protein Standard  
25KD cells with EGF (right 4 lanes) or without (Left 4 lanes) and assorted inhibitors.

Pan Tubulin # ATN02 (microtubule polymerisation assay)



MW marker Novex™ Sharp Pre-stained Protein Standard  
Microtubule polymerisation assay with 25KD cells.